The exploitation of neuronal survival factors in Burkitt's lymphoma and germinal centre B cells

Fungai Natalie Winnie Chirimuuta

A thesis submitted to the University of Birmingham for the degree of DOCTOR OF PHILOSOPHY

School of Immunity & Infection

Institute of Biomedical Research

The Medical School, Vincent Drive

Birmingham, B15 2TT, UK

February 2010

Contents Page

2. Materials and Methods

3. Results

Characterisation of Burkitt's lymphoma B cells and their expression of neurotrophic factor mRNA transcripts

4. **Results**

Expression and autocrine signalling of TrkB and p75NTR receptors and their ligands BDNF and NT-4

5. **Results**

Investigating possible NGF and TrkA signalling via paracrine interactions between Burkitt's lymphoma B cell lines and Follicular Dendritic Cells and possible autocrine signalling effects within Burkitt's lymphoma B cells

5.2 **Results Part I** : Investigating possible NGF and TrkA signalling via paracrine interactions between Burkitt's lymphoma B cell lines and Follicular Dendritic Cells

5.2 **Results PartII** : Investigating possible autocrine signalling effects within Burkitt's lymphoma B cells

6. **Results**

Investigating signalling effects of NGF in Germinal centre B cells and questioning possible NGF and TrkA paracrine signalling with Follicular Dendritic Cells

Figures Tables and Illustrations

1. **Introduction**

2. **Material and Methods**

3. **Results**

4. **Results**

6. **Results**

Acknowledgements

I dedicate this work to the centre of my universe, Mum, Dad, Big and Frog. At times when I had felt like nothing, thinking of you made me pick myself up and carry on. I would not have done this without any of you. I LOVE YOU!

I would like to also thank Professor John Gordon for letting me have a fantastic opportunity to work in a great laboratory. To Professor Martin Rowe for his patience and much needed criticism!

To the Gordon lab/ x-lab members, Dude aka Agata. I love and miss you so much. Remember to call the coast guard for language courses ;-). To the western blotting queen aka Anita Chamba, thank you for the very clever, well thought through advice on how to make the most minging westerns look decent. To lil Anita, thank you for being the source of strength when times were bad. To Michelle for always having a biiiiig hug waiting for me and making me smile.

To Rowe lab members, NuPAGE gel electrophoresis expert extraordinaire aka Wendy. You made me feel welcome in Cancer Studies and greatly appreciate all the help you provided. To Jianmin for putting up with my constant whinging and help with transfection experiments.

To the 4th floor office, I shall miss my neighbours Mahmood and Karine. I would walk into work with a face of thunder and you always managed to make me feel relaxed and happy again. I shall miss the tears of laughter. To Elodie for putting up with my *patro mal* French. To Omar and of course Debbie for all the help on how to do amazing confocal staining. To Dr J, formally known as Master J aka Jenny from the IBR Block….. or Hot Chip Jenny. Thank you so much for being a good friend when I needed a chat and a hug..... and some beer with a lil Hot chip. Kezzinski aka Kezza to the K. MOUNTAIN SIIIIDE! Thank you for inviting me on the best holiday I have ever and will most likely ever be on.

To 4th floor receptions, thank you Alison and Vicki for all your advice, hard work and support. The building would fall apart without such foundations. To Adam for putting up with order forms I handed in without the grant number. Here's to the office that I enter and am always guaranteed a laugh, love and very good advice, Raga, you too are also an IBR corner stone, I shall remember your kind advice when I first came for my interview. And to the lovely Yvonne, for making me laugh out loud on soooo many occasions.

Finally but certainly not least, to my friends in Oxford, Bath, Bristol and Reading. Thank you for putting up with a very stroppy Nat for the past few years.

Thank you, Mazviita, Merci, Gracias!

Abbreviations

aa	Amino acid
BARTs	BamHI-A rightward transcripts
BDNF	Brain Derived Growth Factor (Mature BDNF)
BL	Burkitt’s lymphoma
BSA	Bovine serum albumin
CD	Cluster of Differentiation
CNS	Central Nervous System
CRD	Cystein Rich Domain
DD	Death domain
DMEM	Dulbecco's Modified Eagle Medium
dNTPs	2´-Deoxynucleoside 5´-triphosphates
EBERs	Epstein-Barr encoded small RNAs
EBNA	EBV Nuclear Antigens
EBV	Epstein Barr Virus
FCS	Fetal Calf Serum
IL	Interleukin
ILD	Immunoglobulin-like domain
JNK	c -Jun N-terminal kinase
LatI	Latency one/ I
LatIII	Latency three/ III

LCL	Lymphoblastoid cell line
LMP	Latent membrane protein
LRD	Leucine rich domain
MAPK	Mitogen-activated protein (MAP) kinases
NGF	Nerve Growth Factor (Mature NGF)
NT-3	Neurotrophin 3 (Mature NT-3)
NT-4	Neurotrophin 4 (Mature NT-4)
NTs	Neurotrophic factors
OD	Optical density
$p75^{NTR}$	p75 Neurotrophin Receptor
PBS	Phosphate buffered saline
PI3K	Phosphoinositide 3-kinase
PKC	Protein Kinase C
PLCγ	Phospholipase C-γ
PNS	Peripheral Nervous System
PNS	Peripheral nervous system
ProBDNF	Unprocessed Brain Derived Growth Factor
ProNGF	Unprocessed Nerve Growth Factor
ProNT-3	Unprocessed Neurotrophin 3
ProNT-4	Unprocessed Neurotrophin 4
qRT-PCR	Quantitative real time polymerase chain reaction
RPMI	Roswell Park Memorial Institute

RT-PCR	Reverse transcription polymerase chain reaction
SHC	Src homology and collagen domain protein
TKD	Tyrosine kinase domain
TMD	Transmembrane Domain
Trk	Tyrosine Receptor Kinase
β_2M	β_2 microglobulin

1. Introduction

1.1 Neurotrophic Factors

1.1.1 Discovery, Expression and Function of Neurotrophic factors

Neurotrophins were originally defined as soluble factors which influence neuronal cell survival, death, growth, plasticity and differentiation. The first neurotrophic factor was described by the Italian scientist, Rita Levi-Montalcini at Washington University in 1952. The unknown factor was observed to induce survival of motor neurones shortly removed from developing limb buds in chick embryos (Levi-Montalcini and Angeletti 1968) (Cohen and Levi-Montalcini 1956). Collaborations with Stanley Cohen enabled the production of a bioassay for the soluble factor's ability to induce neurite outgrowth in neuronal cells extracted from the sensory ganglion from a chick embryo. This neurotrophic factor was defined as Nerve Growth Factor (NGF) (Thoenen, Bandtlow et al. 1987)

In order to have a better understanding of this growth factor, animal models were used to knockdown NGF gene expression. Mice models revealed a severely impaired Peripheral Nervous System (PNS), however the Central Nervous System (CNS) neuronal structures and functions remained normal. Inhibiting NGF function by chronic administration of NGF antiserum resulted in adult mice lacking sympathetic ganglion. Interestingly, new born rodents injected with NGF develop enlarged sympathetic ganglia. These observations reveal that NGF is involved in the survival and development of some sensory neurones and the sympathetic nervous system.

In 1978 Yves-Alain Barde came across a neurotrophic factor released by brain derived embryonic glioma cells which also induced survival and growth of sensory neurones (Barde, Lindsay et al. 1978). This unknown factor was purified and added to spinal sensory neurones from chick embryos (Barde, Edgar et al. 1982) Survival and neuronal growth was observed. Importantly, the addition of NGF antiserum did not block the action of this neurotrophin; also the addition of the trophic factor in question does not induce survival in chick sympathetic neurones. The novel neurotrophic factor is now referred to as Brain Derived Neurotrophic Factor (BDNF) expressed within the hippocampus, cerebral cortex, and synapses of the basal forebrain (Hofer, Pagliusi et al. 1990).

NGF and BDNF gene sequences were compared for similarities (Maisonpierre, Belluscio et al. 1990) (Hohn, Leibrock et al. 1990). From these sequence analysis, the third mammalian neurotrophic factor derived from the brain was identified. Neurotrophic factor-3 (NT-3) is also known as Hippocampus-derived neurotrophic factor. Soluble factors from rat hippocampus tissues, were observed to target medial septal neurons and induced neurite outgrowth and cholinergic responses in neurones, specific to this neurotrophin (Ojika and Appel 1984). Transgenic mice lacking NT-3 suffer from server sensory and sympathetic peripheral neuron impairment (Farinas, Jones et al. 1994) (Snider 1994), and also display lack of movement due to deformity of the limbs (Ernfors, Lee et al. 1994).

Further DNA sequence analysis of the neurotrophins enabled the discovery of a fourth neurotrophic factor. High levels of Neurotrophic factor-4 (NT-4) were observed within the ovaries of xenopus (aquatic frogs) and viper (snakes) which is now know to be involved in embryonic chick dorsal root ganglion growth and development (Hallbook, Ibanez et al. 1991). NT-4 DNA sequences were then used to identify the factor within human and rat

genomic DNA which have similar survival effects in dorsal root ganglion survival as the xenopus counterpart (Ip, Ibanez et al. 1992; Ibanez, Ernfors et al. 1993) (Hallbook, Ibanez et al. 1991). Mice lacking the NT-4 gene suffer from server memory loss, indicating the importance of NT-4 for hippocampal dependent memory function (Xie, Sayah et al. 2000).

Collectively known as the mammalian neurotrophic factors, NGF, BDNF, NT-3 and NT-4 are 50 to 60% homologous in their amino acid sequences. In the late 1980's molecular biology techniques were used to sequence DNA for better understanding of the target gene and the protein constructed from it. The most studied neurotrophic factor, NGF was sequenced from mice, revealing a 45kb gene with small 5' exons where four NGF mRNA transcripts are produce by alternative slicing (Selby, Edwards et al. 1987). In mammalian tissue, the NGF complex sedimentation value is 7S. Also known as 7S NGF, the complex is composed of three polypeptides, alpha, beta and gamma (Varon, Nomura et al. 1967) (Smith, Varon et al. 1968). The beta peptide is the biologically active subunit comprised of 241 amino acids (Greene, Shooter et al. 1969), (Dracopoli, Rose et al. 1988).

Once the mRNA has been spliced, a mature NGF dimer is processed thorough a constitutive pathway or secreted as an unprocessed dimer via a regulated pathway. As shown in Illustration 1.1, an 18aa signalling peptide at the amino-terminal is present to for direct modified protein to membranes for sorting then secretion. Within the rough endoplasmic reticulum, the prodomain binds to a sortilin receptor enabling folding of the mature peptide. Non covalent links form between two mature NGF peptides forming a dimer which is then secreted. Unprocessed NGF, also known as ProNGF, can be intracellularly cleavage by endoproteases such as Furin or prohormone convertase 1 (PC1), or extracellularly cleaved by matrix metalloproteinase (MMP) plasmin enzymes, forming mature NGF

peptides (Edwards, Selby et al. 1988), (Seidah, Benjannet et al. 1996), (Mowla, Pareek et al. 1999).

1.1.2 Neurotrophic Factor Receptors

All four mammalian neurotrophins act as secreted ligands that cause target receptor dimerisation It is now known that mammalian neurotrophic factors exert their actions by specifically binding the Tyrosine receptor kinases (Trks). During the late 80s, it was discovered that Trks expressed at varying locations in the body, bind to hormones such as insulin, Epidermal growth factors and platelet-derived growth factor (Carpenter 1987), (Ebina, Ellis et al. 1985), (Yarden, Escobedo et al. 1986). In 1986, Martin-Zanca D., et al identified a novel tyrosine receptor oncogene, structurally related to the tropomyosin gene, within a colon carcinoma biopsy (Martin-Zanca, Hughes et al. 1986). Also known as Tropomyosin related kinases, the novel surface receptor was isolated for nucleotide sequencing and biochemical characterisation, which is now known as Tyrosine receptor kinase A (TrkA) (Martin-Zanca, Oskam et al. 1989), (Klein, Parada et al. 1989).

TrkA is one of three receptor types, TrkB and TrkC were later identified as neurotrophin receptors, having varying binding affinities between the neurotrophins. TrkB, discovered in 1989, shares 57% amino acid sequence homology with TrkA in the extracellular region, and 88% homology with the intracellular catalytic region (Soppet, Escandon et al. 1991).

TrkA preferentially binds NGF however TrkB binds either BDNF or NT-4 with similar affinities and cannot elicit signalling via NGF (Berkemeier, Winslow et al. 1991; Fan, Egles et al. 2000). It was later discovered that NT-3 is the preferential growth factor ligand for TrkC (Lamballe, Klein et al. 1991). On the other hand, NT-3, often referred to as a promiscuous Trk ligand, is

able to bind TrkA and TrkB but with lower affinity than their cognate ligands (Benedetti, Levi et al. 1993; Clary and Reichardt 1994). These receptor-ligand interactions are displayed within Illustration 1.2.

cDNA analysis of Trks has revealed several common receptor protein domains (Middlemas, Lindberg et al. 1991). Trk receptor structure is demonstrated within Illustration 1.3. Trk receptors consists of a, 32aa N-terminal signalling sequence which can be cleaved by peptidases (Kreil 1981). The next extracellular domains are involved in cell signalling. Two cystein rich domains (CRD) flanking three leucine rich motifs (LRM) are present to assist neurotrophic ligand binding which occurs at the second immunoglobulin like domain (ILD). The extracellular domain consists of 11 N-glycosylayion sites. A transmembrane domain was identified, leading onto an intracellular juxtamembrane domain that includes a Shc binding site. The catalytic tyrosine kinase domain, involved in cell signalling, is followed by a region containing a PLC-gamma binding site (Klein, Parada et al. 1989; Martin-Zanca, Oskam et al. 1989; Ninkina, Grashchuck et al. 1997).

Mammalian neurotrophic factors also bind to p75 Neurotrophin Receptors ($p75^{NTR}$). This receptor is structurally homogous to TNF receptors such as CD40-L and Fas which is composed of four cysteine-rich repeating units in the extracellular region. The intracellular region contains a death domain which signals via varying adapter proteins (Radeke, Misko et al. 1987). Due to the lack of enzymatic cytoplasmic activity in the intracellular domain, this receptor is multifaceted, contributing to a variety of biological pathways depending on which ligand it is bound to. Experiments carried out by Herrup K. and Shooter E. M., discovered $p75^{NTR}$ as a potential NGF receptor in sensory ganglia (Herrup and Shooter 1973). Proir to this finding $p75^{NTR}$ was known to bind peptide hormone such as insulin and

glucagon (Cuatrecasas 1971). Considering proinsulin and βNGF evolved from a common gene, ineffect producing proteins with similar homologies, NGF was discovered to act as another $p75^{NTR}$ ligand.

1.1.3 Neurotrophic Factor Receptor Dimerization And Downstream Signalling.

The differences between Trk receptors and $p75^{NTR}$ have to be considered regarding neurotrophin signalling. Proteolytically cleaved neurotrophins, also known as mature neurotrophins, form dimers which bind to two Trk receptors at the cell surface, that inturn, initiate prosurvival downstream signalling via the catalytic tyrosine kinase domain (Ibanez, Ilag et al. 1993). It is now also known that receptor complexes between $p75^{NTR}$ and Trk can occur, binding to one mature neurotrophin dimer which in turn can provide prosurvival signals (Longo, Manthorpe et al. 1997), (He and Garcia 2004). $p75^{NTR}$ on the other hand is also able to bind mature neurotrophin dimers as a single receptor or as a dimerised receptor (He and Garcia 2004). In the absence of TrkA, $p75^{NTR}$ preferentially binds to proneurotrophins causing cell death (Barrett and Bartlett 1994; Casaccia-Bonnefil, Carter et al. 1996). Please refer to illustration 1.4.

Upon binding of mature NGF homodimers, two TrkA receptors are brought together enabling phosphorylation of the intracellular catalytic domain. Trk receptors contain 10 evolutionarily conserved tyrosines in their cytoplasmic domains forming an autoregulatory loop of the tyrosine kinase domain. NGF binding to TrkA induces phosphorylation of three tyrosine residues, involving adaptor proteins such as Phosphoinositide 3-kinase and PLCγ, Src homology and collagen domain protein-1 (SHC). These phosphotyrosine binding

domains initiate downstream signalling through Ras/ Mitogen-activated protein (MAP) kinases, inositol phosphate and/or protein kinase C (PKC) which activate various transcription factors promoting cell survival, proliferation and/or differentiation, as reviewed by (Huang and Reichardt 2003; Reichardt 2006; Skaper 2008).

Signalling via TrkA can be further enhanced within the cell when $p75^{NTR}$ is coexpressed (Berg, Sternberg et al. 1991; Hempstead, Martin-Zanca et al. 1991). However proneurotrophins are associated with p75 dependent cell death via c -Jun N-terminal kinases signalling pathways, in the absence of Trk receptors (Lee, Kermani et al. 2001). On the $p75^{NTR}$ receptor structure, ligands bind and signal at the third and fourth cysteine-rich repeats (Yan and Chao 1991). Cell death can also be induced by $p75^{NTR}$ receptors coupling with other receptor types such as sortilin (Nykjaer, Lee et al. 2004). Sortilin is a trans-golgi protein adaptor, transmembrane protein with multi-ligand receptor binding capability (Bronfman and Fainzilber 2004). Intracellular sortilin is involved in the folding and modification of newly synthesised neurotrophin peptides. Whereas sortilin surface receptors can dimerise with $p75^{NTR}$ initiating cell death upon proneurotrophin binding.

Whether the neurotrophin signalling outcome provides cell death or survival is dependent on various factors such as neurotrophin cleavage and receptor expression patterns. The cell's location is also an influential factor on it's survival during neuronal development.

1.1.4 The Expression Of Neurotrophic Factors

Since neurotrophic factors were initially observed, defined and characterised within the CNS and PNS neuronal populations, they were considered to be trophic factors within these neuronal populations. However as laboratory techniques improved, wider screening methods analysing expression patterns also advanced. In 1992 Ip N.Y. et al, document on NT-4 expression patterns with the use of Northern blotting methods (Ip, Ibanez et al. 1992). Human RNA from various tissues of the body were hybridized with probes specific for NT-4. Surprisingly little to no levels of NT-4 transcripts were detected in the brain, however prostate, thymus, placental and skeletal muscle tissues expressed NT-4 RNA. Work by Blar et al, revel the co-expression of TrkC and TrkB genes in several non-neural tissues, including the tongue, the whisker pad, mesenchyme by in-situ hybridisation experiments in mice (Tessarollo, Tsoulfas et al. 1993).

Prior to these findings there had been evidence for the expression of neurotrophins linked to the immune system. NGF was observed to induce shape changes in platelets, enhance vascular permeability in rat skin and degranulation of mast cells from rats (Bruni, Bigon et al. 1982; Otten, Baumann et al. 1984). Importantly, functional TrkA receptors were documented by Ehrhard P.A et al, where they observe monocyte cytotoxcicity upon NGF administration (Ehrhard, Ganter et al. 1993). Functional TrkA receptors were also found to assist progenitor hematopoetic granulocytes when treated with NGF, inducing proliferation and differentiation (Chevalier, Praloran et al. 1994).

Neurotrophin signalling has also been observed in B lymphocyte development. An important research paper by Torcia M. et al, reveals the dependence of NGF in Memory B cell survival (Torcia, Bracci-Laudiero et al. 1996). NGF has also been shown to induce

proliferation and differentiation in B lymphocytes (Otten, Ehrhard et al. 1989). BDNF on the other hand has been documented to participate in B cell development. BDNF deficient mice have reduced numbers of B cells in the blood, spleen and bone marrow (Schuhmann, Dietrich et al. 2005). This novel neuro-immuno link will be the main focus for this thesis.

1.1.5 Communication Between The Immune And Nervous System

In 1984 Hugo Besedovsky and Edwin Blaclock proposed that “the immune system functions as a diffuse sense organ informing the brain about events related to infection and injury” (Blalock 1984). This bi-directional communication is initiated when the immune system detects a sign of infection then relays signals to the brain via neuronal and/ or humoral routes of transmission. Although controversial, there are suggestions that sensory neurones within the vagus nerve are in direct contact with secondary lymphoid tissues such as lymph nodes, where signals are sent to the brain inducing a “stress response”.

Houmoral routes include various cytokines such as TNF, IL-6 and IL-1 where they are released into the blood vessles following infection. These cytokines are then transported to areas such as the circumventricular organs where the blood brain barrier is weaker or absent. By binding to receptors, signals such as prostaglandins are diffused to the brain parenchyma. In effect, the brain is thought to alter behaviour within the animal due to these signals for infection. As initially documented by Benjamin L. Hart in 1988 from his work on “biological basis of the behaviour of sick animals”, animals respond to sickness by altering sleep and eating patterns and displaying depression symptoms. Hart believed this was an evolved and organised way of fighting infection by letting the body conserve energy (Hart 1988).

Neurotransmitters are then relayed from the brain to blood vessles and lymphoid tissues via the hypothalamic-pituitary-adrenal (HPA) axis or the sympathetic Nervous System (SNS). The HPA axis is a major part of the neuroendocrine connection between the hypothalamus, adrenal glands and the pituitary gland. During the stress response monoamines can be released from adrenal glands into the blood. The SNS is also activated where

neurotransmitters such as dopamine and serotonin are diffused from nerve endings within lymphoid tissues.

B cells can encounter neurotransmitters within lymphoid organs at all stages during their differentiation. The activation of the HPA axis and SNS induce release of dopamine and serotonin which act upon B lymphocytes expressing their receptors and transporters (McKenna, McLaughlin et al. 2002). It is also known that dopamine and serotonin can induce either proliferation or apoptosis in B lymphocytes, depending on concentration (Bergquist, Josefsson et al. 1997).

1.2 B Lymphocyte Development and Maintenance

1.2.1 The Immune System

The immune system of invertebrates is used to defend the body against foreign pathogenic organisms, chemicals or molecules. The immune system is also used to identify and protect against internal defects in the development and functioning of cellular tissue. Innate and adaptive immunity are the two branches of defence used for the body's protection. Innate is non-specific "natural" immunity which utilizes anatomical barriers, phagocytic and inflammatory responses to provide a rapid non-specific protection against intruders. Adaptive immunity on the other hand is long lived specific immunity acts via a humoral or a cell mediated response. Cell mediated defence involves two major groups of cells from the hematopoietic system; cytotoxic T lymphocytes and T helper lymphocytes that target epitopes on the cell surface presented by major histocompatibility complex. The humoral response on the other hand, is maintained by B cells which secrete antibodies that target epitopes found on the cell surface.

B and T lymphocytes arise within the bone marrow; B cells mature in the bone whereas T cells migrate to the thymus.

1.2.2 B-cell Development

There are three stages in B cell development; generation of innate B cells from stem cells, their encounter with antigen and finally, differentiation into memory B cells or plasma B cells. Pluripotent hematopoietic stem cells within the bone marrow produce progenitor B cells which express CD45R and CD43. During early B cell maturation, rearrangement of immunoglobulin DNA occurs. By binding to and secreting IL-7, stromal cells enable the differentiation of progenitor B cells into precursor B cells that contain immunoglobulin heavy chain gene rearrangements.

For a Pre-B cell to continue in development, productive light chain rearrangements need to occur. Due to allelic exclusion one light chain isotope is expressed on each B cell membrane. This B cell will then be committed to have particular antigenic specificity determined by the heavy chain (VDJ) sequence and the light chain (VJ) sequence.

These Pre-B cells then differentiate into mature immunocompetent B cells which express CD45R, IgM, low levels of IgD and the BCR on its surface. Cells are then transferred to secondary lymphoid organs such as the spleen or lymph node for antigen recognition within germinal centres.

The constituents of a germinal centre include activated B cells, T cells, macrophages (also known as tingible body macrophages) and follicular dentritic cells (FDCs) (Butcher, Rouse et al. 1982; Rouse, Ledbetter et al. 1982; Stein, Gerdes et al. 1982).

The germinal centre dark zone is the site where rapidly proliferating mature B cells known as centroblasts, undergo somatic hypermutation of the immunoglobulin variable regions.

Here, variations occur in the form of single base substitutions, insertions and deletions within hyper variable regions. These are the sites that correspond to antigen recognition which specify the type of antigen recognised by the effector B cell via the immunoglobulin receptors. By class switch recombination, cells generate a variety of immunoglobulin classes specific for a variety of antigens.

Centroblasts are then transported into the light zone, rich in dense networks of FDCs, T-Helper cells and tingible body macrophages (TMs), which are scavengers for apoptotic lymphocytes (MacLennan and Gray 1986; Gray 1988). Here the centroblasts are converted into non-dividing centrocytes that intimately interact with the various cells within the germinal centre microenvironment (Gray and Leanderson 1990).

FDCs present native antigen to B cells in order to select high affinity B cells. Low affinity B cells die by apoptosis, therefore a survival function is mediated though B-cell binding to FDCs. Fc epsilon RII, also known as CD23, is expressed by FDCs which induces an anti-apoptotic signal via the BCR-CD21-CD19 complex (Bonnefoy et al., 1993). The adhesion receptors, VCAM, ICAM and CD44 as well as, IL-15 receptor which is known to activate B-cell proliferation, are expressed by the FDCs (Freedman, Munro et al. 1990; Lindhout, Mevissen et al. 1993). As shown by Hase et al, BAFF is able to initiate the production CD19 by activating a B-cell specific transcription factor which in turn enhances proliferation, IgG production, and reactivity to CD154 (CD40 ligand binding to CD40 on TH cells) by BCR/CD19 co-ligation and interleukin-15 (IL-15) (Hase et al., 2004).

Centrocytes then form two types of effector B cells, small memory B cells and large plasmablasts (Coico, Bhogal et al. 1983). Plasmablasts subsequently develop into plasma

cells that secrete antibodies, whereas B cells either remain in the GC or circulate peripheral vessels.

1.2.3 B-Cell Signalling Within The Germinal Centre

Antigen presenting cells such as macrophages and dendritic cells present antigen via MHCII to T-cell receptors on CD8 positive T helper cells. Activated T helper cells then proliferate and secrete cytokines, such as interferon gamma, which in turn activate varying cells within the germinal centre including B cells and FDCs.

B cell activation by soluble antigen requires T helper cell signalling. Initially, antigen binds to surface immunoglobulin receptors on B cells, signals via the B cell receptor and is internalized by endocytosis and processed within the endocytic pathway. Signalling via the B cell receptor initiates the upregulation of surface receptors such as MHC II and its co-stimulatory ligand B7. The B cell then behaves as an antigen presenting cell to T helper cells by expressing the processed antigen present on an MHC II receptor which binds to a T cell receptor. Activated T helper cells then expresses CD40 ligand that binds to CD40 receptor present on B cells, stimulating B cell proliferation and survival via protein tyrosine kinases such as Syk and Lyn, Phospholipase C and transcription factors such as NFκB. B7 receptor then binds CD28 and the release of cytokines such as IL-2, IL-4 and IL-5 bind to cytokine receptors expressed by B cells (Gordon et al., 1989; Liu et al., 1989).

Since most of the B-cell lymphomas originate from germinal centres, their transformation occurs in close association with FDCs in the early stage of tumorigenesis (Li, Yoon et al. 2004).

It is known that FDCs may be involved in lymphomagenesis by providing signalling molecules such as 8D6 and 4G10/CD44. These molecules have been shown to promote

lymphomagenesis within L3055 cells, a human B cell line co-cultured with HK cells, an FDC line.

HK cells also promote L3055 cell line and germinal centre B cell proliferation (Choe, Li et al. 2000; Li, Zhang et al. 2000).

Based on this literature the aims of the investigation were drawn for the study into possible neurotrophic factor signalling in Burkitt's lymphoma B cells and normal germinal centre B cells. Looking further into neurotrophic factor signalling within a germinal centre possible NGF signalling within this germinal centre microenvironment were also questioned by studying possible FDC-B-cell interactions.

1.3 Burkitt's Lymphoma And Epstein Barr Virus

1.3.1 Discovery Of Burkitt's Lymphoma

In 1958, Dennis Burkitt submitted a report on a recently discovered Lymphoma sarcoma in two to fourteen year old children within equatorial parts of Africa (Burkitt 1958; Burkitt 1962). Cancerous growths were observed within the kidneys, adreanal glands, liver, thyroid, heart stomach, ovaries, salivary glands and jaw causing facial disfigurement (Renovanz 1960). These growths were defined as malignant lymphoma in the early 60s by J.N.P. Davis and G.T. O'Conner in Uganda (Burkitt and O'Conor 1961). Without treatment, the children died within four months.

Geographical distribution and race did not influence the prevalence of the lymphoma, suggesting a possible environmental factor. The possible influence of a viral factor was suggested by Professor Davis in 1961 where there were initial speculations on a possible arthropod vector. However, it is now known, the epidemiology of the lymphoma is associated with malaria which weakens the immune system rendering the patient susceptible to viral infection (Old, Boyse et al. 1966).

1.3.2 The Characteristics And Pathogenesis Of Endemic Burkitt's Lymphoma

Histological Burkitt's lymphoma tumour sections obtained from the jaw had been stained in Giemsa and Leishman. Images were described as "a uniform pattern of sheets of immature lymphoid cells interspersed with non-malignant histiocytes which often assume a clear or vacuolated form giving the tumour a characteristic "Starry sky" appearance" (O'Conor and Davies 1960). Due to the high levels of lymphoblast proliferation and apoptosis, tingible-body macrophages ladened with apoptosed tumour cells are observed (Clift, Wright et al. 1963).

A common characteristic of Endemic Burkitt's lymphoma also includes the translocation of *c-myc*, a protooncogene located on chromosome 8 with the immunoglobulin heavy-chain (chromosome 14) or light-chain genes (chromosomes 2 or 22) (Manolov and Manolova 1972; Zech, Haglund et al. 1976; Taub, Kirsch et al. 1982). This translocation is what causes neoplasia in B cells due to the constitutive activation of a *c-myc* oncogene (Erikson, ar-Rushdi et al. 1983). Later it was discovered that a virus drives this translocation.

Epstein M.A. and Barr Y.M. cultivated Burkitt's lymphoma cells from biopsies flown to London from Uganda. The biopsy material was shipped within 50% guinea pig serum in Hanks B.S.S. On arrival cells were fed every three to four days in Eagle's basal medium with 10% human serum and incubated at 37^{o}C. After ten months of continuous culture cells continued to grow as free floating cells that were described having an altered lymphoblast morphology (Epstein and Barr 1965). Some cells in culture had a pear shaped contour however most appeared round under phase contrast microscopy analysis. Larger cells were also observed containing multiple nuclei with basophilic cytoplasms and numerous cytoplasmic vacuoles. Single round cells had a tendency to form doublets and clumps of

five to ten cells. The successful cultivation of Burkitt's lymphoma cell lines were and are still considered a useful tool for investigating the *in vitro* interactions between B cells and EBV.

In 1964 M.A. Epstein and Y.M. Barr collaborated with D. Burkitt, where they obtained biopsy tissue from a maxillary lymphoma excised from a child. These tissues were placed in guinea pig serum and shipped to London from Uganda. The suspending fluid appeared dense containing single round cells shaken from the biopsy. These cells were split in Eagle's basal media containing 5% human serum. Long term cell cultures were achieved enabling further characterisation of the B cells. Within the same year, M.A. Epstein and Y.M. Barr observed small particles within the cytoplasm that resembled Herpes viruses. Further electron microscopy on cell lines obtained from Burkitt's patients verify the virus to be within the Herpes family due to its ability to bud into two viral partials through the plasma membrane and the presence of an outer envelope and a viral capsid (Epstein, Henle et al. 1965).

Burkitts's lymphoma B cells have also been observed to show phenotypic characteristics resembling germinal centre B cells. Klein, U. et al, have documented on the presence of somatically hyper-mutated variable regions within Burkitt's lymphoma cell lines (Klein et al., 1995).

1.3.3 Epstein Barr Virus And B Lymphocytes

From 1964, Epstein T., Barr Y. and Achong B. discovered a herpesvirus which infected cultured cells from African endemic Burkitt's patient tissue samples (Epstein, Achong et al. 1964). EBV is a gammaherpesvirinae virus within the herpesviridae family (Duncan, 2001). It consists of a 173kbp double stranded DNA sequence that multiplies within the nucleus of its host cell. EBV differs from other herpesviridae viruses due to their pathogenicity and are associated with several B-cell lymphomas including Post-transplant lymphoproliferative diseases and Hodgkin's lymphoma. Burkitt's lymphoma is also an EBV associated disease which occurs due to mass proliferation of latently infected B cells at a level which the failure the host's immune system, namely cytotoxic T cells, are unable to control.

EBV viral particles are transmitted orally within saliva (Hoagland, 1955). These particles enter within the nasopharynx through the epithelium lining composed of crypts, underlined by lymphoid tissue (lymphoepithelium) causing pharyngitis (Perry, 1994, Sitki-Green et al., 2003). EBV is speculated to infect, replicate and release viral particles within the stratified squamous epithelium, commonly associated with Infectious Mononucleosis (Henle G., Henle W. Seroepidemiology of the virus Epstein M. A. Achong B. G. eds. The Epstein-Barr Virus, pp. 297-320, Springer-Verlag Berlin 1979). B lymphocytes within the oropharyngeal lymphoid organs are then presumed to be latently infected, initiating the growth of Burkitt's lymphoma cancerous tissues (Greenspan et al., 1985, Babcock et al., 1998) (Rickinson, A. B., and E. Kieff. 1996. Epstein-Barr virus, p. 2397-2446. In B. N. Fields, D. M. Knipe, P. M. Howley, R. Chanock, J. Melnick, T. Monath, B. Roizman, and S. Straus (ed.), Fields virology. Lippincott-Raven, New York, N.Y).

EBV is endocytosed through non-dividing B lymphocyte membranes via a viral membrane glycoprotein binding to the type-two complement receptor, (CR2) also known as CD21 (Fingeroth, Weis et al. 1984). Once uncoated within the cytoplasm, the virus enters the nucleus establishing a state of viral latency. These latently infected B cells undergo proliferation, virus encoded regulatory proteins then prohibit cell death progression by silencing Retinoblastoma and p53 functions (Zhang, Gutsch et al. 1994; Zacny, Wilson et al. 1998). Like many other successful viruses, EBV is also able to manipulate its host's machinery such as cellular proteins involved in apoptosis prevention. For example, the pro-apoptotic protein, Bim, a member of the Bcl-2 family, is down regulated in human B cells infected with EBV (Clybouw et al., 2005). EBV is able to modulate caspase-8 and FLICE-inhibitory protein by preventing Fas-mediated apoptosis (Tepper and Seldin 1999). In vitro, EBV efficiently induces latent infections in B cells that transform to a lymphoblastoid phenotype dependent on constitutively active autonomous signals maintain the latent infection. A small proportion of latently infected B cells can be primed by BZLF1 to induce a lytic EBV infection (Flemington and Speck 1990). Immediate-early transcription activation genes, BRLF1 and BZLF1 orchestrate the production of de novo viral particles by inducing early and late EBV gene expression (Farrell, Rowe et al. 1989; Flemington and Speck 1990). In vitro, latently infected B cells are immortalized by the regulation of EBV latency associated genes which control cell proliferation and survival. Of which includes, six EBV Nuclear Antigens (EBNA) (EBNA-1, 2, -3A, -3B, -3C and -LP), three Latent Membrane Proteins (LMP) (LMP-1, -2A, -2B), BamHI-A rightward transcripts (BARTs) and Epstein-Barr encoded small RNAs (EBERs). Depending on which genes are expressed at one time, alternative latency phenotypes are observed which can be influenced by cytokines such as IL-6 and IL-

10 (Brennan, 2001, Kis et al., 2006b). Table 1.1 is a summary of EBV genes observed within lymphoblastoid cell lines (LCLs) and their functions.

Table 1.1: Summary of EBV gene expression within lymphoblastoid cell lines

EBV Genes	Main Functions
EBNA-1	▪ Required for the replication of viral episomes within latently infected memory B cells cells. ▪ Can bind to BamHI Q promoters, therefore regulate its own expression (Elizabeth R. Leight 2000).
EBNA-2	▪ Similar to NOTCH, enhances and protects against apoptosis (Hsieh, Nofziger et al. 1997). ▪ Controls Lymphocyte with EBV transformation (Cohen and Levi-Montalcini 1956).
EBNA-3A	▪ Can bind to the cellular repressor binding protein RBP-Jk (CBF-1), a component of the Notch signalling pathway (Cludts and Farrell, 1998, Waltzer et al., 1996)
EBNA-3B aka EBNA-4	▪ Can recruit Histone Deacetylase.
EBNA-3C aka EBNA-6	▪ Activates the LMP1 promoter in the presence of EBNA2 (Zhao and Sample 2000).
EBNA-LP aka EBNA-5	▪ Binds to the tumour suppressor proteins Retinoblastoma and p53 for survival against death (Szekely, Selivanova et al. 1993).
LMP-1	▪ Upgregulate anti-apoptosis factors (Bcl-2, A20, Mcl-2) (Izumi 2001). ▪ Mimics a constitutively active CD40-Receptor (Kis, Takahara et al. 2006). ▪ Activates NFkB which inturn switches on survival factors (BAFF, Bcl-XL, Bcl-2) (Elizabeth R. Leight 2000).
LMP-2A	▪ Controls viral lytic phase by inhibiting surface immunoglobulin cross linking within lymphoblastoid cells (Miller, Lee et al. 1994). ▪ Mimics BCR signalling and is involved in B-cell survival (Caldwell, Wilson et al. 1998).
LMP-2B	▪ Regulates viral and cellular gene expression by modulating NFkB (Stewart, Dawson et al. 2004).
EBERs	▪ Induce IL10 transcription for growth within BL (Kitagawa, Goto et al. 2000) ▪ Form complexes with bouble-stranded RNA activated protein kinase, inhibiting the interferon α (Meurs, Chong et al. 1990; Clarke, Schwemmle et al. 1991).
BARTs	▪ Unknown functions.

NOTE: It is worth noting there is difficulty in allocating specific functions for each EBV gene. Through evolution EBV has developed more than one way of enabling proliferation and survival. A vast network of external signals and genes are required at different stages during an infection involving the activation and silencing of various genes. Key:

Genes essential for primary growth transformation (Rickinson, Young et al. 1987; Izumi 2001).

Genes essential for B-cell immortalization (Tomkinson, Robertson et al. 1993).

Genes that can interact with complexes of cellular proteins involved in transcription regulation (Young and Rickinson 2004; Gorzer, Niesters et al. 2006).

During an EBV infection cells can exhibit all types of latency stages depending on the cells location and external survival signals which in turn can alter viral gene expression for survival and proliferation (Thorley-Lawson, 2001).

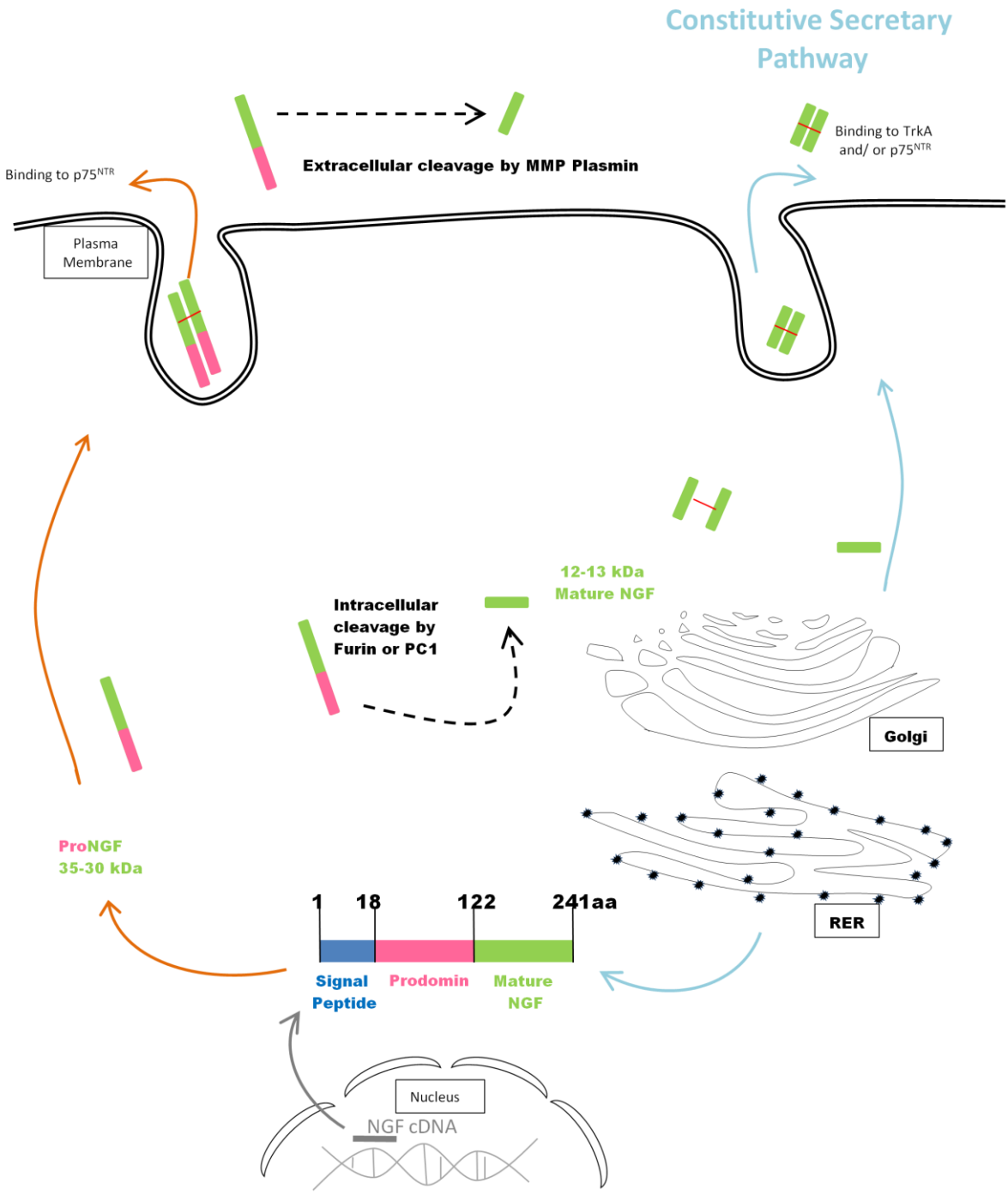

Illustration 1.1: NGF peptide processing dimerization and secretion

Once NGF mRNA is transcribed to a 241 amino acid peptide sequence it is processed within the cytoplasm via a regulated pathway or a constitutive pathway. Peptide processing via the regulated pathway enables secretion of proNGF protein whereas the constitutive pathway enables secretion of mature NGF proteins.

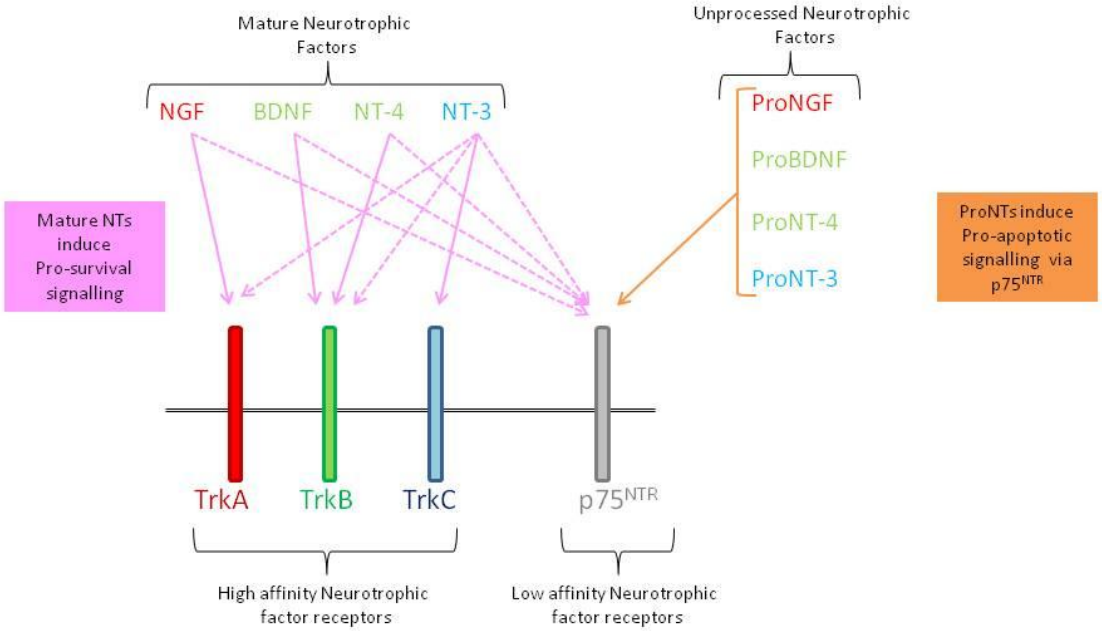

Illustration 1.2: Neurotrophic factors and their receptors

NGF is the cognate ligand for TrkA, BDNF and NT-4 are the cognate ligands for TrkB and NT-3 is the cognate ligand for TrkC. These mammalian mature neurotrophic factors have higher affinity binding to Trk receptors, but low affinity binding to $p75^{NTR}$. ProNGF, ProBDNF, ProNT-4 and Pro NT-4 have higher affinity binding to $p75^{NTR}$.

Key: Low affinity binding: - - -

High affinity binging: ——

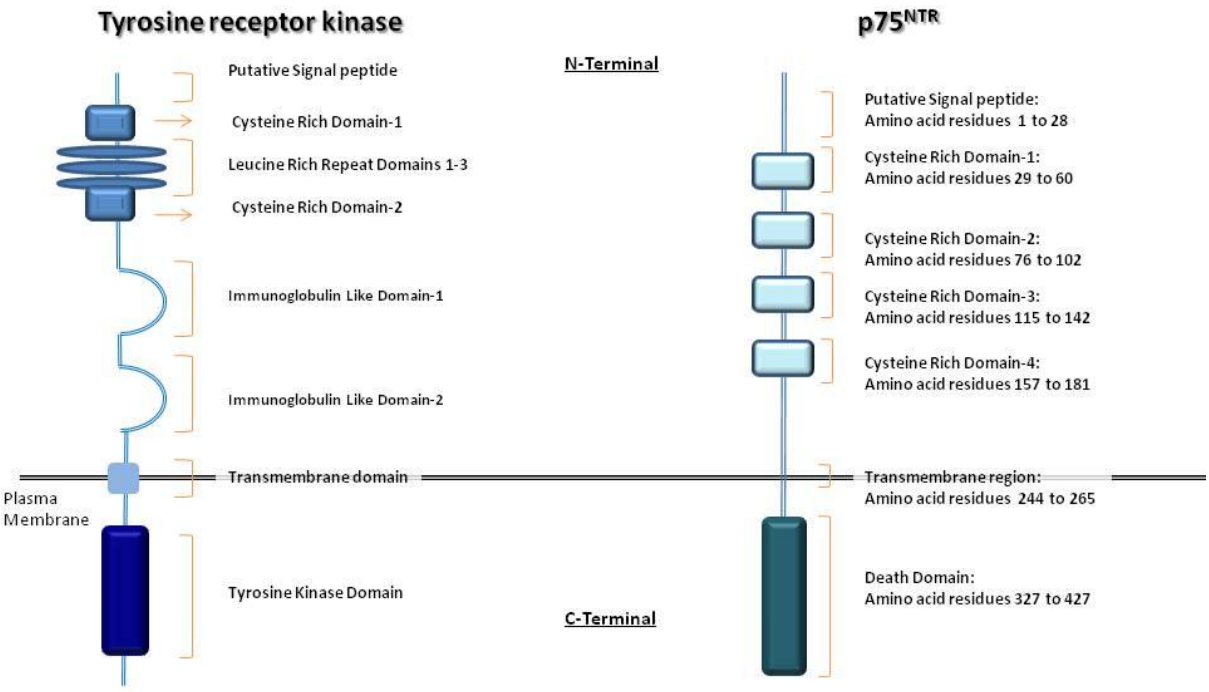

Illustration 1.3: High and low affinity Neurotrophic factor receptor structures

Both Tyrosine receptor kinases and $p75^{NTR}$. Receptors are composed if varying domains that enable neurotrophic factors binding and signalling via intracellular receptor domains.

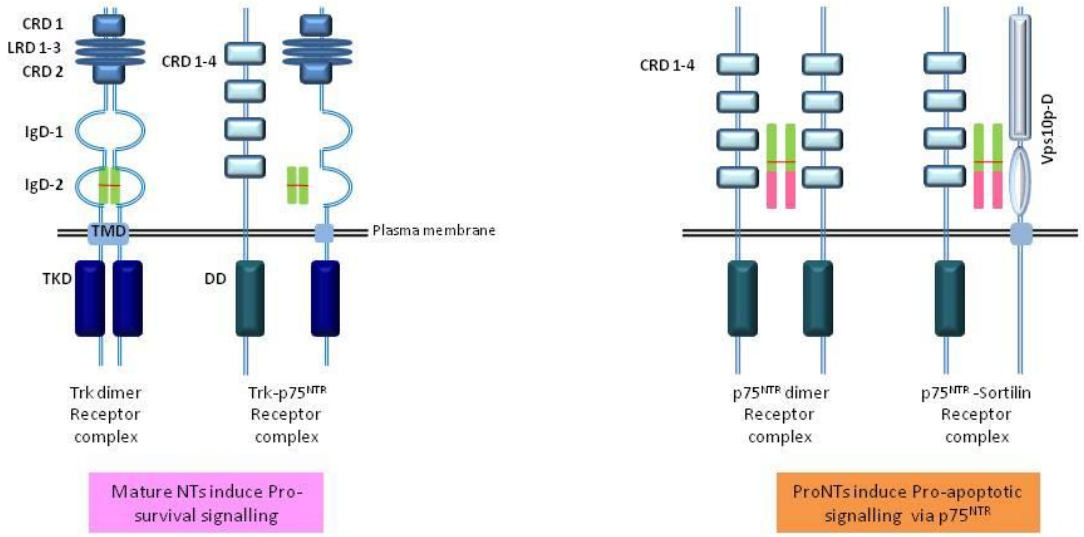

Illustration 1.4: High and low affinity neurotrophic factor receptor dimerization

Upon mature homodimer neurotrophic factors binding to the second immunoglobulin domain of a Trk, receptor homodimerization occurs. Receptor dimerization can also occur between Trk and $p75^{NTR}$ heterodimers enabling receptor autophosphorylation and signalling via the catalytic tyrosine kinase domain for cell survival.

On the other hand, unprocessed neurotrophins bind on to the last two cystein rich domains on $p75^{NTR}$ enabling homodimerization or heterodimerization with sortiln. Downstream signalling via the death domain promotes cell death.

Key: Cystein rich domain (CRD), Leucine rich domain (LRD), Immunoglobulin-like domain (ILD), Transmembrane Domain (TMD), Tyrosine kinase domain (TKD), Death domain (DD).

Aims of the investigation

The main focus for this investigation is to question the expression and signalling outcomes of the four mammalian neurotrophic factors and their high and low affinity receptors in Burkitt's lymphoma B cells lines displaying varying EBV latency phenotypes – to be utilised as specific therapeutic targets for treatment of Burkitt's lymphoma.

The following questions were investigated and analysed within the indicated results chapters

Chapter 3

Do Burkitt's lymphoma B cells displaying varying EBV latency phenotypes express neurotrophic factor mRNA transcripts?

Chapter 4

- Do Burkitt's lymphoma B cells displaying varying EBV latency phenotypes express TrkB, $p75^{NTR}$, BDNF and NT-4 protein?
- To question possible autocrine signalling via TrkB and $p75^{NTR}$ receptors and their ligands NT-4 and BDNF for cell survival and proliferation in Mutu latency III clone J8 Burkitt's lymphoma B cell lines.

Chapter 5

- Do germinal centre B cells, extracted from human tonsils, express neurotrophic factors and receptor mRNA transcripts?
- To question possible paracrine signalling via NGF, secreted by FDCs to signal to B cells via TrkA and P75 receptors to rescue cells from apoptosis, induce proliferation and cell migration in Mutu negative clone 3 Burkitt's lymphoma B cell lines.
- Autocrine signalling via TrkA and P75 receptors and their ligand NGF for cell survival and proliferation in Mutu latency III clone J8 Burkitt's lymphoma B cell lines.

Chapter 6

- Do germinal centre FDC cells, in human tonsils, express NGF protein?
- To question TrkA and $p75^{NTR}$ receptors on germinal centre B cells, signalling in a paracrine manner, with NGF producing FDCs.

2. Materials and Methods

2.1 Cell Culture and Reagents

2.1.1 Cell Culture Media

Cell Culture Media

500mls	RPMI 1640
10%	Foetal Calf Serum
2mM	L-Glutamine
100μg/ml	Penicillin Streptomycin

Cells were grown in Sarstedt cell culture flasks and stored within a 5% CO_2, 37^{o}C incubator. Cells were maintained in RPMI (Roswell Park Memorial Institute) 1640 media (Gibco) containing various amino acids such as L-Serine, required for the production of phosholipids for cellular membranes. RPMI 1640 also contains vitamins, inorganic salts such as Sodium Chloride and Potassium Chloride, for osmotic balance, and other compounds such as Glucose for Adenosine Triphosphate. Phenol Red is an important addictive within media which is used as a pH indicator. Two days after feeding cells, media turns from red to yellow due to the acidic products from cellular metabolism (Moore, Gerner et al. 1967).

Before RPMI 1640 could be used in cell culture, other essential addictives were added. An extra 1% L-Glutamine was added to RPMI 1640 media. As described by Eagle, *et al*, L-Glutamine (Gibco BRL

25030-024) was essential for the survival and growth of mammalian cells and is highly utilized by lymphocytes and other cells within the immune system (Eagle, Oyama et al. 1956; Newsholme, Curi et al. 1999). 1% Penicillin Streptomycin (Gibco BRL 15140-122) was added to prevent microbial contamination. 10% FCS-1621 (first link UK Ltd) was also added and is essential for cell growth.

For long term storage 10^6 cells were pelleted and resuspened per 1 ml of sterile filtered neat FCS containing 5% DMSO. Cells were left in a "Mr Frosty" NALGENE cryo 1^o freezing container containing Isopropanol. Mr Frosty was placed in a -80^{o}C freezer over night to ensure cells were frozen at a rate of 1^{o}C per minute; cells were then placed in liquid nitrogen.

2.1.2 Burkitt's lymphoma cell lines

Within Burkitt's lymphoma endemic areas, this B-cell malignancy is found to harbour EBV genes within infected B cells. However within the western world such as North America, the Burkitt's lymphoma cells are usually negative for the EBV genome (Cohen and Levi-Montalcini 1956).

The following Burkitt's lymphoma cell lines were established at the International Agency for Research on Cancer in Lyon, France; BL41, BL41 with EBV and IARC-171. BL41 is an EBV negative B-Lymphoma cell line with *c-myc* translocations and p53 point mutations (Cohen and Levi-Montalcini 1956; Farrell, Allan et al. 1991).

Two sets of cell lines, BL41 and the MUTU series, displaying varying latency groups were used to compare EBV gene patterns to investigate the expression of varying survival factors. A summary of the cell lines used in this investigation is illustrated below within table 2.

Table 2.1: Burkitt's lymphoma cell lines used within the project

Cell lines	Latency stage	Cellular morphology
BL41	Latency I	Single small cells in suspension with no clumps and a "shiny" appearance under microscope Fast growth observed
BL41 + EBV	Latency III	Bigger size cells in suspension within clumps when compared to BL41 alone.
IARC 171	Latency III	Two morphologies: • Adherent cells are irregular in shape and have a granular appearance. • Cells in suspension form huge "cotton wool" like clumps with very few single floating cells. These cells grow slower than the other Burkitt's lines analysed.
MUTU Neg. Clone 1	N/A	Similar to BL41 and Mutu Lat I cells in appearance, single small cells in suspension.
MUTU Neg. Clone 3	N/A	

MUTU Neg. Clone 4	N/A	Sensitive to apoptosis.
MUTU Lat I Clone 59	Latency I	Similar to Mutu negatives in appearance, single small cells in suspension. Slightly less sensitive to apoptosis than Mutu negatives.
MUTU Lat I Clone 179	Latency I	
MUTU Lat III Clone K5	Latency III	Morphology similar to LCL cell line IARC-171, however the adherent cells were round. These cells also grow as slow as IARC-171 cells.
MUTU Lat III Clone J8	Latency III	

2.1.3 Neurotrophic factor expression positive control cell lines

When this investigation was started, there were limited accessible lines transfected with either neurotrophic factors or their receptors. Therefore to optimise all the reagents and methods used

within this project, cell lines published to express neurotrophic factors and/ or the receptors were obtained and utilised as positive controls.

Table 2.2: Neurotrophic factor positive control cell lines

Cell line	NT expression	Info.	Source/ Reference	Media
NT-2	NGF	NTera-2/D1 is a human teratocarcinoma, neural precursor cell line.	Shiao Chan's group (IBR, UK)	DMEM 10% FCS 2mM L-glut 100 U/ml penicillin 100ug/ml streptavidin
KMS-11	BDNF and TrKB	Multiple myeloma cell line.	(Pearse, Swendeman et al. 2005)	RPMI 10% FCS 2mM L-glut 100 U/ml penicillin 100ug/ml streptavidin
Kelly	TrkA, TrkB and $p75^{NTR}$	Kelly (ACC 355),) is a human neuroblastoma cell line that is predominantly neuroblastic (i.e. does not express a nonneuronal phenotype).	(Martens, Kirschner et al. 2007)	RPMI 10% FCS 2mM L-glut 100 U/ml penicillin 100ug/ml streptavidin
Colo-357	NT-3 and NT-4	Human pancreatic cancer cell line established from a celiac lymph node metastasis of well-differentiated, mucin-containing pancreatic cancer cells	Knut Ketterer (Morgan, Woods et al. 1980)	DMEM 7.5% FCS 2mM L-glut 100 U/ml penicillin 100ug/ml streptavidin
HMC-1	TrkC	Human mast cell leukaemia cell line.	(Tam, Tsai et al. 1997)	RPMI-1640

	10% FCS 2mM L-glut Penstrep.

2.1.4 Reagents used within the investigation

The antibodies, inhibitors, recombinant proteins used within this investigation are illustrated within table 2.3.

Add table 2.3 here

2.2 Measurement of gene expression by Semi-Quantitative Polymerase Chain Reaction

Invitrogen Ltd, Paisley, Scotland:

Oligo(dT) 12-18 Primers (18418-012)

10mM dNTPs Mix (18427-013)

Superscript II reverse transcriptase (18064-014)

100bp DNA ladder (15628-019)

RNase OUT ribonuclease inhibitor (10777-019)

DNAse I reagent (18068-015)

And TRIzol reagent (15596-026)

Qiagen Ltd, West Sussex, UK:

RNeasy mini kit (74104)

Applera, UK:

Amplitaq Gold (N808-0241)

Sigma:

Chloroform (C2432)

Ethanol (E7023)

β-mercaptoethanol (M7154)

Isopropyl alcohol (I9516)

TRIS Base

Boric Acid (B6768)

Injection water (W4502-1L)

Jump start *Taq* DNA Polymerase (D 4184)

Bioline:

Agarose (BIO-41025)

Fisher Scientific, UK, Ltd:

EDTA (BPE-152-1)

2.2.1 RNA extraction and purification

10^7 Cells were seeded during log phase 24hrs post feeding. Using TRIzol (Invitrogen) the RNA extraction procedure was followed according to the manufacturer's instructions. RNA pellets were re-dissolved in nuclease free DEPC- treated water (Ambion). RNA was then purified using an RNeasy Mini kit (Qiagen) according to the manufacturer's instructions. For the RNA concentration calculation, RNA was dissolved in DEPC water, measured using a UV/Vis Spectrophotometer (Jenway).

2.2.2 RT-PCR to obtain cDNA

Reverse Transcription - Polymerase Chain Reaction (RT-PCR) of purified RNA (2μg) was carried out using Invitrogen reagents in a 20μl reaction mix. 10μl of cell sample RNA diluted in injection water was added to 1μl Oligo(dT) 12-18 Primers and 1μl dNTPs. The reaction was heated for 5 minutes at

65°C. 7µl of RT-PCR mix was added. (RT-PCR Mix contains 5X PCR buffer, DTT OUT (0.1M), RNase OUT and injection water). This reaction was heated for 5 minutes at 50°C. 2µl of superscript was added to the RT-positive samples, whereas 2µl of injection water was added to the RT-negative samples. The reaction was left to amplify cDNA at 50°C for 50 minutes and then 70°C for 15 minutes. 30µl of water was added to obtain 50µl of cDNA. This cDNA was aliquoted and stored at -80°C.

2.2.3 RT-PCR experiments

Using specific primers of interest, RT-PCR was used to isolate and amplify known DNA sequences from cellular RNA samples. For each primer analysed the reaction mix was made up according to the concentration of Magnesium Chloride required. Within a 20µl PCR reaction mix, 2µl of cDNA was analysed for each MWG Biotech primer, the primers used are shown in table 2.4. AmpliTaq Gold DNA polymerase (5 units/ul), Magnesium Chloride solution (25mM) and 10x PCR Buffer II reagents were used to analyse all the primers of interest (Applied biosystems). AmpliTaq Gold is derived from a recombinant thermostable DNA polymerase encoded by the Thermus aquaticus DNA polymerase gene inserted within an Escherichia coli host (Lawyer, Stoffel et al. 1989). However the amplification efficiency (amplicon within an agarose gel) for the $p75^{NTR}$ primers were not efficient when using AmpliTaq Gold DNA polymerase, therefore JumpStart Taq DNA polymerase (2.5 units/ul) was used to analyse $p75^{NTR}$ primers. JumpStart Taq DNA polymerase is an antibody inactivated hot start enzyme that prevents non-specific amplification and increases target DNA yield (Sigma).

The following Hot start PCR reaction conditions were used; 95°C for 10 minutes for the initial initiation step, used to denature the DNA template and primers. The initiation step is used to

activate AmpliTaq Gold DNA polymerase which is provided in an inactive form. For the annealing step, various temperatures were used for each set of primers; these differences are due to different melting points. Primers are able to attach to single stranded DNA sequences at the annealing temperature. The temperature is then increased for the extension step to enable DNA synthesis of DNA strands complementary to the primer templates. As shown in table 2.4, the various extension times are due to different lengths of target DNA strands. The annealing and extension steps are then repeated depending on cycle numbers for each primer, followed by the final elongation step which ensures any remaining single stranded DNA is fully extended. The elongation step is the same for all the primers used reaction mixes were left at 72 ^{o}C for 10 minutes.

Add table 2.4 here

2.2.4 PCR product examination

PCR products were run on 1.5% agarose gels containing 0.6μg/ml ethidium bromide within 24 hours from the PCR amplification reaction. Gels were exposed under UV light using a SynGene Bio imaging system (Cambridge, UK). Gels were labelled and printed using Gene Snap software from SynGene, then saved as JPEG files.

2.3 Measurement of gene expression by Real Time Polymerase Chain Reaction

The same cDNA used for RT-PCR experiments was used within quantitative real time PCR (qRT-PCR). 5μl of cDNA was added within a 50μl PCR reaction containing taqman 30 ml tube PCR master Mix (Applied Biosystems) and optimised "house keeping" gene, β_2-Microglobulin (β_2M) primers and

probes, together with TrkB primers and probes in multiplex RT-PCR experiment. Triplicate reactions for each cell line were conducted within 96 well optical reaction plates (Applied Biosystems). FAM and VIC fluorescence was measured using an ABI prism detection 7900HT SDS machine.

Raw fluorescence values were obtained using the SDS v2.2 software. Once the base line was set for each experiment, relative TrkB fluorescence values were calculated from β_2M fluorescence for each cell line using excel spread sheets. This calculation was obtained by subtracting the β_2M levels from the TrkB fluorescence values. Positive increases in fluorescence were then plotted for each line.

2.4 Measurement of protein expression by Western blots

2.4.1 Whole cell extracts

Urea Buffer

9M	Urea
50mM	Tris pH 7.5

10^7 cells in log phase (24 hours post addition of fresh media to ensure cells are at log growth phase) were pelleted at 13,000g (8400 rpm) for 5 minutes. Pellets were resuspended and washed twice in 10mls of room temperature, sterile phosphate buffered saline (PBS). A final wash was completed within eppendorfs containing 1ml of room temperature PBS, spun at 13,000g. Pellets were flicked to

resuspend, 100µl of 9M Urea buffer was added to each pellet. Cells were vortexed, to mix and then placed on ice.

Each pellet was sonicated for 20 seconds, well sonicated pellets frothed at the top and were easily taken up into a p200 yellow Gilson pipette tip to ensure minimum viscosity. If pellets were larger, they were resonicated for a further 20 seconds with a 1 minute interval.

2.4.2 Quantifying protein concentration

Protein concentrations were measured using the Bio-Rad, Bradford assay (catalogue number 500-0006) (Bradford 1976). The acidic dye (Coomassie Brilliant blue G-250) binds to solubilised protein, the colour of the dye intensifies depending on the concentration of protein present. The samples were then measured at a wavelength of 595nm using a spectrophotometer.

When comparing this protein determination procedure with the Lowry method, variations in protein concentrations are observed. As seen below in table 3 the concentration of Bovine serum albumin (BSA) using the Bio-Rad method is double compared to the Lowry method. This information was obtained from the manufacturer's manual (Bio-Rad 2006).

Table 2.4 : Comparison of varying protein determination methods

		Assay Results (Protein mg/ml)		
		Biuret	Lowry	Bio-Rad
1.	Alcohol dehydrogenase	5.8	5.0	7.8
2.	α-Amylase	6.8	6.0	8.3
3.	Bovine serum albumin	9.7	8.4	21.1
4.	Carbonic anhydrase	8.8	8.9	13.0
5.	Catalase	7.6	6.3	9.7
6.	α-Chymotrypsin	9.4	11.6	7.8
7.	Cytochrome c*	25.7	11.3	25.3
8.	Ovalbumin	10.2	10.1	9.4
9.	Fibrinogen	6.2	7.3	7.8
10.	Gamma globulin (rabbit)	9.4	11.8	8.0
11.	β-Galactosidase	9.5	9.9	7.9
12.	Hemoglobin (bovine)*	16.2	8.3	19.9
13.	Histones	9.7	9.2	15.8
14.	Hemocyanin	6.6	5.4	9.2
15.	Lysozyme	10.4	12.6	9.9
16.	Myoglobin*	13.7	7.9	20.7
17.	Ovomucoid	7.8	8.3	5.9
18.	Pepsin	9.8	12.4	4.1
19.	Ribonuclease	11.8	15.9	5.3
20.	Trypsin inhibitor (soy)	9.1	10.3	6.1
21.	Transferrin	8.5	9.0	12.6
22.	Trypsin	11.4	15.5	4.9
23.	Thyroglobulin	7.7	8.2	9.3
Average		10.1	9.5	10.9
*Average		8.8	9.6	9.2

* The second average eliminates from the figures the values for the three colored proteins shown by asterisks.

BSA is of interest from this table since it was used to make up the protein concentration standards. Concentrations of 0.2, 0.4, 0.6, 0.8 and 1.0 mg/ml were made up in distilled water and frozen at -20^{o}C.

For each protein determination assay, distilled water was used a blank control to calibrate the spectrophotometer. The BSA standards were defrosted and measured in duplicates within disposable, 10mm Fisherbrand cuvettes to obtain a standard curve. The linear regression line and the R-squared (line of best fit) value was then calculated. Once duplicate values of the samples measured were entered onto an excel spread sheet the concentration of protein was then calculated using the example shown Illustration 2.1.

These calculations shown in Illustration 2.1 were used to work out amount of cell lysate protein and the amount in microliteres required to add to gel sample buffer, used for western blot analysis.

Illustration 2.1 goes here

2.4.3 Protein sample preparation

Gel sample buffer (2X)

0.4M	Sodium 2-mercaptoethanesulfonate (MESNA)
125 mM	Tris-HCl pH 6.8
20%	Glycerol
4%	SDS
0.004%	Bromophenol blue

The protein determination example shown in Illustration 2.1 shows an example calculation for BL41. The lysate was diluted 1 in 20 using distilled water. 980µl of the Bio-Rad dye reagent concentrate (diluted 1 in 5 using distilled water) was added to a 1 ml cuvette, this was completed in duplicate for more accurate readings. 20µl of diluted cell lysate/BSA standard was added and mixed using a pipette tip; the reaction was left for 15 minutes. The spectrophotometer was calibrated at 595nm using the blank sample (980µl of diluted Bio-Rad dye reagent with 20µl of distilled water). The BSA standard's optical density (OD) were measured in duplicate and used to plot the standard curve on an Excel spreadsheet. Both sets of the sample lysate (Abs 1 and 2) were measured and applied into the spreadsheet calculation shown in Illustration 2.1.

The mean value and protein concentration was calculated as shown in the red and orange boxes. For the protein concentration calculation the mean absorbance was divided by the value of the Y axis taken from the standard curve (Y=1.1043) multiplied by the dilution factor (20). (The X axis value was not taken into consideration since the value was very low).

Since BSA standards were used for the standard plot the protein concentration was divided in two due to the difference in the Bio-Rad assay and the Lowry assay as shown in table 2.4. This calculation is displayed within the yellow box.

To calculate the number of microlitres required to obtain 100μg of protein, 100 was divided by the protein calculation, as shown within the green box. Illustration 2.1 shows that 17.8μl of the BL41 cell lysate will contain 100μg of protein.

Therefore in order to dilute the lysate with gel sample buffer, 100μg of cell lysate is diluted to give a final volume of 50μl, an equal volume of gel sample buffer (2X stock) is then added. Glycerol is present within the sample buffer to help the protein sink to the bottom of the well within the staking gel. Bromophenol blue is the tracking dye added to follow the electrophoresis run. Gel sample buffer also contains MESNA which breaks down disulphide bonds and helps preserve the protein sample, ready to load into a western blot gel. MESNA is a non-smelly equivalent to Beta-2-mercaptanol. The final concentration of the lysate ready to load was 100μg in 100μl or 1μg in 1μl. 20μl of ready to load samples were used to load the NuPAGE Noxex gels. The loading samples were then stored at -20^{o}C.

2.4.4 Western blot analysis

Running buffers

TrisBase running buffer

MOPS buffer

Blotting Buffer

25 mM Tris-base

192 mM Glycine

20% Methanol

I-Block with Tween buffer (IBT blocking buffer)

0.4% Casein in PBS

0.05% Tween-20

0.02% NaN_3

The Invitrogen NuPAGE gel electrophoresis western blot technique was used within this project. Depending on the aims for each experiment different types of gels were used. NuPAGE Novex Bis-Tris gels, at 10% and gradient gels (4-12%) (MOPS) were used to analyse 50kDa to 10kDa protein, whereas 7% NuPAGE Novex Tris-Acetate gels were used to analyse 50kDa to 200kDa protein.

The gel electrophoresis apparatus was set up using an XCell SureLock Mini-Cell apparatus. To ensure an even distribution of volts thorough out the apparatus, running buffers containing SDS and glycine were used. Tris-Acetate SDS running buffer from InVitrogen was diluted 1 in 20 and used for Tris-Acetate gels, whereas MOPS SDS running buffer 1x was used for Bis-Tris gels. Ready to load lysate samples within gel sample buffer were heated at 100^{o}C for 5 minutes on a heat block. (Subsequent use of these lysates required heating at 80^{o}C after they are thawed from -20^{o}C to re-solubilise protein.) SDS within the sample buffer and the application of heat ensures di-sulphide bonds are broken down, disrupting secondary and tertiary peptide structures by applying a negative charge to the amino acids (Laemmli 1970).

As soon as the samples were heated and cooled for 5 minutes, 20µl of loading sample lysate was carefully pipetted into each well. Within either the first or last well, 20µl (diluted 15 to 25) of SeeBlue Plus2 Pre-Stained Standard molecular weights were added as markers to determine protein size. Table 2.5 shows the molecular weight markers for both types of gels used.

Table 2.5 : Chart indicating size for molecular weight markers on the gels used

Protein	Approximate Molecular Weights (kDa)				
	Tris-Glycine	Tricine	NuPAGE® MES	NuPAGE® MOPS	NuPAGE® Tris-Acetate
Myosin	250	210	188	191	210
Phosphorylase	148	105	98	97	111
BSA	98	78	62	64	71
Glutamic Dehydrogenase	64	55	49	51	55
Alcohol Dehydrogenase	50	45	38	39	41
Carbonic Anhydrase	36	34	28	28	n/a
Myoglobin Red	22	17	17	19	n/a
Lysozyme	16	16	14	14	n/a
Aprotinin	6	7	6	n/a	n/a
Insulin, B Chain	4	4	3	n/a	n/a

NuPAGE® Novex
Bis-Tris 4-12% Gel

This chart was used to mark the correct molecular weight sizes in kDa for each western blot (Invitrogen 2002).

Bis-Tris gels were run at 200Volts for 50 minutes whereas Tris-Acetate gels were run 160Volts for 1 hour.

One Invitrogen polyvinylidene difluoride PVDF membrane was pre-soaked in methanol for 10 seconds; this step was required since PVDF membranes are hydrophobic. Membranes were then

soaked in blotting buffer together with two filter paper sheets for at least 5 minutes to ensure the complete surface was wet for the transfer step. Protein was then transferred from the gel to the PVDF membrane by applying 30Volts (250 milliamps) for 1 hour 20 minutes when using a Bis-Tris gel, and 35Volts (250 milliamps) for 1 hour 30 minutes when using a Tris-Actetate gel. In each case the voltage remained constant throughout the transfer therefore the milliamps were set higher than the amount required. The blots were aligned to ensure protein within the gel moved from the negatively charged cathode core towards the positively charged anode onto the PVDF membrane. To ensure efficient transfer, blotting pads were also soaked in blotting buffer to ensure a steady current is able to move through the gel (Towbin, Staehelin et al. 1979).

Once the transfer was completed, blots were labelled and soaked in I-Block (Applied Biosystems Inc) with Tween (IBT) buffer for 1 hour at room temperature or at 4^{o}C overnight to block excess binding sites on the PVDF membrane.

2.4.5 Primary and secondary antibodies

Phosphate buffered saline with Tween (PBST)

58mM Na_2HPO_4

17mM $NaH_2PO_4.H_2O$ } Pre-mixed tablets

68mM NaCl

0.1% Tween-20

Primary antibodies were diluted at varying concentrations (see experimental reagents table 2.3) within in IBT and stored at 2^{o}C. The number of times each diluted antibody mix was used to probe a PVDF membrane was recorded then discarded once it had been used 10 times.

Membranes were probed for 2 to 4 hours at room temperature or at 4^{o}C over night. The primary antibody was replaced within the 30 ml tube to be re-used and the blots were washed with Phosphate buffered saline with Tween (PBS-T) to remove excess primary antibodies from the membrane for 30 minutes. The appropriate secondary antibody was selected to match the host species of the primary antibody. Table 2.6 lists the alkaline phosphatase secondary antibodies used and their dilutions.

Table 2.6 : Working concentrations of alkaline phosphatase conjugated secondary antibodies used for western blotting

Secondary Antibodies in IBT	Source and Catalogue number	Final working dilution
AP-anti-mouse IgG	BioRad 170-6520	1/10,000
AP-anti-rabbit IgG	BioRad 170-6518	1/10,000
AP-anti-goat IgG	Sigma A4062	1/40,000

10ml of secondary antibody was made up and probed for 30 minutes at room temperature, then discarded after first use.

2.4.6 Exposure of bands on film

Alkaline Phosphatase assay buffer (10X)

0.1M Diethanolamine pH 9.5

1mM $MgCl_2$

To ensure excess secondary antibodies were efficiently washed off the membranes, blots were washed for at least an hour with five PBS-T changes. The container with which the membrane was being washed in was changed after the first wash cycle to ensure a complete removal of secondary antibodies off the membrane. The blot was then soaked in 10mls of 1x Alkaline Phosphatase assay buffer for 2 minutes twice. 800µl CDP-star chemiluminescent substrate was left to soak on the

membrane for 15 minutes within a plastic sleeve. The developer was spread across the membrane to ensure and even layer of developer across the surface of the blot.

Excess developer was squeezed out from the plastic sleeve and dried to prevent drops of developer reacting with the film (Amersham chemiluminescence film). Each blot was taped onto the cassette which was wiped with tissue to ensure a completely dry surface. Initially blots were exposed for 2 minutes. Depending on the strength of the antibody and how long the membrane was probed for, film exposure times were either increased or decreased to produce clear bands on the film within the expected molecular weight. The blots showing the best exposure times were scanned and saved for analysis.

Once the films were scanned and the results were obtained, excess CDP-star chemiluminescent substrate was washed off the blot twice, using 30mls of PBS-T. 10mls of PBS-T was then added to a plastic sleeve containing the blot; this was then sealed and stored at 4^{o}C.

2.4.7 Stripping Blots for reprobing

Sodium Dodecyl Sulfate (SDS) wash buffer

62.5 mM Tris-HCl pH 6.8

2% SDS

Stripping buffer

50 mM sodium 2-mercaptoethasulfonate (MESNA)

62.5 mM Tris-HCl pH 6.8

2% SDS

Once a membrane had been probed with a primary and secondary antibody, it was either stored at 4^{o}C within 10mls of PBS-T or stripped to re-probe with other primary antibodies. The advantage of this method allows direct comparison of varying antibodies corresponding to different epitopes of different molecular weights within one blot.

Blots were removed from the PBS-T wash and placed in a fresh plastic sleeve. 15mls of pre-heated stripping buffer was added to the blot which was sealed and added within a water bath set at 55^{o}C. Blots were heated for 15 minutes; then temporarily removed and shaken to ensure an even distribution of stripping buffer over the entire membrane surface. Blots were then quickly returned to the 55^{o}C water bath and left for another 15 minutes.

MESNA was washed off the blots with 30mls of SDS wash buffer (NB; MESNA is a non-smelly and more stable alternative to β-mercaptoethanol). Blots were then washed three times in 30mls of PBS-T for 10 minutes each. The blot was blocked with IBT blocking buffer for one hour at room temperature or over night at 4^{o}C. The blot was then ready to be re-probed with a primary antibody. It is worth noting that this method is an efficient process and will produce clear blots, however the blots become less clear if stripped and re-probed 5 times or more.

2.5 Measurement of protein expression by Flow cytometry

FACS buffer

500ml	PBS
25ml	Goat Serum Donor Herd
5 ml	10% Sodium Azide

Fix Buffer- 2% Paraformaldehyde

500µl	Paraformaldehyde (37 wt. % in solution)
9.5ml	Distilled water

Permeabilization buffer

0.01g	Saponin
10mls	PBS

Flow cytometry is a method used to measure the size, shape of cells and to identify specific surface or intracellular molecules from a suspension of live cells travelling though a laser. Within this investigation FACSCalibur, a Becton Dickinson Immunocytometry Systems modular bench top flow cytometry was used to analyse live cells stained for specific surface markers.

For each FACS experiment each cell line used was analysed using three different variables. Each cell line was divided into three FACS tubes for analysis. Cells within the "Cells Alone" tube were treated with 50µl of FACS buffer alone, used as a negative staining control to draw a dot plot of viable cells (no antibodies present). Cells within the "Negative antibody (irrelevant antibody) and secondary antibody" tubes are cells treated with an appropriate negative control antibody depending on the

immunoblobulin class of the primary antibody. And finally cells within the "Primary and secondary antibody" tubes contain the target antibody which will bind to the surface protein being studied; the appropriate secondary antibody will then allow fluorescence of this surface protein. Table 2.7 is a summary illustrating these experimental variables.

Table 2.7: Experimental set up for FACS analysis

Experimental variables	Staining stage 1 (50μl)	Staining stage 2 (50μl)	Expected results
"Cells alone"	FACS Buffer	FACS Buffer	Negative
"Negative antibody with secondary antibody"	Negative antibody diluted in FACS Buffer	Secondary antibody diluted in FACS Buffer	Negative

"Primary antibody and secondary antibody"	Primary antibody diluted in FACS Buffer	Secondary antibody diluted in FACS Buffer	Positive

2.5.1 Flow cytometry – Surface staining

24 hours post feeding, the number of mls required to obtain 2.5 million cells was calculated for each cell line. Cells were spun down at 13,000g (8400 RPM) for 5 minutes and washed twice in 10ml of PBS to remove excess FCS protein. 3 mls of FACS buffer was added to the pelleted to resuspend the cells. 1 ml of each cell line was aliquoted into three labelled FACS tubes (5ml polystyrene round bottom falcon tubes). A p1000 Gilson pipette was used to accurately aliquot 1ml, containing 500,000 cells into each tube. These tubes were then spun to pellet the cells enabling them to stick to the tube surface; excess FACS buffer was then aspirated.

Within the first stage of the staining method, antibodies were diluted in FACS buffer; 50µl was then aliquoted to the correctly labelled tubes. As shown in table 2.7 one set of cells were used as a "cells alone" negative control, 50µl of FACS buffer alone was added to these cells. The appropriate antibodies (negative control and primary antibodies being tested) were applied to the other tubes within the experiment. Cells were then left on ice for 45 minutes; cells were then washed within 4mls of FACS buffer.

For the second staining stage, cells were incubated in 50µl of FACS buffer with FITC conjugated secondary antibody; no secondary antibody was added to the cells alone control. The secondary antibody was left to react with the cells on ice whilst covered in foil to remove external light during the 45 minute incubation time. Cells were then washed in 4mls of FACS buffer and fixed using 500µl of FACS FIX buffer to fix the cell membranes. FACS tubes were then stored at 4^{o}C wrapped in foil. Although cells could have been kept and measured seven days post staining, all the FACS analysis experiments results were recorded 24hrs (at the most) post staining.

2.5.2 Flow cytometry – Intracellular staining

24 hours post feeding, the number of mls required to obtain 1.5 million cells was calculated for each cell line. Cells were spun down at 13,000g (8400 RPM) for 5 minutes and washed twice in 10ml of PBS to remove excess FCS protein. Within the 30 ml tube, cells were then treated with 150µl of 2% paraformaldehyde for 5 minutes, to fix the cellular plasma membrane. Cells were then washed in cold PBS, and treated on ice for 5 minutes with 750µl of 0.1% saponin which form pores on their plasma membranes. After a wash step in 10mls of 0.1% saponin cells were then left on ice for 5 minutes in 150µl of neat FCS (the same serum used in cell culture "L3 serum"). Serum was washed off the cells with another 10ml 0.1% saponin wash. 3 mls of 0.1 saponin was added to each 30 ml tube. 1 ml of each cell line was aliquoted into three labelled FACS tubes. A p1000 Gilson pipette was used to accurately aliquot 1ml, containing 500,000 cells into each tube. These tubes were then spun to pellet the cells enabling them to stick to the tube surface.

For the first stage of the staining method, negative control and antibodies of interest were diluted in 0.1% saponin; no antibody was added in the cells alone negative control. 50μl was then aliquoted to the appropriate labelled tubes which were then left on ice for 45 minutes. Cells were then washed within 4mls of 0.1% saponin.

As for the second staining stage, cells were incubated in 50μl of 0.1% saponin with FITC conjugated secondary antibody; no secondary antibody was added to the cells alone control. Cells were treated on ice whilst covered in foil to remove external light during the 45 minute incubation time. For the final wash step cells were then washed in 4mls of FACS buffer, the new goats serum within FACS buffer is used to re-seal the cellular plasma membranes. These cells were then fixed using 500μl of FACS FIX buffer to fix the cell membranes.

2.5.3 Flow cytometry Results Analysis - FlowJo

Staining results was analysed using the FACSCalibur flow cytometer. Dot plots of side scatter and forward scatter light emissions were recorded using Cell Quest Pro software. Green fluorescence (FITC-1 staining) was recorded for each variable within each cell line and saved for analysis.

FlowJo software (Version 6.3.2) was used to analyse dot plots for each experimental variable. Viable cells within the cells alone dot plot were gated and used to directly compare and analyse the various antibody combinations. Histograms were drawn to observe any possible shifts in fluorescence to compare appropriate negative control with the primary antibodies.

2.6 Measurement of protein expression by Confocal Microscopy

DABCO

90% Glycerol

10% PBS

2.5g/100ml DABCO (Sigma D2522)

Confocal microscopy was used to view fixed and fluorescently stained protein in cells. Cells were mounted on glass slides, their images were viewed and captured by a Zeiss Axiovert 100M microscope. The LSM 510 software was used to analyse the fluorescent images.

10^6 cells at log growth phase and at a viable count of 80% or more were counted and washed in PBS at room temperature. Pelleted cells were then fixed in 100μl of 2% Paraformaldehybe for 10 min on ice. Once washed in cold PBS, cells were incubated in 1ml 0.1% saponin at room temperature for 5 min, and then washed in 10ml 0.1% saponin. Next, cells were either stained for target protein or F-actin.

To stain for target protein, permeabilized cells were then incubated with primary antibody diluted in cold 50μl 0.1% saponin within FACS tubes for 1hr on ice. Cells were then washed twice in 2mls of cold 0.1% saponin and incubated with the isotype specific fluorescently conjugated secondary antibody diluted in 50 μl cold 0.1% saponin for 30 minutes on ice. At this step, cells were incubated within a dark container to maintain the fluorescence of the light sensitive secondary conjugates. The secondary antibodies applied for confocal analyses are illustrated within the table below.

Table 2.8: Working concentrations of secondary antibodies used for confocal analysis

Secondary Antibodies in IBT	Source and Catalogue number	Working Conc.
Donkey anti-Goat IgG FITC	Santa Cruz – SC2024	5μg/ml
Goat anti-Mouse IgG (H&L) TRITC	SouthernBiotech - 1031-03	1μg/ml
Goat anti-Mouse IgG2a TRITC	SouthernBiotech - 1080-03	1μg/ml
Goat anti-Mouse IgG1 FITC	SouthernBiotech - 1072-02	5μg/ml
Alexa Fluor 633 Goat anti-Mouse IgM	Invitrogen - A-21046	2μg/ml
Alexa Fluor® 488 Goat anti-Rabbit IgG (H&L)	Invitrogen - A-11008	5μg/ml
Alexa Fluor 488Goat anti-Mouse IgG (H&L)	Invitrogen - A-11001	2.5μg/ml

Cells were then washed in cold 0.1% saponin. To stain for F-actin re-arrangement cells were stained with 250ng/ml phalloidin conjugated with TRITC (Sigma - 77418) for 30 minutes on ice and within a dark container. Cells were then washed in cold 0.1% saponin.

For nuclear staining, cells were incubated with 10μg/ml DAPI diluted in 50μL of cold 0.1% saponin at room temperature for 5 minutes.

Multispot glass slides were washed initially in 500μl of 100% ethanol and rinsed four times in 20mls of distilled water. Slides were air dried before use.

To seal membranes, cells were washed in cold PBS and resuspended in 2mls PBS. 100ul of cells were added per spot, then left to air dry in the dark. Once dry, 20μl of DABCO was added per spot to

prevent fluorophores fading. Cover slips were added on top and sealed with clear nail polish at the edges of the slide.

Prior to viewing slides were kept wrapped in foil at 4^{o}C. All slides were viewed and captured within 24 hours of staining using a Zeiss Axiovert 100M microscope.

2.7 Enzyme-linked immunosorbent assay

Two Enzyme-linked immunosorbent assay (ELISA) kits were used within this investigation. One kit was used to measure BDNF protein and was obtained from Chemicon (Cat. Number CYT306). The second kit, used to measure NGF protein was obtained from Signosis (Cat. Number EA0406).

2.7.1 Intracellular and extracellular BDNF ELISA kit – Sample preparation and incubation

<u>Homogenization buffer</u>

100mM Tris HCl, pH7

2% BSA

1M NaCl

4mM EDTA.Na^{2}

2% Triton X-100

0.1% Sodium Azide

5μg/ml Aproptinin

157μg/ml Benzamide

17μg/ml PMSF- Calpain inhibitor

To prepare test samples, 10^6 cells were pelleted from media. Supernatant was used to analysed extracellular BDNF whereas cell pellets was lysed in 100ul of pre chilled homogenisation buffer to analyse intracellular BDNF protein. Cells were pippeted to break their membranes and left at 4^oC for 30 minutes. Cells were then centrifuged for 30 minutes at 4^0C. This supernatant was used to assess intracellular BDNF protein.

To prepare BDNF standards, manufactures' instructions were followed. Serial dilutions of Human recombinant BDNF standard controls were performed, producing the following concentrations, 0pg/ml (diluent alone), 7.82pg/ml, 15.63pg/ml, 31.25pg/ml, 62.5pg/ml, 125pg/ml, 250pg/ml and 500pg/ml.

100μl of duplicate BDNF standard controls were added to the 96 well immunoplate pre-coated with rabbit anti-human BDNF polyclonal antibody. 100μl of duplicate cell lysate samples were also added to the pre-coated 96 well plate and left to incubate overnight at 4^oC.

The wells were then washed and incubated with 100μl biotinylated mouse anti-BDNF monoclonal antibody for 3 hours at room temperature. Wells were washed then treated with streptavidin-HRP conjugate solution at room temperature for 1 hour within a dark container. Once washed 100μl of TMB/E substrate was added (producing a blue colour) to incubate for 15 minutes within a dark container. The reaction was stopped by adding 100μl of stop solution (producing a yellow colour).

2.7.2 Intracellular and extracellular NGF ELISA kit – Sample preparation and incubation

Like the BDNF cell lysate sample preparation, 10^6 cells were pelleted from media. Cell culture supernatant was used to analyse extracellular NGF and 100μl of homogenized cell lysates were used to analyse intracellular NGF protein.

To prepare NGF standards, manufactures' instructions were followed. Serial dilutions of Human recombinant βNGF standard controls were performed, producing the following concentrations, 0pg/ml (diluent alone), 15.63pg/ml, 31.25pg/ml, 62.5pg/ml, 125pg/ml, 250pg/ml, 500pg/ml and 1000pg/ml.

100μl of duplicate βNGF standard controls were added to the 96 well immunoplate pre-coated with rabbit anti-human NGF antibody. 100μl of duplicate cell lysate samples were also added to the pre-coated 96 well plate and at room temperature for 1 hour.

The wells were then washed and incubated with 100μl biotinylated rabbit anti-NGF antibody for 1 hour at room temperature. Wells were washed then treated with streptavidin-HRP conjugate solution at room temperature for 45 minutes within a dark container. Once washed 100μl of TMB substrate was added (producing a blue colour) to incubate for 30 minutes within a dark container. The reaction was stopped by adding 50μl of stop solution (producing a yellow colour).

2.7.3 Optical density readings for ELISA plates

ELISA plates were read using a Molecular devises E-Max precision micropate reader at a wavelength of 450nM ("λ1 only" settings). Soft MaxPro v311 was the software used to analyse the readings, which were then transferred to Microsoft excel for further analysis.

2.8 Assessment of DNA synthesis by thymidine incorporation

The rate of cell division was obtained by treating cells with varying reagents then exposed to thymidine ([^{3}H]Thy) (Amersham International). [^{3}H]Thy is incorporated by proliferating cells during S-phase DNA synthesis. 96 well flat bottomed microculture (Nunc) plates were used to culture 200μl

of quadruplet cell samples at densities and for varying periods of time. Burkitt's lymphoma B cells were then pulsed with 50μl of [^{3}H]Thy during the last 4 hours of culture, whereas germinal centre B cells were pulsed during the last 12 hours of culture.

Cells were then harvest onto filter mats (Cox Scientific) using a Skatron cell harvester model 11051 (Helis Bio Ltd, Newmarket, UK). Radioactivity, per well, was measured samples using a liquid scintillaton counter (Betaplate) over 60 seconds. Mean counts per minutes were calculated for quadruplicate wells and results expressed as mean thymidine incorporation counts per cell sample.

2.9 Assessment of lymphocyte cell division using CFSE dye

Carboxyfluorescein succinimidyl ester (CFSE) is a membrane permeable, fluorescently labelled dye used to stain live cells in order to track proliferation rate which diminishes over time due to the progressive halving of CFSE fluorescence within daughter cells following each cell division (Lyons and Parish 1994).

10^7 cells were washed twice in 10mls PBS and the pellet resuspended in 1ml 5μM CFSE. Cells were then incubated for 10 minutes at room temperature on a gentle shaker. 1ml of culture media with 10% FCS was added to quench the labelling reaction. Cells were then washed twice in 20mls PBS and resuspended in culture media. 100μl per well of $2x10^5$ cells/ ml cells were then treated with varying reagents diluted in 10% Culture media on 96 well plates for 48 hours.

The total volume (200μl) of cells was then added to polystyrene FACS tubes containing 100μl of PBS. 10,000 cells were acquired and the CFSE fluorescence levels were measured using a FACSCalibur flow cytometer. CFSE levels were analysed for each treatment and compared to control treated cells using FlowJo software.

2.10 Assessment of cell viability by propidium iodide stain

Propidium Iodide (PI) is a fluorescent compound that binds to non-viable cells. Upon treatment with varying reagents and for varying time points, quadruplicate cell samples cultured within 96 well plates ($2x10^5$ cells/ ml), were pooled into polystyrene FACS tubes and washed in 2mls of PBS at room temperature. Cells were then kept on ice until use. 4μl of 100μg/ml PI was added per FACS tube then immediately analysed using a flow cytometry Becton Dickinson FACScalibur for intensity in PI staining using FL-2 lasers. 10,000 cells were measured for each sample and analysed using FlowJo software v2.2.

2.11 Assessment of cell viability by propidium iodide co-stained with Phiphilux

To measure viable, early apoptotic, late apoptotic and necrotic cells treated with varying reagents, quadruplicate cell samples cultured within 96 well plates ($2x10^5$ cells/ ml), were pooled into polystyrene FACS tubes and washed in 2mls of PBS at room temperature. 30μl of the caspase substrate Phiphilux-G_1D_2 (OncoImmunin, Inc. – A304RIG) was added per cell pellet (PhiPhilux fluorescence intensity increases when it is cleaved by active caspases). Centrifugation speeds and times were followed from according to the manufactures instructions. Tubes were incubated within a dark 37^{o}C tissue culture incubator for 1 hour. Once washed in 2mls of cold PBS cells were gently resuspended in 350μl of flow cytometry buffer (provided within the kit) and kept on ice, wrapped in foil. Immediately before running each sample, 4μl of 100μg/ml PI was added per FACS tube and analysed using the flow cytometry Becton Dickinson FACScalibur. 10,000 cells were collected to measure the intensity of Phiphilux fluorescence using FL-1 lasers, and PI fluorescence using FL-3 lasers.

This dual staining is then analysed using FlowJo software. Cells populations were distributed into PI low/ Caspase low (viable), PI low/ Caspase high (early apoptotic), PI high/ Caspase high (late apoptotic) and PI high/ Caspase low (necrotic) populations.

2.12 Human tonsil sections and Germinal centre B cell isolation

2.12.1 Human tonsil tissue section preparation and staining

Human tonsil, obtained from a young adult at routine tonsillectomy was sliced into 5mm thick sections. These sections were then wrapped in aluminium foil, snap-frozen in liquid Nitrogen, and stored at –70°C in grip-sealed polythene bags until use. The frozen tonsil sections were embedded in OCT compound (Miles, Inc., Elkhart, IN) and 5μm cryostat sections were mounted onto 4-spot glass slides. These were air dried for 1 h, then fixed in acetone at 4°C for 20minutes, dried, and stored in sealed polythene bags at –80°C.

When used for staining, sections were left to thaw at room temperature for 15 minutes, then washed in a gently stirred PBS bath for 10 minutes. Sections were then stained with 100μl of diluted primary antibody, over night at 4^{o}C within a damp sealed container.

Excess primary antibody was then carefully tipped off the sections which were washed for 10 minutes in a PBS bath. Secondary antibodies used for confocal staining are illustrated below.

100μl of diluted secondary antibodies were added per tissue section at left in a dark, damp sealed container for 3 minutes at room temperature. Excess secondary antibody was then carefully tipped

off the sections that were washed for 10 minutes in a PBS bath protected from light to preserve the conjugated fluorescence.

Immunofluorescencent images were viewed using a Zeiss Axiovert 100M microscope. Images were then analysed using LSM v510 software.

2.12.2 Isolation of germinal centre cells

Human tonsils, obtained from young adults at routine tonsillectomy were finely minced in RPMI 1640 media without any additional supplements. The cell suspension was subjected to two rounds of T cell depletion using 2% 2-aminoethyl-isothiouronium bromide-treated sheep red blood cells (TCS Microbiology, Botolph Claydon, UK– SB068). B cells were then isolated by centrifugation through a 60% Percoll gradient (Pharmacia, Uppsala, Sweden). Cells were then incubated with four primary mouse antibodies, 2.5μg/ml anti-IgD polyclonal mouse monoclonal antibody (Sigma – HJ9), 10μg/ml anti-CD39 (AC2), 1/100 anti CD14 (61D3) and anti 10μg/ml anti-CD3 antibody (OKT3) for 30 minutes at 4^{o}C. Once washed twice in RPMI 1640 media cells were resuspended in 1ml PDS containing 1% BSA. Sheep anti Mouse IgG dynabeads were added to bind to the four primary mouse antibodies, for 30 minutes at 4^{o}C. A 4 to 1 ratio of beads to total cell numbers were added to ensure high purity levels of germinal centre B cells depletion. Germinal centre B cells (IgD-ve, CD39-ve, CD3-ve and CD14-ve) were isolated from five rounds of magnetic separation and kept on ice prior to use.

2.12.3 Phenotyping tonsillar germinal centre B cells

Cell surface staining was competed to phenotype freshly isolated germinal centre B cells. 10^5 cells were added to polystyrene FACS tubes and washed in 2ml cold PBS. Cells were gently resuspened in 50µl and dual-stained for 7µg/ml RPE conjugated anti-CD3 (Dako – R0810) and 4µg/ml FITC conjugated anti-CD19 (Dako – F0768) as well as 4µg/ml PE conjugated anti-CD38 (Phamigen - 31015) and 1µg/ml FITC conjugated anti-IgD (Dako – F0059). Cells were stained for 30 minutes on ice then washed in 2mls of cold PBS. Cells were resuspeded in 350µl of FACS buffer. 10,000 cells were collected to measure the intensity of FITC fluorescence using FL-1 lasers, and RPE or PE fluorescence using FL-3 lasers. Data was analysed using FlowJo software.

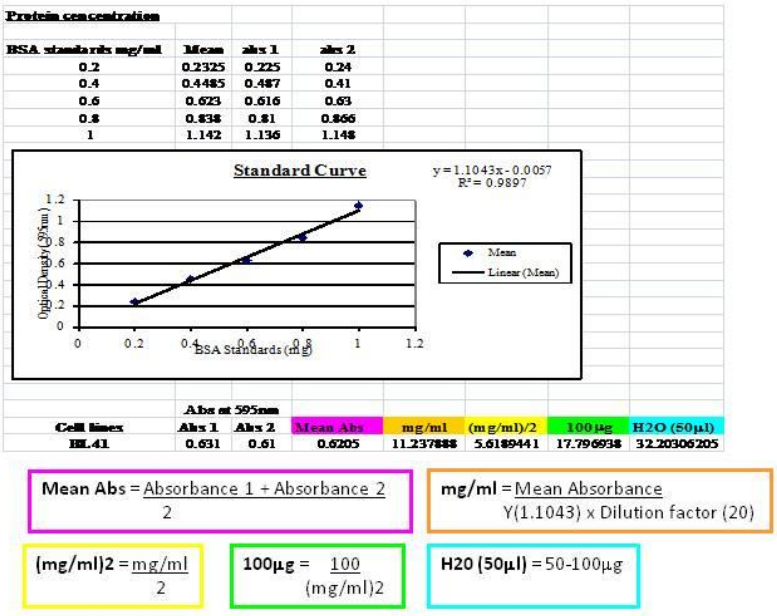

Illustration 2.1: Excel spreadsheet displaying the method of determining protein concentration using OD readings from the Spectrophotometer.

An example of an excel spreadsheet showing equations used to work out protein concentrations values in BL41 cells

Key: Bovine serum albumin (BSA), Absorbance (Abs)

Table 2.3 Antibodies, inhibitors and recombinant protein used within the investigation

Reagents	Company/ Collaboration	Application and Working Concentration
Neurotrophin Antibodies		
NGF (N3279) Mouse monoclonal IgG1 Clone 25623.1	Sigma	Neutralisation (20μg/ml), Immunofluorescence (15μg/ml), Flow cytometry (5μg/ml)
NGF(AF256NA) Goat IgG	R&D	Immunofluorescence (10μg/ml), Immunoblotting (5μg/ml).
BDNF (GF35L) Mouse monoclonal IgG1 clone 35928.11	Calbiochem	Neutralisation (10μg/ml), Immunoblotting (15μg/ml), Flow cytometry (4μg/ml)
NT-4 (Ab9824) Goat polyclonal	Abcam	Neutralisation (10μg/ml), Immunoblotting (5ng/ml), Flow cytometry (1μg/ml)
Neurotrophin Receptor Antibodies		
TrkA (AF175) Goat IgG	R&D	Immunofluorescence (10μg/ml)
Phospho-TrkA-Y490 (4619) Rabbit monoclonal IgG	Cell Signaling	Immunoblotting (2μg/ml)
TrkB (794) SC-12 Rabbit polyclonal affinity purified	Santa Cruz Biotech.	Immunofluorescence (4μg/ml), Immunoblotting(1μg/ml)
TrkB (H-181) SC-8316 Rabbit polyclonal	Santa Cruz Biotech.	Immunofluorescence (4μg/ml), Immunoblotting(1μg/ml)
Phospho-TrkB-Y705 (Ab52191)	Abcam	Immunoblotting(2μg/ml)
$p75^{NTR}$ – MLR2 and MLR3 Mouse monoclonal IgG2a	Robert R.Rush (2006;158-109) Flinders University, Australia	Neutralisation (100μg/ml), Immunofluorescence(11μg/ml), Flow cytometry (2.5μg/ml)
$p75^{NTR}$ –9992 Rabbit polyclonal	M.V. Chao NYU Langone Medical Center, New York, USA	Immunoblotting (1μg/ml),

Reagents	Company/ Collaboration	Application and Working Concentration
Trk Inhibitors		
K252a (K1639)	Sigma	TrkA and TrkB inhibition (50nM to 10μM)
TrkAd5	David Dawbarn University of Bristol, UK	TrkA inhibition (1μM to 25μM)
TrkBd5		TrkB inhibition (1μM to 25μM)
GW441756-Hydrochloride (G3420)	Sigma	TrkA inhibition (1nM to 100μM)
Erk and Akt inhibitors		
PD98059 (9900)	Cell signaling	Erk inhibition (1μM to 200μM)
LY294002 (9901)	Cell signaling	Akt/ PI3K inhibition (1μM to 200μM)

Reagents	Company/ Collaboration	Application and Working Concentration
Recombinant Protein		
Human recombinant β-NGF (256-GF)	R&D	NGF bioassay, treatment (100ng/ml or otherwise stated)
Human recombinant BDNF (11343375)	ImmunoTools	Treatment (50ng/ml or otherwise stated)
Human recombinant NT-4 (268-N4)	R&D	Treatment (50ng/ml or otherwise stated)
Human recombinant ProBDNF	Vincent Ellis , University of East Anglia, Norwich, UK	Treatment (50ng/ml)

Reagents	Company/ Collaboration	Application and Working Concentration
Erk and Akt Antibodies		
Erk1/2 p44/42 MAPK Rabbit monoclonal IgG (9102)	Cell Signaling	Immunofluorescence (0.4µg/ml), Immunoblotting (0.5µg/ml), Flow cytometry (0.4µg/ml)
Phospho-Erk1/2 p44/42 MAPK Thr202/Tyr204. Rabbit monoclonal IgG (4370)	Cell Signaling	Immunofluorescence (1µg/ml), Immunoblotting(0.1µg/ml), Flow cytometry (2µg/ml)
Akt Rabbit polyclonal IgG (9272)	Cell Signaling	Immunofluorescence (1µg/ml), Immunoblotting(0.1µg/ml), Flow cytometry (1µg/ml)
Phospho-Akt Ser473. Rabbit IgG (9271)	Cell Signaling	Immunofluorescence (0.4µg/ml), Immunoblotting(0.1µg/ml), Flow cytometry (0.4µg/ml)

Table 2.4 Primer sequences and PCR conditions

Primers	Forward sequence	Reverse sequence	Initial Initiation temperature and time		Initiation temperature and time		Annealing temperature and time		Cycle Nos	Extension temperature and time		Reference
			°C	Min	°C	Min	°C	Min		°C	Min	
β-Actin	5'CAGGGTACATGGTGGTGCC3'	5'AGCGGGAAATCGTGCGTG3'	95	10	95	0.30	55	0.30	26	72	1	Designed by Liz Meredith
TrkA	5'CAATACTTCAGTGATGCCTGTGTTC3'	5'AGCCTCACGCTGGAAGTCCT3'	95	10	95	1	62	0.30	35	72	2	Designed by Liz Meredith
Pan-TrkB	5'CCCACTCACATGAACAATGG3'	5'TCAGTGACGTCTGTGGAAGG3'	95	10	95	1	60	0.30	35	72	0.30	(Nassenstein et al., 2006)
TrkB Variants A&C	5'AGGGCAACCCGCCCACGGAA3'	5'GGATCGGTCTGGGGAAAAG3'	95	10	94	1	62	1	36	72	1	(Pearse et al., 2005)
TrkC	5'GGAGTCCAAGATCATCCATGTGGA3'	5'CATTCCAAATTTGGACCGTCGACC3'	95	10	95	1	55	0.30	35	72	2	(Besser and Wank, 1999)
$p75^{NTR}$	5'TACATAGCCTTCAAGAGGTGGAACA3'	5'AAGCTTCTCCACCTCCTCCC3'	95	10	95	1	62	1	35	72	2	Designed by Liz Meredith
BDNF	5'AACAATAAGGACGCAGACTT3'	5'TGCAGTCTTTTTGTCTGCCG3'	95	10	94	1	62	1	36	72	1	(Pearse et al., 2005)
NGF	5'CAGGACTCACAGGAGCAAGC3'	5'GCCTTCCTGCTGAGCACACA3'	95	10	94	0.30	60	0.30	32	72	0.30	(Iannone et al., 2002)
NT-3	5'GTATCTCATGGAGGATTACGTGGG3'	5'TGTTCTCTGAAGTCAGTGCTCGGA3'	95	10	94	1	55	0.30	36	72	0.30	(Besser and Wank, 1999)
NT-4	5'CAGTACTTCTTTGAAACCCGCTGC3'	5'GACGCAGGCAGTGTCAATTCGA3'	95	10	95	1	65	0.30	36	72	2	Designed by Liz Meredith

3. Results

Characterisation of Burkitt's lymphoma B cells and their expression of neurotrophic factor mRNA transcripts

3.1 Introduction

Nearly all African Burkitt's lymphoma patient tumours are EBV positive. Increasing evidence for the involvement of EBV in Burkitt's lymphoma pathogenesis has been provided, questioning how the virus controls its host via the expression of latency genes. In order to efficiently investigate these viral-cellular interactions model Burkitt's lymohoma cell lines have been established to yield clues to the understanding of EBV. Two main patterns of EBV gene expression are observed. Freshly isolated and cultured Burkitt's lymphoma cells from tumour display only one EBV latent gene, EBNA1 (Rowe, Rowe et al. 1987). This EBV gene expression phenotype is described to have latency I characteristic. However, in vitro infection of primary resting B cells with EBV produces an EBV transformed lymphoblastoid cell line (LCL) which displayed all six EBNA latent proteins and three Latent membrane proteins. These LCLs are described to have a latency III phenotype. LCLs are a good model for the study of uncontrolled proliferation as that observed in Burkitt's lymphoma tissues and other EBV associated malignancies, particularly in immunosupresed patients with post-transplant proliferative diseases.

Considering *c-myc* translocations coincide with cell death, it is possible that the main function for EBV gene expression is to oppose these apoptotic effects enabling Burkitt's lymphoma pathogenesis. Examples of this include EBV proteins such as EBNA and BARF1 which are known to prevent cell apoptosis (Kennedy, Komano et al. 2003; Sheng, Decaussin et al. 2003). EBERs also promote cell survival via the up regulation of IL10 (Kitagawa, Goto et al. 2000).

To further investigate the involvement of EBV latency gene expression Burkitt's lymphoma pathogenesis, model cell lines displaying varying latency phenotypes were analysed within the investigation.

As mentioned before, the use of cells displaying latency I phenotype is a good model for Burkitt's lymphoma which behave like original Burkitt's tumours.

Work by Gregory C.D. *et al.,* in 1990 document on the establishment of varying Burkitt's lymphoma clones from a tumour biopsy (Gregory, Rowe et al. 1990). At the period of time in culture, when EBV latency phenotype altered, morphologically distinct cell populations were separated and characterised. LCL-like cells which grew in clumps and contained cytoplasmic projections were fractioned from small, round, free floating single cells. These cell lines were named as the Mutu Burkitt's lymphoma line. Clones of single round cells were described to have a group I phenotype based on morphological and surface antigen expression. Consequently, LCL clones were known to display a group III morphological phenotype. Once characterised for the expression of EBV latency proteins, group I cells were shown to express only EBNA1, which in turn displays a latency I EBV gene expression phenotype. Group III cells on the other hand expressed all five EBNA proteins, LMP and lytic cycle antigens, displaying a latency III phenotype.

Cell lines have also been established from rare non-EBV associated sporadic Burkitt's lymphoma cases. These EBV negative cell lines include BL41, which was first established at the International Agency for Research on Cancer (IARC) in Lyon, France. Experimental infection of cell lines such as BL41 with the transforming EBV strain, B95.8 resembled the phenotype and EBV gene expression patterns observed within in vitro infected normal B cells (Calender, Billaud et al. 1987).

The initial aim within this investigation was to question the expression patterns of neurotrophic factors and receptors within Burkitt's lymphoma cell lines displaying varying EBV latency phenotypes. Additional research using Burkitt's lymphoma model lines by questioning EBV gene patterns and the control of the cellular proteins, neurotrophic factors and receptors could provide further insights to viral-cellular communication in Burkitt's lymphoma. The involvement of neurotrophic factor signalling in B cells has previously been documented by several laboratories.

In 1987 Thorpe L.W. and Perez-Polo J.R. discovered that rat spleen B and T lymphocytes express NGF-receptor which can induce cell proliferation upon NGF treatment (Thorpe and Perez-Polo 1987). Subsequently, Otten U. *et al.,* document on the expression of NGF receptors within human spleen and lymph node tissues. Importantly they also discovered that NGF induced proliferation and differentiation in human B lymphocyte (Otten, Ehrhard et al. 1989). Further research by Edling A.E., *et al.,* show the expression of NT-4, BDNF and their receptor TrkB as well as NGF expression in human B cells (Edling, Nanavati et al. 2004).

Neurotrophic factor expression and signalling can also be associated with haematological malignancies. Hodgkin Reed Sternberg cells obtained from Hodgkin lymphoma, express TrkA and TrkB receptors which can be phosphorylated upon ligand binding (Renne,

Willenbrock et al. 2005). The B cell neoplasm, Multiple myeloma tumour cells also express BDNF and its receptor TrkB. In this case, BDNF acts as a potent growth factor, inhibits apoptosis induced by dexamethasone, enhances cell survival and acts as a chemoattractant (Pearse, Swendeman et al. 2005; Hu, Sun et al. 2006).

This increase in evidence on the involvement of neurotrophic factor signalling in cancers of the immune system has lead to the main focus for this section of the investigation. Here the aim is to explore neurotrophic factor mRNA expression patterns in characterised Burkitt's lymphoma B cells.

3.2 Results

3.2.1 Morphological characteristics of a series of model Burkitt's lymphoma lines

Two sets of Burkitt's lymphoma B cell lines were provided displaying varying EBV latency and cellular phenotypes. The first set from an EBV negative Burkitt's lymphoma patient, comprise the EBV tumour line BL41; an EBV convertant of this line, BL41+EBV strain B95.8, established by in vitro infection of the original tumor line and IARC-171, an EBV transformed lymphopblastoid line generated by in vitro infection of normal B cells from the blood of this patient. The second set are subclones of the Mutu- Burkitt's lymphoma line, two EBV negative clones, two latency I and two latency III clones (Gregory, Rowe et al. 1990). Figure 3.1 shows the differences in cell morphology between EBV negative/ latency I cells compared to those expressing EBV latency III genes. EBV negative cells appear as free floating, small circular single cells in suspension (figure 3.1a), while Latency III cells appear in clumps with some single cells in suspension (figure 3.1b).

3.2.2 Verification of EBV gene expression patterns in the model Burkitt's lymphoma lines

Burkitt's lymphoma lines were screened using antibodies specific to each EBV latency protein. Protein lysates were obtained from each line 24 hours post feeding to ensure the cells were at growth phase. The first set of whole cell extracts were prepared and ran on 7% polyacrylamide with SDS gels (Tris-Acetate buffer) under reducing conditions. Samples were then screened for EBNA1, EBNA2, EBNA3a, EBNA3b, EBNA3c, LMP1 and LMP2a (figure 3.2a).

The lymphoblastoid cell line, IARC-171 expressed all latent proteins analysed. BL41+EBV strain B95.8 shows weaker expression of EBNA3c and LMP1, with undetectable EBNA3b and LMP2a expression. Mutu latency III clone J8 show similar expression patterns to BL41+EBV, whereas Mutu latency III clone K5 is probably a micture if ENB loss and latency III cells.

Since EBNA-LP is composed of proteins with multiple molecular weights, a 4 to 12% polyacrylamide with SDS gradient gel (Bis-Tris buffer) under reducing conditions, was used to display a larger range in molecular weight proteins (figure 3.2b). BL41+EBV lines show strong protein expression at ~20kDa and ~30kDa. IARC-171 on the other hand shows weaker levels of proteins running at a wide range of molecular weights. All Mutu lines were negative for EBNA-LP with the use of this antibody.

3.2.3 Analysis of mRNA expression of Neurotrophic factors and their receptors in Burkitt's lymphoma cell lines

To examine the expression of neurotrophic factors and their receptors, RNA was extracted from all Burkitt's lymphoma cell lines and analysed by semi-quantitive RT-PCR. Following amplification of target sequences, samples were run on agarose gels containing 0.6μg/ml ethidium bromide and visualised under UV light. β-actin primers were used to monitor the presence of equal cDNA levels within RT positive samples (figure 3.3.1). All PCR results are representatives of three independent RNA extractions and PCR experiments.

NGF specifically binds to TrkA. Although expression of the receptor, TrkA was observed within all Burkitt's lymphoma B cell lines, transcript expression of its NGF ligand was undetectable across the set of lines analysed (figure 3.3.2).

The expression levels of NT-4, BDNF and their specific receptor TrkB, were also examined. Both BDNF and NT-4 primers lie within one exon and can therefore pick up non-specific genomic DNA, therefore RT negative cDNA was compared to RT positive cell samples (figure 3.3.3). BDNF PCR products were present within all RT positive Burkitt's lymphoma cell lines and absent within the RT negative controls. Weak expression of NT-4 PCR products were observed within all cell lines, however non-specific genomic DNA was also amplified within all the RT negative sample.

Two primer sets were used to examine TrkB expression. The first primer sets recognize all TrkB variants and are named “Pan TrkB primers”. The second set on the other hand only recognizes the two full length TrkB variants A and C; this set is named “variants A & C TrkB primers”. All EBV negative cell lines, and the Mutu latency I clone 59 lacked detectable transcripts specific for all TrkB variants. BL41+EBV and Mutu latency I clone 179 only expressed Pan-TrkB transcripts where as IARC-171 and both Mutu clones expressed all TrkB transcript variants.

Which specific variants are upregulated by the latency III phenotype however, remains unknown. For these experiments to be repeated, it would be worth knowing which specific variants are upregulated by designing semi-quantitative RT-PCR primers specific for unique regions on each TrkB variant.

NT-3 specifically binds to TrkC receptor. The NT-3 primers used also lie within one exon therefore RT positive PCR products were compared to RT negative samples to ensure specificity of transcript detection. Expression of NT-3 transcripts was observed within all cell lines; however it was remarkable that these expression levels seemed to decrease with acquisition of a latency III phenotype (figure 3.3.4). Based on the concluding remarks for latency characteristics of Mutu latency III clone K5; where a heterogeneous population may be present, the few latency III cells within the culture may influence the lower expression levels of NT-3 transcripts observed. All EBV negative and Mutu latency I lines show strong transcript levels whereas latency III lines show weaker NT-3 levels. The RT-negative control samples for NT-3 expression did not pick up any genomic DNA rendering the NT-3 results a true positive.

In contrast to the reproducible results obtained for other neurotrophic factors and receptor transcript assays, variation of TrkC expression between RNA extractions within the lines analysed therefore, three independent results for TrkC mRNA expression are shown. These results were inconclusive but suggest that very low levels of transcripts may be present in most of the cell lines, but with no obvious correlation to latency phenotype.

RT-PCR experiments were conducted to question $p75^{NTR}$ expression levels. NGF, BDNF, NT-3 and NT-4 bind to $p75^{NTR}$ receptor with lower affinity than their cognate Trk receptors. Most Burkitt's lymphoma B cell lines analysed express $p75^{NTR}$ transcripts regardless of EBV latency phenotype with the exception of Mutu latency I clone 179.

3.2.4 Quantitative analysis of TrkB mRNA

Using real time PCR methods, Pan-TrkB primers were used to quantify TrkB transcripts within characterised Burkitt's lymphoma lines. VIC labelled Beta-2 Microglobulin (B2M) primers and FAM labelled TrkB primers were designed and optimised to be used in a duplex RT-PCR detection system. mRNA levels of TrkB were calculated relative to B2M levels for each Burkitt's lymphoma cell line (figure 3.4). Consistent with RT-PCR data shown within figure 3.3.3, latency III cells expressed detectable levels of TrkB transcripts compared to their EBV negative or latency I counterparts. The multiple myeloma cell line, KMS-11 was used as the positive control.

A summary of the data analysing expression of EBV latency proteins, neurotrophic factors and their receptors in the model Burkitt's lymphoma B cell lines is illustrated within Table 3.1.

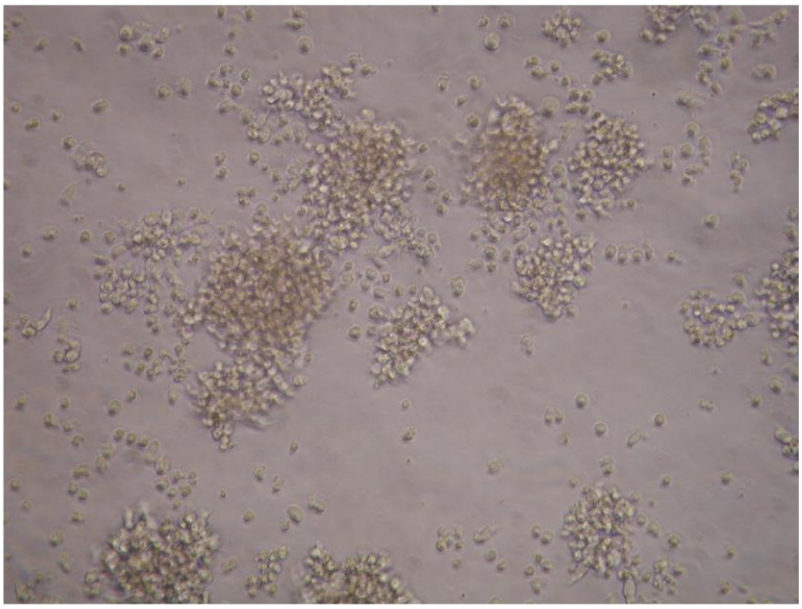

Figure 3.1a

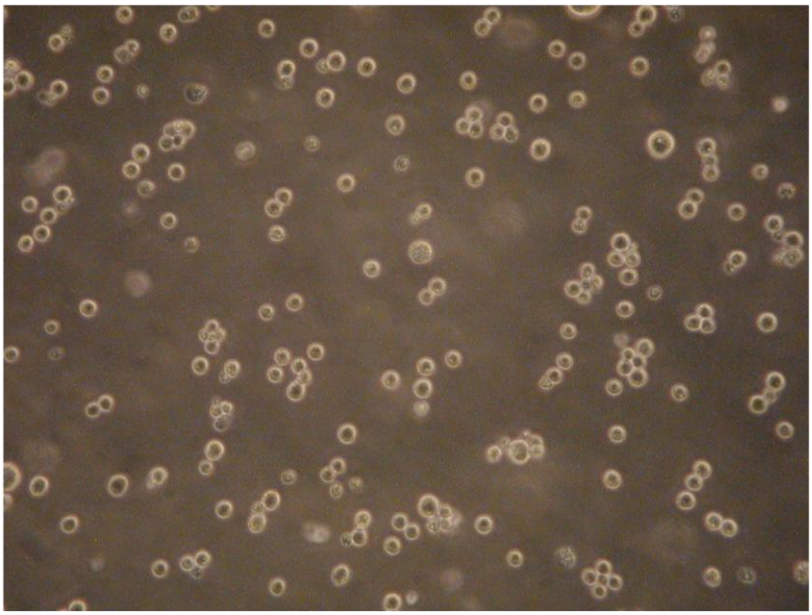

Figure 3.1b

Figure 3.1: Differences in cell morphology between EBV negative and latency III Burkitt's lymphoma cell lines

Phase bright images of IARC-171 lymphoblastoid cells in culture (figure 3.1a) showing differences in morphology between EBV negative BL41 Burkitt's lymphoma cells (figure 3.1b).

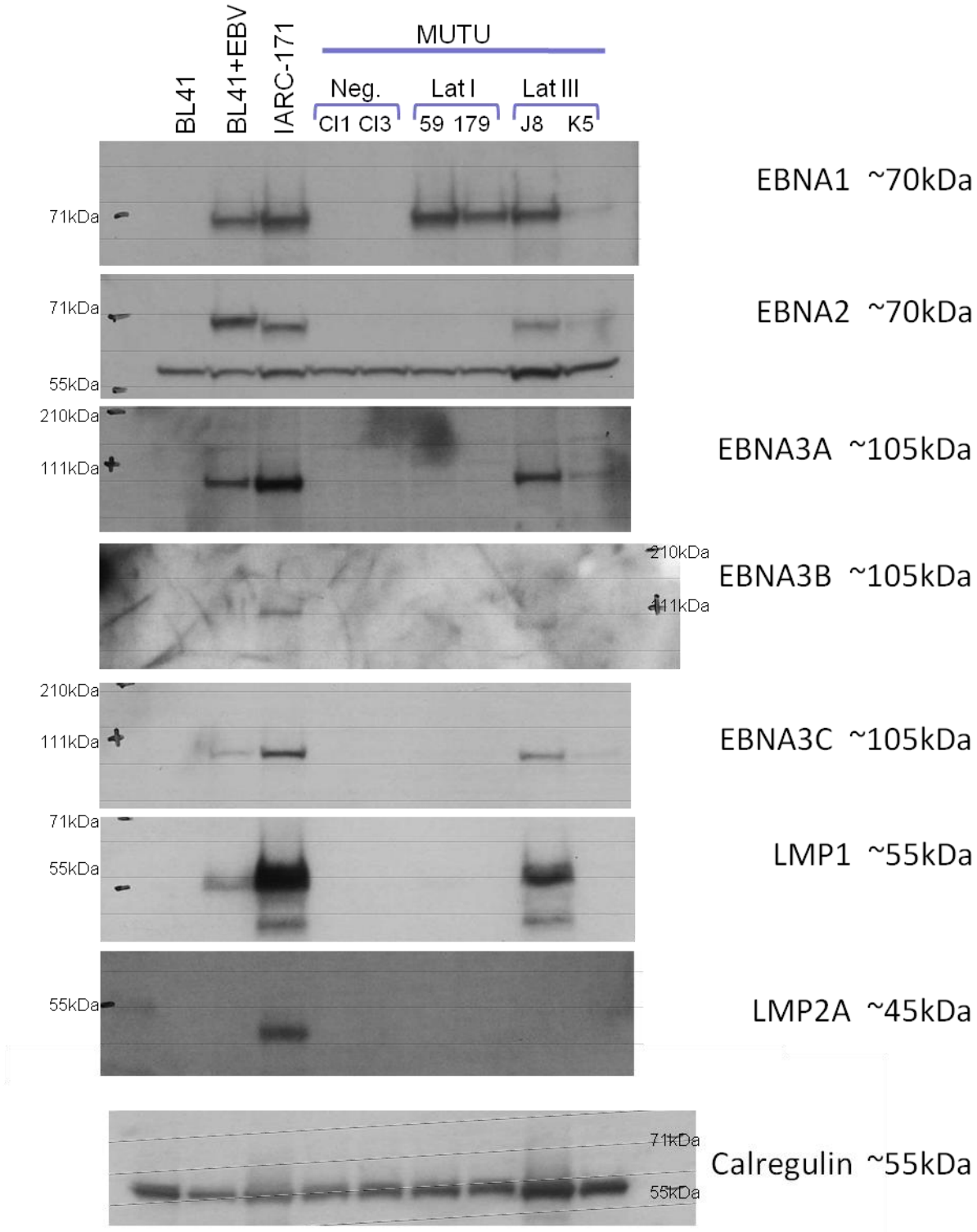

Figure 3.2a: The expression of EBV latency proteins in Burkitt's lymphoma B cell lines
Western blot results showing whole cell extracts (10μg protein) run within 7% Acrylamide Tris-Acetate NuPAGE Gels. BL41 and MUTU negatives do not express any Latency III proteins. The MUTU Lat I cell lines only express EBNA1, whereas MUTU Latency III cell lines Clone J8 and IARC 171 expressed all EBV latency protein as expected. MUTU Lat III clone K5 on the other hand did not express EBNA3B, LMP1 and 2A, although weak expression of other latency genes was observed. Calregulin was used as the loading control.

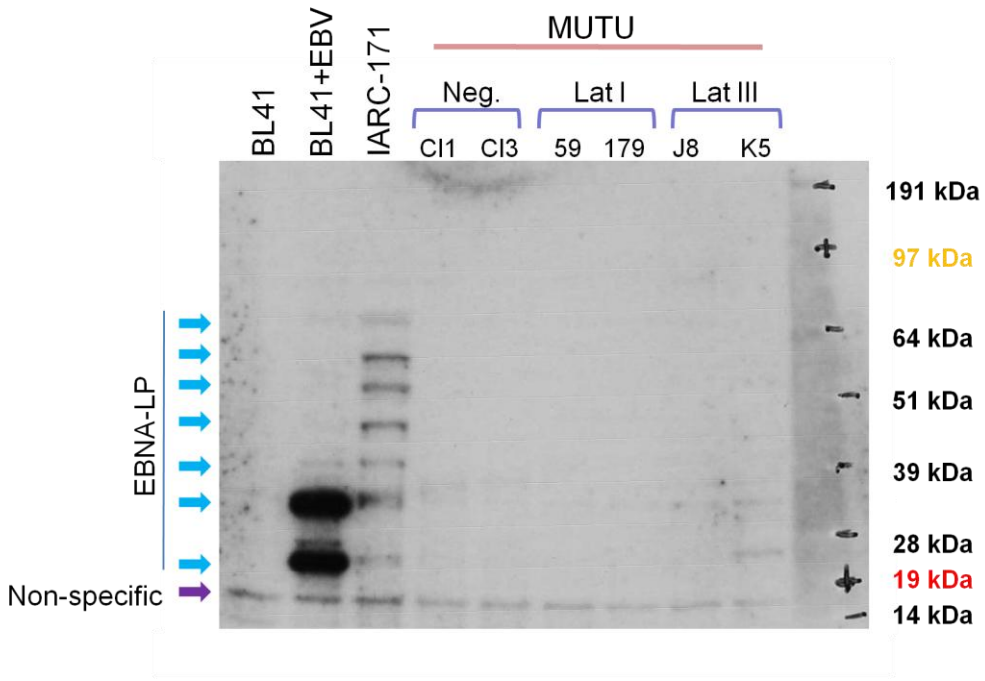

Figure 3.2b: The expression of EBNA-LP in Burkitt's lymphoma B cell lines
Western blot of Burkitt's lymphoma lines probed for EBNA-LP. BL41+EBV and IARC 171 are the only cell lines found to express EBNA-LP. Strong protein expression was observed at ~20kDa and at ~30kDa within the BL41+EBV cell line. Multiple bands were observed within the IARC 171 cell line.

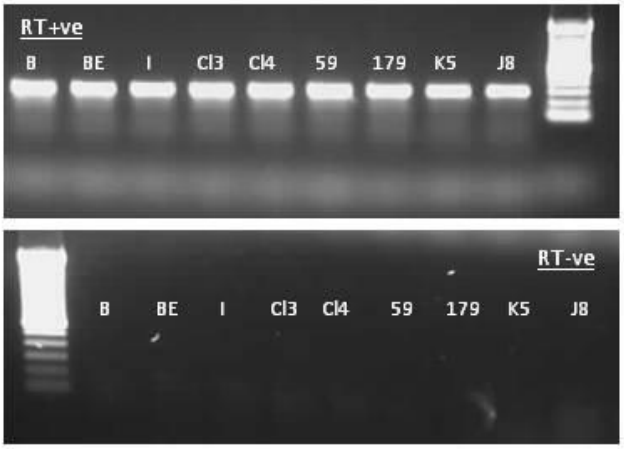

Figure 3.3.1: mRNA transcripts of β-actin in Burkitt's lymphoma B cells
RT-PCR primers specific for β-actin were used in an RT-PCR reaction producing a 300bp amplicon. RT positive and negative products were separated on a 1.5% agarose gel containing ethidium bromide and visualised under UV light.
Representatives of three independent experiments are shown.

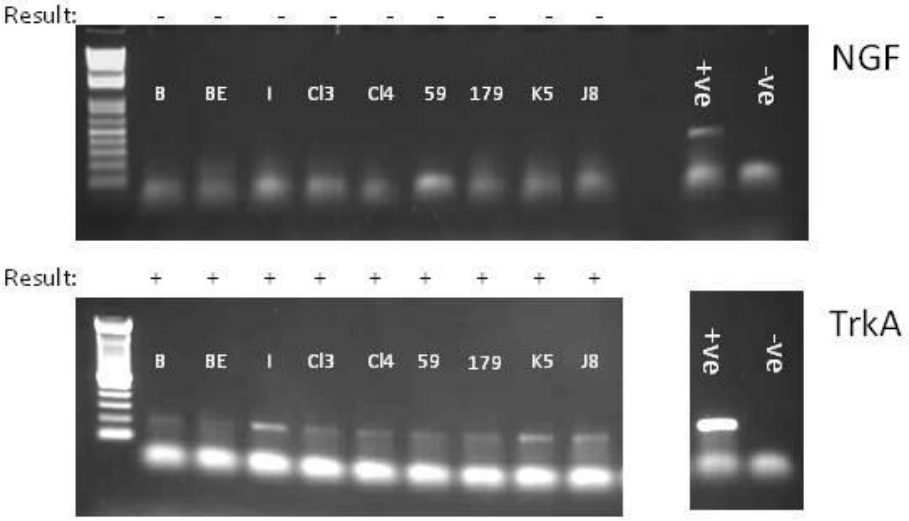

Figure 3.3.2: mRNA transcripts of NGF and its' receptor TrkA in Burkitt's lymphoma B cells
RT-PCR primers specific for NGF producing a 325bp amplicon, and for TrkA producing a 200bp amplicon were used in RT-PCR reactions. Products were separated on 1.5% agarose gels containing ethidium bromide and visualised under UV light. The interpretation (detected specific product "+" or no specific product "-") of the gels is indicated in the results above each gel image. RNA extracted from NT-2 cells was used as the positive control for NGF whereas RNA from KELLY cells was used for the TrkA RT-PCR control.
Representatives of three independent experiments are shown.

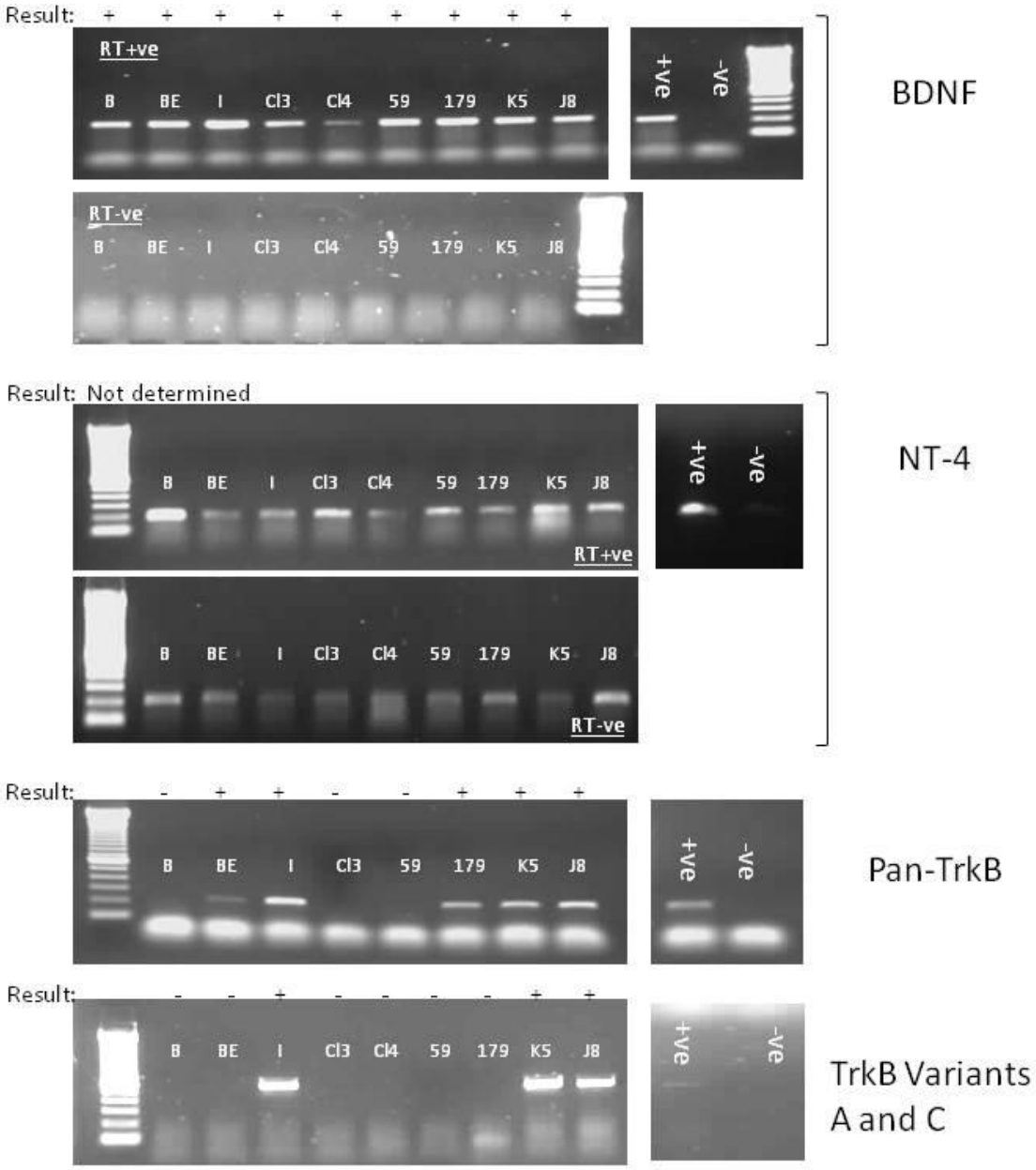

Figure 3.3.3: mRNA transcripts of BDNF, NT-4 and their receptor TrkB in Burkitt's lymphoma B cells

RT-PCR primers specific for BDNF producing a 221bp amplicon, NT-4 producing a 201bp amplicon, Pan-TrkB producing a 221bp amplicon and TrkB variants A and C producing a 574bp amplicon were used in an RT-PCR reaction. Products were separated on 1.5% agarose gels containing ethidium bromide and visualised under UV light. The interpretation (detected specific product "+" or no specific product "-") of the gels is indicated in the results above each gel image. The multiple myeloma cell line, KMS-11 was used as a positive control for BDNF expression whereas Colo-357 was used as the NT-4 control. cDNA extracted from KMS-11 cell line was used as the control for TrkB mRNA transcripts. Representatives of three independent experiments are shown.

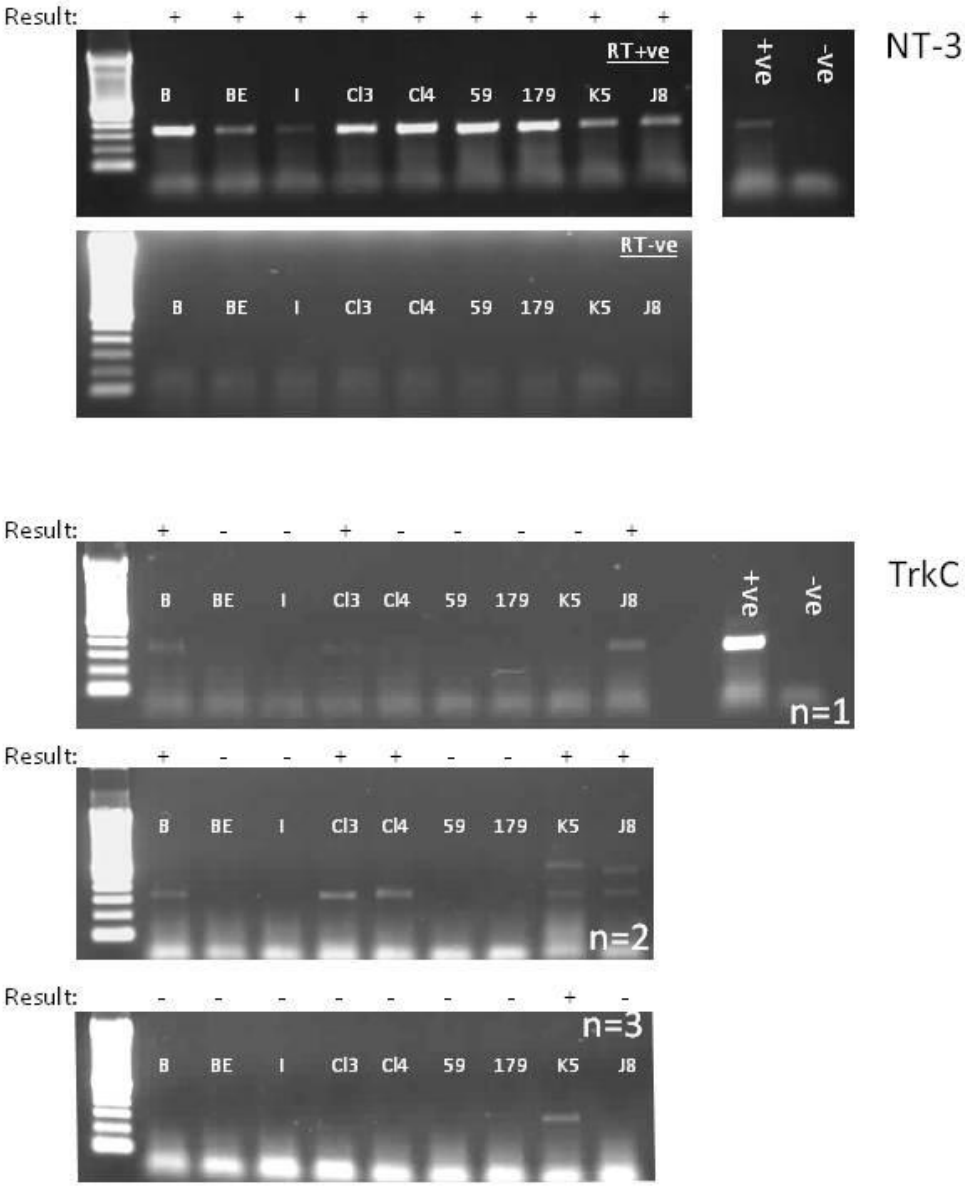

Figure 3.3.4: mRNA transcripts of NT-3 and its' receptor TrkC in Burkitt's lymphoma B cells

RT-PCR primers specific for NT-3 producing a 343bp amplicon and TrkC producing a 363bp amplicon were used in an RT-PCR reaction. Products were separated on 1.5% agarose gels containing ethidium bromide and visualised under UV light. The interpretation (detected specific product "+" or no specific product "-") of the gels is indicated in the results above each gel image. cDNA obtained from Colo-357 cells were used as NT-3 controls, on the other hand, HMC-1 cDNA was used as the control in TrkC RT-PCR experiments.

A representative of three independent experiments is shown for NT-3 RT-PCR analysis.

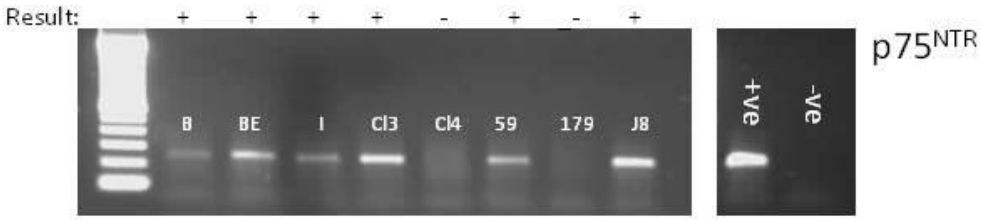

Figure 3.3.5: mRNA transcripts of the low affinity receptor $p75^{NTR}$ in Burkitt's lymphoma B cells

RT-PCR primers specific for $p75^{NTR}$ producing a 246bp amplicon were used in an RT-PCR reaction. Products were separated on 1.5% agarose gels containing ethidium bromide and visualised under UV light. A representative of three independent experiments is shown for NT-3 RT-PCR analysis. The interpretation (detected specific product "+" or no specific product "-") of the gels is indicated in the results above each gel image. cDNA extracted from KELLY cells was used as the RT-PCR control.

A representative of three independent experiments is shown.

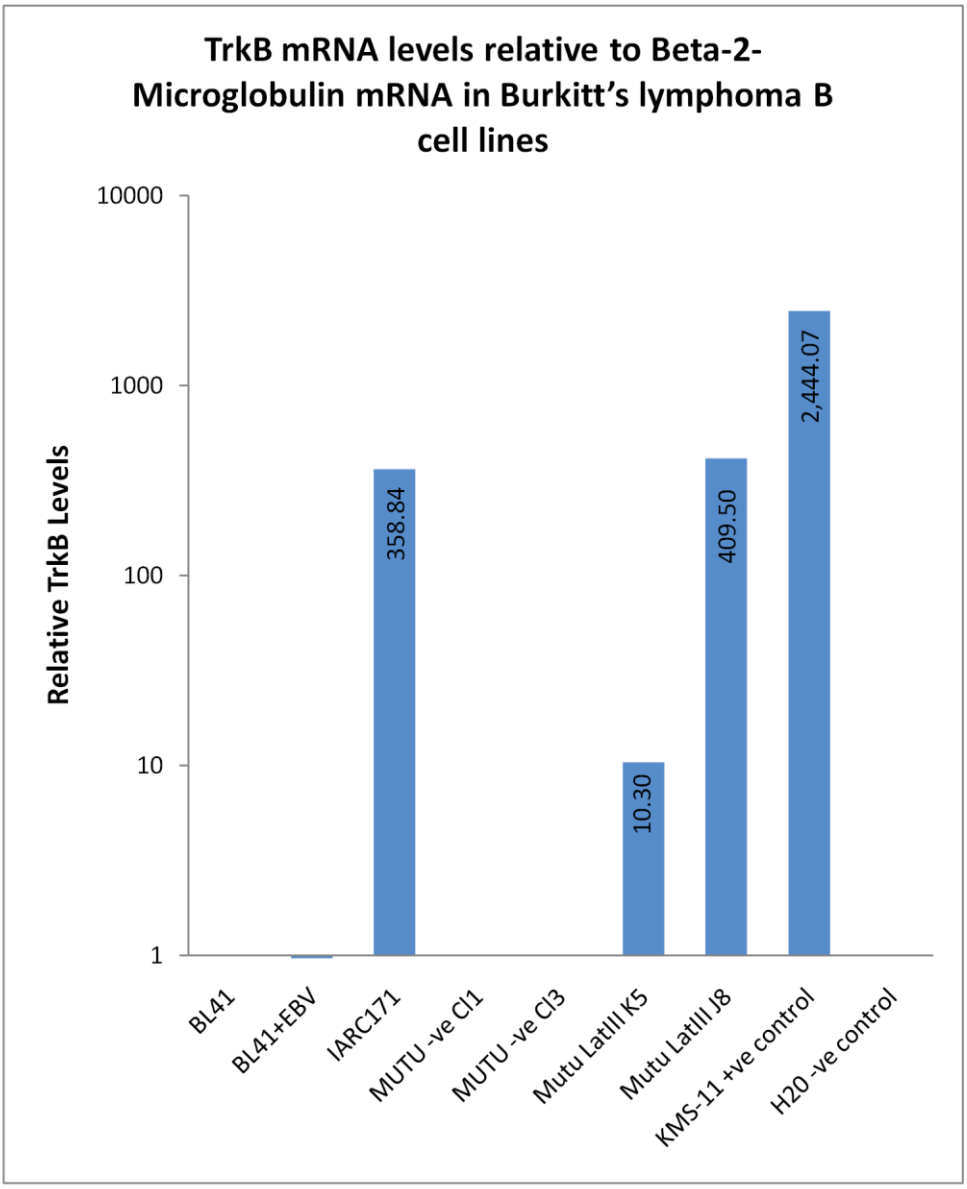

Figure 3.4: Real time-PCR data showing relative TrkB mRNA levels to β-2-Microglobulin mRNA levels in Burkitt's lymphoma B cells

Relative levels of mRNA specific for Pan-TrkB variants were caculated compared to mRNA levels of Beta-2 Microglobulin from Multiplex Real time PCR rections. Mean TrkB levels from three independent sets of mRNA extractions are displayed.

Table 3.1: Summary representing the expression of EBV latency proteins and RT-PCR mRNA transcript experiments on neurotrophic factors and their receptors within Burkitt's lymphoma cell lines

	BL41	BL41 + EBV	IARC 171	Mutu -VE		Mutu Lat I		Mutu Lat III	
				Clone 3	Clone 4	Clone 59	Clone 179	Clone K5	Clone J8
EBV Latency Proteins									
LMP1	-	-	+	-	-	-	-	-	+
LMP 2A	-	-	+	-	-	-	-	-	-
EBNA1	-	+	+	-	-	+	+	+	+
EBNA2	-	+	+	-	-	-	-	+	+
EBNA3A	-	+	+	-	-	-	-	+	+
EBNA3B	-	+	+	-	-	-	-	-	+
EBNA3C	-	+	+	-	-	-	-	+	+
EBNA-LP	-	+	+	Not determined					
Neurotrophic Factors and Their Receptors									
NGF *	-	-	-	-	-	-	-	-	-
BDNF	+	+	+	+	+	+	+	+	+
NT-3	+	+	+	+	+	+	+	+	+
NT4/5	Not determined								
$p75^{NTR}$	+	+	+	+	-	+	-	+	+
TrkA	+	+	+	+	+	+	+	+	+
Pan-TrkB	-	-	+	-	-	-	-	+	+
TrkB A&C	-	+	+	-	-	-	+	+	+
TrkC	-/+	-	-	-/+	-/+	-	-	-/+	-/+

* See Results Chapter 5 for further NGF expression results

3.3 Discussion

Freshly isolated Burkitt's lymphoma cell lines can change in EBV latency phenotype when cultured. Over time, these cells can shed viral episomes changing their phenotype from latency III to an EBV latency I/ negative line. To ensure the cell lines provided for the investigation were true to their EBV latency phenotypes morphologies were closely examined and recorded whilst in culture. This was important for interpreting data produced from future neurotrophic factor signalling experiments. As shown within figure 3.1, latency three cells form clumps in culture, differences in cell morphologies between Mutu latency III clone J8 and K5 were observed. Clone J8 cells retained their characteristic clumping morphology, whereas clone K5 cells appeared to have much smaller clumps with a very high proportion of free floating single cells in suspension. Further evidence of viral episome shedding was observed when screening the cells for EBV latency proteins. Comparing Mutu latency III clones, J8 cells expressed stronger levels of EBNA1, EBNA2, EBNA3a and EBNA3c. K5 cells on the other hand lacked LMP1 and EBNA3b proteins expressed within J8 clones. BL41 lines infected with EBV also lacked EBNA3b proteins, however it is worth noting, the antibody used to probe for EBNA3b is relatively weak and may not have been sensitive enough to detect expression within EBV infected BL41 lines and Mutu latency III K5. Differences in molecular weight for EBNA2 protein between BL41+EBV and IARC 171 indicating possible variation in EBV virus strain however this is unlikely since both lines were in vitro infected with EBV stain B95.8. Immunoprecipitation and mass spectrometry analysis would be a useful experiment to further analyse whether the proteins detected are true EBNA2 proteins.

LMP2a expression however was only observed within the LCL line, IARC-171. This result is either due to antibody sensitivity or a true representation of LMP2a expression within the two Mutu latancy III lines. LMP2a is a mimic for BCR signalling in EBV infected B cells, these signalling events, together with LMP1 are essential for survival and growth are essential in maintaining the latency III phenotype. Taking this into consideration it would be beneficial to question LMP2a expression using an alternative antibody and to also examine gene expression within the two Mutu latency III lines.

The expression pattern for EBNA-LP is consistent with previous EBNA-LP expression as documented by Finke J. *et al,*. Here, they investigated on EBV infected BL41 cells where two EBNA-LP proteins, one at approximately 30kDa and the other at roughly 20kDa are observed (Finke et al., 1987). The RT-PCR results shown in figure 3.2b for BL41+EBV cells are consistent with these results. Although IARC 171 was not included as one of the LCLs analysed within Finke, J. *et al's* study, proteins observed within IARC 171 ranging from 20kDa to 65kDa lysates resemble EBV infected B cells illustrated within the publication.

However, EBNA-LP expression was not observed within any of the Mutu clones. The reason for this is due to the antibody used, JF186, which recognises specific sites of the EBNA-LP antigen present within BL41+EBV and IARC 171 cell lines, however this antigen is not present in Mutu lines (communication with Professor Rowe.)

Prior to each RT-PCR experiment, amplicons from positive control cell lines such as Kelly and KMS-11 were run out on a 1.5% agarose gel. Extracted DNA was obtained using a Qiagen gel extraction kit and sent to MWG Biotech Ltd (Covent Garden, London) for sequence

verification. Primers specific for each neurotrophic factor and receptor were then used within a series of RT-PCR experiments.

Three independent RNA extractions were performed for all Burkitt's lymphoma lines to be screened for the expression of neurotrohic factors and receptor mRNA transcripts. For each RNA extraction, a β-Actin RT-PCR test was completed to ensure cDNA was successfully obtained for each cell sample (figure 3.3.1).

All Burkitt's lymphoma lines expressed TrkA transcripts regardless of EBV latency phenotype, however the lack of its ligand, NGF was observed (figure 3.3.2). This lack in NGF mRNA expression was unexpected considering previous publications show NGF expression in B cells. As shown by Torcia M. *et al.,* NGF is synthesised and signals in an autocrine manner through its receptor TrkA and $p75^{NTR}$ within memory B cells (Torcia, Bracci-Laudiero et al. 1996). Further evidence on NGF expression in B cells was documented by Coppola V. *et al.,* and Bracci-Laudiero L. *et a.l*. (Coppola, Barrick et al. 2004; Bracci-Laudiero, Aloe et al. 2005). However based on the RT-PCR experiments, the lack of NGF expression is observed in all Burkitt's lymphoma B cells and possibilities of paracrine signalling with NGF expressing cells will later be question within the investigation.

Transcripts for TrkB ligands on the other hand, are expressed within all Burkitt's lymphoma lines. Publications have been submitted showing bioactive BDNF secretion from B cells can support neuronal survival in vitro (Kerschensteiner, Gallmeier et al. 1999). As for NT-4 expression in B cells, there is currently limited literature on this neurotrphic factor however NT-4 mRNA expression has been documented in murine lymphocytes (Barouch, Appel et al. 2000). The expression of NT-4 transcripts was observed within all Burkitt's lymphoma lines. Their cognate receptor, TrkB is formed of varying isoforms therefore two primer sets were

used to screen for TrkB expression. Using the Pan-TrkB primers, expression was only observed within latency I and latency III cell lines, excluding Mutu latency I clone 59 (figure3.3.3). This expression pattern is possibly due the presence of EBNA1 within this set of Burkitt's lymphoma lines. TrkB primers recognising variants A and C on the other hand only detected transcripts within IARC-171 and both Mutu latency III clones. The initial postulations from these results may indicate the co-expression of TrkB and LMP1 within these lines, except Mutu latency III clone K5. The lack of full length TrkB variants A and C in EBV negative and latency I lines revel a possibility in the up regulation of TrkB in latency III tumour cells. The up regulation of TrkB for tumour survival and progression has been indicated for a number of neuronal and nonneuronal solid tumours (Ricci, Greco et al. 2001; Sakamoto, Kitajima et al. 2001). Like Multiple myeloma, Burkitt's lymphoma latency III cells express TrkB and may respond to BDNF promoting tumour growth (Pearse, Swendeman et al. 2005).

As for NT-3 expression, all lines reguardless of EBV phenotype express NT-3 transcripts, however the level of expression seemed to correlate with EBV phenotype. With increasing EBV phenotype from EBV negative to latency III, cells seem to have a decrease in NT-3 expression levels. As of yet, there are no publications investigating the changes in neurotrophic factor expression levels between EBV latency groups, however there is evidence for changes in expression levels between activated and non-activated lymphocytes. Stimulating B cells obtained from PBMCs with heat-inactivated *Staphylococcus aureus* increases their expression of soluble BDNF (Kerschensteiner, Gallmeier et al. 1999). It is a possibility that normal B cells have high levels of NT-3 mRNA which decrease upon EBV infection. Although NT-3 binds with its cognate receptor TrkC, it

is the most promiscuous of the mammalian neurotrophic factors which can also signal via TrkA and TrkB at a lower affinity together with the low affinity receptor $p75^{NTR}$ but (Ibanez 1994; Ibanez 1998).

The need for stronger NT-3 levels in EBV negative lines may be linked to the lack of full length TrkB within these cells as discussed above. The expression of TrkC however was not clear from the RT-PCR experiments completed. Varying transcript levels were detected between Burkitt's lymphoma RNA extractions (figure 3.3.4). Overall, TrkC expression was only observed within EBV negative BL41 line, Mutu negative clones and Mutu latency III clones therefore the expression of this receptor was conclude to not be EBV latency specific.

BDNF, NT-3 and NT-4 expressed by Burkitt's lymphoma B cells could signal through their cognate receptors and the low affinity receptor $p75^{NTR}$ in Burkitt's lymphoma B cells. The expression of $p75^{NTR}$ transcripts were observed within all Burkitt's lymphoma lines excluding Mutu latency I clone 179 (figure 3.3.5). Mature EBV negative B cell lines have been previously show to have increased membrane expression of $p75^{NTR}$ and TrkB when deprived of serum for 24 to 72 hours (Fauchais, Lalloue et al. 2008). $p75^{NTR}$ signalling for proliferation can occur in B cells obtained from patients with chronic lymphocytic leukaemia (Waage, Liabakk et al. 1992), and the activation of mantel zone B cells with anti-immunoglobulin and IL-4 or IL-2, increases receptor expression of $p75^{NTR}$ (Zola, Flego et al. 1993).

4. Results

Expression and autocrine signalling of TrkB and $p75^{NTR}$ receptors and their ligands BDNF and NT-4

4.1 Introduction

The conclusions drawn based on TrkB and $p75^{NTR}$ expression, from the previous chapter, illustrate that latency III Burkitt's lymphoma lines, IARC-171 and Mutu clone J8 show clear, detectable mRNA expression for full length TrkB whereas their EBV negative counterparts, BL41 and Mutu negative clones and EBV latency I clones lacked detectable full length TrkB mRNA. On the other hand, all Burkitt's lymphoma lines expressed the high affinity TrkB ligands NT-4 and BDNF.

The main focus for this chapter is to explore protein expression of TrkB and $p75^{NTR}$ receptors in Burkitt's lymphoma B cell lines previously characterised. The expression of their ligands NT-4 and BDNF will also be investigated. Ligand expression confirmation is important since possible autocrine signalling may occur in Burkitt's lymphoma lines. For this question to be answered, downstream signalling effects on cell survival and proliferation within the Mutu clone J8 latency III Burkitt's lymphoma line will be analysed by the use of varying receptor and/ or ligand inhibitors.

4.1.1 Alternatively spliced TrkB variants

The TrkB gene contains 24 exons that are influenced by alternative promoters, splicing, and polyadenylation sites. In effect, the *TrkB* gene can create at least 100 isoforms that can encode around 10 proteins (Klein, Parada et al. 1989). However by using RT-PCR and

Northern blot analysis, it is known that three major protein isoforms are generated by the *TrkB* gene (Middlemas, Lindberg et al. 1991). A TrkB full length receptor, a isoform lacking the tyrosine kinase domain (TrkB-T1), and an isoform lacking the tyrosine kinase domain but containing an Shc binding site (TrkB T-Shc) (Klein, Conway et al. 1990; Shelton, Sutherland et al. 1995). There are 5 well characterised mammalian TrkB isoforms, displayed within illustration 4.1.

Like the full length TrkB, TrkB-T1 variant can bind and activate to neurotrophins and is internalized, but due to the lack of a kinase domain it cannot signal catalytically (Biffo, Offenhauser et al. 1995). However its specific function remains controversial.

As for TrkB-T-Shc, it is a truncated variant which contains a Shc-binding site in the juxtamembrane domain but lacks the kinase domain and has a unique truncated C terminus. T-Shc is predominantly expressed in the brain, but its role is so far mostly unknown (Haapasalo, Sipola et al. 2002). TrkB-T-Shc is generated by the use of a new alternative exon 19.

4.1.2 TrkB phosphorylation and downstream signalling

BDNF and or NT-4 ligand binding can result in receptor dimerisation of either two TrkB receptor dimers or one TrkB with a $p75^{NTR}$ receptor (Bibel, Hoppe et al. 1999). This occurs at the cell surface resulting in autophosphorylation of intracellular tyrosine residues (Stephens,

Loeb et al. 1994; Inagaki, Thoenen et al. 1995). TrkB autophosphorylation occurs on five BDNF inducible cytoplasmic tyrosine site: Y484, Y670, Y674, Y675, and Y785 as displayed in illustrated 4.2 (Guiton, Gunn-Moore et al. 1994; Middlemas, Meisenhelder et al. 1994).

As reviewed by Huang E.J. and Reichardt L.F., phosphorylated tyrosines act as docking sites for adaptor proteins containing PTB or SH2 domains which in turn activate Ras-Raf-Erk, Phosphoinositide 3-kinases (PI3-K), PLC-γ-Ca^{2+} and NFκB pathways (Wooten, Seibenhener et al. 1999; Foehr, Lin et al. 2000; Kaplan and Miller 2000; Huang and Reichardt 2003). The tyrosine site, Y484, lies within the intracellular juxtamembrane region of TrkB and is predicted to be the binding site for the PTB domain of the SHC adapter protein (Nimnual, Yatsula et al. 1998; Xing, Kornhauser et al. 1998). Shc recruits the Grb2 adaptor protein complexed with SOS which is exchanged with Ras. Activated Ras then stimulates varying downstream pathways including PI3-K which produce phosphatidylinositides generated by phosphatiyinositde-dependent protein kinase (PDK-1) and PI3-K. These three phosphoinositides activate protein kinase Akt which then phosphorylates sereval proteins important in promoting cell survival.

Substrates of Akt phosphorylation include anti-apoptotic proteins such as Bad, a member of the Bcl-2 family which prevents apoptosis when phosphorylated. It has also been shown that NT-3 signalling, involving PI3-K, can orchestrate anti-apoptotic effects on cultured cortical neurons (Liot, Gabriel et al. 2004).

Activated Ras can also stimulate Raf which phosphorylates Erk 1 and Erk 2 by MEK1 or MEK 2 (English, Pearson et al. 1999). Rsk are Erk 1 and Erk 2 substrates that activate CREB which regulates genes associated with differentiation and survival (Riccio, Ahn et al. 1999). Neurotrophin signalling involving Erk activation is shown by the addition of BDNF to intact

adult hippocampus which allows long lasting synaptic strengthening, acting through Erk-Mek signalling adaptors.

TrkB signalling can also regulate cell proliferation in the development of murine embryonic central nervous system precursors (Bartkowska, Paquin et al. 2007). Here, it was noted that Erk and not Akt signalling is involved in cell proliferation of cortical precursors in vivo. Upon phosphorylation of the tyrosine kinase residue, Y-484, Shc is phosphorylated then signals via adaptor proteins such as Ras, Erk1/2 and c-fos enhancing protein synthesis (McCarty and Feinstein 1999). The three autophosphorylation sites, tyrosine Y670, Y674 and Y675 lie within a structurally flexible activation loop, inside the TrkB catalytic domain (illustration 4.1). When phosphorylated it is presumed that SH2 and/ or PTB domain-containing proteins interact with one or more of the activation loop phosphotyrosines inducing mitogenesis via Erk1/2 and c-fos synthesis (McCarty and Feinstein 1998).

Hence, to question whether Burkitt's lymphoma B cell lines express TrkB and/ or $p75^{NTR}$ protein, three anti-$p75^{NTR}$ antibodies and two Anti-TrkB antibodies were used for analysis. The regions the antibodies recognise on the TrkB and the $p75^{NTR}$ structures are annotated within illustration 4.3 and 4.4. To question possible autocrine signals via TrkB and/ or $p75^{NTR}$, Burkitt's lymphoma latency III B cells were exposed to varying TrkB and or/$p75^{NTR}$ inhibitors discussed below.

4.1.3 Inhibitions for TrkB signalling

The most commonly documented neurotrophic factor receptor signalling inhibitor is K252a, an alkaloid-like compound isolated from the *Nocardwpsis* species of soil fungi

(1987;142:43). K252a is a membrane permeable, staurosporine analog and an inhibitor of Ca^{2+}/calmodulin-dependent protein kinases, phosphorylase kinases, many tyrosine and serine/threonine kinases (Ruegg and Burgess 1989; Elliott, Wilkinson et al. 1990; Chin, Murray et al. 1999). As reported by Smith R.J. *et al.*, K252a was initially discovered as an inhibitor of protein kinase C signalling in human polymorphonuclear neutrophils at an IC_{50} of 0.58μM (Smith, Justen et al. 1988). Inhibition of degranulation in neutrophils can also be observed upon K252a treatment at high IC50 values, 0.1–10 μM.

The inhibition of NGF signalling by K252a, was first tested in rat pheochromocytoma cells (PC12) which revealed an inhibition of NGF induced neurite outgrowth and the phosphorylation of various kinases including tyrosine hydroxylase at a concentration of 100nM (Hashimoto 1988). After a report by Berg M.M. *et al.*, K252a was demonstrated to act directly on NGF specific signal transduction in PC12 cells by inhibiting tyrosine phosphorylation and kinase activity of TrkA in a does dependent manner (Berg, Sternberg et al. 1992).

K252a is now used to inhibit TrkA, TrkB and TrkC signalling in varying cell types, investigating different neurotrophic factor signalling effects. Some examples of where K252a has been used as a Trk inhibitor include investigations on breast cancer cells, which normally express high levels of TrkA and are resistant to cell death. Upon K252a treatment, anoikis resistance was diminished (Lagadec, Meignan et al. 2009). K252a also inhibits NGF induced human aortic endothelial cell migration (Dolle, Rezvan et al. 2005), as well as inhibiting TrkB and BDNF autocrine signalling, promoting the proliferation of retinoblastoma tissue and retinoblastoma cell lines (Stephan, Zakrzewski et al. 2008).

However, it is worth noting that K252a is regarded as a high-affinity but nonselective kinase inhibitor known to disrupt Akt kinase (PKB), protein kinase CR (PKC-R), Ca++/calmodulin kinase II (CamKII), and cGMP-dependent protein kinase (PKG) (Hashimoto, Nakayama et al. 1991). Since K252a is not a specific inhibitor for Trk signalling, its effects were compared to a TrkB receptor analogue.

TrkB-domain 5 (TrkAd5) was constructed after the discovery of BDNF and NT-4s' specific binding site on the TrkB receptor structure. This binding site lies within the extracellular part of TrkB known as the immunoglobulin-like domain 5 (please refer to Trk receptor structure – illustration 1.3) (Holden, Asopa et al. 1997; Watson, Fahey et al. 2006). The TrkBd5 receptor analogue acts by binding to BDNF or NT-4, which in turn out competes with any extracellular BDNF and/ or NT-4 ligand. This 5th domain structure was cloned, purified and tested in vitro and in vivo for its inhibitory effects on TrkB signalling.

TrkBd5 binds with NT-4 and BDNF ligands with no significant binding with NGF (Banfield, Naylor et al. 2001; Naylor, Robertson et al. 2002). Upon nerve injury BDNF induced release from microglia is observed causing chronic constriction injury. TrkBd5 has been shown to attenuate the effects of chronic constriction injury (neuropathic pain) of the sciatic nerve from 20 day old rats by binding to BDNF (Lu, Biggs et al. 2009).

4.1.4 $p75^{NTR}$ cleavage and signalling inhibition

Since the latency III lines characterised in chapter 3 express both high and low affinity receptors for BDNF and NT-4, $p75^{NTR}$ signalling will also be of interest within this study. Upon phorbol ester treatment within cells expressing $p75^{NTR}$, a zinc dependent metalloprotease cleavage thought to be an α-secretase, induces shedding of the extracellular domain, leaving a membrane bound carboxy-terminal fragment (CTF) (DiStefano, Chelsea et al. 1993; Zampieri, Xu et al. 2005). $p75^{NTR}$, like the Notch receptor, then transmits its signals to the nucleus via an intracellular domain (ICD), cleaved from the transmembrane region of a CTF fragment by γ-secretase (Kanning, Hudson et al. 2003). A study by Kenchappa R. S., *et al*, using sympathetic neurones from rats, examined $p75^{NTR}$ cleavage upon ligand binding (Kenchappa, Zampieri et al. 2006). After a 2 day culture in 20ng/ml NGF, cells were treated with the $p75^{NTR}$ high affinity ligand, ProBDNF, it's low affinity receptors, BDNF and NGF as well as PMA for up to 24 hours. PMA, BDNF and ProBDNF ligands induced full length receptor (~75kDa) cleavage, producing a CTF (~30-24kDa), and an ICD fragment (~25-19kDa), whereas NGF ligand did not induce receptor cleavage. These $p75^{NTR}$ domains were identified by western blotting. The anti-$p75^{NTR}$ 9992 antibody used within the publication was provided by Moses Chao at New York University School of Medicine, USA. This antibody is a rabbit polyclonal, raised against the intracellular domain of $p75^{NTR}$ which recognises the full length $p75^{NTR}$ protein, the CTF as well as the ICD (Kanning, Hudson et al. 2003). This antibody was used within this study to detect any $p75^{NTR}$ protein in the characterised Burkitt's lymphoma B cell lines and to show possible $p75^{NTR}$ signalling by receptor cleavage.

Previously, it has been shown that ProBDNF or ProNGF can induce cell apoptosis in sympathetic neurons via $p75^{NTR}$ by outcompeting their mature equivalent proteins BDNF or

NGF which promote cell survival, growth, and differentiation (Chun and Patterson 1977; Teng, Teng et al. 2005). The co-expression of TrkA and $p75^{NTR}$, within these sympathetic neurons prevents ProNGF from stimulating $p75^{NTR}$ proteolysis but signalling via the mature form, NGF ligand. This is consistent with previous findings that TrkA expression inhibits γ-secretase dependent $p75^{NTR}$ cleavage (Kanning, Hudson et al. 2003).

Upon cleavage, the ICD can bind to varying proteins involved in cell apoptosis. These include, TRAF6, NRIF, NADE, Rac, NRAGE and Necdin. For apoptosis induction, the C-terminal domain of TRAF6 (TNF receptor associated factor) directly interacts with the death effector domain of pro-caspase 8, and the N-terminal RING domain, which is required for activation of caspase 8 (Khursigara, Orlinick et al. 1999; Yeiser, Rutkoski et al. 2004). NRIF (neurotrophin receptor interacting factor) is a ubiquitously expressed zinc finger protein which is a selective mediator for $p75^{NTR}$-dependent JNK activation and apoptosis in sympathetic neurones (Casademunt, Carter et al. 1999; Linggi, Burke et al. 2005). NRAGE (Neurotrophin Receptor–interacting MAGE homolog) binds $p75^{NTR}$ in the presence of NGF and can block the physical associated between $p75^{NTR}$ and TrkA (Salehi, Roux et al. 2000). When overexpressed in sympathetic neuron precursor cells, NRAGE induces NGF dependent apoptosis and cell cycle arrest. Necdin, also a member of the MAGE family, is a growth suppressor protein predominantly expressed in post-mitotic neurones. When $p75^{NTR}$ is over expressed in neuroblastoma cells, necdin is translocated to the proximity of the plasma membrane, reducing its association with the transcription factor E2F1, and enabling E2F1-induced death (Kuwako, Taniura et al. 2004).

The expression of $p75^{NTR}$ protein will be the initial task when investigating $p75^{NTR}$ signalling in Mutu latency III clone J8 cells. Next, the induction of apoptosis by ProBDNF will then be

explored. Possible $p75^{NTR}$ autocrine signalling in Mutu latency III clone J8 cells will then be addressed with the use of $p75^{NTR}$ antibodies to neutralise signalling.

These antibodies were obtained from collaboration with Robert A. Rush from Flinders University in Australia. Three functional monoclonal antibodies to human $p75^{NTR}$ were raised in knockout mice as illustrated within a publication by Mary-Louise Rogers *et al*,. (Rogers, Atmosukarto et al. 2006). These three monoclonal antibodies were names MLR1, MLR2 and MLR3. They recognise the ligand binding, extracellular domain region of $p75^{NTR}$ and can be used to detect $p75^{NTR}$ protein by western blotting, flow cytometry and immunohistochemistry methods. MLR1, MLR2 and MLR3 are biologically active antibodies that can neutralise NGF induced cell death in an NSC-34 mouse cell line which expressed $p75^{NTR}$ but lack TrkA (Turner, Murray et al. 2004).

Illustration 4.1: TrkB transcript variants

Isoform A

This variant (a; also known as Full length or wild type TrkB) encodes the full-length protein that contains the tyrosine kinase catalytic domain. This is the longest isoform (a).

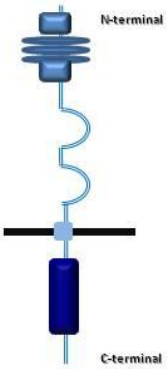

NCBI protein Reference:
NP_006171.2
Protein: 838aa
Core protein: 93.844kDa

NCBI mRNA Reference:
NM_006180.3
mRNA: 5608 bp

Isoform B

This variant (b; also known as TrkB-T1) uses an alternate terminal exon (exon 16 in PMID 11798182), which results in a truncated protein with a distinct C-terminus. Transcripts containing this alternate terminal exon have been detected in multiple tissues. The protein lacks the catalytic domain translational frameshift.

NCBI protein Reference:
NP_001007098.1
Protein: 477 aa
Core protein: 53.069kDa

NCBI mRNA Reference:
NM_001007097.1
mRNA: 7111 bp

Isoform C

This variant (c) includes the tyrosine kinase catalytic domain and omits an internal coding exon (17), resulting in a slightly shorter isoform (c).

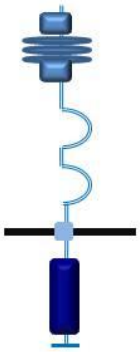

NCBI protein Reference:
NP_001018074.1
Protein: 822 aa
Core protein: 92.017kDa

NCBI mRNA Reference:
NM_001018064.1
mRNA: 5560 bp

Isoform D

This variant (d) uses an alternate terminal exon compared to transcript variant a. The resulting protein (isoform d, also known as TrkB-T-Shc) lacks the tyrosine kinase catalytic domain.

NCBI protein Reference:
NP_001018075.1
Protein: 553 aa
Core protein: 61.012kDa

NCBI mRNA Reference:
NM_001018065.2 mRNA:
8340 bp

Isoform E

This variant (e) uses an alternate terminal exon and omits a small internal coding exon compared to transcript variant a. The resulting protein (isoform e, also known as TrkB-T-Shc) lacks the tyrosine kinase catalytic domain.

NCBI protein Reference:
NP_001018076.1
Protein: 537 aa
Core protein: 59.185kDa

NCBI mRNA Reference:
NM_001018066.2
mRNA: 8292 bp

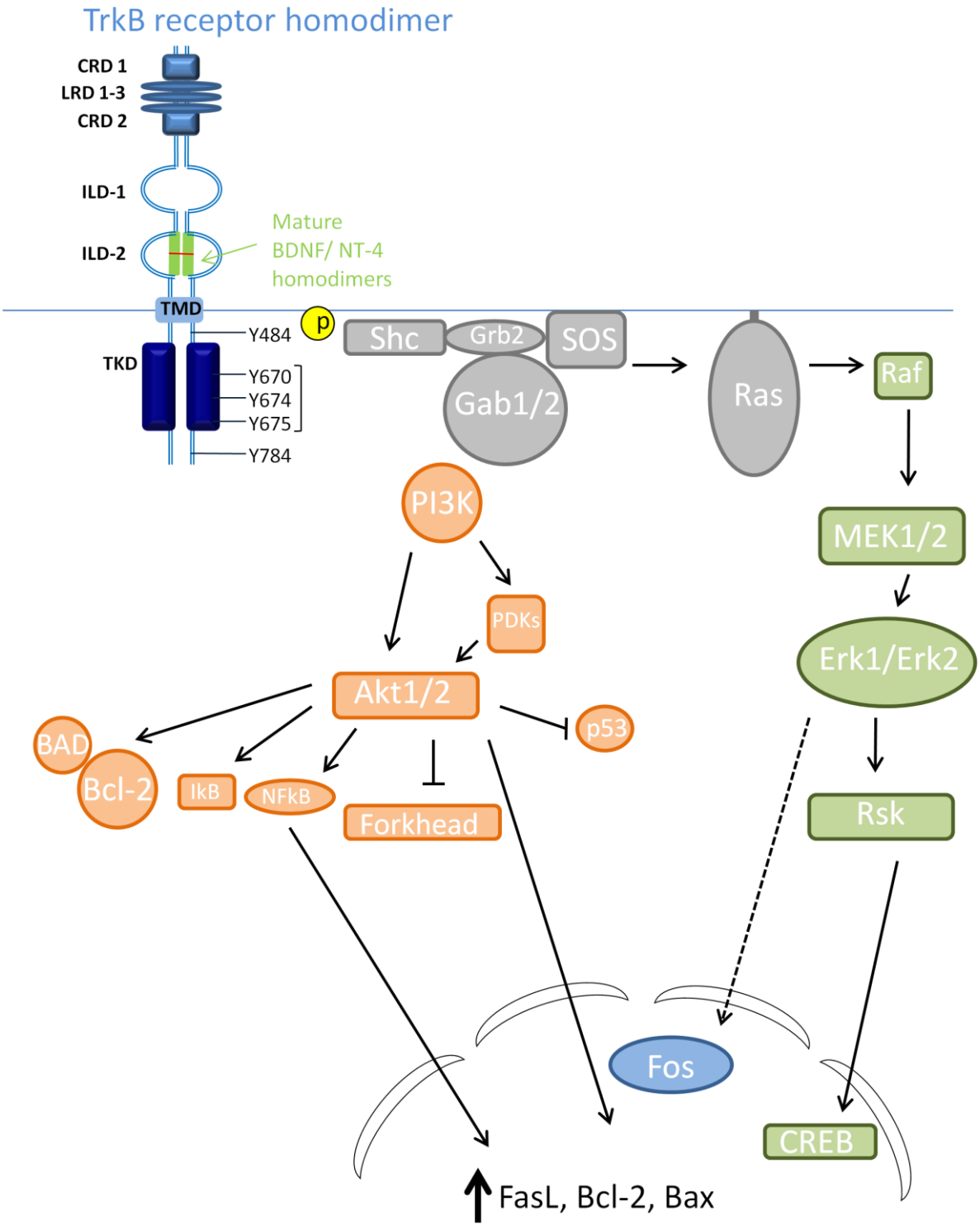

Illustration 4.2: Downstream TrkB signalling via Erk and Akt adaptor proteins
Upon binding of a BDNF/ NT-4 homodimer to the second immunoglobulin domain on full length TrkB receptor, receptor dimerization occurs inducing autophosphorylation. Adapter proteins then induce signalling pathways upregulating cell survival and or proliferation via Erk and/ or Akt.
(Note: Erk and/ or Akt induced activation can also occur upon BDNF/ NT-4 homodimers binding to TrkB:p75^{NTR} heterodimers.)

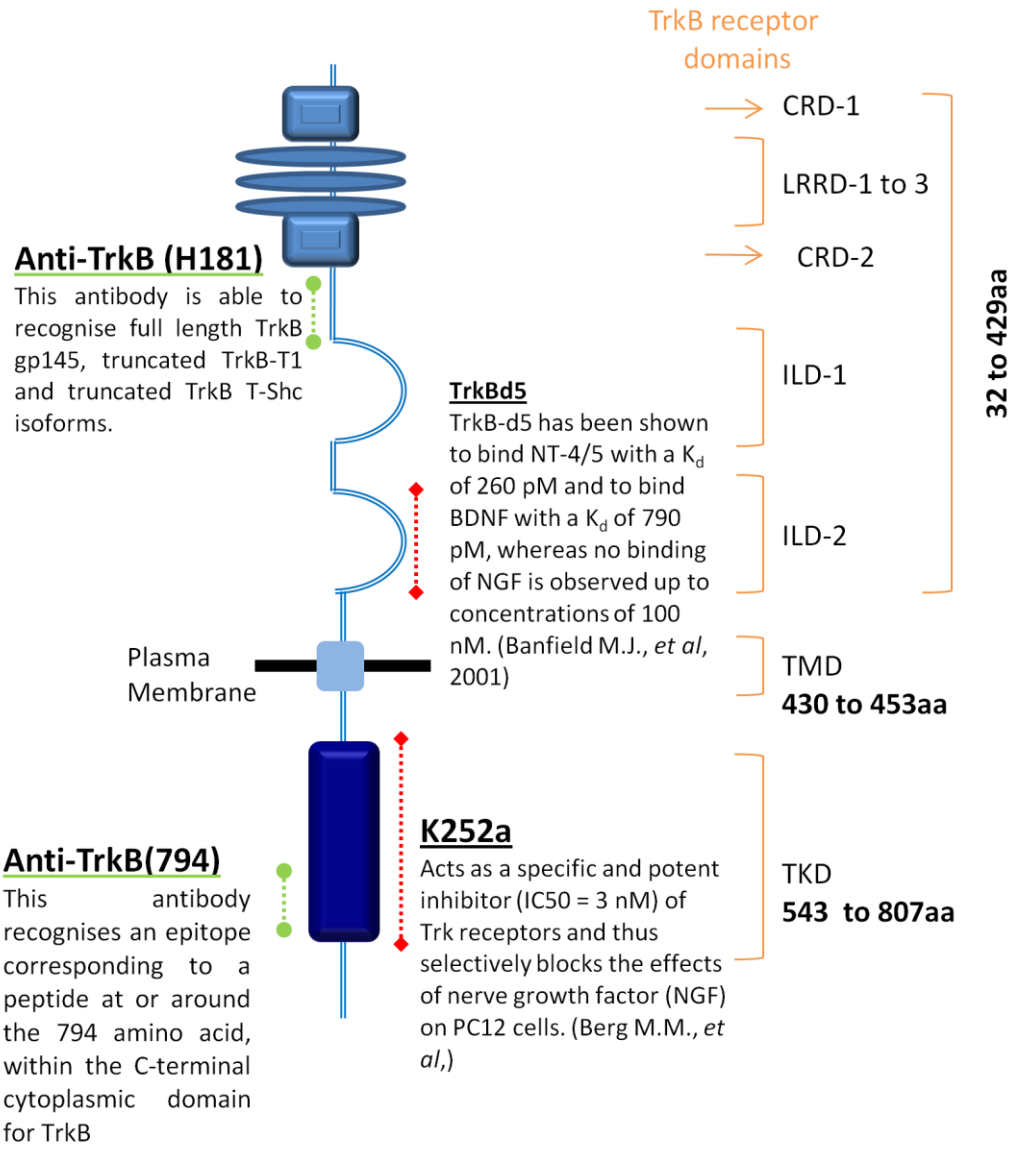

Illustration 4.3: TrkB receptor antibodies and inhibitors applied within the investigation
TrkB receptor domains and amino acid numbers are displayed. The reagents used to recognise TrkB protein by antibodies or inhibit TrkB signalling are displayed and annotated at the receptor regions they recognise/ hinder.
Key: Amino acids (aa), Cystein rich domain (CRD), Leucine rich domain (LRD), Immunoglobulin-like domain (ILD), Transmembrane Domain (TMD), Tyrosine kinase domain (TKD).

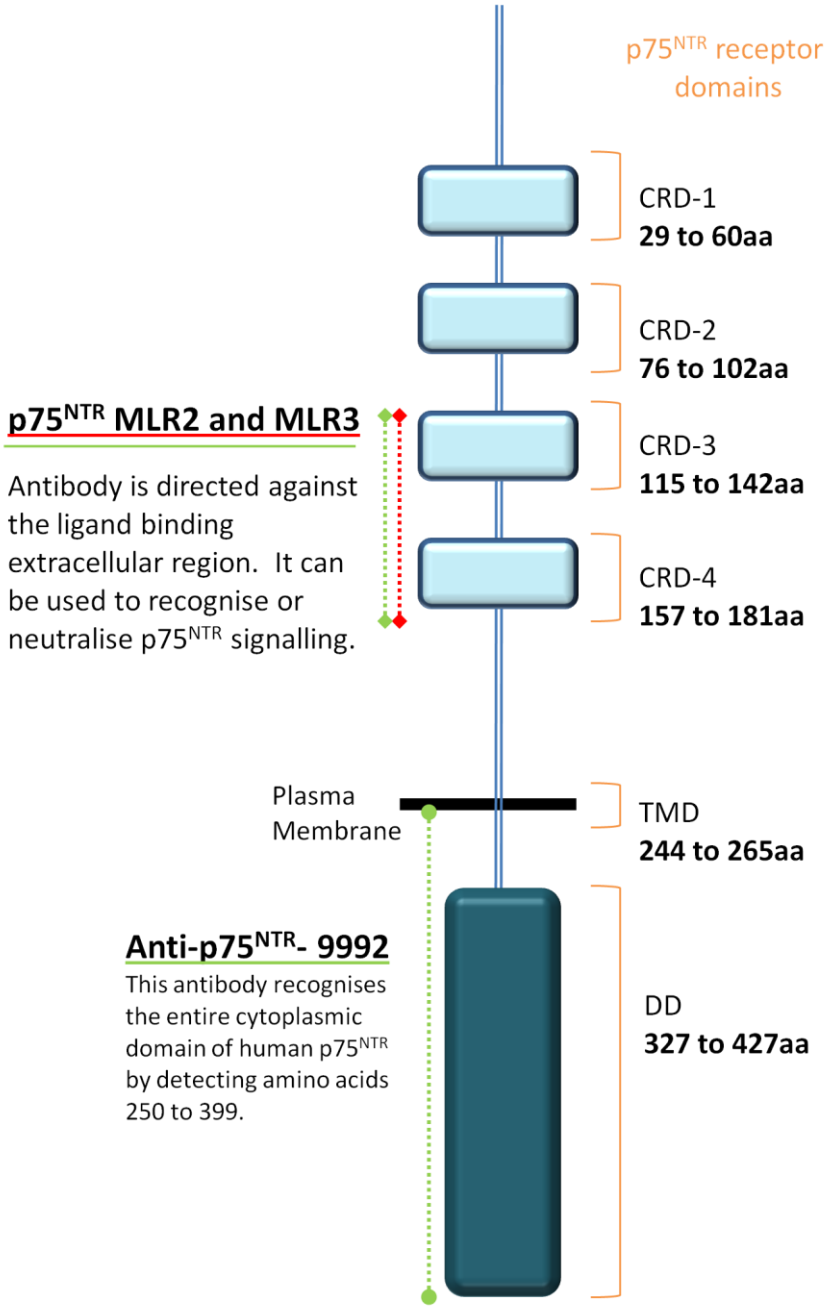

Illustration 4.4: p75^{NTR} receptor antibodies and neutralising antibodies applied within the investigation

p75^{NTR} receptor domains and amino acid numbers are displayed. The reagents used to recognise p75^{NTR} protein by antibodies or inhibit p75^{NTR} signalling are displayed and annotated at the receptor regions they recognise/ hinder. MLR antibodies were used to identify and neutralise p75^{NTR} protein.

Key: Amino acids (aa), Cystein rich domain (CRD), Transmembrane Domain (TMD), Death domain (DD).

4.2 Results

4.2.1 The expression of TrkB protein in Burkitt's lymphoma B cell lines by western blotting methods

To screen the previously characterised Burkitt's lymphoma lines for TrkB protein, two antibodies recognising varying TrkB receptor epitopes were applied for protein analysis. The first being, TrkB (794) which recognises an epitope corresponding to a peptide at or around the 794 amino acid, within the C-terminal cytoplasmic domain for TrkB. This antibody therefore can only recognize full length TrkB isoforms A and C.

20μg of Mutu negative clone 3, Mutu latency I clone 59, Mutu latency III clone J8 and IARC-171 protein samples were loaded per well. Once run within a 7% polyacrylamide with SDS gradient gel (Tris-Acetate buffer) under reducing conditions, samples were transferred onto PVDF membranes. Samples were probed using the TrkB (794) antibody alone or TrkB (794) antibody pre-treated with its specific peptide (figure 4.1.1). A table was drawn illustrating known TrkB isoforms and their core or glycosylated molecular weights. These molecular weights were obtained from the National Center for Biotechnology Information (NCBI), protein database linked with PubMed.

All Burkitt's lymphoma B cell lines analysed expressed a ~70kda band. According to the TrkB isofrom table shown in figure 4.1.1 this ~70kDa protein does not correspond to any of the known TrkB isoforms and is therefore an unknown protein. Mutu latency III clone J8 and IARC-171 lines on the other hand, expressed a ~145kda protein which may indicate

glycosylated full length TrkB protein. This full length TrkB protein was not detected in EBV negative clone 3 and EBV latency I clone 59 lines.

As expected, the peptide blocker prevented antibody binding to TrkB protein within all Burkitt's lymphoma samples although the unknown ~70kDa band was also diminished within all the cell lines analysed. His led to question wether the 70 kDa protein is a true TrkB protein.

There are publications where a 70kDa TrkB protein had been detected by western blotting methods. For example, a 70kDa protein can be detected in TRK-transformed NIH3T3 cells (Mitra, Martin-Zanca et al. 1987; Ohmichi, Decker et al. 1991). This 70kDa TrkB protein was shown to be preferentially located within the cytoplasm and can be phosphorylated in vivo, therefore the 70kDa band observed in all Burkitt's lymphoma lines may represent a genuine TrkB protein, however it is unknown which TrkB isoform is detected. For this to be further investigated mass spectronomy would be needed to secuence the unknown peptide for verification.

The second antibody used to probe for TrkB protein was Anti-TrkB (H181) which recognises an epitope corresponding to a peptide at or around the 181 amino acid, within the N-terminal extracellular domain for TrkB. At this epitope, the antibody is able to recognise full length TrkB gp145, truncated TrkB-T1 and truncated TrkB T-Shc isoforms.

20μg of Mutu negative clone 3, Mutu latency I clone 59, Mutu latency III clone J8, IARC-171 protein samples and 2μg of wild type (WT) HEK293 and TrkB transfected HEK293 cell samples were loaded per well. Once run within a 4% to 12% polyacrylamide with SDS gradient gel (Bis -Tris buffer) under reducing conditions, samples were transferred onto

PVDF membranes. All Burkitt's lymphoma lines analysed express ~61kDa, ~59kDa and ~53kDa proteins which may represent unglycosylated TrkB T-Sch (isoforms D), unglycosylated TrkB T-Sch (isoforms E) and unglycosylated TrkB T-1 (isoform B), respectively (figure 4.1.2).

Detected proteins running at a kDa range lower than ~51kDa were also observed on the western blot, however these proteins do not correspond to any known TrkB isoforms and may indicate degraded protein or the antibody may detect unspecific protein. To repeat this experiment I would be useful to initially do an SG substrate blocking step first. This method blocks the secondary antibody from binding directly onto protein transferred onto a PVDF which would in turn be detected by alkaline phosphatase chemiluminescent enzyme.

The same blot is magnified in figure 4.1.3 displaying TrkB isoforms at higher molecular weights. The ~94kDa to ~95kDa protein may represent unglycosylated full length TrkB protein which was observed in all Burkitt's lymphoma lines and TrkB transfected HEK293 cells. The ~94kDa band is thought to be full length TrkB core protein since HEK293-TrkB cells were transfected with just the full length TrkB protein, hence truncated isoforms would not be detected. Hence, the detection of only unglycosylated full length TrkB protein in transfected HEK293 cells is further indication that the ~61kDa to ~53kDa bands detected may represent truncated TrkB protein since these bands are absent within the transfected line.

The unglycosylated TrkB core peptide is also registered to migrate at around the 95kDa molecular weight, according to the NCBI, protein database. It is however unknown why transfected TrkB protein is not glycosylated within these HEK293s. This is unexpected since

previous publications on TrkB transfected HEK293 cells show fully glycosylated full length TrkB protein, viewed on western blots (Narisawa-Saito, Iwakura et al. 2002).

On the other hand, weak expression of the glycosylated ~145kDa, full length TrkB protein was observed within Mutu latency III clone J8 and a stronger band within IARC 171 cell samples but not the EBV negative or latency I samples.

To ensure the ~94kDa to ~95kDa bands suspected to be unglycosylated full length TrkB, and the ~145kDa bands suspected to be glycosylated full length TrkB protein are genuine proteins, all cell lines shown in figure 4.1.3 should ideally be treated in tunicamycine and/ or PNGase. These inhibitors disrupt N-glycosylation sites; therefore the predicted results would indicate all Burkitt's lymphoma lines and TrkB transfected HEK293 lines to express the ~94kDa to ~95kDa unglycosylated TrkB protein and the detection of the ~145kDa bands detected in latency III lines should be diminished. This experiment was not competed due to time restrictions.

Also, the expression of TrkB full length protein does not directly correspond to the PCR data concluded from the previous chapter, where TrkB isoform variants corresponding to full length TrkB mRNA were only detected within latency III Burkitt's lines. Within figure 4.1.3, the expression of full length TrkB protein is presumed to be expressed within all Burkitt's lymphoma cell lines, nonetheless the protein expressed seemed to migrate at ~94 to ~95kDa which may represent the unglycosylated, core TrkB protein. On the other hand, protein migrating at ~145kDa which may represent glycosylated full length TrkB protein was only detected within latency III lines.

The lack of detectable full length TrkB mRNA variants and yet the expression of full length unglycosylated TrkB protein within EBV negative and latency I lines may be due to the RT-PCR method which being too insensitive to detect full length TrkB transcripts in EBV negative Burkitt's lymphoma lines that may be present but at lower levels compared to the latency III lines. It is therefore also possible that EBV latency may upregulate full length TrkB mRNA transcript levels and this may influence the upregulation of glycosylated full length TrkB protein.

In conclusion, Burkitt's lymphoma cells lines that express full length TrkB mRNA variants also seem to express glycosylated full length TrkB protein as observed with the use of two different Anti-TrkB antibodies. It would however be useful to verify the multiple proteins observed by extracting protein from a western blot gel and extracting the peptides running at varying molecular weights. These proteins would then be sequenced to confirm the varying TrkB isoforms detected. Another method for verification could involve transfecting Mutu latency III lines with a full length specific TrkB expression silencer such as an siRNA. It would also be of great benefit to compare results from this experiment with the transfection of an siRNA that specifically targets truncated TrkB isforms. Any bands diminshed from the samples on a western blot may help also identify the proteins observed.

Add figs 4.1

4.2.2 The expression of TrkB protein in Burkitt's lymphoma B cell lines by confocal imaging

The TrkB (H-181) antibody was also used to screen for TrkB proteins using confocal imaging analysis. Burkitt's lymphoma lines were permeabilized with 0.1% saponin and probed for TrkB protein and DAPI nuclear stain (figure 4.2). A FITC- conjugated secondary antibody was used to observe any specific TrkB antibody bound to cells and viewed under confocal microscopy. Any TrkB antibody staining observed was compared to its non-immune isotype control.

The images shown in figure 4.2.1 are representatives of two independent experiments. Mutu negative clone 3 and Mutu latency I clone 59 staining were weak but positive (figure 4.2.1a) compared to Mutu latency III clone J8 and IARC-171 cells which show stronger TrkB protein staining (figure 4.2.1b). It can be noted that the positive TrkB stain is specific due to the lack of FITC-conjugated staining within the isotype controls for each cell line analysed.

To directly compare TrkB staining images between the Burkitt's lymphoma cell lines, the third confocal staining experiment is illustrated in figure 4.2.2 showing just TrkB staining. The isotype controls were negative for this set of images (data not shown), however an example of the control staining is shown for the positive control cell line KMS-11. From

these confocal images and the TrkB western blot results, it can be conclude that higher TrkB protein levels were observed with increasing EBV latency phenotype.

Analysing the western blotting data and the confocal images shows some correlation between the two methods for TrkB protein expression. Looking at western blots shown in figures 4.1.1 and 4.2.1, total TrkB protein levels seem to increase slightly from cells displaying an EBV negative phenotype compared to those with a latency III phenotype due to the number of bands detected.

This correlation of increasing total TrkB protein with increasing EBV latency is more clearly defined within the confocal images. The reason for this may be that the TrkB (H181) antibody may have higher affinity for certain TrkB isoforms when applied to PVDF membranes for western blotting as opposed to when it is applied to permeablised cells for confocal imaging. Hence more TrkB isoform structures and possibly degraded TrkB protein may be detected on a western blot membrane compared to permeablised cells.

So far it can be concluded that all Burkitt's lymphoma B cell lines analysed express truncated TrkB protein whereas those displaying latency III characteristics reveal higher total TrkB protein staining and detectable glycosylated full length TrkB protein.

Add figs 4.2

4.2.3 The expression of $p75^{NTR}$ protein in Burkitt's lymphoma B cell lines

Here, $p75^{NTR}$ protein expression levels were analysed within the same Burkitt's lymphoma lines. A $p75^{NTR}$ specific antibody ($p75^{NTR}$ 9992) provided by M.V. Chao, was applied for expression analysis by western blotting methods. This antibody recognises the entire cytoplasmic domain of the human $p75^{NTR}$ structure. 20μg of protein samples were run within a 4 to 12% polyacrylamide with SDS gradient gel (Bis-Tris buffer) under reducing conditions and transferred onto PVDF. Samples were then probed for $p75^{NTR}$ protein (figure 4.3).

The human neuroblastoma cell line, Kelly was used as a positive control for $p75^{NTR}$ protein expression. Several immunoreactive protein species were detected within the positive control, as well as all Burkitt's lymphoma lines. As well as the full length $p75^{NTR}$ ~75kda band, various bands with molecular weights ranging from ~35kDa to ~65kDa were also observed on the membrane within all cell lines analysed. These bands possibly represent degraded protein or immature nascent protein that is not fully glycosylated.

As shown in chapter 3, all Burkitt's lymphoma B cells express $p75^{NTR}$ mRNA with the exception of Mutu negative clone 4 and Mutu latency I clone 179 (figure 3.3.5). However $p75^{NTR}$ protein levels in Mutu latency I clone 179 lines were detected, although weaker compared to other Burkitt's samples (figure 4.3). A discrepancy between Protein and RT-PCR expression was also observed in the expression of $p75^{NTR}$ protein in Mutu negative

clone 4 line. This may be due to the sensitivity of the RT-PCR method in its lack of detecting low levels of $p75^{NTR}$ transcripts, particularly in Mutu negative clone 4 and Mutu latency I clone 179. On the other hand, the correlations between $p75^{NTR}$ mRNA and protein expression levels are similar within all other Burkitt's lymphoma lines analysed.

Next, $p75^{NTR}$ protein expression was analysed in the Burkitt's lymphoma cell lines by flow cytometry. Two $p75^{NTR}$ specific antibodies (MLR2 and MLR3), obtained from a collaboration with Robert A. Rush, were compared (Rogers, Atmosukarto et al. 2006).

Initially, to optimise antibody concentrations, Kelly cell line was used as a control. Intracellular as well as extracellular expression was detected from both $p75^{NTR}$ antibodies MLR2 and MLR3 (Figure 4.4.1). Higher levels of $p75^{NTR}$ protein were detected when Kelly cells were permablised compared to the live cell staining. Intercellular $p75^{NTR}$ expression levels were then analysed in Burkitt's lymphoma B cells using both MLR2 (figure 4.4.2) and MLR3 (figure 4.4.3).

Add figs 4.3 & 4

As shown in figure 4.4.2 and 4.4.3, detectable $p75^{NTR}$ protein was observed in all Burkitt's lymphoma lines.

However, EBV negative Mutu clone 3 lines expressed lower levels of $p75^{NTR}$ protein compared to all other EBV positive lines analysed. This is true for both MLR2 and MLR3 $p75^{NTR}$ antibodies tested by flow cytometry, however these $p75^{NTR}$ protein levels do not correlate with data obtained from $p75^{NTR}$ mRNA expression by RT-PCR (figure 3.3.5) or $p75^{NTR}$ expression by western blotting (figure 4.3). The differences in protein correlation levels maybe due to different antibody specificities between the anti-$p75^{NTR}$ MLR antibodies and that obtained from M.V. Chao.

As discussed by L. He and M.H. Fox, the differences in flow cytometry and western blotting methods include the accessibility of protein binding for the monoclonal antibodies. Cell lysate proteins separated by electrophoresis and transferred to membrane are more accessible compared to protein within intact, permeablised cells (He and Fox 1996).

Differences in flow cytometry and western blotting detection levels may also be altered depending on how the cells are permeablised for confocal staining. Burkitt's lymphoma lines shown in figure 4.2.2 were fixed in 2% paraformaldehyde then permeablised in 0.1%

saponin, this may have altered the epitope on the cell surface, affecting antibody specificity and binding.

However, it can be concluded that all Burkitt's lymphoma cell lines characterised, express $p75^{NTR}$ protein, regardless of their EBV latency phenotype.

4.2.4 The expression of BDNF and NT-4 protein in Burkitt's lymphoma B cell lines

Since Burkitt's lymphoma cell lines express TrkB and $p75^{NTR}$ receptor proteins, it was worth questioning protein expression of the receptor ligands, BDNF and NT-4. This was completed using specific antibodies for expression analysis by western blotting methods. 20μg of protein samples were run within a 4 to 12% polyacrylamide with SDS gradient gel (Bis-Tris buffer) under reducing conditions and transferred onto PVDF. Initially, samples were probed using an Anti-NT-4 primary antibody (figure 4.5.1).

All cell lines expressed a ~14kDa NT-4 specific protein, as compared to human recombinant NT-4 control (figure 4.5.1). The ~28kDa band observed within the recombinant protein sample may correspond to a mature NT-4 dimer but was not observed within any of the cell samples analysed, however this maybe due to the concentration of lysate added to the well, hence it would be useful to compare NT-4 protein expression in higher Burkitt's lymphoma cell lysate concentrations.

To compare the data obtained from the NT-4 western blot, NT-4 protein expression was analysed by flow cytometry. Burkitt's lymphoma cell lines together with the NT-4 positive control line (Colo-369) were permeabilized in 0.1% saponin and stained for NT-4 (figure 4.5.2). Gated cells are shown within the dot plots. These gates were then used to acquire 10,000 permeabilized and stained cells, measuring NT-4 expression levels using FL-1 laser settings. Histograms were used to display FL-1 levels for each cell line comparing secondary antibody alone stained cells, isotype control with secondary antibody stained cells and primary antibody with secondary antibody stained cells. Add figs 4.5

The flow cytometry data reveals expressed of NT-4 protein in all Burkitt's lymphoma lines analysed supporting the results obtained from NT-4 the western blots.

Next BDNF protein expression was analysed by western blotting methods (figure 4.6.1). This BDNF blot revealed many bands of various sizes. Mature BDNF is presumed to run at ~14kDa, as compared to the human recombinant BDNF control. All Burkitt's lymphoma B cell lines expressed this ~14kDa band. As for the BDNF homodimer which is alleged to run at ~27kDa, was detected only within the Mutu latency III clone J8 cell line.

Unprocessed, Pro-BDNF is presumed to run at ~35kDa, whereas its dimer is possibly what is observed at ~55kDa, ~57kDa and/ or ~60kDa. The multiple bands detected may also correspond to the multiple BDNF variants illustrated in table 4.1, which may be post-translationally modified. These BDNF variants are further discussed within this chapter's discussion section. Calregulin was used as the loading control.

On the other hand, although the levels are low, BDNF protein was detected within all Burkitt's lymphoma lines using flow cytometry analysis (figure 4.6.2). These protein levels show some correlation with the multiple bands detected by western blotting methods.

Add figs 4.6 and Table 4.1

Looking at the ~52 to ~60kDa ProBDNF bands in figure 4.6.2, stronger levels of protein are observed in IARC-171, latency I and III Mutu lines. As for the EBV negative line, the ~60kDa band is absent and shows lower levels of the ProBDNF protein presumed to run at ~55kDa and ~57kDa. Hence these ProBDNF bands may be readily detected by flow cytometry analysis.

In all, like NT-4, BDNF protein can be detected in all Burkitt's lymphoma B cell lines analysed. However both NT-4 and BDNF are secreted proteins, hence the best protein expression analysis method is by using an ELISA and comparing intracellular and extracellular protein. Research funds were only available to purchase one ELISA kit, which detected BDNF protein.

Upon secretion into the cellular environment, BDNF can bind and signal via extracellular TrkB and/ or $p75^{NTR}$ receptor domains. Therefore, intracellular and extracellular BDNF protein was measured for each Burkitt's lymphoma B cell line by ELISA (figure 4.7). When

cells from culture were centrifuged, pellets were used as intracellular samples, whereas supernatant was used as extracellular samples. For intracellular samples, 10^6 cells were lysed using the ELISA homogenisation buffer (review ELISA materials section within the materials and methods chapter for details). Specifically bound BDNF protein was detected by horseradish peroxidase enzyme, colour detection. OD values (read at 450nM) were collected for standard BDNF protein and for each cell line. BDNF concentrations for each cell line sample were then calculated using the linear regression equation from the standard curve graph (y = 0.001x + 0.0782). Kelly and KMS-11 cell lines were used as positive controls for the expression of BDNF protein. Add figs 4.7

In conclusion all Burkitt's lymphoma B cell lines expressed intracellular BDNF protein. Mutu cell lines expressed between 48.3 to 52.3 pg/ml intracellular BDNF protein. IARC 171 on the other hand expressed 110.3 pg/ml intracellular BDNF protein. Secreted BDNF obtained from cell culture supernatant was observed in all Burkitt's lines excluding Mutu negative clone 3.

Importantly, it is worth noting that the levels of intracellular and extracellular BDNF in MUTU latency I clone 59 and MUTU latency III clone J8 have very similar intracellular and extracellular BDNF concentrations, although IARC 171 cell line expressed the highest level of extracellular BDNF protein within all lines analysed. As for the control lines, Kelly and KMS-11, the highest levels of intracellular BDNF protein were recorded however, very low to undetectable levels of extracellular BDNF protein were observed.

BDNF protein was not detected in the media cells were grown in or the background control used to dilute the BDNF standards. Hence, all BDNF protein detected was obtained solely

from the cells. Burkitt's lymphoma cells lines displaying varying EBV latency phenotypes can therefore secrete detectable BDNF protein within the cellular environment.

4.2.5 The effects on cell survival upon TrkB:p75^{NTR} autocrine signalling inhibition in Mutu latency III clone J8 Burkitt's lymphoma B cell line

So far, it can be presumed that glycosylated full length TrkB receptors may dimerise with themselves and/ or with p75^{NTR} and induce autocrine signalling upon NT-4 or/ and secreted BDNF binding in Burkitt's lymphoma cell lines displaying a latency III phenotype.

To question whether TrkB:p75^{NTR} signalling is implicated in cell survival, a dose response to their inhibitors were utilized to assess the levels of live, early, late and necrotic cells 24 hours post treatment. Cells were then stained with a membrane permeable fluorochrome-labelled dye, PhiPhiLux which enables the measurement of caspase 3 activities, distinguishing early and late apoptotic cells. The fluorochrome generated by proteolytic cleavage of the caspase 3 substrate is proportional to the concentration of activated

caspase 3 within the cell sample. Prior to sample measurement by flow cytometry, propidium iodide (PI) was added to each cell sample to distinguish live cells from necrotic cells.

TrkB signalling was initially inhibited by treating cells with TrkBd5 which inhibits the fifth domain on the TrkB receptor (figure 4.8.1). A dose range from 1μM to 50μM TrkBd5 inhibitor concentration was added to Mutu latency III clone J8 cells for 24 hours. Control media (CM) and Tris buffer (TRIS), the vehicle control for TrkBd5 were used as control treatments compared to TrkBd5 treated cells. Mutu latency III clone J8 cells treated with 1μM TrkBd5 enabled cells survival and increased the number of live cells compared the control treated cells. At a concentration of 5μM and 10μM TrkBd5, reduced levels of live cells were observed, with higher early, late apoptotic and necrotic Mutu latency III cells. However 45.7% cells were early apoptotic at a concentration of 25μM whereas 71.1% of cells were late apoptotic at a concentration of 50μM. Therefore by inhibiting TrkB signalling in Mutu latency III clone J8, cells die from apoptosis.

The effects observed by TrkBd5 inhibition were compared to another Trk inhibitor, K252a. Between 50nM and 5μM concentrations of K252a live cell numbers decreased, as late apoptotic cell numbers increased (figure 4.8.2). Representative mean cell percentages from three independent experiments are displayed together with their standard error bars. This result is similar to that observed by inhibiting TrkB signalling alone, where cells die from apoptosis at higher concentrations of inhibitors.

To question whether $p75^{NTR}$ signalling is also involved in cell survival, increasing concentrations of the neutralising antibodies MLR2 and MLR3 were added to Mutu latency III clone J8 cells (figure 4.8.3). Interestingly, inhibiting $p75^{NTR}$ signalling by steric hindrance of extracellular $p75^{NTR}$ interactions with the specific antibodies does not inhibit cell survival. On the contrary, by adding $p75^{NTR}$ antibody MLR2 at a concentration of 50μg/ml and MLR3 at 10μg/ml, the highest level of live cells were observed. Therefore unlike TrkB, inhibiting $p75^{NTR}$ signalling does not induce cell death but may enable cell survival in Mutu latency III clone J8 cells.

Add figs 4.8.1 to 4.8.3

Since downstream TrkB signalling may involve Erk and Akt adapter proteins, the next experiment was to inhibit either Erk or Akt signalling and to question their effects on cell survival (figure 4.8.4). Between 1μM and 200μM Erk and Akt inhibitor concentrations were used in a dose response assay. Inhibiting Akt signalling by adding increasing concentrations of LY294002 resulted in a decrease in live cells but a gradual increase in necrotic cells. As for Erk inhibition, PD98059 used between 1μM to 50μM concentrations seemed to show similar live, early, late apoptotic and necrotic levels of cells with some late apoptotic cells and yet more necrotic cells compared to those control treated. Highest levels of late apoptotic cells were observed in cell treated in 100μM of PD98059, whereas those treated in 200μM PD98059 show the highest level of necrotic cells. Hence, inhibiting either Akt or Erk

signalling by adding their inhibitors at very high concentrations for 24 hours, induces cell necrosis in Mutu latency III clone J8 lines.

Add figs 4.8.4

At this point it can be concluded that Mutu latency III clone J8 cells express both TrkB and $p75^{NTR}$ receptors and their ligands BDNF and NT-4. Inhibiting TrkB signalling hinders cell survival by inducing apoptosis, while $p75^{NTR}$ inhibition may slightly enhance cell survival. However for this question to be looked at in more detail, it would be useful to treat cells in the same inhibitors and analysed cell lysates by a western blot probed for Poly (ADP-ribose) polymerase and Caspases such as 3, 8 or 9. Unfortunately due to time constraints and available funds these antibodies were not included in the investigation.

From these dose response experiments, the working concentrations of the inhibiters were determined. K252a was used at 0.5μM concentration, TrkBd5 used at 4.5μM, p75 neutralising antibodies (MLR2 and MLR3) used at 100μg/ml and Akt inhibitor (LY294002) and Erk inhibitor (PD98059) used at 50μM/ml. To ensure these inhibitors are targeting TrkB signalling, the next step was to question TrkB phosphorylation upon treatment with these TrkB inhibitors.

4.2.6 The inhibition of autocrine dependent TrkB phosphorylation in Mutu latency III clone J8 Burkitt's lymphoma B cell line

K252a is the most frequently used tyrosine kinase inhibitor within publications on neurotrophic factor signalling pathways. However K252a is known to inhibit TrkA, TrkB and TrkC signalling whereas TrkBd5 is a TrkB receptor specific inhibitor. TrkBd5 was therefore also utilised to question TrkB phosphorylation in MUTU latency III clone J8 cells. Since

$p75^{NTR}$ co-localises with TrkB during NT-4 and/ or BDNF dependent signalling, a neutralising $p75^{NTR}$ antibody (MLR2) was also used to question autocrine signalling.

ProBDNF protein has a higher affinity to $p75^{NTR}$ compared to TrkB receptor. The effects of exogenous ProBDNF treatment were also analysed and compared to the inhibition of NT-4 and BDNF neutralisation as well as TrkB and $p75^{NTR}$ inhibition, with the addition of ProBDNF treatment.

Neutralising antibodies specific for TrkB ligands, NT-4 and BDNF were included in the investigation to investigate if TrkB receptor phosphorylation is ligand dependent. These NT-4 and BDNF signalling inhibitors were then compared to the effects of the well documented K252a inhibitor.

Mutu latency III clone J8 cells were treated with these signalling inhibitors for one hour. 20μg of cell lysate samples were collected and run within 10% polyacrylamide with SDS gradient gels (Bis-Tris buffer) under reducing conditions and transferred onto PVDF. Samples were probed using a TrkB receptor antibody which recognises phosphorylated tyrosine residue Y705 protein (figure 4.9). These blots were then stripped and re-probed with an antibody that recognises full TrkB protein (TrkB H-181).

Mutu latency III clone J8 cells expressed both NT-4 and BDNF ligands. Inhibiting NT-4 or BDNF individually by steric hindrance of extracellular NT-4 and BDNF interactions with their specific antibodies (Anti-NT-4 used at 10μg/ml and Anti-BDNF used at 20μg/ml), TrkB phosphorylation was maintained; therefore NT-4 and BDNF are individually able to

phosphorylate TrkB. However when both ligands were inhibited (NT-4 Ab + BDNF Ab) TrkB phosphorylation is undetectable.

Mutu latency III clone J8 cells also express both $p75^{NTR}$ as well as full length TrkB receptors. When $p75^{NTR}$ alone was inhibited (Anti-$p75^{NTR}$ used at 100μg/ml) TrkB phosphorylation was still observed, however, by adding TrkBd5 inhibitor (TrkBd5 used at 4.5μM/ml), lower levels of TrkB phospho-protein were detected when compared to control treated Mutu J8 cells. On the other hand, by inhibiting both TrkB and $p75^{NTR}$ receptors ($p75^{NTR}$ Ab + TrkBd5) undetectable levels of TrkB phosphoprotein are observed.

Treatment with exogenous ProBDNF (ProBDNF used at 50ng/ml), which binds $p75^{NTR}$ was able to inhibit TrkB phosphorylation. Together with the inhibition of TrkB and p75 receptors (ProBDNF + $p75^{NTR}$ Ab + TrkBd5) or NT-4 and BDNF ligands (ProBDNF + NT-4 Ab + BDNF Ab), ProBDNF treatment resulted in undetectable levels of phospho-TrkB.

K252a on the other hand inhibits Trk kinase activity which when added alone (at 0.5μM/ml) inhibited TrkB phosphorylation. Upon the addition of human recombinant NT-4 and human recombinant BDNF exogenous TrkB ligands (both added at 50ng/ml), the levels of inhibition by K252a were slightly reduced by the observation of weak TrkB phospho-protein in cells treated in K252a plus the two human recombinant TrkB ligands.

Control cells were treated in either control media, DMSO, vehicle control for K252a or TRIS buffer, vehicle control for TrkBd5 for one hour. TrkB Phosphorylation was observed within all control cell samples, showing autocrine signalling via TrkB and $p75^{NTR}$ and their ligands NT-4 and BDNF.

Although the Anti-phospho-TrkB antibody used, recognised the ~95kDa band, protein running at ~50kDa to 10kDa were observed. Initially it was suspected that these unknown lower molecular weight bands may correspond to proteolytically degraded TrkB phosphor protein, however cell lysate samples were prepared with the appropriate protease inhibitors. Other possible explanations may involve unspecific secondary binding to lower molecular weight proteins. To eliminate this in future experiments it would be of interest to use an SG substrate blocker prior to the primary antibody incubation.

Importantly used as a control, when this blot was stripped and reprobed for TrkB protein expression using the Anti-TrkB (H181) antibody, all cell samples treated within the varying inhibitors expressed the full length glycosylated (~145kDa) and unglycosylated (~92kda) TrkB proteins. Although, Mutu latency III clone J8 cells treated in Anti-$p75^{NTR}$ antibody, the cell lysate concentration is slightly lower compared to the other cell samples on the blot. This inaccuracy is due to loading amounts during sample preparation.

Add figs 4.9

In conclusion, inhibiting both NT-4 and BDNF ligand signalling or both TrkB and $p75^{NTR}$ receptors, inhibits TrkB phosphorylation. However when either ligand or receptor is inhibited individually, TrkB phosphorylation is maintained. Therefore TrkB phosphorylation is dependent on TrkB, $p75^{NTR}$ and both NT-4 and BDNF. The addition of ProBDNF however, hinders this TrkB:$p75^{NTR}$ and NT-4:BDNF signalling pathway.

Although the results from the western blot are informative of TrkB phosphorylation in Mutu latency III clone J8 lines, to confirm that the addition of either Anti-NT-4 and Anti-BDNF neutralising antibodies, TrkBd5 and Anti-$p75^{NTR}$ neutralising antibody, ProBDNF protein or K252a truly inhibit TrkB phosphorylation, the effects of these inhibitor combinations could be compared to control treated in Mutu latency III clone J8 cells treated in Lambda Protein Phosphatase. This enzyme inhibits phosphorylated serine, threonine and tyrosine residues.

Also, to ensure that Anti-$p75^{NTR}$ antibody specifically targets $p75^{NTR}$ signalling, an Anti-Phospho-$p75^{NTR}$ antibody should be incorporated in the above experiment. However, during the time these experiments were conducted, this antibody was not commercially available.

The next sets of experiments were with taken to ask whether TrkB:$p75^{NTR}$ downstream signalling involves the Erk and/or Akt adaptor proteins.

4.2.7 The effect on cell proliferation upon TrkB:$p75^{NTR}$ autocrine signalling inhibition in Mutu latency III clone J8 Burkitt's lymphoma B cell line

To question the functional outcomes for TrkB:$p75^{NTR}$ signalling in Mutu latency III clone J8 lines, inhibitors were added in culture to observe any changes in cell proliferation. Cells

were stained with CFSE dye then cultured with varying TrkB: $p75^{NTR}$ signalling inhibitors for 48 hours. Histograms were plotted showing CFSE levels on day two; control media treated cells were compared to varying inhibitors as illustrated in figure 4.10.

Anti-IgM (2μg/ml) and Mitomycin C (40μg/ml) were used as positive controls to inhibit cell proliferation (figure 4.10.1). Both Anti-IgM and Mitomycin C slowed cell proliferation in Mutu latency III clone J8 cells as expected. Inhibiting Akt and Erk phosphorylation by treatment with their inhibitors LY294002 and PD98059 respectively, also slowed cell growth. PD98059, however, inhibited cell proliferation to a lesser extent compared to LY294002.

Adding the tyrosine kinase inhibitor, K252a inhibits cells proliferation in latency III Mutu cells. To ensure tyrosine kinase signalling was inhibited, exogenous human recombinant TrkB ligands BDNF and NT-4 were also added together with the K252a treatment which also prevented cell growth. This is further confirmation that inhibiting K252a inhibits the TrkB signalling pathway. DMSO was used as the vehicle control for K252a, which slowed cell growth but to a lesser extent compared to K252a.

Inhibiting TrkB ligands BDNF or NT-4 individually had no effect on cell proliferation, however when both ligands are inhibited within one treatment, cell proliferation was reduced in Mutu latency III clone J8 cells (figure 4.10.2).

The specific inhibitor for TrkB receptor, TrkBd5, also reduced cell proliferation. This inhibitor was compared to its vehicle control Tris buffer which had no effect on cell growth. Moreover, inhibiting the low affinity receptor $p75^{NTR}$ in Mutu latency III clone J8 cells had no effect on cell proliferation.

On the other hand, inhibiting both TrkB and $p75^{NTR}$ receptors slowed cell proliferation; however this was of a lesser extent compared to inhibiting TrkB signalling alone.

ProBDNF protein, which has a higher binding affinity for $p75^{NTR}$, was added to culture (figure 4.10.3). ProBDNF alone slows cell proliferation compared to control treated cells. This inhibition was slightly increased by adding neutralising antibodies for BDNF and NT-4, together with ProBDNF protein treatment. Interestingly, inhibiting the TrkB receptor, and enabling $p75^{NTR}$ signalling by adding ProBDNF, significantly hinders cell proliferation in Mutu latency III clone J8 cells.

Add figs 4.10

Taken together, these results indicate that inhibiting TrkB signalling by either inhibiting the receptor alone or its ligands BDNF and NT-4, reduces cell proliferation therefore TrkB enhances cell growth. While, inhibiting TrkB receptor and promoting $p75^{NTR}$ signalling by adding its high affinity ligand, ProBDNF, $p75^{NTR}$ signalling slows cell proliferation compared to control treated cells which signal via both TrkB and $p75^{NTR}$.

It would however be useful to compare these CFSE histograms by using another cell proliferation assay such as an MTT kit or simply counting live versus apoptotic cells by either using a haemocytometer in trypan blue stained cells or by simply staining with PI and acquiring cells on a flow cytometer.

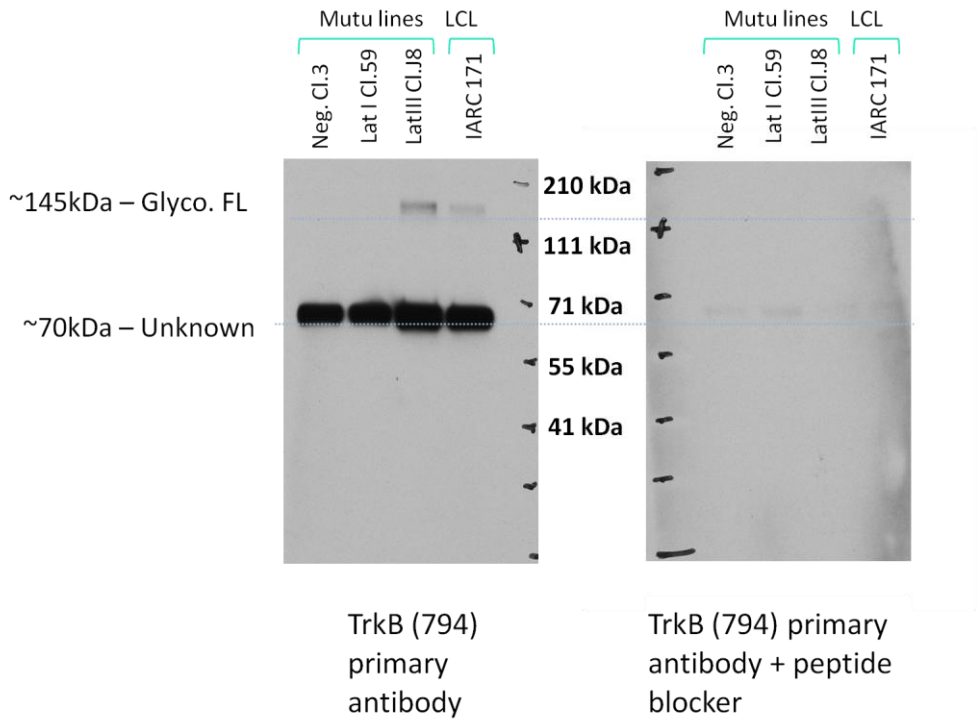

TrkB Isoforms		
Glycosylated Full length TrkB	Isoform A	~145kDa
Unglycosylated Full length TrkB	Isoform A	~94kDa
Glycosylated TrkB T-1	Isoform B	~95kDa
Unglycosylated TrkB T-1	Isoform B	~53kDa
Unglycosylated Full length TrkB (without exon 17)	Isoform C	~92kDa
Unglycosylated TrkB T-Sch (without tyrosine catalytic domain)	Isoform D	~61kDa
Unglycosylated TrkB T-Sch (without tyrosine catalytic domain)	Isoform E	~59kDa

Figure 4.1.1: The expression of TrkB proteins in Burkitt's lymphoma B cell lines
Western blot showing whole cell extracts (20μg protein) run within 7% polyacrylamide with SDS gels (Tris-Acetate buffer) under reducing conditions. Blots were probed for TrkB (794) primary antibody alone or TrkB (794) antibody with the blocking peptide. Full length TrkB protein is annotated according to the corresponding kDa sizes indicated within the TrkB isoforms table. Specifically bound antibodies were detected by an alkaline phosphatase chemiluminescent method and blots exposed to photographic film.

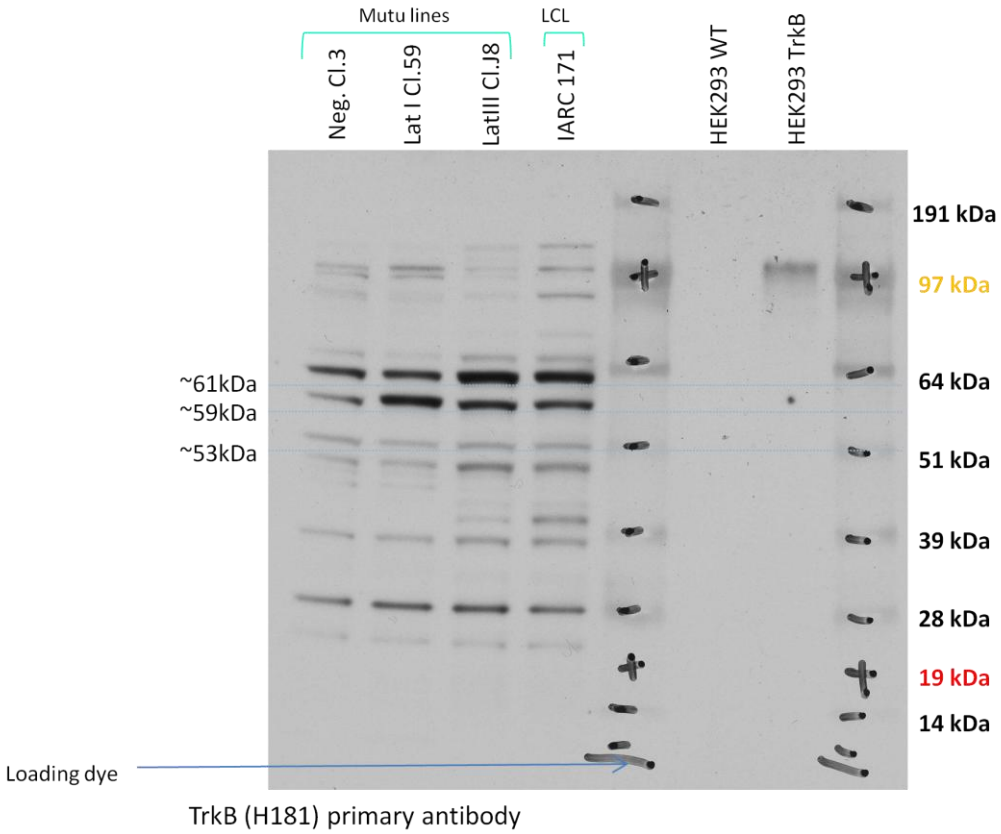

TrkB Isoforms		
Glycosylated Full length TrkB	Isoform A	~145kDa
Unglycosylated Full length TrkB	Isoform A	~94kDa
Glycosylated TrkB T-1	Isoform B	~95kDa
Unglycosylated TrkB T-1	Isoform B	~53kDa
Unglycosylated Full length TrkB (without exon 17)	Isoform C	~92kDa
Unglycosylated TrkB T-Sch (without tyrosine catalytic domain)	Isoform D	~61kDa
Unglycosylated TrkB T-Sch (without tyrosine catalytic domain)	Isoform E	~59kDa

Figure 4.1.2: The expression of TrkB isoforms in Burkitt's lymphoma B cell lines
Western blot showing whole cell extracts (20µg protein) run within a 4% to 12% polyacrylamide with SDS gel (Bis-Tris buffer) under reducing conditions. TrkB (H181) was the primary antibody used. Detected truncated TrkB is annotated according to the corresponding kDa sizes indicated within the TrkB isoforms table. Specifically bound antibodies were detected by an alkaline phosphatase chemiluminescent method and blots exposed to photographic film.

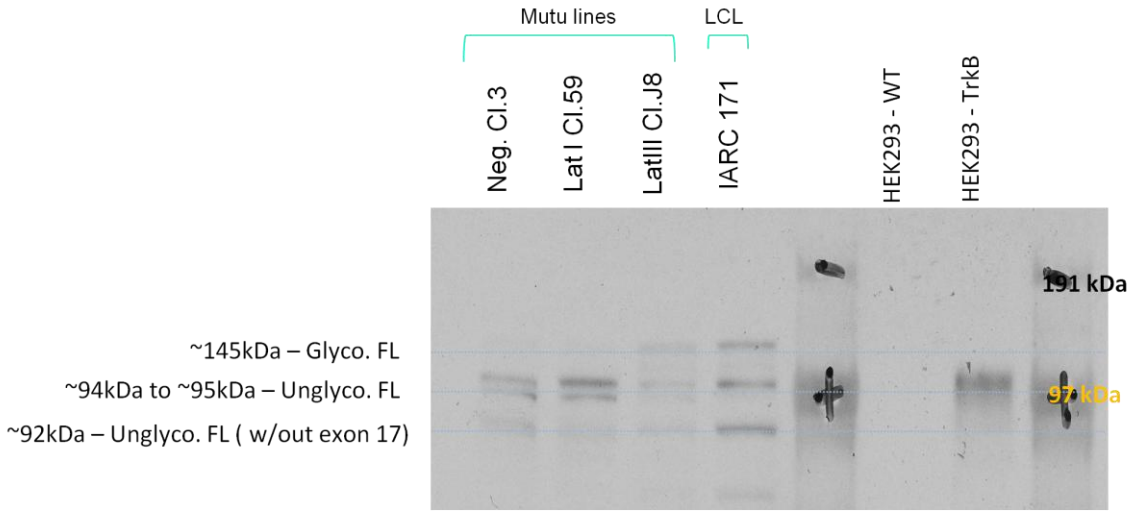

Figure 4.1.3: The expression of full length TrkB isoforms in Burkitt's lymphoma B cell lines
Western blot showing whole cell extracts (20µg protein) run within a 4% to 12% polyacrylamide with SDS gel (Bis-Tris buffer) under reducing conditions. TrkB (H181) was the primary antibody used to probe both western blots shown. Specifically bound antibody was detected by an alkaline phosphatase chemiluminescent method and blots exposed to photographic film.

The expression of glycosylated full length TrkB (Glyco. FL), unglycosylated full length TrkB (Unglyco. FL) and unglycosylated full length TrkB without exon 17 (Unglyco. FL w/out Exon 17) in Burkitt's lymphoma B cells are illustrated.

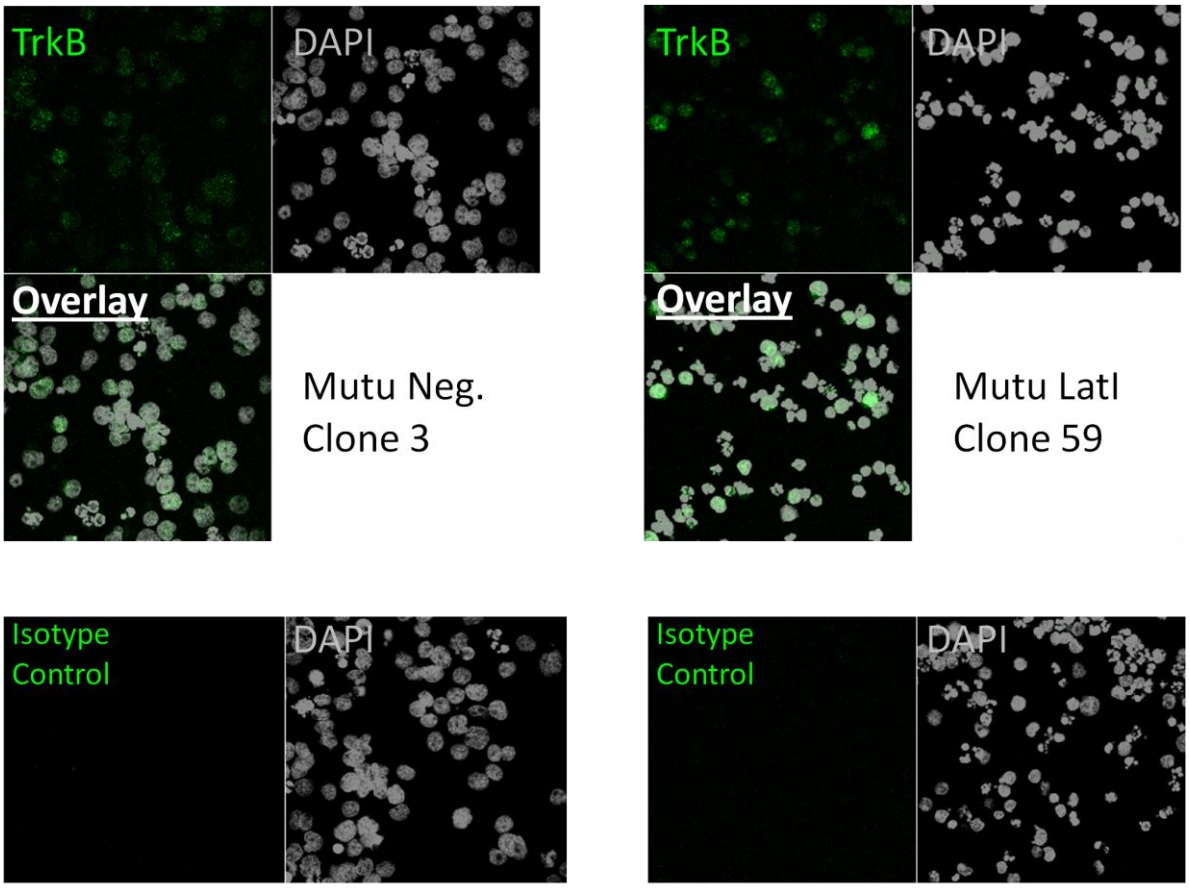

Figure 4.2.1a: The expression of TrkB protein in Burkitt's lymphoma B cell lines Mutu negative clone 3 and Mutu latency I clone 59

Confocal images showing permeablised Burkitt's lymphoma B cells stained for TrkB (H-181) primary antibody (this antibody recognises TrkB gp145, TrkB-T1 and TrkB-T-Shc isoforms) and DAPI nuclear stain. Specifically bound TrkB antibodies were detected by FITC-congugated secondary antibodies then viewed under an LSM laser miscroscope. Immunoglobulin specific isotype controls were also used to compare primary antibody staining. A representative of two independent experiments are shown.

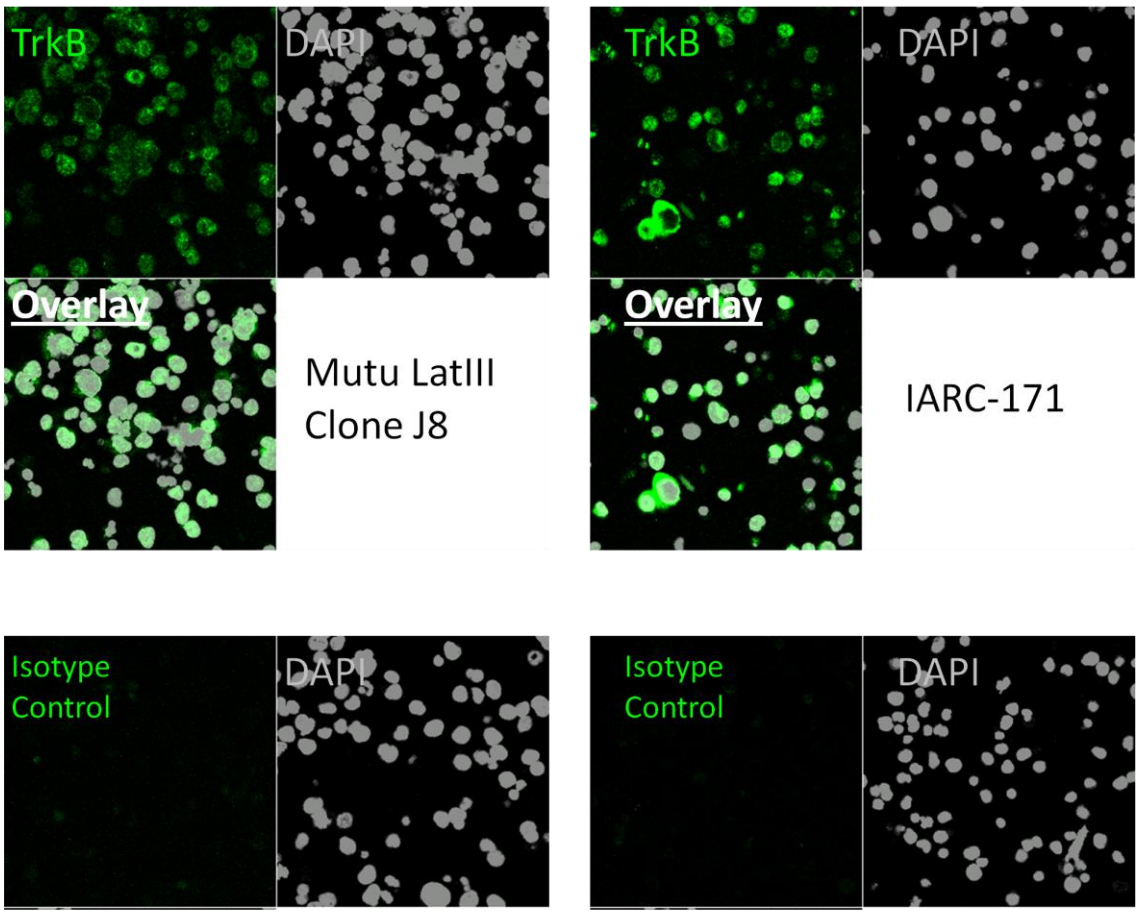

Figure 4.2.1b: The expression of TrkB protein in Burkitt's lymphoma B cell lines Mutu latency III clone J8 and IARC-171

Confocal images showing permeablised Burkitt's lymphoma B cells stained for TrkB (H-181) primary antibody (this antibody recognises TrkB gp145, TrkB-T1 and TrkB-T-Shc isoforms) and DAPI nuclear stain. Specifically bound TrkB antibodies were detected by FITC-congugated secondary antibodies then viewed under an LSM laser miscroscope. Immunoglobulin specific isotype controls were also used to compare primary antibody staining. A representative of two independent experiments are shown.

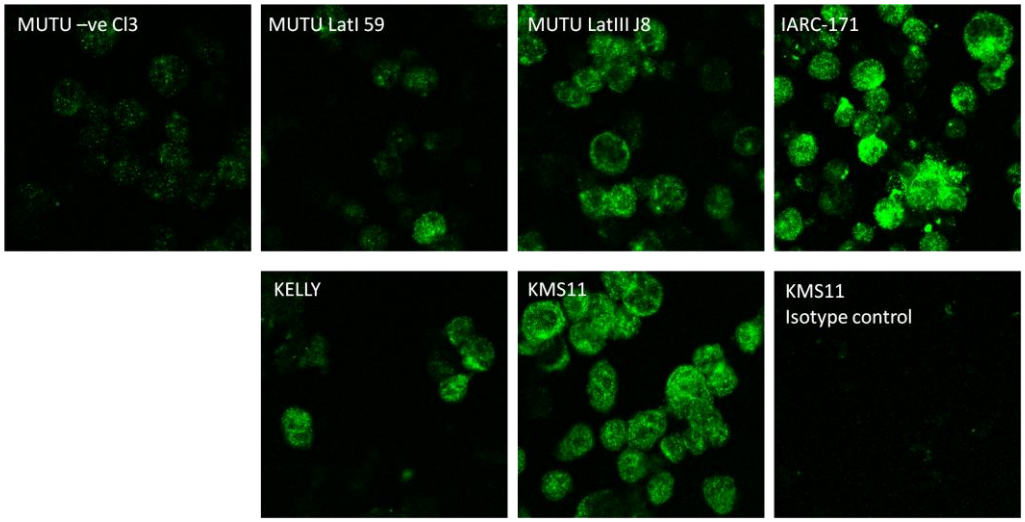

Figure 4.2.2: The expression of TrkB protein in Burkitt's lymphoma B cell lines
Confocal images showing permeablised Burkitt's lymphoma B cells stained for TrkB (H-181) primary antibody and DAPI nuclear stain. Specifically bound TrkB antibodies were detected by FITC-conjugated secondary antibodies then viewed under an LSM laser microscope. Immunoglobulin specific isotype controls were also used to compare primary antibody staining .

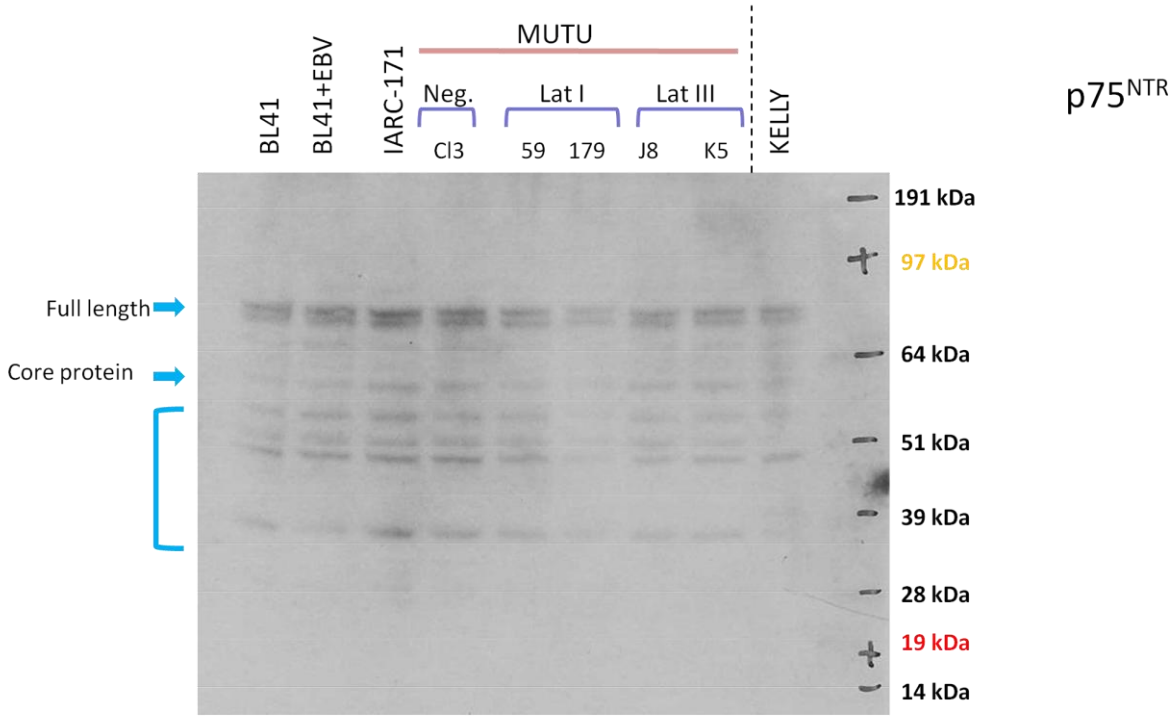

Figure 4.3: The expression of $p75^{NTR}$ in Burkitt's lymphoma B cell lines
Western blot of Burkitt's lymphoma lines probed for $p75^{NTR}$. All Burkitt's lymphoma lines express $p75^{NTR}$ protein as indicated with a blue arrow. Protein ranging from ~65kDa to 35kDa were also detected by the antibody. (n=3)

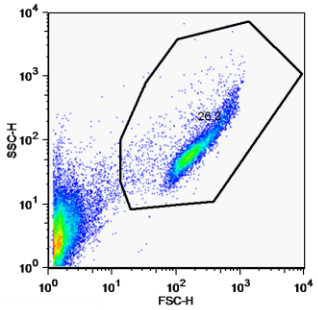

Unpermeablized live cells

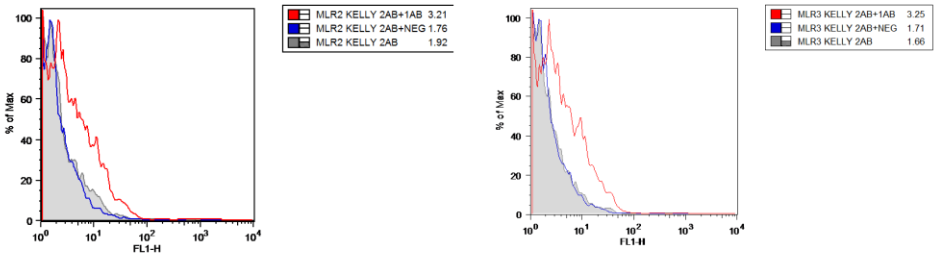

Permeablized cells

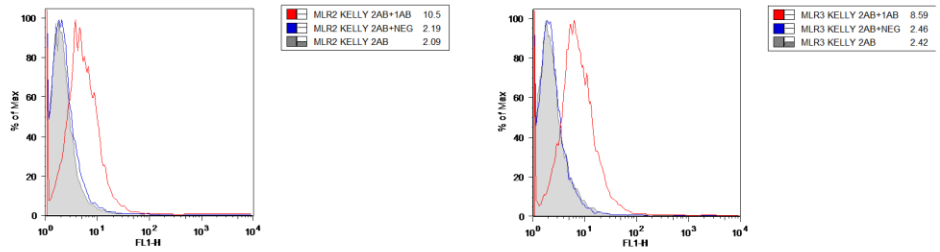

Figure 4.4.1: The expression of p75^{NTR} in positive control line KELLY

Unpermeabilized and permeabilized KELLY cells stained for flow cytometry analysis using two antibodies, MLR2 and MLR3, specific for p75^{NTR}. The dot plot shown above displays the population of 10,000 gated cells collected for FITC measurement.

MLR2 and MLR3 were the primary antibodies used (1AB) and compared to the isotype control (NEG). A secondary antibody directly conjugated with FITC (2AB) was used to detect specifically bound p75^{NTR} antibodies. Mean FITC levels were displayed from each histogram.

A representative of three independent experiments is shown.

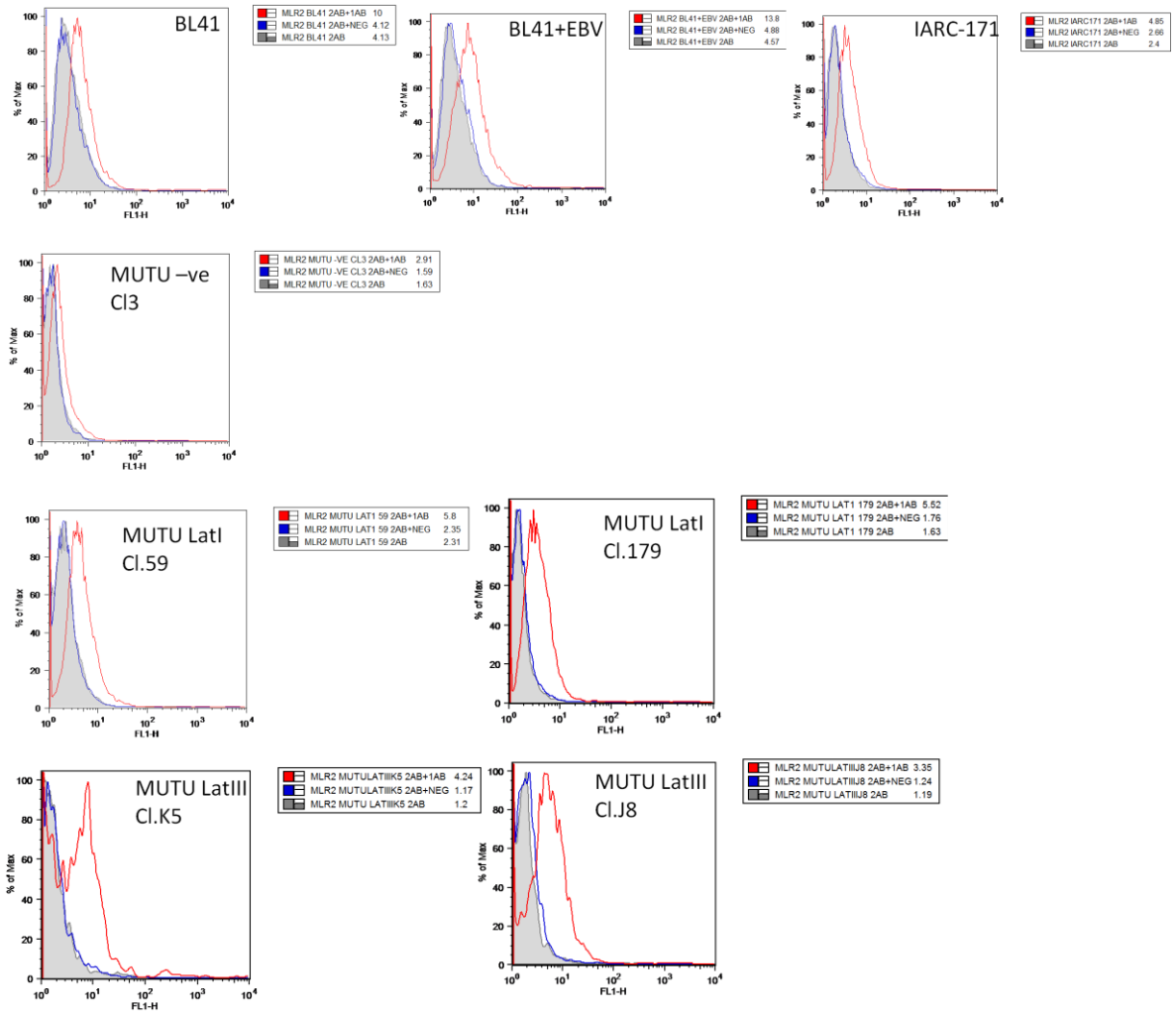

Figure 4.4.2: The expression of p75^{NTR} in Burkitt's lymphoma B cell lines

Permeabilized Burkitt's lymphoma B cells stained for flow cytometry analysis using MLR2 antibody specific for p75^{NTR}.

MLR2 was the primary antibody used (1AB) and compared to its isotype control (NEG). A secondary antibody directly conjugated with FITC (2AB) was used to detect specifically bound p75^{NTR} antibody. Mean FITC levels were displayed from each histogram.

A representative of three independent experiments is shown.

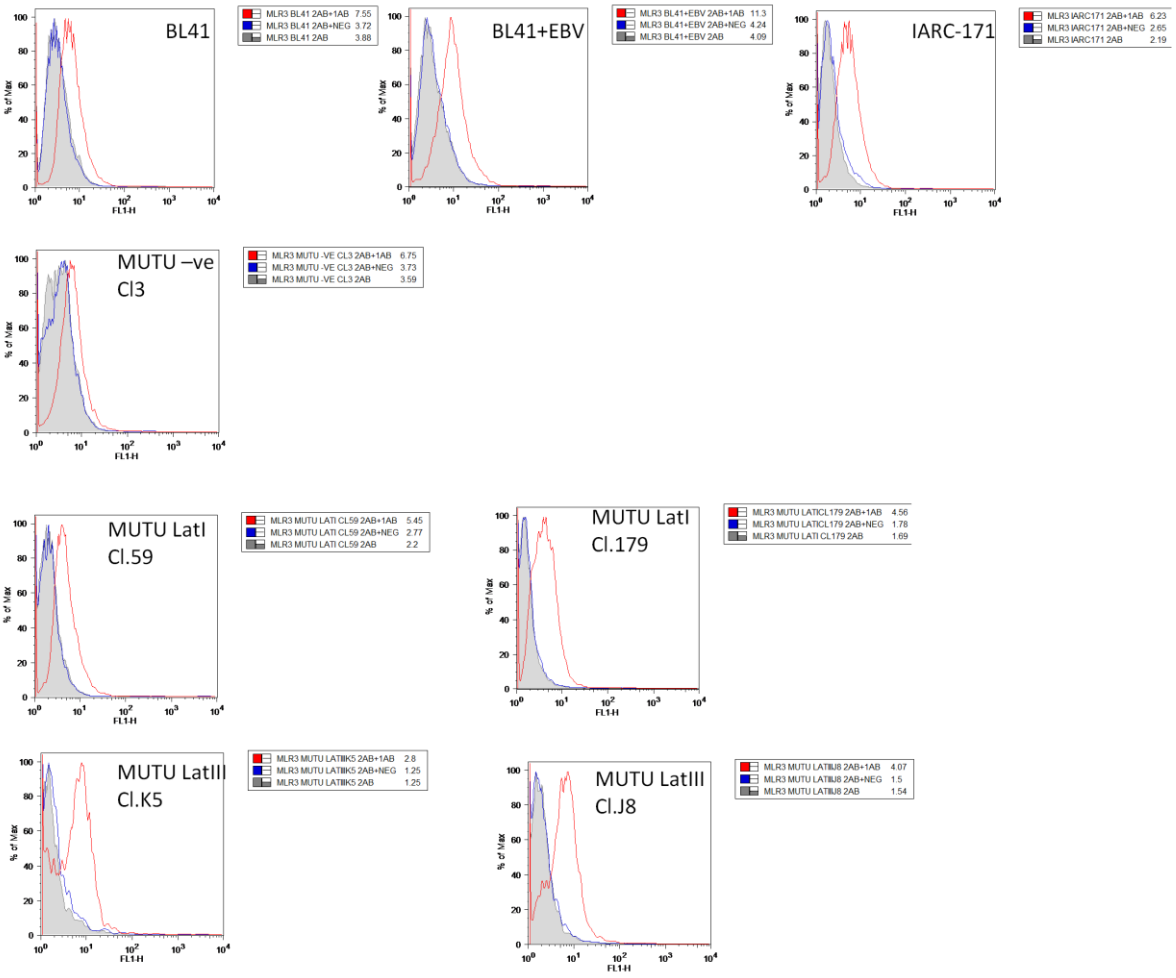

Figure 4.4.3: The expression of p75^{NTR} in Burkitt's lymphoma B cell lines

Permeabilized Burkitt's lymphoma B cells stained for flow cytometry analysis using MLR3 antibody specific for p75^{NTR}.

MLR3 was the primary antibody used (1AB) and compared to its isotype control (NEG). A secondary antibody directly conjugated with FITC (2AB) was used to detect specifically bound p75^{NTR} antibody. Mean FITC levels were displayed from each histogram.

A representative of three independent experiments is shown.

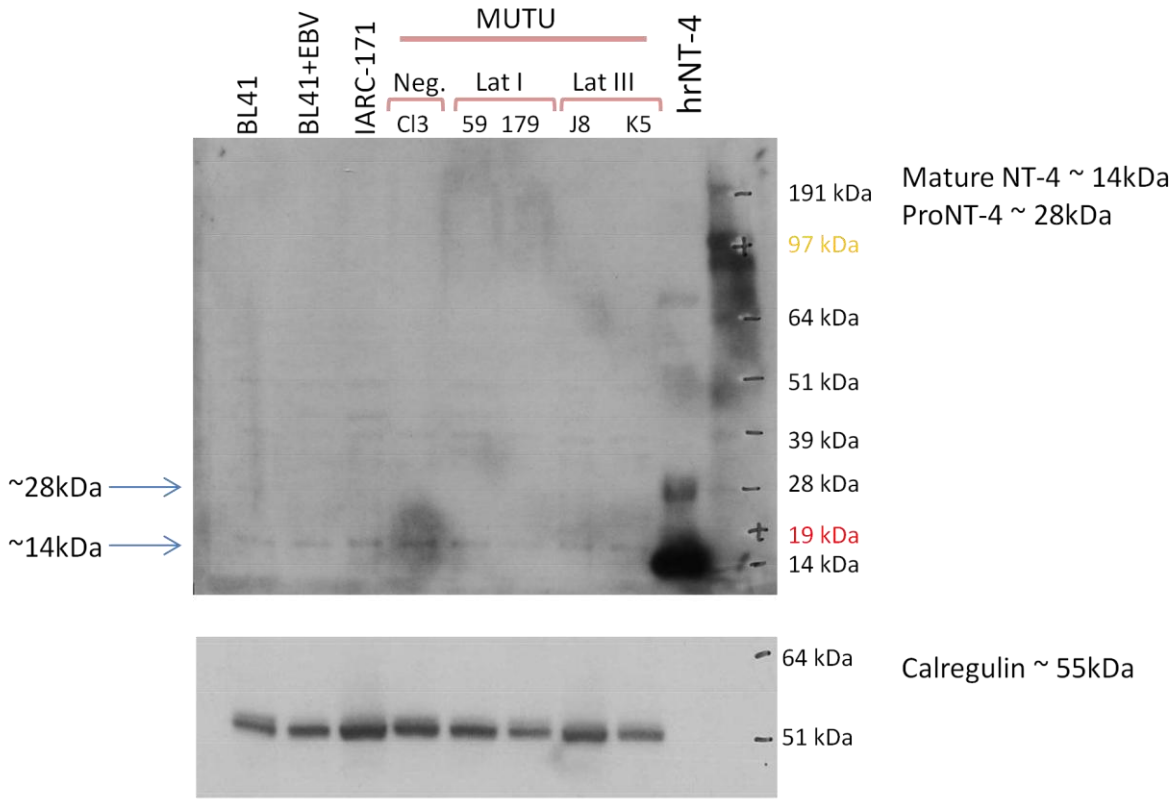

Figure 4.5.1: Western blotting expression analysis of TrkB ligand NT-4 in Burkitt's lymphoma B cells
Western blot showing whole cell extracts (20μg protein) run within a 4 to 12% polyacrylamide with SDS gradient gel (Bis-Tris buffer) under reducing conditions. NT-4 (Ab-9824) was the primary antibody used. 5μg of Human recombinant NT-4 (hrNT-4) was used as an NT-4 protein control. Specifically bound antibodies were detected by an alkaline phosphatase chemiluminescent method and blots exposed to photographic film. The same blot was stripped and re-probed for the loading control, Calregulin (n=3).

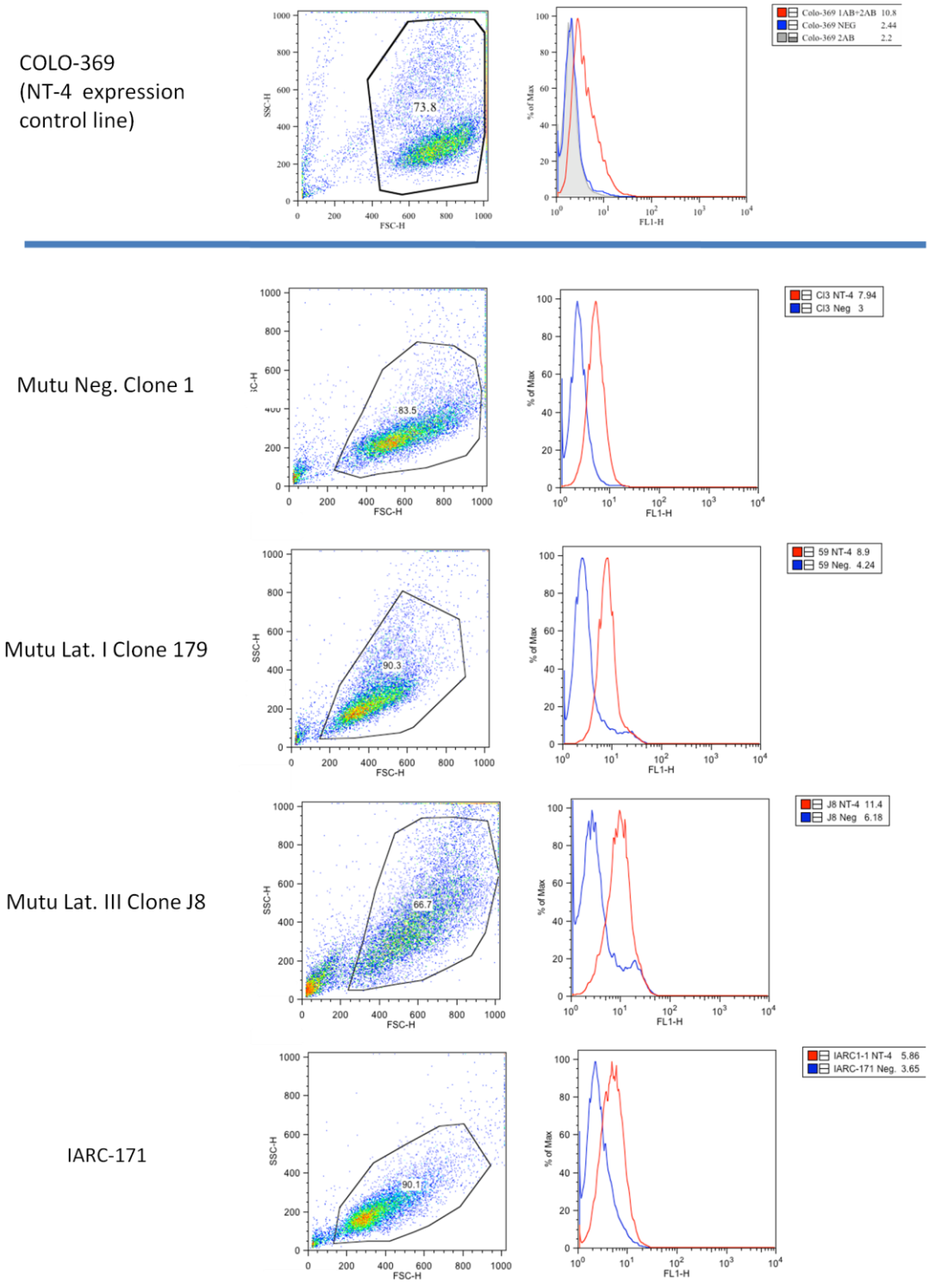

Figure 4.5.2: Flow cytometry expression analysis of TrkB ligand NT-4 in Burkitt's lymphoma B cells
Permeabilized Burkitt's lymphoma B cells stained with NT-4 antibody for Flow cytometry analysis . Dot plots display the gated population of cells collected for FITC measurement. NT-4 was the primary antibody used and compared to its isotype control (Neg.). A secondary antibody directly conjugated with FITC was used to detect specifically bound NT-4 antibodies. Mean FITC levels were displayed from each histogramme (n=3).

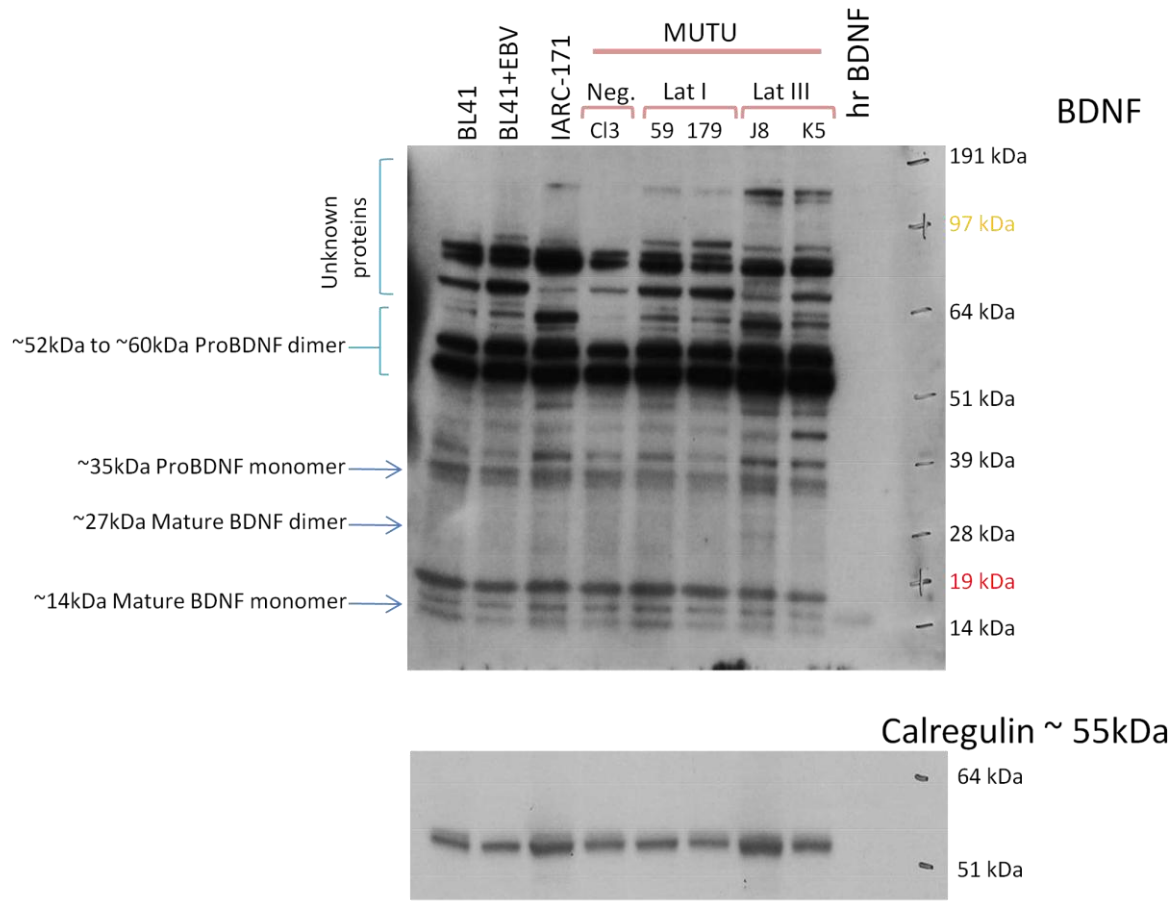

Figure 4.6.1: The expression of TrkB ligand BDNF in Burkitt's lymphoma B cells
Western blot showing whole cell extracts (20μg protein) run within a 4 to 12% polyacrylamide with SDS gradient gel (Bis-Tris buffer) under reducing conditions. BDNF (GF35L) was the primary antibody used. 1μg of Human recombinant BDNF (hrBDNF) was used as the BDNF protein control. Specifically bound antibodies were detected by an alkaline phosphatase chemiluminescent method and blots exposed to photographic film (n=3).

Table 4.1: Alternatively spliced human BDNF variants

Variant	BDNF Isoforms	aa	NP number	Da	Notes (aka)
Variant 1	isoform a preproprotein	247 aa	NP_733931	27,836	IX
Variant 2	isoform a preproprotein	247 aa	NP_733928	27,836	IIc, BDNF2C, or 2-5
Variant 3	isoform b preproprotein	255 aa	NP_733927	28,890	I, BDNF1, or 1-5
Variant 4	isoform a preproprotein	247 aa	NP_001700	28,736	VIb or BDNF5
Variant 5	isoform a preproprotein	247 aa	NP_733929	27,836	IV, BDNF4, or 3-5
Variant 6	isoform c preproprotein	262 aa	NP_733930	29,835	VIIb, BDNF6B, or 4I-5
Variant 7	isoform a preproprotein	247 aa	NP_001137277	27,836	IIa or BDNF2A
Variant 8	isoform a preproprotein	247 aa	NP_001137278	27,836	IIb or BDNF2B
Variant 9	isoform a preproprotein	247 aa	NP_001137279	28,736	III or BDNF3
Variant 10	isoform a preproprotein	247 aa	NP_001137280	28,736	Va
Variant 11	isoform a preproprotein	247 aa	NP_001137283	28,736	V-VIII-VIIIh
Variant 12	isoform a preproprotein	247 aa	NP_001137284	28,736	Vh
Variant 13	isoform a preproprotein	247 aa	NP_001137285	28,736	VIa
Variant 14	isoform a preproprotein	247 aa	NP_001137286	28,736	VIb-IXbd
Variant 15	isoform a preproprotein	247 aa	NP_001137287	28,736	VIIa or BDNF6A
Variant 16	isoform a preproprotein	247 aa	NP_733931	28,736	IXabd
Variant 17	isoform d preproprotein	276 aa	NP_001137281	31,134	Vb

Variants 1, 2, 4, 5, and 7-16 encode the same isoform (a) and differ in the 5' UTR and represents use of an alternate promoter compared to variant 1

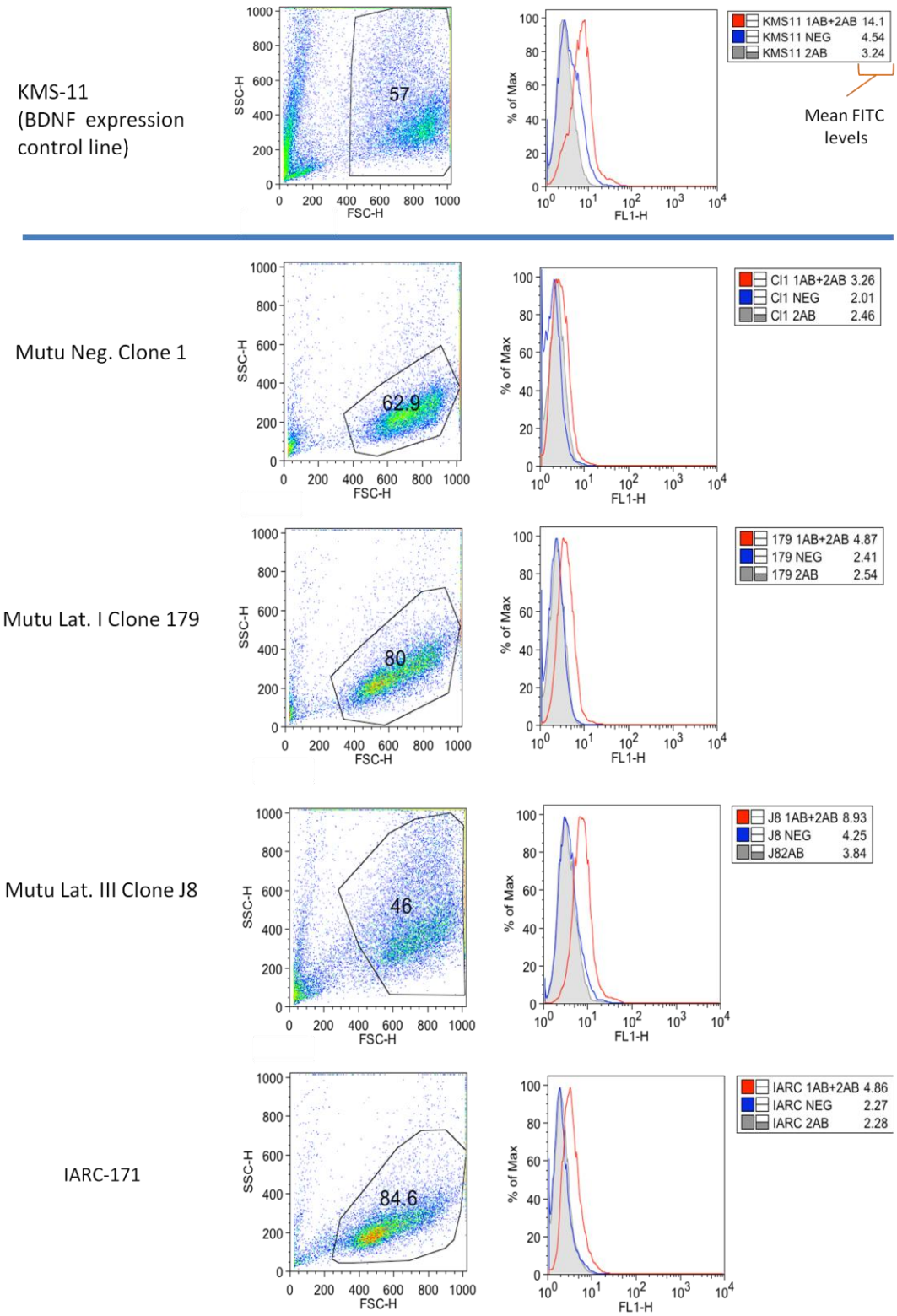

Figure 4.6.2: The expression of TrkB ligand BDNF in Burkitt's lymphoma B cells

Permeabilized Burkitt's lymphoma B cells stained with BDNF antibody for Flow cytometry analysis . Dot plots display the population of gated cells collected for FITC measurement. BDNF (GF35L) was the primary antibody used (1AB) and compared to its isotype control (NEG). A secondary antibody directly conjugated with FITC (2AB) was used to detect specifically bound BDNF antibodies. Mean FITC levels were displayed from each histogramme (n=3).

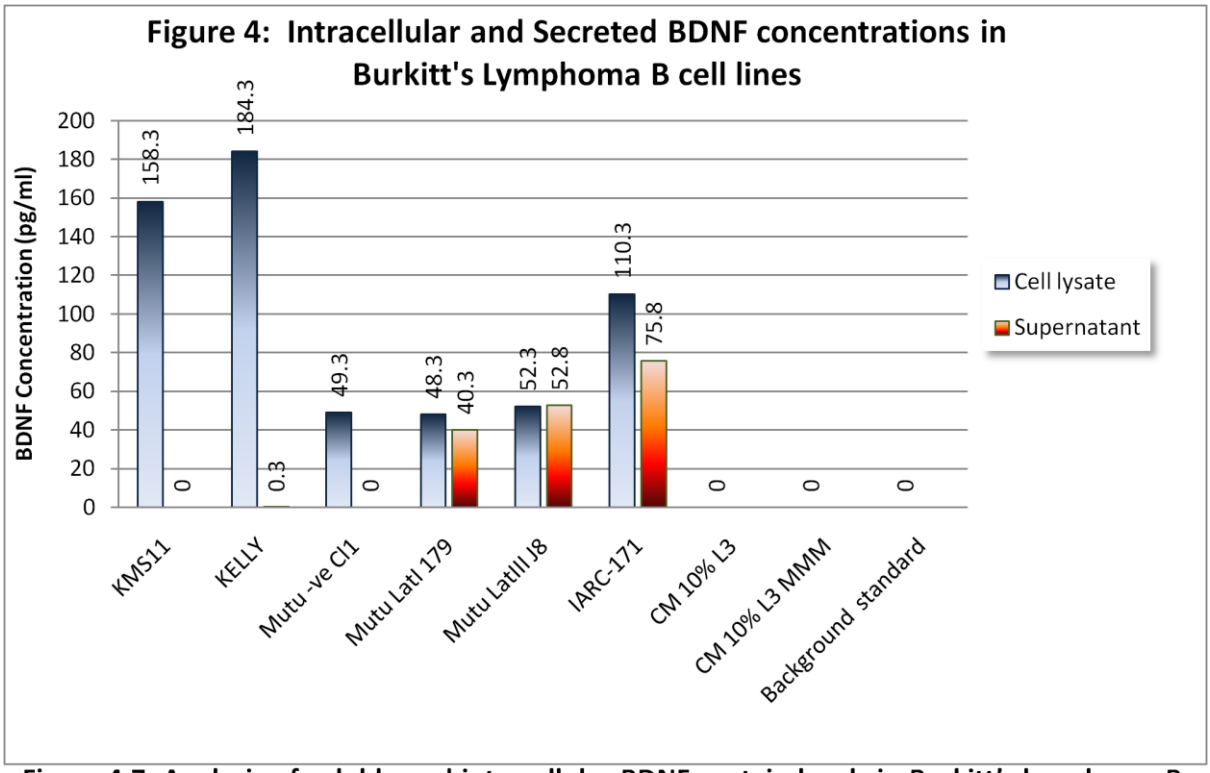

Figure 4.7: Analysis of soluble and intracellular BDNF protein levels in Burkitt's lymphoma B cells. Intracellular and extracellular protein obtained from Burkitt's lymphoma B cell lines were added to a BDNF antibody pre-coated 96-well plate. Specifically bound antibody was detected by horseradish peroxidise enzyme, colour detection measured on a spectrophotometer at an optical density of 450nM.

A linear regression equation (y = 0.0001x + 0.0782) was used to calculate actual BDNF concentrations in the Burkitt's lymphoma cell lines and the BDNF control cell lines KMS-11 and KELLY.

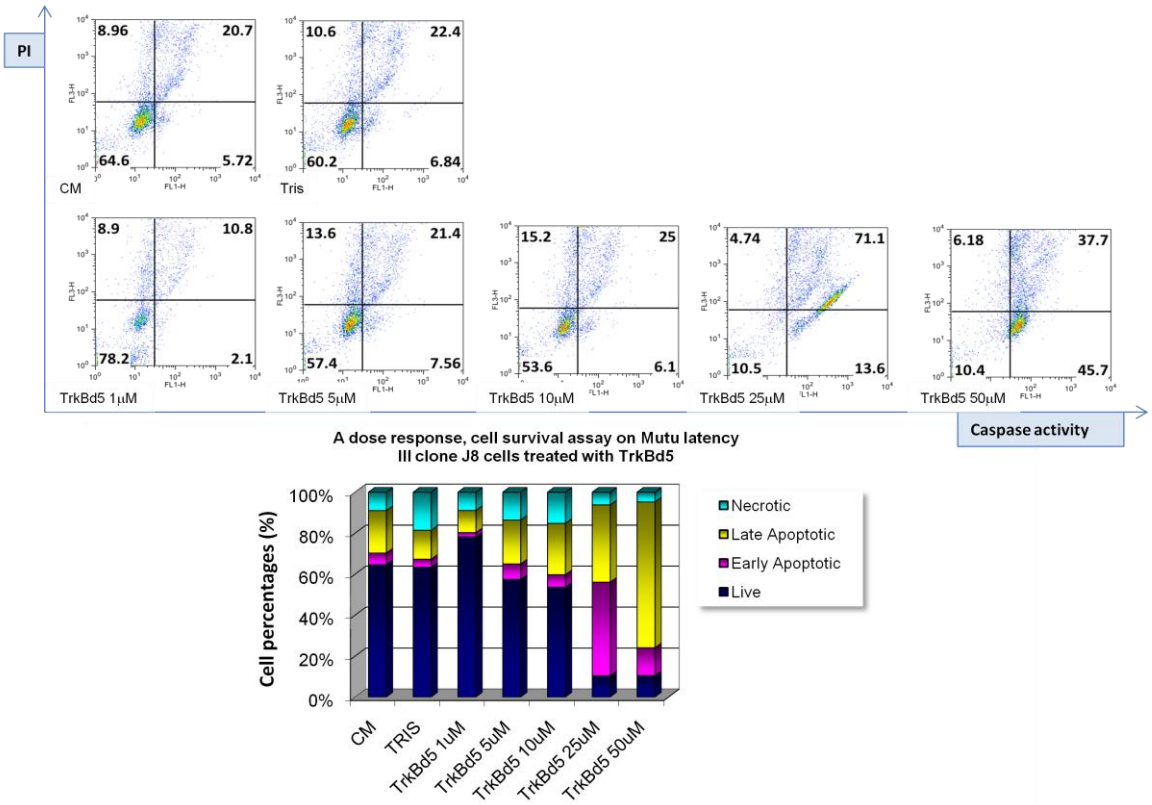

Figure 4.8.1: Cell survival assay on Mutu latency III clone J8 cells treated with TrkB signalling inhibitor TrkBd5
Dose response analysis on cells treated in control media (CM), Tris buffer (TRIS-vehicle control for TrkBd5) and TrkB signalling inhibitor, TrkBd5 for 24 hours. PI/PhiPhiLux stained cells were measured by flow cytometry for live cells, early, late apoptotic and necrotic cells.

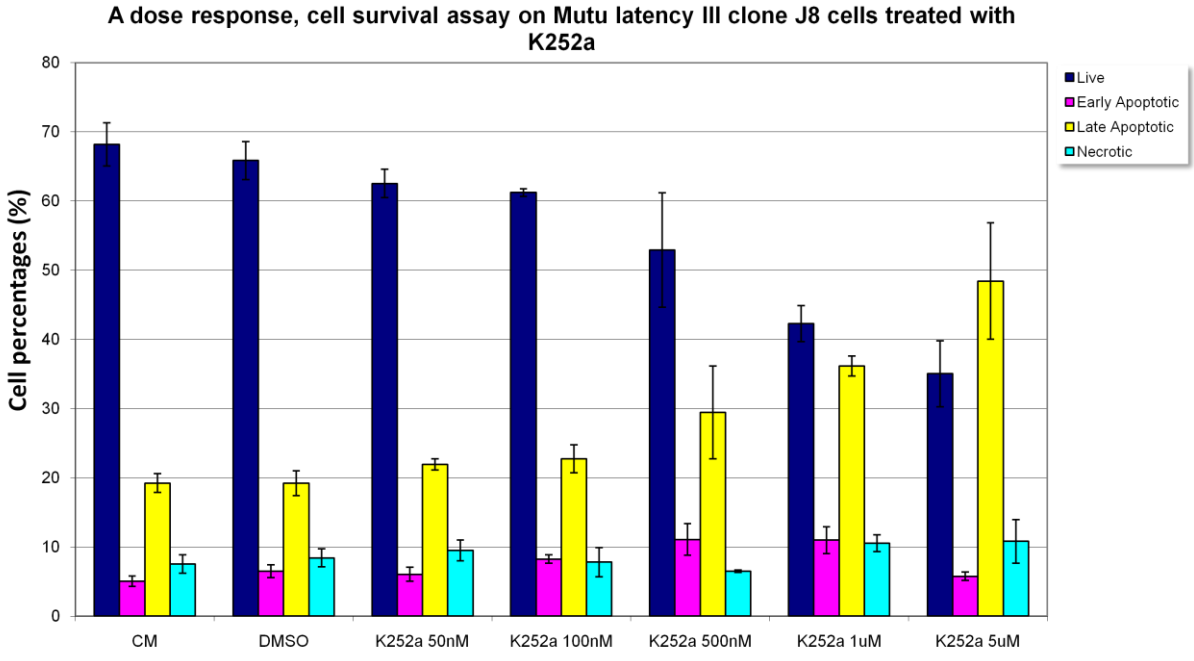

Figure 4.8.2: Cell survival assay on Mutu latency III clone J8 cells treated with Trk signalling inhibitor K252a
Dose response analysis on cells treated with 50nM to 5μM K252a for 24 hours. PI/PhiPhiLux stained cells were measured by flow cytometry for live cells, early, late apoptotic and necrotic cells. Mean cell percentages and standard deviation error bars were calculated between three independent experiments.

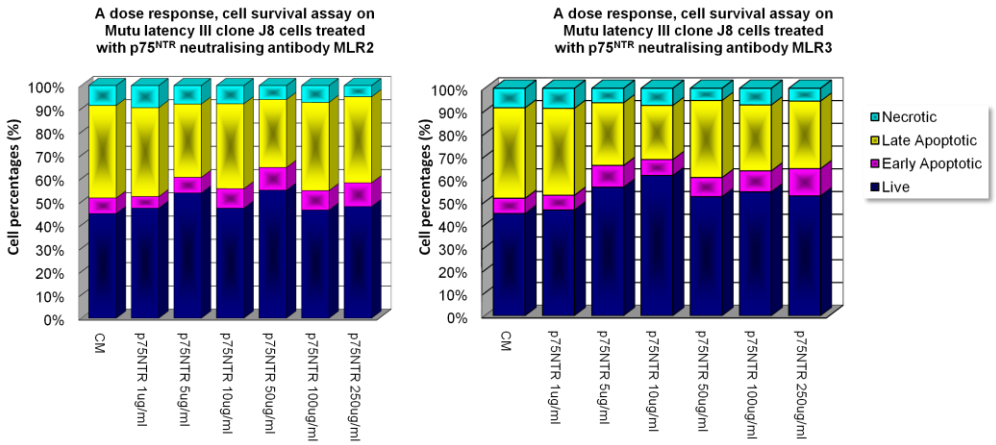

Figure 4.8.3: Cell survival assay on Mutu latency III clone J8 cells treated with p75^{NTR} signalling inhibitors MLR2 and MLR3
Dose response analysis on cells treated with either MLR2 or MLR3 antibodies for 24 hours. PI/PhiPhiLux stained cells were measured by flow cytometry for live cells, early, late apoptotic and necrotic cells.

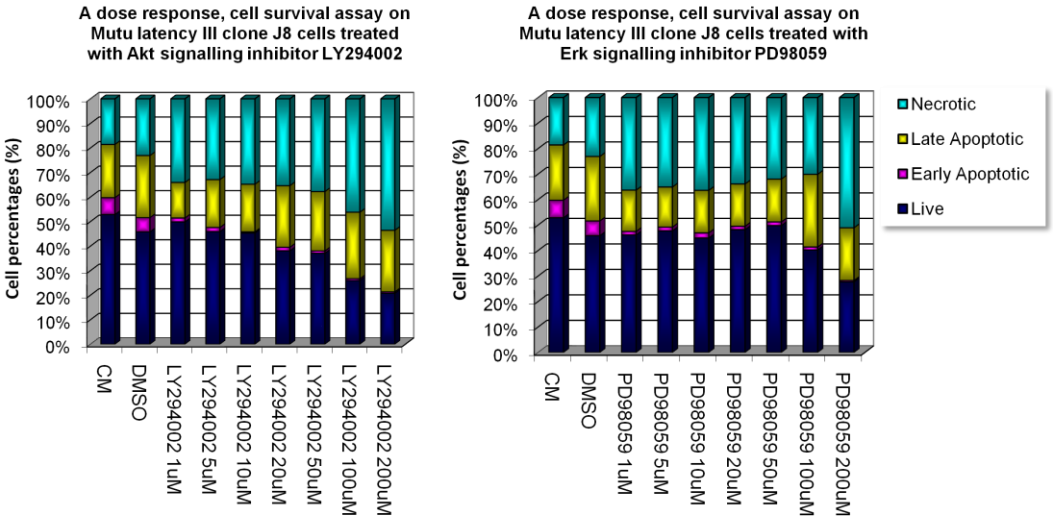

Figure 4.8.4: Cell survival assay on Mutu latency III clone J8 cells treated with Akt and Erk signalling inhibitors LY294002 and PD98059
Dose response analysis on cells treated with either LY294002 or PD98059 for 24 hours. PI/PhiPhiLux stained cells were measured by flow cytometry for live cells, early, late apoptotic and necrotic cells.

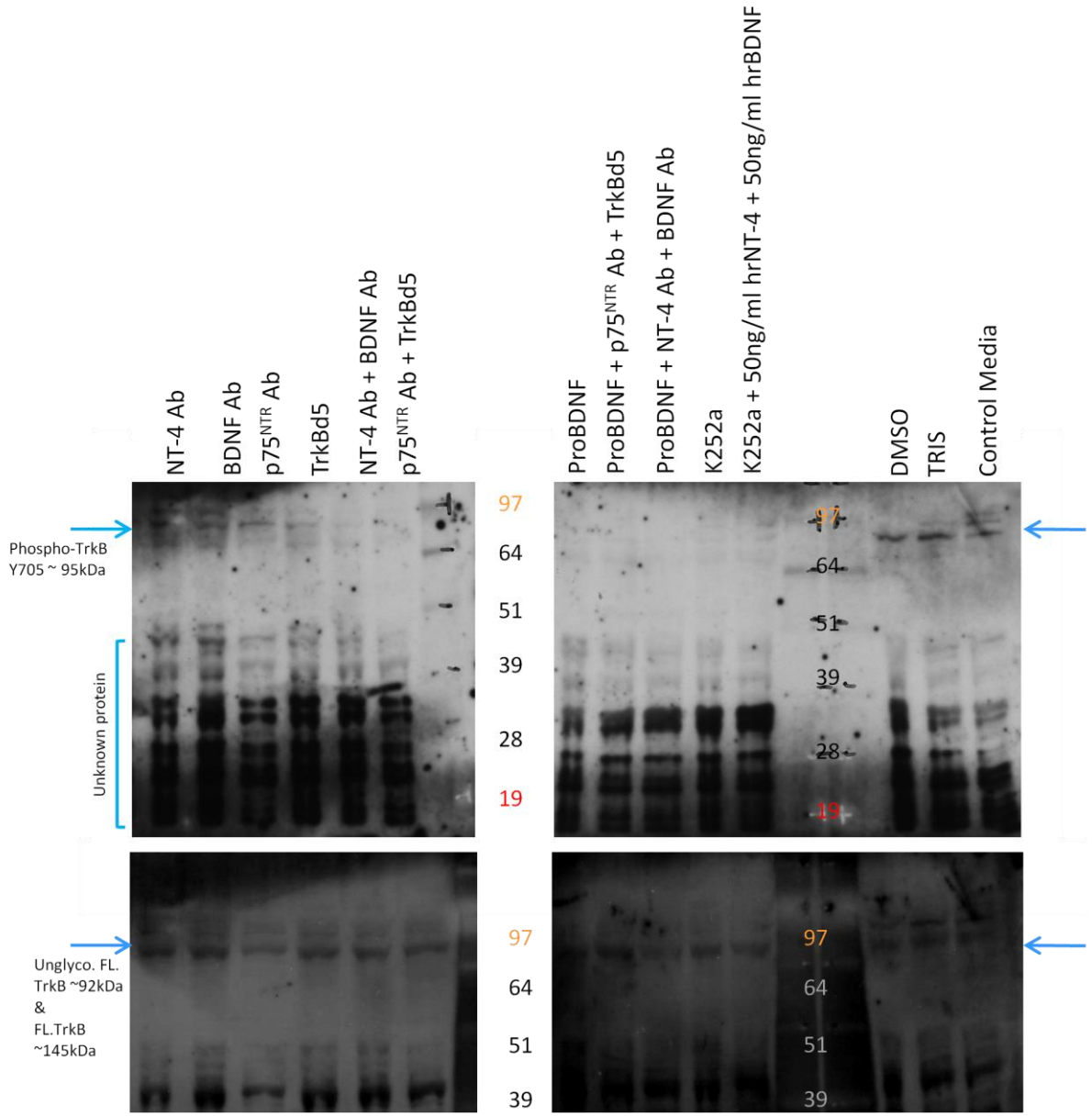

Figure 4.9: Inhibiting autocrine TrkB:NT-4 and BDNF signalling by BDNF and NT-4 antibodies, TrkB domain-5 analogue, p75^{NTR} antibody and K252a treatment in MUTU latency III clone J8 cells

Western blot showing whole cell extracts (20µg protein) run within a 10% polyacrylamide with SDS gradient gel (Bis-Tris buffer) under reducing conditions and transferred onto PVDF. Phospho-TrkB (Y705) was the primary antibody used. Specifically bound antibodies were detected by an alkaline phosphatase chemiluminescent method and blots exposed to photographic film.

Blots were then stripped in MESNA stripping buffer, blocked in IBT buffer then re-probed for Full-TrkB using TrkB (H-181) antibody. Specifically bound antibodies were detected by an alkaline phosphatase chemiluminescent method and blots exposed to photographic film (n=3).

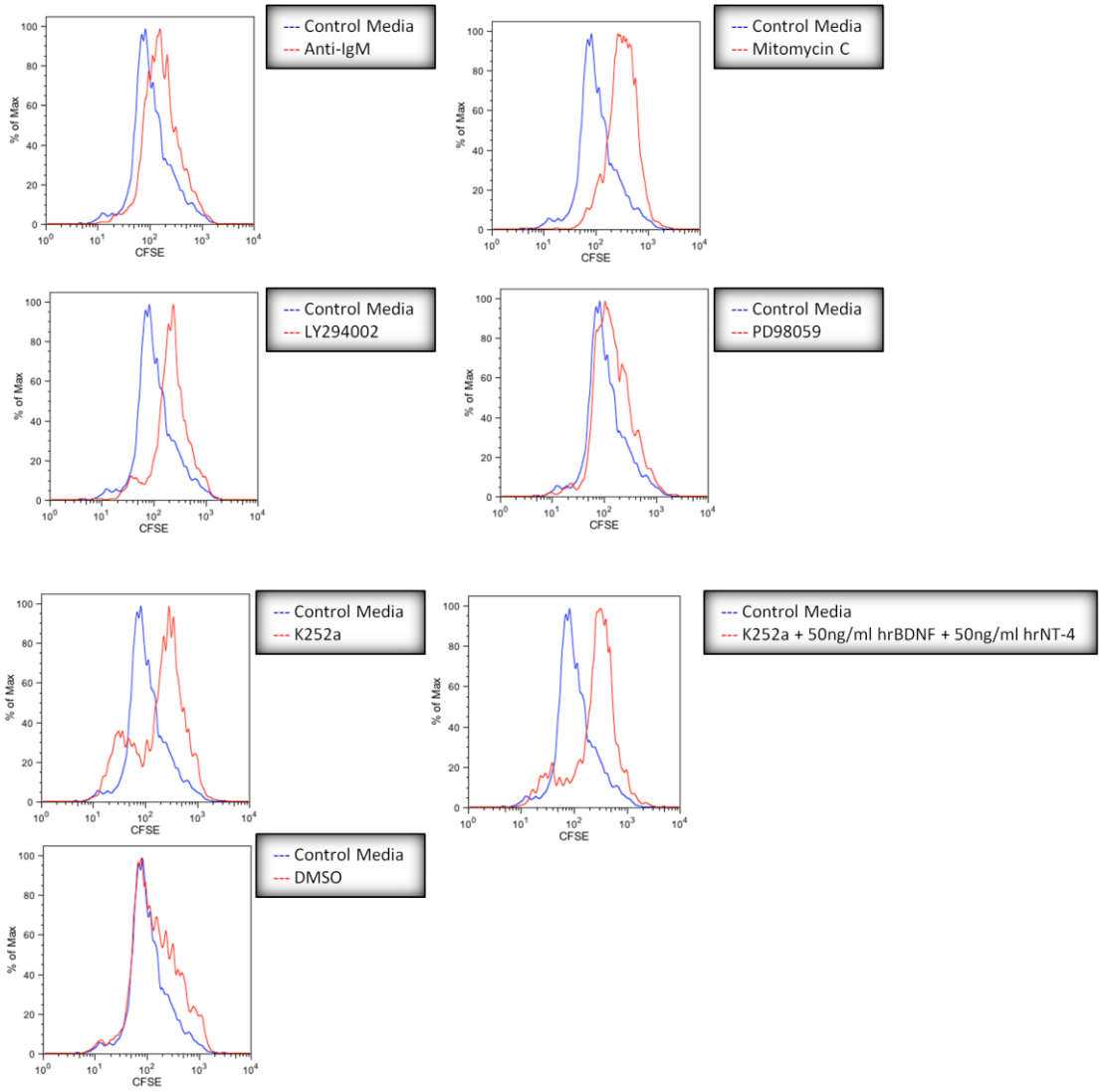

Figure 4.10.1: The effects on cell proliferation in Mutu latency III clone J8 cells treated with various TrkB:p75^{NTR} signalling inhibitors

Mutu latency III clone J8 cells were treated with CFSE dye then cultured with the inhibitors, Anti IgM, Mitomycin C, Akt inhibitor (LY294002), Erk inhibitor (PD98059), Trk signalling inhibitor K252a and its vehicle control, DMSO. Human recombinant BDNF (hrBDNF) and NT-4 (hrNT-4) protein were also added to K252a treated cells. Cells were treated for 48 hours. CFSE dye levels were measured by flow cytomerty, control treated cells were compared to each inhibitor individually (n=4).

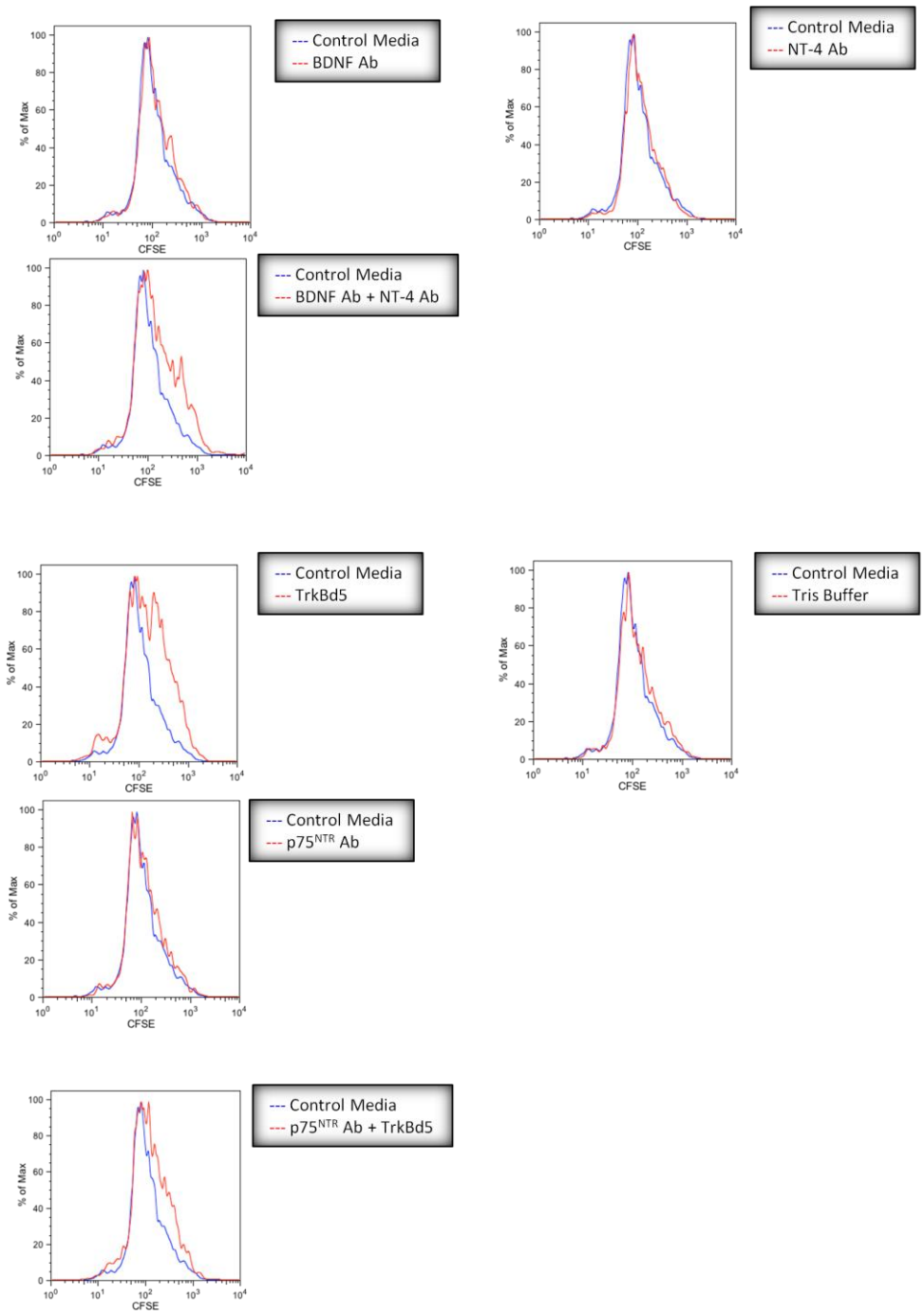

Figure 4.10.2 The effects on cell proliferation in Mutu latency III clone J8 cells treated with various TrkB:p75^{NTR} signalling inhibitors

Mutu latency III clone J8 cells were treated with CFSE dye then cultured with the inhibitors, neutralising antibodies for p75^{NTR} (MLR2), BDNF and NT-4, the specific inhibitor for TrkB receptor domain 5, TrkBd5 and its vehicle control Tris buffer. Cells were treated for 48 hours. CFSE dye levels were measured by flow cytomerty, control treated cells were compared to each inhibitor individually (n=4).

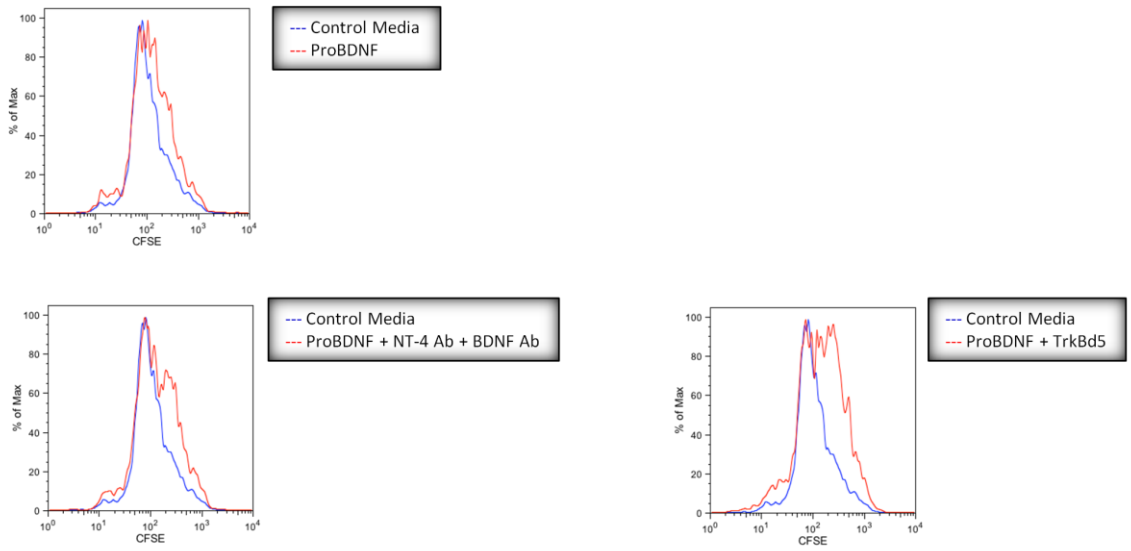

Figure 4.10.3 The effects on cell proliferation in Mutu latency III clone J8 cells treated with various TrkB:p75^{NTR} signalling inhibitors
Mutu latency III clone J8 cells were treated with CFSE dye then cultured with the inhibitors, ProBDNF protein, the specific inhibitor for TrkB receptor domain 5, TrkBd5 and neutralising antibodies for BDNF and NT-4. Cell were treated for 48 hours. CFSE dye levels were measured by flow cytomerty, control treated cells were compared to each inhibitor individually (n=4).

4.3 Discussion

The main conclusions from this part of the investigation are that Burkitt's lymphoma B cells express the neurotrophins BDNF and NT-4 and their receptors, TrkB and p75^{NTR} and that Mutu latency III clone J8 cells express functional full length TrkB and p75^{NTR} receptors which signal via their ligands in an autocrine manner for cell survival and proliferation.

4.3.1 BDNF and NT-4 expression and signalling discussion

The expression of BDNF protein in all Burkitt's lymphoma B cell lines analysed was observed by flow cytometry, western blotting and ELISA methods. BDNF has been shown to have

varying functions in B cells such as B cell development. According to a study by Schuhmann B. *et al*., paracine signalling between bone marrow stromal cells expressing BDNF which binds to Pre-BII cells, expressing $p75^{NTR}$ and truncated TrkB, plays a significant role in B cell development (Schuhmann, Dietrich et al. 2005). Mice deficient in BDNF have considerable B cell number reductions in Blood, spleen and bone marrow.

The detection of mature BDNF (~14kDa) and ProBDNF (~35kDa) within all Burkitt's lymphoma B cell lines was observed, however many other BDNF proteins with varying molecular weights were also detected. The human BDNF gene consists of 11 exons which respond to 9 promoters producing 17 sliced variants expressing the same protein, encoded from exon 8 (Pruunsild, Kazantseva et al. 2007). When glycosylated, these variants may produce multiple BDNF protein corresponding to varying molecular weights, as shown in figure 4.9.2.

Different BDNF spliced variants are expressed within diverse regions of the brain and other peripheral organs such as the spleen (Liu, Lu et al. 2006). The splice variants usage within peripheral immune organs are significantly different from those in brain tissue (Kruse, Cetin et al. 2007). In activated T cells for example, an upregulation of certain BDNF splice variants were observed, however the specific differences in function between the variants are unknown.

The observation of multiple BDNF protein within the western blot is also likely to represent varying BDNF dimmers. Mature BDNF can form homodimers for binding to TrkB receptor homodimers or TrkB:$p75^{NTR}$ heterodimers. Mature BDNF homodimers are presumed to form ~27kDa proteins which were detected within Mutu latency III clone J8 cell, but

undetected within other latency III lines indicating a possible clonal variant since its expression seems to not be latency phenotype specific (Roland, Stefan et al. 1994).

ProBDNF can also form homodimers for preferential binding to $p75^{NTR}$ coupled with receptors such as sortilin. These ProBDNF homodimers can form biologically active proteins ranging from ~50kDa to 60kDa (Roland, Stefan et al. 1994). Therefore, protein detected at ~55kDa, ~57kDa and/ or ~60kDa are presumed to be ProBDNF dimmer proteins observed within the BDNF western blot for the Burkitt's lymphoma cell samples. However it is also possible that ProBDNF may activate TrkB. Work by Fayard B. *et al*., show that ProBDNF induces TrkB tyrosine phosphorylation, activation of Erk pathways, and neurite outgrowth in COS-7 cells, hence it is a possibility that ProBDNF maybe secreted and may be involved in TrkB autophosphorylaton in Mutu latency III clone J8 cells (Fayard, Loeffler et al. 2005).

Proteins also detected by the BDNF antibody, running above 64kDa are unknown. If this experiment on BDNF expression was to be repeated, it would be worth pre-incubating the PVDF membrane with secondary antibody. An SG substrate should then be applied to be attached to any secondary antibody bound to the PVDF. Once the blot is washed and blocked, the BDNF primary antibody should then be applied as normal. The secondary antibody will then be re-applied to bind primary BDNF antibodies for detected by alkaline phosphatase chemiluminescence.

Pre-incubation with the secondary antibody and the SG substrate ensures any unspecifically bound secondary antibody is eliminated. Another suggestion to be considered if the experiment is to be repeated is to compare cells that express BDNF and those that are negative for BDNF expression.

RN46A is a neuronal cell line derived from rat raphe nuclei. The raphe nucleus is a moderate-size cluster of nuclei found in the brain stem which releases serotonin. These cells were used within a study on autocrine BDNF secretion and serotonergic differentiation in neuronal cells of the CNS within adult rats (Eaton and Whittemore 1996). These cells were transfected with a plasmid containing the cDNA sequence for rat BDNF. Wild type RN46A cells are negative for BDNF but efficiently express BDNF when transfected.

Control transfected and BDNF transfected RN64A cell samples could be compared to samples from the Burkitt's lymphoma lines within the same gel to ensure the various BDNF bands detected are specific for BDNF, although, a mature BDNF antibody which reacts to both human and rat BDNF protein will need to be used. It would also be informative to obtain an antibody which also recognised rat and human ProBDNF proteins detected at higher molecular weights.

Extracellular and intracellular BDNF expression was explored in Burkitt's lymphoma B cell lines by the use of a pre-coated sandwich ELISA kit, however it is worth noting that this ELISA kit does not distinguish between mature BDNF and ProBDNF protein. All Burkitt's lymphoma cell lines expressed detectable levels of intracellular BDNF, whereas only latency I and latency III cell lines secreted detectable levels of BDNF within their cell culture supernatant (figure 4.11).

The addition of either NGF or BDNF is able to induce neurite outgrowth in PC12 lines transfected with TrkB. There are suggestions in the literature that BDNF secreted by B cells is bioactive (Kerschensteiner, Gallmeier et al. 1999), therefore to test this using latency I and latency III Burkitt's lines, PC12 cells transfected with functional full length TrkB receptors

were treated with supernatant from latency I and latency III Burkitt's lymphoma lines for 14 days (data not shown).

TrkB transfected PC12 lines produced neurite outgrowth when treated with 50ng/ml of human recombinant BDNF protein, whereas supernatant obtained from latency I Burkitt's lymphoma lines did not induce neurite outgrowth. The lack of neurite outgrowth was possibly due to the half life for secreted BDNF protein within culture, therefore in the next experiment, TrkB transfected PC12s were treated every 48 hours with fresh supernatant; however this experiment was also unsuccessful. In this case it was proposed that the lack of neurite outgrowth in cells treated in culture supernatant may be due the concentration of secreted BDNF. Based on the BDNF ELISA experiment, the highest concentration of BDNF detected in culture supernatant was within IARC-171 supernatant containing 75.8 pg/ml BDNF compared to unstimulated B cells obtained from PBMCs which secreted 250pg/ml and 750pg/ml when stimulated, as documented by Kerschensteiner, M. *et al,* (Kerschensteiner, Gallmeier et al. 1999).

All Burkitt's lymphoma B cells lines analysed possessed detectable levels of NT-4 protein, however there is limited literature on NT-4 expression and function in human B lymphocytes. NT-4 mRNA however, has been documented to be expressed at basal levels in T and B splenocytes obtained from mice (Barouch, Appel et al. 2000). Whereas, within humans, NT-4 has been detected in alveolar and interstitial macrophages (Hikawa, Kobayashi et al. 2002), eosinophil granulocytes (Laurenzi, Beccari et al. 1998) monocyte-derived macrophages (Samah, Porcheray et al. 2008) and slow- and fast-twitch muscle fibers (Walker and Schon 1998).

4.3.2 TrkB expression discussion

Like BDNF, NT-4 binds and signals via TrkB and $p75^{NTR}$ and has been shown to induce neurite outgrowth and cell survival in embryonic trigeminal ganglia and trigeminal ganglion neurons excised from rat tissue (Ibanez, Ernfors et al. 1993). As seen in Mutu latency III clone J8 cells, NT-4 also signals for survival through TrkB but can also induce cell death through $p75^{NTR}$ within sensory neurones (Agerman, Baudet et al. 2000).

Other examples of BDNF and NT-4 signalling via TrkB have also been suggested during dendritic cell maturation which corresponds to an increase in the expression of HLA-DR and CD80, markers for antigen presentation (Bratke, Maruschke et al. 2007). TrkB expression was observed to be increased within maturing, human monocyte-derived dendritic cells and is linked to cell survival.

The expression of glycosylated full length TrkB protein (145kDa) was detected within the latency III lines, Mutu clone J8 and IARC-171 (figure 4.4), whereas glycosylated TrkB-T1 (95Kda)was detected in latency I, III and EBV negative Burkitt's lymphoma lines. Importantly, unglycosylated TrkB-T1 protein was only observed within EBV negative and latency I lines.

During embryogenesis BDNF and full length TrkB are highly expressed in neurones of the central nervous system. At later stages in postnatal development, truncated TrkB-T1 variants become more abundant (Allendoerfer, Cabelli et al. 1994; Armanini, McMahon et al. 1995; Biffo, Offenhauser et al. 1995). Screening adult rat cerebellar cDNA libraries

reveals TrkB-T1 contains the TrkB extracellular domain, as well the transmembrane region, but lacks the kinase domain (Middlemas, Lindberg et al. 1991).

TrkB.T1 is a functional receptor which when overexpressed, can increase the proliferation of neural progenitors (Tervonen, Ajamian et al. 2006). TrkB-T1 can internalise and store BDNF in biologically active forms and release it depending on the BDNF concentration within the cellular environment; this inturn can regulate extra cellular BDNF levels (Biffo, Offenhauser et al. 1995; Rubio 1997; Alderson, Curtis et al. 2000).

TrkB-T1 has also been shown to be involved in cell morphology. Over expression of full length TrkB receptors increases proximal dentritic branching, whereas TrkB-T1 promotes elongation of distal dendrites in cortical cells (Yacoubian and Lo 2000). TrkBT-1 can also act in a ligand independent manner by altering cellular morphology in neuroblastoma lines; forming outgrowth of filopodia and processes in transfected neuroblastoma cell lines (Haapasalo, Saarelainen et al. 1999). Interestingly, full length TrkB expression, suppresses the formation of filopodia and processes outgrowth in cells co-transfected with both full length and truncated TrkB. The inhibitory effects from full length TrkB were inhibited upon k252a treatment. Therefore, depending on levels of full length and truncated TrkB receptor expression, their signalling functions can be counteracted.

Overexpression of TrkB-T1 can also form filopodia in hippocampal neurones; this TrkB-T1 signalling cascade involves $p75^{NTR}$ but is independent from ligand binding. Importantly, the co-expression of TrkB-T1 and full length TrkB hinders dendritic filopodia formation.

Notwithstanding, heterodimerization of full length and truncated TrkB which can inhibit autophosphorylation of the tyrosine kinase domain (Haapasalo, Koponen et al. 2001). Co-

expression of truncated and full-length TrkB cDNAs in sympathetic neurons reduces the ability of full length TrkB to induce particular BDNF-dependent events such as neuronal survival (Ninkina, Adu et al. 1996). Xenopus oocyte transfected with full length and truncated TrkB can form non-functional heterodimers, inhibiting the full length TrkB response upon BDNF stimulation (Eide, Vining et al. 1996).

Another truncated TrkB receptor, that contains an Shc-binding site in the juxtamembrane domain, but lacks the kinase domain and has a unique truncated C terminus is known as TrkB T-Shc. Co-immunoprecipitation experiments from human brain tissue show that TrkB-T-Shc is not autophosphorylated by full length TrkB, indicating that it could also be a negative regulator of TrkB signalling in the brain (Stoilov, Castren et al. 2002).

Taken together, the truncated TrkB receptors may therefore act as naturally occurring dominant negative modulators in cells co-expressing full length and truncated TrkB. On the other hand TrkB-T1 may support and even promote full length TrkB signalling.

It is known that BDNF and TrkB play an important role in modulating the plasticity of the adult hippocampus. TrkB-T1 receptors have been postulated to prolong the availability of neurotrophin by acting as depots for BDNF. Since BDNF can occur as a homodimer it can be speculated that these dimers contain two binding sites, one interacting with a full length receptor such as that on glial cells, and the other with a truncated receptor present on a growing axon, thereby promoting cell-cell interactions (Schneider and Schweiger 1991).

The specific functions of full length and truncated TrkB receptors in Burkitt's lymphoma are unknown. However based on the literature it can be presumed that full length and truncated TrkB receptors within latency III Burkitt's lymphoma B cells lines may work

together promoting cell survival and proliferation. In this case, cells would be control treated since latency III lines express TrkB and their receptors. However when treated with the tyrosine kinase signalling inhibitor K252a, full length TrkB is inhibited whereas truncated TrkB (negative for the tyrosine kinase domain), should remain active. K252a inhibits cell growth and proliferation therefore it is possible that truncated TrkB-1 expression is not involved in cell survival within Mutu latency III clone J8 lines.

EBV negative and latency I Burkitt's lymphoma cells on the other hand, express glycosylated truncated TrkB-T1. Functional signalling via TrkB and BDNF pathways in these cell lines were not investigated due lack of glycosylated full length TrkB protein expression. To test the hypothesis whether there are differences in full length TrkB and TrkB-T1 signalling compared to truncated TrkB-T1 signalling alone, the experiments conducted within this investigation TrkB and BDNF signalling would need to be applied using EBV negative and latency I Burkitt's lymphoma Mutu cell lines. It would also be highly beneficial to compare any results from these tests by using TrkB negative cell lines transfected with either TrkB-T1 or full length TrkB cDNA. Including these transfected lines would eliminate any signalling differences observed between the Burkitt's lymphoma lines, influenced by EBV latency phenotype.

Ways in which EBV influences its host cell are still being discovered. Previously a publication by Eggers S.D.Z. and Windebank A.J. demonstrated that peripheral resting human B cells have undetectable levels of TrkB mRNA expression through the use of TrkB RT-PCR primers which recognise all variants (Scott D. Z. Eggers and Anthony J. Windebank 1996). Epstein-Barr Virus Transformation Induces Expression of TrkB mRNA in Human B Lymphocytes). By

transforming B cells obtained from the same doner with EBV, enables the detection of Pan-TrkB mRNA expression.

EBV transformed B cells have also been seen to translate functional TrkB receptors that are phoshorylated upon BDNF treatment (Schenone, Gill et al. 1996). Conversely, B cell transformation by EBV did not upregulate $p75^{NTR}$ expression or TrkA and TrkC mRNA expression, therefore TrkB expression seems to be linked EBV gene expression.

From RT-PCR and western blotting, data not shown, it was concluded that LMP1 transfected BJAB cells express strong LMP1 protein, strong TrkB protein but weak levels of TrkB mRNA. LMP1 transfected DG75 lines on the other hand show weaker LMP1 protein levels, weaker TrkB protein expression and yet stronger TrkB mRNA levels. Although the mRNA data did not match the TrkB protein levels detected by western blotting methods, it was speculated that these differences may have been due to the sensitivity for each method.

For each RT-PCR experiment, 40ng/ml of cell sample RNA was loaded per PCR reaction, whereas 20ug/ml of protein was loaded per well within an SDS-PAGE gel for western blotting. Since protein and RNA concentrations were considered for each method as opposed to cell numbers, the two methods cannot e directly compared in terms of expression levels.

The differences in TrkB expression between the two methods are also possibly due to TrkB protein influencing its gene expression. The high expression level of TrkB protein in LMP1 transfected BJAB cells may have a negative feedback loop which could down regulate TrkB

mRNA within the cell. Whereas, low expression of TrkB protein in LMP1 transfected DG75 cells may induce a positive feedback loop that may increase TrkB mRNA expression.

Other reasons for the difference in mRNA and protein expression may include TrkB specific microRNAs (miRNAs) which act by binding to target mRNA and either cleave or reduce translation efficiency of that mRNA sequence. The miRNAs 9, 125a, and 125b have been shown to bind truncated TrkC receptors in neuroblastoma tumors, decreasing cell growth (2007: 104, 7957). TrkB specific miRNAs however have yet been discovered, however it is probable that EBV encoded miRNAs may influence TrkB expression.

The possibility that LMP1 may upregulate TrkB protein expression was also tested in Mutu latency III clone J8 and IARC-171 cells transfected with an LMP1 specific siRNA (data not shown). Unfortunately the LMP1 expression levels within siRNA transfected Mutu and IARC-171 cells were not lessened compared to the control transfected samples.

4.3.2 TrkB and $p75^{NTR}$ autocrine signalling discussion

Autocrine signalling within Mutu latency III was scrutinized by use of various receptor and ligand inhibitors. Although informative results were obtained from the use of tyrosine kinase inhibitor, K252a, it was worth comparing this inhibitors' effect with the more specific inhibitor TrkBd5. This was beneficial for comparing the resulting data since these TrkB inhibitors act by inhibiting differing sites within the receptor structure.

K252a is considered to be a less specific Trk signalling inhibitor. As well as inhibiting tyrosine kinase signalling, K252a can also induce cell cycle arrest and apoptosis in TrkA and TrkB expressing glioma cells, by inhibiting cyclin-dependent kinases (Chin, Murray et al. 1999).

K252a is now regarded to be an inhibitor of varying kinases and neurotrophic factor signalling. These varying kinases include calmodulin-dependent protein kinase (McGinnis, Wang et al. 2001), protein kinase C (Yamada, Iwahashi et al. 1987) and other serine/threonine protein kinases including MAPKs (Pan, Zhang et al. 2005).

To strengthen data obtained from TrkB signalling experiments by the use of K252a inhibitor in Mutu latency III clone J8 cells, TrkBd5 was directly applied to the experiment as the more specific inhibitor. As mentioned previously within the chapter, TrkBd5 is an analogue for the 5^{th} domain on the TrkB receptor structure, known to be the binding site for BDNF. However it is also worth noting that BDNF can bind to a site spanning the third leucine-rich domain and the second cystein cluster domain (please refer back to the TrkB receptor structure shown in illustration 1.2.) (Haniu, Montestruque et al. 1997).

It has also been shown that peptides corresponding to the leucine rich motif sequence, can effectively bind and block BDNF, NT-4 and NT-3 binding to the extracellular domain of TrkB (Windisch, Auer et al. 1995). Therefore it is possible that Mutu latency III clone J8 cells treated with TrkBd5, secreting BDNF, may still be able to signal via the third leucine-rich domain and the second cystein cluster domain on TrkB, however the proliferation and cell survival were efficiently inhibited upon TrkBd5 treatment and there is currently no literature on the signalling outcomes of BDNF binding with the third leucine-rich domain and the second cystein cluster domain on TrkB.

If TrkB and BDNF autocrine signalling was to be investigated further in Burkitt's lymphoma B cell lines, the use of a large variety of TrkB signalling inhibitors, possessing differing inhibition mechanisms would be highly beneficial. An example includes the novel tyrosine kinase inhibitor CEP-751 (KT-6587), which is an indolocarbazole derivative (Hu, Sun et al.

2008). Nonetheless, its mode of action against Trk signalling receptors has not yet been documented.

As for the mature neurotrophic factor low affinity receptor $p75^{NTR}$, its expression was observed within all Burkitt's lymphoma lines analysed. Within Trk and $p75^{NTR}$ positive cells, the expression level balance between the two receptors could influence signalling for cell survival or cell death. Cell survival can be signalled via Trk pathways whereas $p75^{NTR}$ can signal for cell death. Scenarios where disruptions in this balance, favouring $p75^{NTR}$ signalling to induce cell death include diseases such as Alzheimer's.

The catalytic activity of □-secretase is dependent on its prestilin subunit, a multi-transmenbrane aspartyl protease. Mutations in presenilin-1 gene are known to induce familial Alzheimer's disease (Citron, Westaway et al. 1997). Mutations arise from the effects of □-secreatase-dependent processes of amyloid precursor protein and the subsequent formation of amyloid. As documented by Hatchet C.S. et al., familial Alzheimer's mutations, namely M146V mutations, induce $p75^{NTR}$ cleavage, releasing the ICD promoting cholinergic neuronal cell death (Hatchett, Tyler et al. 2007).

$p75^{NTR}$ is synthesized as ~59-60kDa precursor which is subsequently glycosylated to produce a full length, 75kDa receptor. $p75^{NTR}$ cleavage was observed upon inhibition of TrkB signalling in Mutu latency III clone J8 cells compared to control treated Mutu cells (data not shown). This therefore indicates that $p75^{NTR}$ cleavage is either at a low levels or absent within Mutu latency III clone J8 cells. This may be due to full length TrkB signalling, inhibiting $p75^{NTR}$ cleavage by co-localising with $p75^{NTR}$ forming heretodimers. In this case the balance is shifted in the favour of TrkB signalling for cell survival.

On the other hand, inhibiting TrkB kinase domain signalling by K252a enhanced $p75^{NTR}$ cleavage, tipping the balance in favour of $p75^{NTR}$ dependent cell death in Mutu latency III clone J8 cells. $p75^{NTR}$ cleavage is also heightened by its high affinity receptor ProBDNF compared to BDNF protein in cells treated with K252a. The ~35kDa ProBDNF monomers were detected within all Burkitt's lymphoma lines indicating endogenous ProBDNF which may be secreted by Mutu latency III clone J8 cells. Inhibiting TrkB signalling by K252a addition alone had a slight increase in $p75^{NTR}$ cleavage whereas the addition of K252a and exogenous ProBDNF increased $p75^{NTR}$ cleavage further showing biologically active ProBDNF within Mutu latency III clone J8. On the other hand, if these experiments were to be repeated, the addition of another Trk signalling inhibitor could help verify the results obtained. Novel inhibitors such as AZ-23 which acts as a potent and selective Trk kinase inhibitor could be used as a treatment for cancer (Thress, Macintyre et al. 2009).

Neurotrophin signalling via TrkB:$p75^{NTR}$ and their ligands may therefore aid B cell survival and proliferation in EBV transformed Burkitt's lymphoma B cells providing a possible novel axis as a tumour prophylaxis. Burkitt's lymphoma B cells also express detectable TrkA mRNA, however lack detectable NGF transcripts, therefore TrkA and NGF signalling pathways within EBV negative and EBV latency I cell lines were to be investigated within the next results chapter.

5. Results

Investigating possible NGF and TrkA signalling via paracrine interactions between Burkitt's lymphoma B cell lines and Follicular Dendritic Cells and possible autocrine signalling effects within Burkitt's lymphoma B cells

5.1 Introduction

In line with the previous chapter on TrkB signalling, TrkA expression and signalling was investigated in Burkitt's lymphoma B cell lines. This chapter is split into two sections. The main focus for the first section was to study novel bi-directional neurotrophic factor communication between FDCs and Burkitt's lymphoma B cells and to question possible FDC roles in lymphomagenesis. As concluded from chapter 3, TrkA mRNA transcripts were detected in all Burkitt's lymphoma cell lines analysed, yet, transcripts of its' specific ligand, NGF were not observed, hence the hypothesis for a paracrine signalling effect.

The results gained from this first section of the chapter where used to drew the second hypothesis, asking whether TrkA and NGF autocrine signalling takes place in Burkitt's lymphoma B cell lines.

Possible source of NGF within the germinal centre (GC) microenvironment has been shown to be provided from T cells (Lambiase, Bracci-Laudiero et al. 1997); however there is currently no data on NGF secretion by follicular dendritic cells (FDCs). FDCs were therefore questioned as possible sources of NGF within a GC.

5.1.1 The function of FDCs within a germinal centre micro-environment

First described as “a non-lymphoid population of embryonic non-phagocytic reticulum cells” by A. Maximow, FDCs are CD45 negative, multi-nucleated cells which form dense three-dimentional structures within the light zone of germinal centre follicles (Gerdes, Stein et al. 1983; Schriever, Freedman et al. 1989).

FDCs within the GC assist B cell maturation by taking up antigen attached to antibodies or by presenting antigen complement complexes for centroblasts (Klaus, Humphrey et al. 1980). High affinity B cell selection then occurs by inducing class switch recombination, forming centrocytes within the light zone (Liu, Joshua et al. 1989). Many centrocytes die of apoptosis and yet cells with higher affinity for antigens receive signals for survival by interacting with FDCs (Fliedner, Kesse et al. 1964).

As summarised in illustration 5.1, FDC and B-cell interactions involve varying receptors and ligands for specific functions including cell proliferation, survival and adhesion, as well as upregulating CD19, CD154 and IL15 binding. Germinal centres are also known to play a central role in the formation of memory B cell (Klaus, Humphrey et al. 1980; Kunkl and Klaus 1981; MacLennan and Gray 1986).

Add ill 5.1

It was proposed by Babcock G. J. *et al*., that upon entry, EBV infects B cells within the submucosal membrane, and that these B cells enter the germinal centre to differentiate into EBV positive, sIgD negative memory B cells released within peripheral blood (Babcock, Decker et al. 1998). There are indications of EBV positive cells to be of GC origin. For example, the expression of *GCET1* (Germinal Centre B cell Expressed Transcript-1) gene which codes for a serpin (Frazer, Jackson et al. 2000) is expressed in EBV positive B cells.

Normally expressed in germinal B cells, *GCET1* is also expressed within Burkitt's lymphoma cell lines (Paterson, Horvath et al. 2007). Other examples of GC B cell markers observed in Burkitt's lymphoma lines include CD10, CD38 and CD77 (Gregory, Tursz et al. 1987; Mangeney, Richard et al. 1991; Mangeney, Lingwood et al. 1993). Again, like GC B cells, Burkitt's lymphoma B cells lack markers such CD39, CD23, CD25 and CD71 (Gregory, Tursz et al. 1987). Drawn from these observations it seems that Burkitt's lymphoma B cells undergo B cell maturation through GCs by interacting with T cells and FDCs. The main focus within the first section of this chapter was to ask if neurotrophic factors and their receptors signal between Burkitt's lymphoma B cells and FDCs. One possible link between FDCs and B cells via neurotrophic factors may involve $p75^{NTR}$. FDCs have been shown to express $p75^{NTR}$ protein within paraffin embedded histological sections (Maeda, Matsuda et al. 2002). Hence, Mutu latency III clone J8 cells which secrete BDNF, may bind and signal to FDCs.

To question these, two FDC cell lines were utilized. The first being, FDC1 cell line, provided by Clark E.A. which was compared with the HK cell line provided by Choi Y.S.

The FDC1 cell line was generated by shearing human tonsils and digesting them with DNase and collegenase (Schriever, Freedman et al. 1989; Clark, Grabstein et al. 1992). When cultured, the large adherent cells with elongated extensions were isolated and grown in culture. Initially, these cells were used to investigate CD40 signalling within the germinal centre. Like true FDCs, the FDC1 cell line express CD11b, CD14, CD29, CD40, CD54. CD73, CD74 and VCAM-1. The cells lack CD11c, CD22, CD18, CD25, CD45 and T-cell markers. Human B cells and B cell lines have been shown to bind to FDC1 lines and in the presence of anti IgM and/ or agonistic CD40 mAb, can induce B cell proliferation. Importantly, T cells do not bind to the FDC1 cell line and yet B cells bind via VLA-4 and VCAM-1.

Another very similar FDC cell line, HK, was found to express CD21, CD23, DRC-1, CD40, VCAM-1, ICAM-1 and HJ2 (Kim, Zhang et al. 1994). Anti CD3 Ab activates T cells that bind and stimulate HK cells showing T cells stimulate resting B cells and support B cell maturation by stimulating FDC development.

Both FDC cell lines are considered to be useful tools in studying surface molecular markers and cytokines expressed by FDCs. Within this section of the thesis, FDC1 and HK cell lines were initially characterised for known FDC markers and screened for the expression of NGF mRNA transcripts and protein.

5.1.2 TrkA phosphorylation and downstream signalling

The functional effects upon NGF treatment were also analysed in Burkitt's lymphoma B cells. NGF has been shown to induce an array of biological effects in B cells such as cell survival, cell proliferation and cell migration. B cells and B cell lines have been shown to express $p75^{NTR}$ and TrkA which is phosphorylated upon exogenous NGF addition (Melamed, Kelleher et al. 1996; D'Onofrio, de Grazia et al. 2000).

NGF and IL2 stimulation increases the mitogenic effect of the T-independent B cell mitogen, Staphylococcus aureus Cowan I strain in tonsillar and peripheral human B cells (Brodie and Gelfand 1992). NGF has also been shown to induce a dose-dependent increase in human B-cell DNA synthesis (Otten, Ehrhard et al. 1989), enhances IgG4 production in cultures of human tonsillar B cells (Kimata, Yoshida et al. 1991), increases F-actin content, microfilament assembly and phosphorylation of paxillin in human B cells (Melamed, Turner et al. 1995).

Upon TrkA phosphorylation, NGF, induces the tyrosine phosphorylation and activation of MAP-kinase (Franklin, Brodie et al. 1995), tyrosine phosphorylation of Shc and its association with Grb2 as well as inducing Vav phosphorylation and the activation of Ras downstream signalling (Melamed, Patel et al. 1999).

In terms of cell survival, NGF is said to rescue B cell lines from apoptosis induced by anti-IgM (Kronfeld, Kazimirsky et al. 2002). NGF may also act in an autocrine manner by signalling for cell survival within memory B cells and Hodgkin lymphoma derived, Hodgkin-Reed Sternberg cells (Torcia, Bracci-Laudiero et al. 1996; Renne, Minner et al. 2008).

An additional signalling outcome upon NGF stimulation includes cell migration which has been demonstrated in primary melanoma cells (Shonukan, Bagayogo et al. 2003), mast cells (Sawada, Itakura et al. 2000), macrophages (Kobayashi and Mizisin 2001), microglial cells (De Simone, Ambrosini et al. 2007) and Schwann cells (Anton, Weskamp et al. 1994).

5.1.3 Inhibitions for TrkA signalling

The second part of this chapter will be to ask possible autocrine NGF signalling via TrkB within Burkitt's lymphoma B cells. These signalling effects were investigated in EBV negative Burkitt's lymphoma cell lines by using TrkA signalling inhibitors. Reagents used to observed TrkA protein and inhibit TrkA signalling at illustrated in illustration 5.2. K252a signalling inhibition effects were compared to the specific TrkA inhibitors TrkAd5 and GW441756.

TrkA-domain 5 (TrkAd5) is a receptor analogue that acts by binding to NGF which in turn out competes with any extracellular NGF binding to TrkA.

Add Ill 5.2 here

TrkAd5 was the first of the analogues to be designed and constructed after the discovery of NGFs' specific binding site on the TrkA receptor structure. This binding site lies within the extracellular part of TrkA known as the immunoglobulin-like domain 5 (Please refer to Trk receptor structure – illustration 1.3) (Holden, Asopa et al. 1997; Watson, Fahey et al. 2006). The TrkAd5 receptor analogue acts by binding to NGF which in turn out competes with any extracellular NGF. This 5th domain structure was cloned, purified and tested in vitro and in vivo for its inhibitory effects on TrkA signalling.

TrkAd5 inhibits NGF dependent neurite outgrowth and cell survival in PC12 cells (Watson, Fahey et al. 2006). As shown by De Vries A. *et al.,* 20ng/ml of NGF induces hyper-responsiveness of isolated guinea pig tracheal rings following application of histamine (de Vries, van Rijnsoever et al. 2001). Treatment with TrkAd5 prior to the addition of NGF was able to inhibit hyper-responsiveness to histamine. Importantly, TrkAd5 shows no significant binding to BDNF, providing further evidence that domain 5 regions on TrkA and TrkB regulate specificity for cognate ligand binding (Ultsch, Wiesmann et al. 1999; Robertson, Banfield et al. 2001).

Within this investigation, TrkAd5 was compared a potent, selective TrkA kinase inhibitor known as GW441756 that is able to inhibit TrkA-induced cell death in cell lines over expressing TrkA (Wood, Kuyper et al. 2004; Jung and Kim 2008). GW441756 has also been shown to inhibit DNA damage due to the accumulation of γH2AX leading to apoptosis in SK-N-MC and U2OS cells over expressing TrkA (Jung, Kim et al. 2008; Jung and Kim 2008).

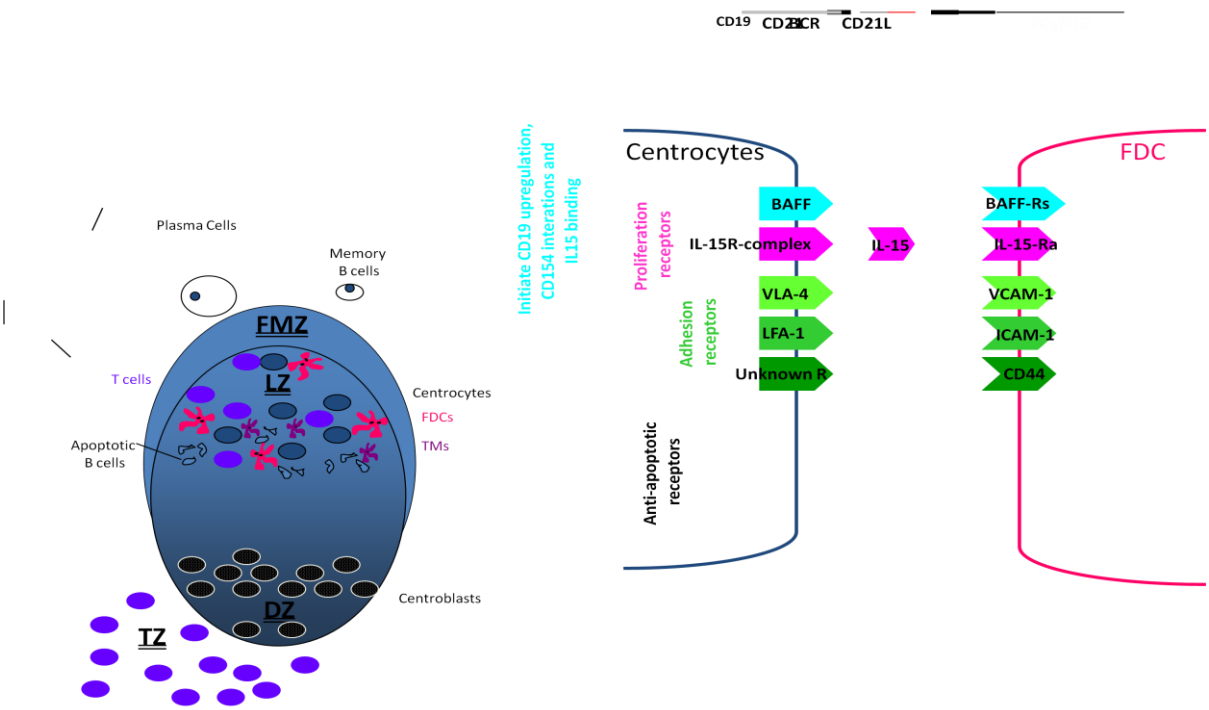

Illustration 5.1: Germinal centre micro-environment and B-cell to FDC interactions
Germinal centre zone, dark zone (DZ), light zone (LZ), follicular mantle zone (FMZ) and T cell rich area (TZ) are displayed. FDC and B-cell centrocyte interactions are also summarised, identifying the effects of these signalling interactions promoting B-cell growth, development and survival.

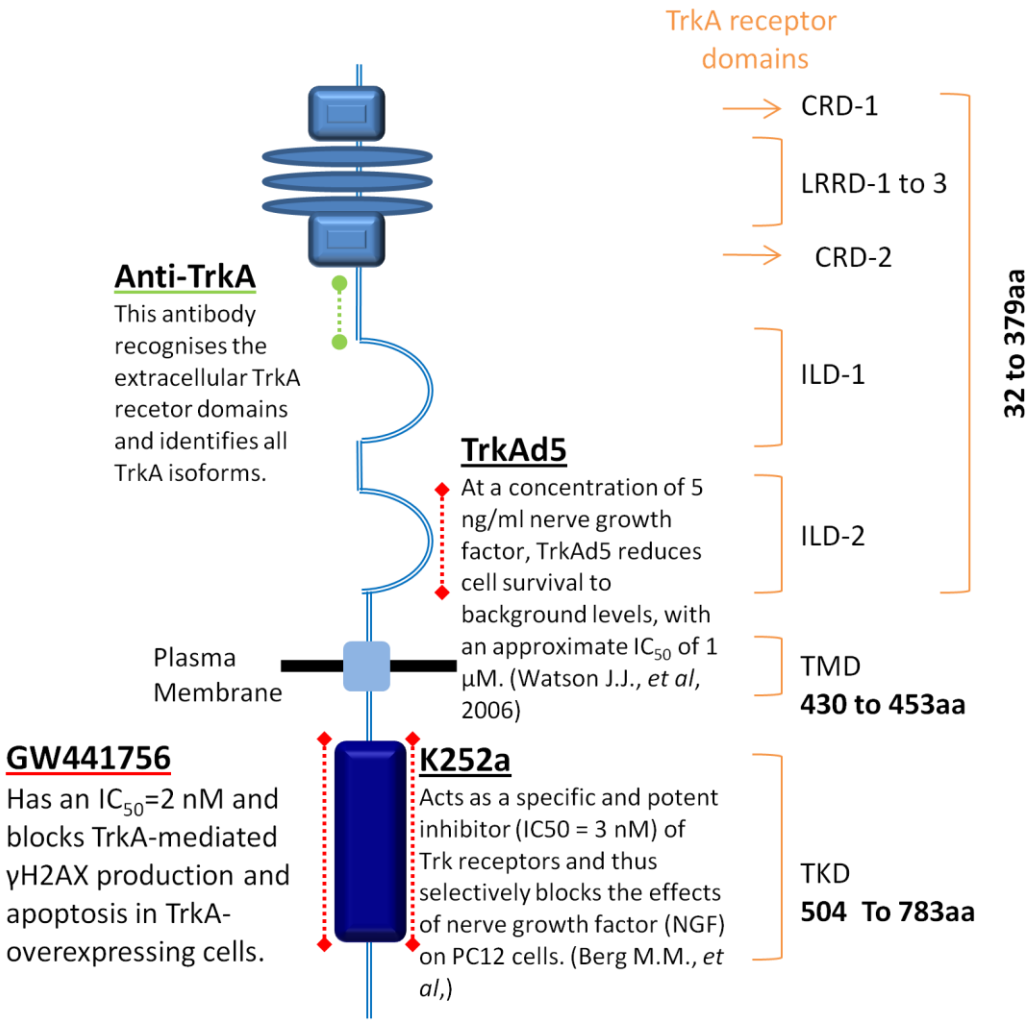

Illustration 5.2: TrkA receptor antibodies and inhibitors applied within the investigation
TrkA receptor domains and amino acid numbers are displayed. The reagents used to recognise TrkA protein by antibodies or inhibit TrkA signalling are displayed and annotated at the receptor regions they recognise/ hinder.

5.2 Results Part I : Investigating possible NGF and TrkA signalling via paracrine interactions between Burkitt's lymphoma B cell lines and Follicular Dendritic Cells

5.2.1 The characterisation of FDC-like lines, FDC1 and HK

To question possible FDC-B-cell interactions via neurotrophic factors, HK and FDC1 cells were initially characterised for known published FDC markers. These antibodies are known to react with normal FDCs by human tonsil histological staining (communication with Dr. D Hardie, University of Birmingham, UK). The FDC-like cell lines were then screened for neurotrophic factor mRNA and NGF protein expression.

The antibodies used for flow cytometry analysis on FDC1 and HK cell surface markers are shown in table 5.1 below.

Table 5.1: FDC markers used to characterise FDC lines

FDC Markers	Information	Reference
BU10	"Birmingham University" FDC marker	(Johnson et al., 1986)
FD6 – 88.6	FDC marker	
8D6 - FDC-SM-8D6 aka CD320	8D6 increases plasma cell generation in the GC and IgG secretion.	(Li, Zhang et al. 2000)
CD106 – VCAM-1	CD106 contributes to leukocyte adhesion.	(Freedman et al., 1990)
3C8	3C8 protein is a prostacyclin synthase.	(Li et al., 2000)

These antibodies were used to stain HK and FDC1 cells for flow cytometry analysis. It is proposed that CD19 is expressed by FDCs isolated from human tonsils therefore an anti-CD19 antibody was also included within these experiments as shown in figure 5.1. Very low levels of FDC marker surface expression was detected when cells live cells were stained (data not shown), therefore HK and FDC1 cells were permeabilized within each experiment.

HK cells reveal low but detectable levels of CD19, FD6, 8D6 and CD106. As for BU10 and 3C8 and HK cells reveal high levels of protein. As for the FDC1 line, low levels of BU10 and 3C8 were observed. Undetectable to weak levels of CD19, FD6, 8D6 and CD106 were observed. Representatives from three independent experiments are shown. HK cells therefore revealed higher levels of characteristic FDC marker expression patterns compared to FDC1 cell line.

Other FDC marker antibodies such as CD21 and CD23 were also included to screen for FDC1 and HK cells (data not shown), however due to time constraints these antibodies were not fully optimised for use. It is also worth noting that cells were only used until they reached pass number 7. It was observed that cells kept in culture after 7 passages had diminished levels of BU10 and 3C8 expression (data not shown).

Fig 5.1 add here

cDNA was then extracted from both FDC- like lines to test for β-actin to ensure equal levels of cell sample cDNA within each PCR experiment (figure 5.2.1). FDC-1 like cell samples were then tested for BAFF mRNA, also known to be expressed in FDCs. Both HK and FDC-1 show detectable levels in figure 5.2.2, IARC-171 cell line was used as a positive control. $p75^{NTR}$ expression had also been reported in FDCs, HK and FDC-1 cell lines show detectable levels of

p75^{NTR} mRNA transcripts within figure 5.2.3, although, HK cells seem to reveal a stronger level of p75^{NTR} transcripts compared to the FDC-1 line, as well as the positive control line, Kelly.

Overall, both FDC like lines expressed detectable BAFF and p75^{NTR} mRNA transcripts. To test further, the expression of p75^{NTR}, MLR2 antibody for p75^{NTR} was used to stain permeabilized HK and FDC-1 cells for flow cytometry analysis (figure 5.3). Representatives from three independent experiments are shown. Kelly cell line was used as the positive control line. Both FDC-1 and HK cells show detectable levels of p75^{NTR} protein by flow cytometry analysis compared to the control like Kelly cells.

Therefore, as expected HK and FDC1 lines express BAFF mRNA transcripts and p75^{NTR} transcripts and protein, as well as known FDC markers, namely BU10 and 3C8.

Fig 5.2 and 5.3 add here

5.2.2 The expression of Neurotrophic factors and their receptors in FDC-like lines, FDC1 and HK

So far it has been shown that FDCs express $p75^{NTR}$ protein. Hence Mutu latency III clone J8 cells which secrete BDNF, may bind and signal to FDCs. To question further the possibility that FDCs may interact with B cells within the germinal centre via neurotrophic signalling pathways, cDNA extracted from FDC-1 and HK cells was tested for neurotrophic factor and receptor mRNA transcripts by RT-PCR (figure 5.4).

To ensure equal levels of cDNA was present between the FDC-1 like lines β-actin primers were used (figure 5.4.1). These samples were then test for TrkA and TrkB mRNA transcripts. Although HK cells show stronger levels of TrkA mRNA, FDC-1 cells also reveal detectable transcripts. TrkB variants A and C transcripts were not detected in either FDC-like line. But HK cells show detectable transcripts corresponding to Pan-TrkB variants which may include truncated TrkB mRNA. FDC-1 lines on the other hand, lacked any detectable Pan-TrkB variants.

As for NGF and BDNF, transcripts were detected within both HK and FDC-1 lines (figure 5.4.2). HK cells show stronger levels of NT-3 transcripts compared to FDC-1, however both lines also show detectable NT-3 transcripts within RT positive lines compared to RT negative lines. NT-4 primers on the other hand reveal detectable transcripts within the RT positive and negative samples, therefore these results were rendered inconclusive.

Add fig 5.4 here

Overall, it is probable that FDCs can signal in an autocrine manner via TrkA and NGF and/ or NT-3. As for possible TrkB signals, HK lines may signal via truncated TrkB and BDNF and/ or NT-3. These results, together with the data on FDC markers, are summarised in table 5.1.

It is however also possible that FDCs may communicate with B cells via BDNF in a paracrine manner via truncated TrkB expressed by Mutu negative clone 3 cell lines that show undetectable levels of BDNF secretion compared to their latency III equivalent line, Mutu clone J8.

Add Table 5.1 here

5.2.3 The expression of NGF protein in FDC-like cell line, HK

Based on the characterisation of FDC-likeness, HK cells seem to show stronger levels of FDC markers compared to FDC-1 lines. Therefore HK cells are characteristically more FDC-like in terms of their expression for known FDC markers; hence HK cells were then carried forward within the investigation. In terms of possible paracrine signalling, FDCs were hypothesised to provide NGF to B cells such as Burkitt's lymphoma B cells which lack detectable NGF mRNA transcripts. To test this it was first essential to further question NGF expression in HK cells.

HK cells and the NGF control line, NT-2, were initially permeabilized then stained for NGF protein for flow cytometry analysis (figure 5.5). Both NT-2 control cells and HK cell show detectable NGF protein. Also, HK cells seem to have higher levels of NGF protein compared to NT-2 cells.

NGF protein expression was also analysed by confocal microscopy (figure 5.6). HK cells were grown on coverslips pre-coated with 5% poly L-Lysine, until 70 to 80% confluent. Cell were then permeabilized and stained for NGF using two different NGF antibodies from separate companies. Permeabilized cells stained with NGF (AF256NA) antibody show strong NGF stain which is considered specific by comparing the isotype control stain (figure 5.6.1). Cells stained using NGF (N3279) also show strong NGF expression (figure 5.6.2). The isotype control for this NGF antibody was also negative for any staining.

Next NGF protein expression was then compared to $p75^{NTR}$ expression in HK cells. NGF primary antibodies were detected using a green fluorescence secondary antibody for confocal microscopy, whereas the $p75^{NTR}$ antibody was detected using a red florescence secondary antibody (figure 5.6.3). Both primary antibodies were added at the same time and excess antibody was washed off. Specifically bound primary antibody was detected using the two secondary antibodies, also added at the same time. This was completed to question possible co-localised staining of $p75^{NTR}$ protein and NGF. A representative of three independent experiments is shown.

Add fig 5.5 and 5.6 here

Based on the confocal images shown in figure 5.6.1 to figure 5.6.3, NGF staining in HK cells is spread throughout the cellular cytoplasm. As for $p75^{NTR}$, the stain pattern seems to be localised around the cell nucleus. However this pattern of staining may be due to the anti-NGF antibody being more sensitive compared to the $p75^{NTR}$ antibody.

Since FDCs produce NGF protein observed within the cytoplasm, the next question to ask whether FDCs secrete NGF for possible paracrine signalling to germinal centre B cells. To do this, cell lysates obtained from HK and NT-2 cells were applied to measure the amount of NGF by an ELISA kit.

Initially, a standard curve was drawn from a serial dilution of human recombinant NGF protein. NGF dilutions ranging from 15pg/ml to 1000pg/ml were measured and OD readings were obtained. Raw OD readings for the NGF positive control cell line, NT-2 and four separate HK cell lysates were compared with the background standard.

These OD readings were carried forward to measure picograme concentrations of NGF protein based on the linear regression equation. The OD reading from the background control (used to dilute the NGF standards) was subtracted from each cell sample's OD reading. NGF concentrations were then calculated and plotted within figure 5.7.

Add fig 5.7

The NGF positive control line, NT-2, produced the highest detectable levels of intracellular NGF protein (451pg/ml), whereas, secreted the lowest levels of NGF protein within the supernatant (49pg/ml). As for HK cells, similar levels of secreted NGF were detected (128pg/ml to 113pg/ml) compared to intracellular NGF levels (159pg/ml to 123pg/ml). In all, NGF can be secreted by FDC-like cell line, HK. However, it is worth noting that this level of NGF secretion was not able to induce neurite outgrowth in PC12 cells (data not shown). The possible reason for a lack in biological activity maybe due to low levels of NGF protein concentration secreted by the FDC line.

To answer whether FDCs express could provide NGF paracrine signalling to TrkA expressing Burkitt's lymphoma B cells, the next part of the investigation was to further investigate the expression of TrkA protein in Burkitt's lymphoma B cell lines.

5.2.4 The expression of TrkA protein in Burkitt's lymphoma B cell lines

For TrkA and NGF paracrine signalling to occur between B cells and NGF producing FDCs, functional TrkA receptors will need to be expressed in B cells. As concluded within chapter 3, Burkitt's lymphoma B cell lines displaying varying EBV latency phenotypes, show detectable levels of TrkA mRNA.

The great advantage of confocal imaging is that it can show heterogeneity in the amount of protein within a cell line culture, while western blotting can only show the average amount for the whole cell population. Therefore Burkitt's lymphoma lines with varying EBV latency phenotypes were permeabilized and stained for TrkA protein using a primary TrkA antibody (figure 5.8). Specifically bound TrkA antibodies were detected using FITC conjugated secondary antibodies which were then examined by confocal microscopy.

Mutu negative clone 3 and Mutu latency I clone 59 cells express TrkA protein. Mutu negative cells reveal strong peripheral staining, whereas the majority of Mutu latency I cells show weaker cytoplasmic staining with few cells in suspension showing stronger staining levels.

Mutu latency III clone J8 cells and IARC-171 cells also stain for TrkA protein. Like Mutu latency I cells, Mutu latency III cells show cytoplasmic staining patterns with few cells in

suspension with stronger staining patterns. IARC-171 cells on the other hand, like Mutu negative cells, show peripheral TrkA staining.

Add fig 5.8 here

Interestingly, all Burkitt's lymphoma lines reveal heterogeneous patterns of TrkA staining. This is observed particularly in latency III cells Mutu clone J8 and IARC-171 with some live cells in suspension showing clear DAPI nuclear staining but lack any TrkA staining. This staining pattern was observed within all three independent repeats for TrkA staining.

In all, Burkitt's lymphoma B cell lines express TrkA mRNA and protein but lack detectable NGF mRNA, whereas FDC-like cell lines express NGF mRNA and protein. It has been noted that exogenous NGF includes a variety of downstream function effects in various cell types including B cells. The next section of this chapter will investigate NGF signalling in Burkitt's lymphoma cell lines.

5.2.5 Biological activity assessment for human recombinant NGF in PC12 cells

The , human recombinant NGF used to question cells survival, proliferation as well as cell migration in EBV negative Burkitt's lymphoma B cells was initially tested to ensure it was biologically active. To investigate this, PC12 cells were cultured on plates, pre-coated within Poly-D-lysine and rat tail collagen (figure 5.9). Cells were left in control media or cultured with 100ng/ml NGF within media for 7 days. Differences in cellular morphology were analysed by confocal microscopy and phase contrast microscopy.

100ng/ml of human recombinant NGF induced neurite outgrowth in PC12 cell cultures within 7 days hence the NGF used is biologically active at this concentration. This recombinant NGF then used to assess downstream signalling effects in Burkitt's lymphoma B cell lines.

Add fig 5.9 here

5.2.6 The downstream signalling effects upon exogenous NGF treatment within Mutu negative clone 3 cells

NGF is able to induce varying signalling outcomes in a variety of cells. It has been shown by Melamed I. *et al.*, that F-actin rearrangement and assembly can be observed upon NGF addition in human B cells (Melamed, Turner et al. 1995). Changes in the cell cytoskeletal arrangement may be involved in the actual transduction of signals from the surface receptor, leading to cell activation and proliferation. Since this cytoskeletal re-arrangement is time dependent, Mutu negative clone 3 cells were exposed to 100ng/ml NGF for 1 minute, 2 minutes, 5 minutes and 10 minutes (5.10.1). Cell were then stained for F-actin and viewed under confocal microscopy.

Without treatment (control media) F-actin levels remain low with weak phalloidin stain throughout the cell cytoplasm and the cellular periphery. However within a minute of NGF addition, cells show strong levels of phalloidin staining at the cell membrane. After two minutes of NGF exposure, Mutu cells reveal a more uniform spread of F-actin staining, with some cells in culture showing brighter staining than other cells. However, at 5 and 10 minutes of NGF treatments the phalloidin stain is weak and closely resembles the staining

observed in control treated cells. Hence NGF induces rapid F-actin rearrangement in Mutu negative clone 3 cells.

Add fig 5.10 here

It is also known that NGF can signal via TrkA causing receptor dimerization and phosphorylation. Downstream signalling pathways involve adaptor proteins such as Erk and Akt signalling for cell survival, differentiation and/ or proliferation.

Akt phosphorylation was then investigated in Mutu negative clone 3 cells treated with 100ng/ml NGF for 2 minutes, 5 minutes and 10 minutes. Cells were then washed and lysed. Protein lysates were then extracted and run through a 4 to 12% polyacrylamide with SDS gradient gel (Bis-Tris buffer) under reducing conditions, samples were transferred onto PVDF. Samples were probed using either an Akt antibody or a Phospho-Akt antibody (figure 5.10.2).

Erk phosphorylation was also examined within NGF treated Mutu negative lines. This time cells were treated at varying time points then fixed and stained for Phospho-Erk protein for confocal microscopy analysis (figure 5.10.3).

To test whether Erk Phosphorylation induced by NGF is TrkA phosphorylation dependent, Trk signalling inhibitor K252a, as well as TrkA inhibitors GW441756 and TrkAd5, were compared to control treated cells (Figure 5.10.4).

Akt phosphorylation was detected in control treated Mutu negative cells hence background signalling in Mutu negative clone 3 cells produces some Akt phosohorylation howver, within 2 minutes of NGF treatment, Akt phosphorylation is observed (figure 5.10.2). This level of phosphorylation is maintained 10 minutes post NGF addition.

Peripheral Erk Phospho-protein staining was detected within control treated Mutu cells but at low levels (figure 5.10.3). By treating cells with NGF, Erk Phosphorylation staining steadily increased from 30 seconds and peaked at 10 minutes. Levels of Phospho-Erk protein started to diminish 15 minutes and at 30 minutes post NGF addition, levels of detectable protein had reduced to similar levels observed in control treated Mutu cells. Erk signalling inhibitor PD98059, inhibited NGF induced Erk phosphorylation 10 minutes post NGF addition in Mutu negative cells.

However to ensure NGF induced Erk Phosphorylation was dependent on TrkA phosphorylation, Trk inhibitors K252a, GW441756 and TrkAd5 were used to pre-treat the Mutu cells before addition of NGF for 10 minutes (figure 5.10.4). Erk phosphorylation was inhibited when TrkA signalling was also withdrawn, hence Erk Phosphorylation, induced by NGF in Mutu negative clone 3 cells, is TrkA dependent.

5.2.7 The effects of exogenous NGF in Burkitt's lymphoma B cell lines treated in Anti-IgM

To question the possibility that NGF may act in B cells by signalling for cell survival, an experiment published by Kronfeld et al., where anti-IgM induced cell death was inhibited upon NGF treatment within Ramos cells (Kronfeld, Kazimirsky et al. 2002). The Ramos cell line was derived from an EBV negative Burkitt's lymphoma tumour biopsy and shares many phenotypic characteristics of the original tumour (Klein, Giovanella et al. 1975). These Ramos cells were treated in 10μg/ml anti-IgM which induced cell death but addition of 100ng/ml NGF lowered the percentage of non-viable cells by ~50%. Importantly, a pre-incubation with 50ng/ml K252a inhibits the anti-cell death effect observed by NGF. This experiment was repeated using Ramos cells and L23055 cells. L3055 cells are also EBV Burkitt's lymphoma B cell lines used to compare Ramos cells (figure 5.11.1).

The addition of 100ng/ml human recombinant NGF had little effect in comparison to control treated Ramos cells, however NGF seems to slightly decrease the percentage of live (PI low) L3055 cells compared to those in control media (figure 5.11.1). 2μg/ml anti-IgM efficiently induced cell death; however 100ng/ml NGF was unable rescue both cell lines analysed. The

reasons for this lack of rescue was initially presumed to be limited NGF within culture therefore a dose response experiment was conducted using 50ng/ml, 100ng/ml and 200ng/ml of human recombinant NGF in Ramos cells (figure 5.11.2) and another EBV negative line, BL41 cells (figure 5.11.3).

Add fig 5.11 here

As previously shown, anti-IgM induces cell death in Ramos cells treated for 24 hours however no rescue effect was observed in Ramos cells treated in either 50ng/ml, 100ng/ml or 200ng/ml NGF concentrations (figure 5.11.2).

BL41 cells were also tested to question if NGF can rescue cells from cell death (figure 5.11.3). Unfortunately, like Ramos cells, 50ng/ml, 100ng/ml or 200ng/ml NGF is unable to rescue BL41 cells treated in 2μg/ml anti-IgM.

A summary showing four independent apoptosis experiments in BL41 and L3055 cells are shown within figure 5.11.4.

Mean PI low cells and standard error bars from four independent experiments using L3055 cells are shown on figure 5.11.4a and those for BL41 cells are shown in figure 5.11.4b. All together, these results shown that human recombinant NGF is unable to rescue Ramos, L3055 and BL41 Burkitt's lymphoma cells from apoptosis induced by anti-IgM. It is also with noting that NGF alone does not increase the numbers of live cells in either Ramos, L3055 or BL41 lines compared to control treated cells.

5.2.8 The effects of exogenous NGF in Burkitt's lymphoma B cell proliferation

Since NGF does not seem to induce cell survival in EBV negative Burkitt's lymphoma B cells lines, and it seemed to not induce cell proliferation when added alone in culture, this was worth further testing the effects of NGF treatment on cell proliferation. This time EBV negative Mutu clone 3 cells were initially treated in CFSE dye and cultured with varying concentrations of NGF for 24 hours (5.12.1).

According to the mean CFSE dye levels from three independent experiments, shown in figure 5.12.1b, there seems to be a difference in CFSE dye levels between control cells and those treated in 50ng/ml NGF. However this is a slight difference as clearly seen within the histograms displayed in figure 5.12.1a. On the other hand, there does not seem to be any effect upon treatment with 100ng/ml or 200ng/ml NGF treatment.

Cell proliferation rates were also measured by the assessment of DNA synthesis. Mutu negative cells were treated in 2μg/ml Anti-IgM, as a proliferation inhibition control, 1μg/ml CD40-L, as a proliferation promoter control and compared to 100ng/ml NGF (figure 5.12.2).

Add fig 5.12 here

As expected, anti-IgM inhibited cell proliferation in Mutu negative clone 3 cells; whereas CD40-L stimulation promoted a slight increase in cell proliferation when compared to control treated cells (figure 5.12.2). 100mg/ml NGF on the other hand, seems to inhibit rather than promote cell proliferation, but of a lesser extent than anti-IgM treatment. This is a discrepancy compared to the previous results obtained from the CFSE stain in Mutu negative cells treated with 100ng/ml NGF, where proliferation levels were similar to control treated cells (Figure 5.12.1). This disparity may be due to the differences in methods used. CFSE dye is diminished over time as cells proliferate, whereas thymidine is incorporated into dividing cells, hence the thymidine method could also be used to observe any changes in cell viability upon treatment considering live cell uptake thymidine, whereas static, no-dividing viable cells would still maintain high levels of CFSE dye. Hence the thymidine incorporation assay may indicate cell death in Mutu negative clone 3 lines upon treatment with 100ng/ml NGF over 24 hours which is not as clearly defined in the CFSE assay. For this set of experiments to be repeated, Mutu negative clone 3 cells lines could be analysed for PI absorbance when treated for 24 hours in 100ng/ml NGF.

On the other hand, Ramos, L3055, BL41 or Mutu negative clone 3 cells do not show any signs of cell proliferation upon treatment with 50ng/ml, 100ng/ml or 500ng/ml human recombinant NGF.

5.2.9 The effects of exogenous NGF in Burkitt's lymphoma B cell migration

The last set of experiments show that NGF does not seem to induce cell proliferation or rescue from cell death, thus the signalling outcome by exogenous NGF were still unknown. Next, it was speculated that NGF may induce cell migration in Burkitt's lymphoma cells. To test this hypothesis, cells were placed within the top chamber of transwell membrane inserts. Chemoattractants were added within the bottom chamber and cells were left to migrate for 6 hours.

Stromal cell-Derived Factor-1 (SDF-1) also known as CXCL-12, was used as the positive control chemoattractant and compared to varying concentrations of NGF for Mutu negative clone 3 cell migration. To ensure Mutu negative clone 3 cells respond to CXCL-12, cells were tested for the CXCL-12 receptor, CXCR4 by flow cytometry (5.13.1).

Mutu negative cells were then placed within the top chamber on transwell membrane plates. The chemokine in question, the CXCL-12 control or human recombinant NGF, were placed within the bottom well of the transwell membrane plate. Plates were incubated for

6 hours. The numbers of cells within the top and bottom wells were counted using a flow cytometer. Cell migration percentages were calculated and compared between Mutu cells exposed to low NGF concentrations (50ng/ml to 100pg/ml) shown in figure 5.13.2a, and high NGF concentrations (100ng/ml to 100μg/ml) shown in figure 5.13.2b.

Add figure 5.13 here

Mutu negative cells express the CXCR4 receptor for CXCL-12. CXCL-12 was then used as a control chemoattractant and compared to NGF. Low NGF concentrations of NGF do not induce cell migration as shown in figure 5.13.2a. Higher NGF concentrations also do not promote cell migration in Mutu negative cells (figure 5.13.2b). It is however worth noting that the migration percentages observed are very low in number, even within those cells exposed to CXCL-12.

CXCL-12 induced cell migration was then compared to Mutu negative cells exposed to culture supernatant from HK cells and the cell line used as a positive control for NGF expression, human neural precursor, NT-2 cells (figure 5.13.3). Although, CXCL-12 induces cell migration in Mutu negative clone 3 cells, supernatant from HK cells had no effect on cell migration, whereas supernatant from NT-2 cells promoted cell migration. Importantly, Mutu negative cells pre-treated with TrkA inhibitor, GW441756, then exposed to NT-4 supernatant show reduced cell migration percentages. Whereas, Mutu negative cells pre-treated with TrkAd5 reveal slightly higher levels of inhibition in cell migration.

Therefore a chemokine expressed in NT-2 cells induced cell migration. This chemokine is speculated to be, or involves NGF since pre-treating Mutu cells with TrkA inhibitors, greatly reduces cell migration numbers in Mutu negative cells. However NGF alone did not induce such an effect in migration.

Part I discussion

The human recombinant NGF used in the experiments within this part of the results chapter was previously shown to induce neurite outgrowth in PC12 cell cultures within 7 days, therefore the lack of biological function within EBV negative cell lines, treated with NGF, are genuine results.

It is possible that NGF and another unknown secreted protein may induce B cell migration as observed in figure 5.13.3, where Mutu negative clone 3 cells migrated towards media obtained from NT-2 cells. Firstly, this result was unexpected since HK cells showed higher levels of secreted NGF compared to NT-2 cells within the ELISA assay (figure 5.7.3). And yet media obtained from NT-2 cells induced cell migration which was NGF:TrkA signalling pathway specific due to the inhibition in migration when Mutu negative cells were pre-treated with TrkA signalling inhibitors. The unknown protein that may act with NGF or may

be controlled by NGF and TrkA signalling to induce cell migration is possibly not expressed in HK cells.

Notwithstanding, that basal Erk and Akt phosphorylation was detected in Mutu negative clone 3 lines, NGF induce a further increase in phosphorylation. Also, Erk phosphorylation was blocked upon NGF stimulation in Mutu negative cells treated with varying TrkA signalling inhibitors. Therefore, exogenous NGF activates Mutu cells by signalling through TrkA for Erk and Akt dependent activity, however the outcomes for this signalling cascade are currently known.

Due to the observation of basal Erk and Akt phosphorylation in Mutu negative cells, and the lack of a survival or cell growth signalling outcome upon exogenous NGF addition, the hypothesis within this part of the thesis was altered to question possible NGF and TrkA autocrine signalling in Mutu negative cells.

5.2 Results PartII : Investigating possible autocrine signalling effects within Burkitt's lymphoma B cells

5.2.10 The production of NGF protein in Burkitt's lymphoma B cell lines

To examine possible NGF protein expression in Burkitt's lymphoma B cells lines, Mutu negative, latency I and latency III cells were permeabilized and stained for NGF protein for flow cytometry analysis (figure 5.14.1). All Burkitt's lymphoma B cell lines were also screened for NGF protein expression by western blotting methods (figure 5.14.2).

Interestingly, NGF protein was detected within Mutu negative clone 3 cells, Mutu latency I clone 179 and Mutu latency III clone J8 cells (figure 5.14.1).

NGF expression was also analysed by using western blotting methods. Like HK cells, Mutu negative clone 3 cells expressed low levels of NGF protein compared to Mutu latency I, Mutu latency III and IARC-171 cells which show higher levels of detectable protein (figure 5.14.2). ~25kDa and ~32kDa proteins were detected buy the NGF antibody, presumed to be proNGF proteins. Both ~25kDa and ~32kDa bands were observed at equal levels within all Mutu and HK cells analysed.

Add fig 5.14 here

In all, Burkitt's lymphoma B cells express NGF protein. EBV negative Mutu lines reveal similar levels of NGF expression to HK cells, whereas latency I and latency III cell lines show higher levels of NGF protein by ELISA and western blotting methods.

In turn, Burkitt's lymphoma B cells express NGF protein and its receptors TrkA and $p75^{NTR}$. The focus for this part of the investigation was then altered to investigate the possible TrkA:$p75^{NTR}$ and NGF autocrine signalling pathways in Mutu negative clone 3 cells.

5.2.11 The effect on cell death upon TrkA autocrine signalling inhibition in Mutu negative clone 3 Burkitt's lymphoma B cell line

To investigate TrkA and NGF autocrine signalling in Mutu negative clone 3 cells, the induction of cell death was analysed within cells treated with various TrkA:$p75^{NTR}$ and NGF signalling inhibitors. 24 hours post treatment cells were stained for PhiPhiLux and propidium iodide. Cells were then measured by flow cytometry for the induction of apoptosis or necrosis (figure 5.15).

Dose response assays using TrkA inhibitors were initially completed using TrkAd5. Cells were treated in 1μM to 25μM TrkAd5 inhibitor for 24 hours (figure 5.15.1). Caspase-3 activity was measured by phiphilux staining and cell necrosis was measured by PI absorption. As seen in the cell proliferation assay, TrkAd5 had no effect on cell survival in Mutu negative clone 3 cells.

The TrkA inhibitor GW441756 was also used in a dose response assay for cell apoptosis in Mutu negative clone 3 cells (figure 5.15.2). GW441756 concentrations ranging from 0.1nM to 100μM were added to cells treated in culture for 24 hours. Dot plots shown in figure 5.15.2a show the majority of Mutu negative cells are live (81.8%) within control media. Between 0.1nM and 1μM GW441756, majority of Mutu negative cells remain within the same quadrant within the dot plot, displaying live cells. From a concentration of 5μM to 50μM GW441756, majority of Mutu negative cells displayed early apoptotic staining patterns. Finally, at a concentration of 100μM GW441756, the majority of cells (90.2%) were late apoptotic.

Looking at the same data plotted within a graph (figure 5.15.2b), it is clear that there is a big shift in live cells to early apoptotic cells between 1μM and 5μM GW441756. This clear gap was also observed within the following figure (figure 5.15.3).

The GW441756 dose response experiment was repeated. Mean live, early, late apoptotic and necrotic cell percentages within each dot plot were calculated from three independent experiments. This data, displayed in figure 5.15.3, also displays the standard deviation error bars form each experiment.

Between concentrations of 0.1nM and 1μM, the GW441756 inhibitor had no effect on Mutu negative cell survival. However between 5μM and 50μM concentrations, GW441756 induced early apoptosis in Mutu cells. In turn, increasing the GW441756 concentration to 100μM induced late apoptosis in Mutu cells.

Add figure 5.15.1 to 5.15.3 here

To pin point the concentration at which GW441756 shifts cells from live to early apoptotic cells, the dose response experiment was repeated to focus on concentrations between 1μM and 5μM GW441756 (figure 5.15.4a).

GW441756 inhibitor has no effect on Mutu cell lines at 500nm and 1μM concentrations. However from 2μM to 10μM, GW441756 induced early apoptosis in Mutu negative cells. A further increase in GW441756 concentration from 50μM to 100μM increase the number of late apoptotic cells.

GW441756 induced early, then late apoptosis in Mutu negative cells by inhibiting TrkA phosphorylation as shown in figure 5.15.4b. Although TrkA phosphorylation was still detectable at a GW441756 concentration of 50μM, phosphorylation levels were diminished compared to control treated Mutu cells. Importantly, TrkA levels remained the same within all cell samples.

The induction of apoptosis by GW441756 was then compared to K252a. Concentrations ranging from 50nM to10μM were analysed within a dose response experiment for cell survival (figure 5.15.5). K252a treated cells were compared to control media treated cells and those treated with the K252a vehicle control, DMSO. DMSO added was at an equivalent level to the 10μM K252a concentration. Mean cell percentages for live, early, late apoptotic and necrotic cells are displayed with their standard error bars from three independent experiments.

At low K252a concentrations ranging from 50nM to 100nM, no changes in the levels of live Mutu cells were observed. As the K252a concentration was increased from 500nM to

10μM, the proportion of live cells was diminished, with a steady increase in late apoptotic cells (5.15.5). At a concentration of 10mM, K252a induced late apoptosis in Mutu negative cells.

Unlike GW441756, K252a induced late apoptosis in Mutu negative cells by inhibiting TrkA phosphorylation as shown in figure 5.15.6. Although TrkA phosphorylation was still detectable at a K252a concentration of 0.5μM, phosphorylation levels were undetectable at a concentration of 1μM, compared to control treated Mutu negative cells. Importantly, full TrkA levels remained the same within all cell samples.

Add fig 5.15.4 to 5.15.6 here

A dose response experiment was also completed using Akt inhibitor, LY294002 and Erk inhibitor PD98059 (5.15.7). By increasing the concentration of LY294002 from 1μM to 200μM, increased the proportion of late apoptotic Mutu negative cells. Hence the induction of apoptosis in Mutu negative clone 3 cells by TrkA inhibition may involve Akt signalling.

As for Erk inhibition, PD98059 had no effect on cell survival. A concentration of 1mM to 200mM was used. Erk signalling inhibition therefore may not be involved in the cell survival of Mutu negative clone 3 cells.

Add fig 5.15.7 here

In all, based on these dose response experiments, the working concentrations of the inhibitors were determined. GW441756 was used at a concentration of 5μM, K252a was used at 1μM, TrkAd5 (like TrkBd5) used at 4.5μM, $p75^{NTR}$ neutralising antibodies (MLR2 and MLR3) used at 100μg/ml and Akt inhibitor (LY294002) and Erk inhibitor (PD98059) used at 50μM/ml.

5.2.12 The effect on cell proliferation upon TrkA:p75^{NTR} autocrine signalling inhibition in Mutu negative clone 3 Burkitt's lymphoma B cell line

To study autocrine signalling pathways within the EBV negative Mutu clone 3 line, TrkA and p75^{NTR} signalling inhibitors and neutralising NGF antibodies were added within the culture to question their effects on cell proliferation. Mutu negative cells were initially dyed with CFSE and treated with varying TrkA or NGF inhibitors for 48 hours. The differences in CFSE dye levels were measured by flow cytometry analysis (figure 5.16).

The negative controls, Anti-IgM (2μg/ml) and Mitomycin C (40μg/ml), were used as inhibitors for cell proliferation (Figure 5.16.1). Proliferation was inhibited by Anti-IgM and Mitomycin C in Mutu negative clone 3 cells. Interestingly, the Akt inhibitor, LY94002 (50μM/ml), slows cell proliferation in Mutu negative cells; however Erk inhibitor, PD98059

(50μM/ml), had no effect on cell proliferation. Therefore Akt signalling seems to be involved in cell proliferation within Mutu negative clone 3 lines.

Three TrkA inhibitors were added within this experiment. Tyrosine kinase signalling inhibitor K252a (1μM/ml), TrkA receptor domain 5 analogue TrkAd5 (4.5μM/ml) and the selective aza-oxindole, GW441756 (5μM/ml), were compared in their abilities to inhibit cell proliferation. K252a inhibited cell proliferation compared to control treated cells and those treated with the K252a vehicle control, DMSO.

Add figure 5.16 here

The TrkA domain 5 inhibitor, TrkAd5 had no effect on cell proliferation inhibition, whereas GW441756 abridged cell proliferation but to a lesser extent compared to K525a. The neutralising antibody for $p75^{NTR}$ signalling on the other hand, had no effect on cell proliferation in Mutu negative clone 3 cells.

Unexpectedly, the NGF neutralising antibody (20 μg/ml) also had no effect on Mutu negative clone 3 cell proliferation.

Considering the possibility that TrkA may for heterodimers with p75NTR, it is possible that TrkA signalling alone in Mutu negative cells is required for cell proliferation since inhibiting $p75^{NTR}$ shows no effect in growth inhibition. However TrkA and NGF may signal for cell proliferation since inhibiting TrkA signalling via K252a or GW441756 slows cell proliferation.

Signalling for cell proliferation also involves Akt signalling however based on these results, it is known of Akt signalling occurs due to TrkA phosphorylation.

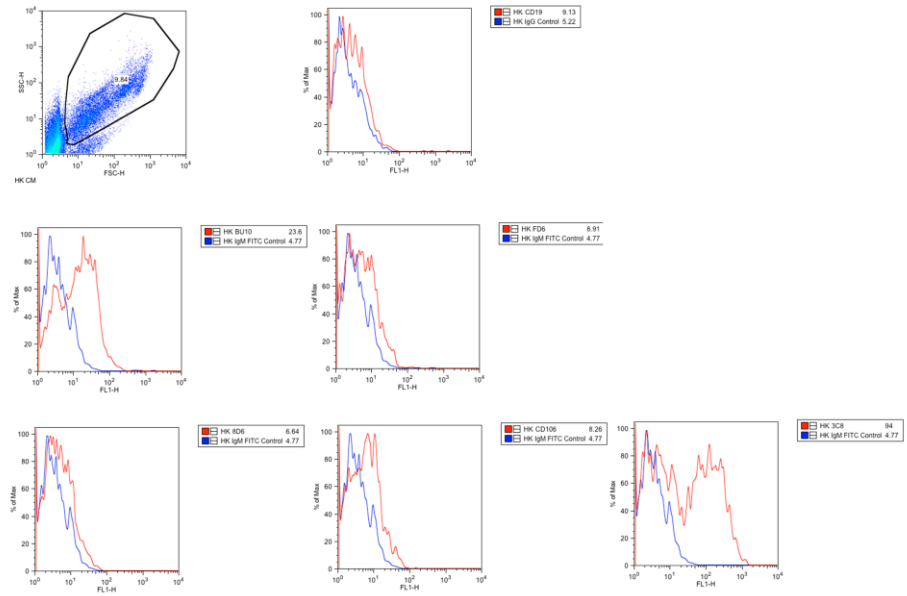

Figure 5.1.1: Characterising Follicular dendritic like–cell line, HK, for known surface markers by flow cytometry analysis
Permeabilized HK cells stained for flow cytometry analysis using CD19, BU10 FD6, 8D6, CD106 and 3C8 antibodies. The dot plot, show above, displays the population of cells collected for FITC measurement, gates were drawn from PI low cells taken from culture.
The primary antibodies used were compared to the isotype control within each histogram displayed. A secondary antibody directly conjugated with FITC was used to detect specifically bound primary antibody. Mean FITC levels were displayed from each histogram.
A representative of three independent experiments is shown.

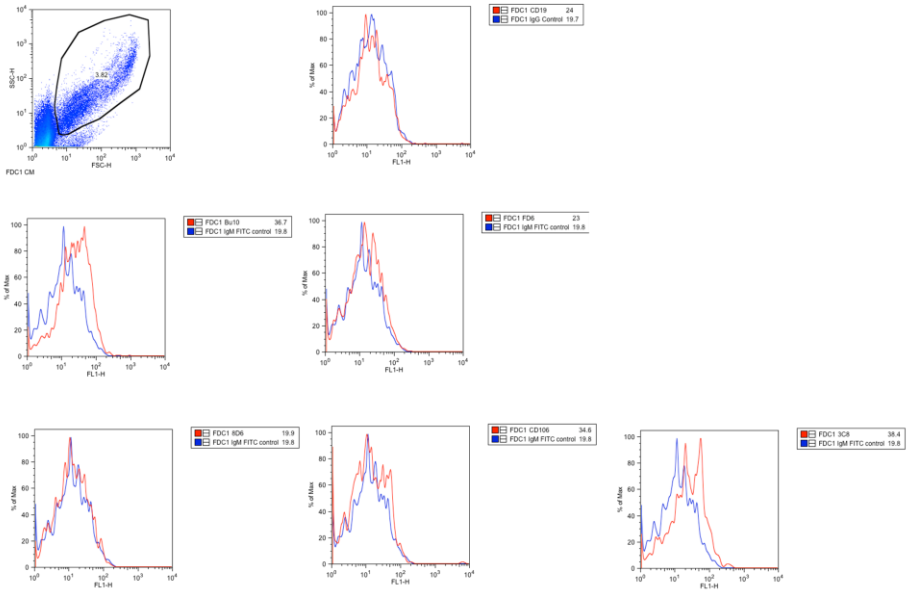

Figure 5.1.2: Characterising Follicular dendritic like–cell line, FDC-1, for known surface markers by flow cytometry analysis
Permeabilized FDC1 cells stained for flow cytometry analysis using CD19, CD21, CD23 BU10 FD6, 8D6, CD106 and 3C8 antibodies. The dot plot, show above, displays the population of cells collected for FITC measurement, gates were drawn from PI low cells taken from culture.
The primary antibodies used were compared to the isotype control within each histogram displayed. A secondary antibody directly conjugated with FITC was used to detect specifically bound primary antibody. Mean FITC levels were displayed from each histogram.
A representative of three independent experiments is shown.

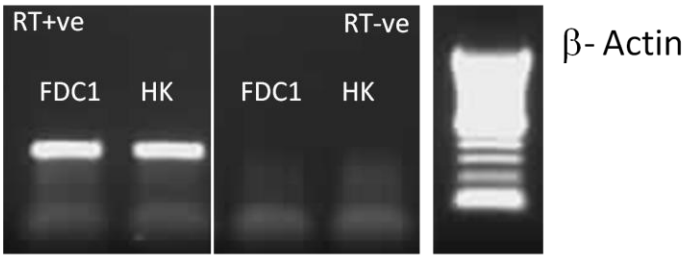

Figure 5.2.1: mRNA transcripts of β-actin in FDC-like lines FDC-1 and HK
RT-PCR primers specific for β-actin were used in an RT-PCR reaction producing a 300bp amplicon. RT positive and negative products were separated on a 1.5% agarose gel containing ethidium bromide and visualised under UV light.
Representatives of three independent experiments are shown.

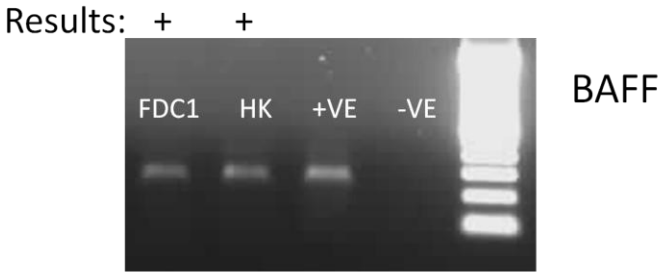

Figure 5.2.2: mRNA transcripts of BAFF in FDC-like lines FDC-1 and HK
RT-PCR primers specific for BAFF were used in an RT-PCR reaction producing a 250bp amplicon. RT positive and negative products were separated on a 1.5% agarose gel containing ethidium bromide and visualised under UV light.
Representatives of three independent experiments are shown.

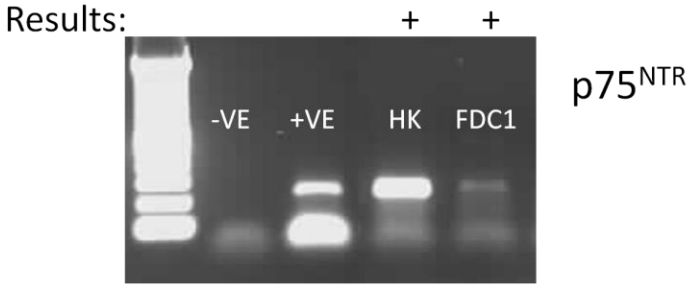

Figure 5.2.3: mRNA transcripts of $p75^{NTR}$ in FDC-like lines FDC-1 and HK
RT-PCR primers specific for $p75^{NTR}$ were used in an RT-PCR reaction producing a 246bp amplicon. RT positive and negative products were separated on a 1.5% agarose gel containing ethidium bromide and visualised under UV light.
Representatives of three independent experiments are shown.

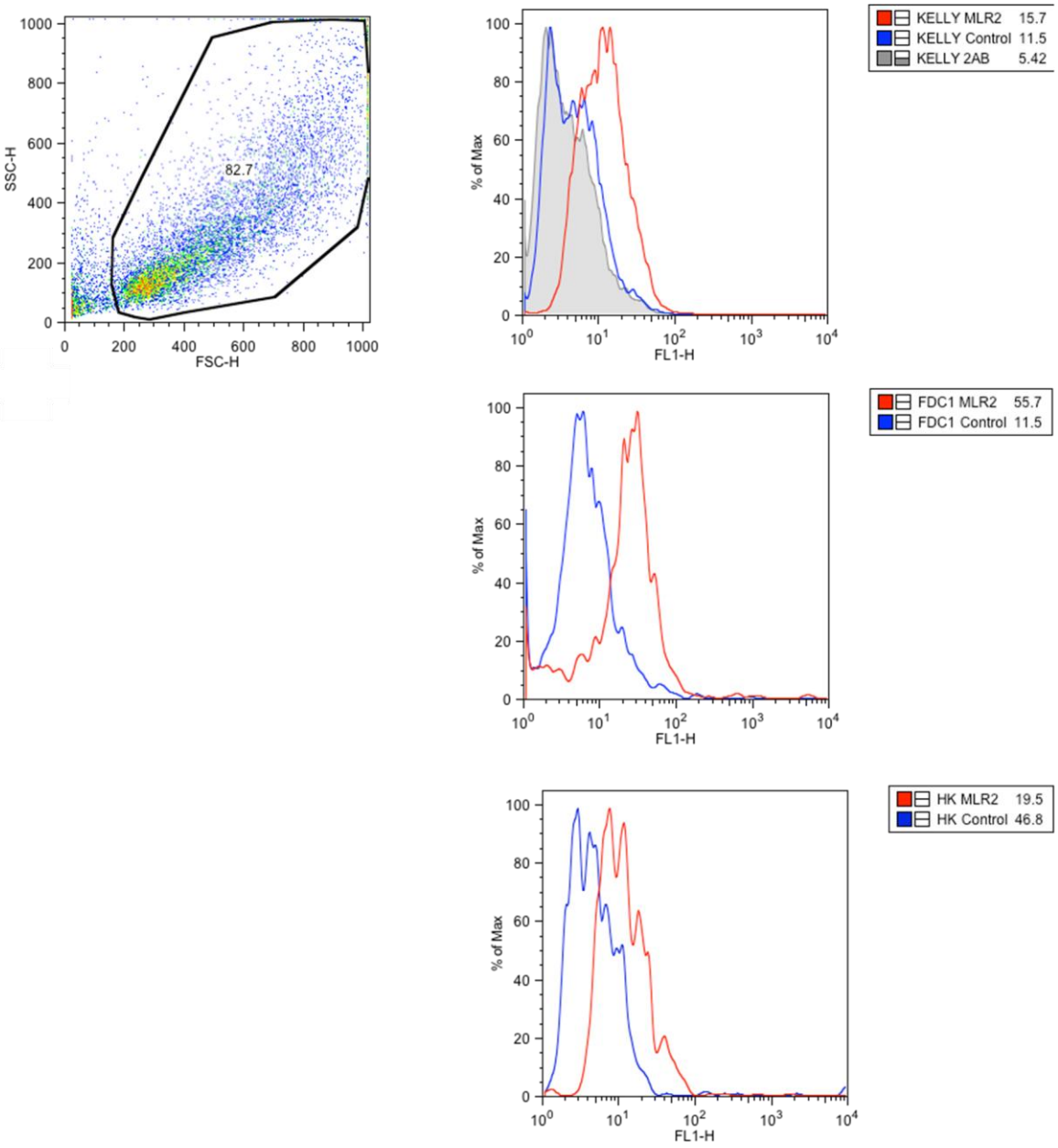

Figure 5.3: Characterising Follicular dendritic like–cell lines for p75^{NTR} expression
Permeabilized Kelly, FDC-1 and HK cells stained for flow cytometry analysis using p75^{NTR} antibody (MLR2) The dot plot, show above, displays the population of cells collected for FITC measurement, gates were drawn from PI low cells taken from culture.
The primary antibodies used were compared to the isotype control within each histogram displayed. A secondary antibody directly conjugated with FITC was used to detect specifically bound primary antibody. Mean FITC levels were displayed from each histogram.
A representative of three independent experiments is shown.

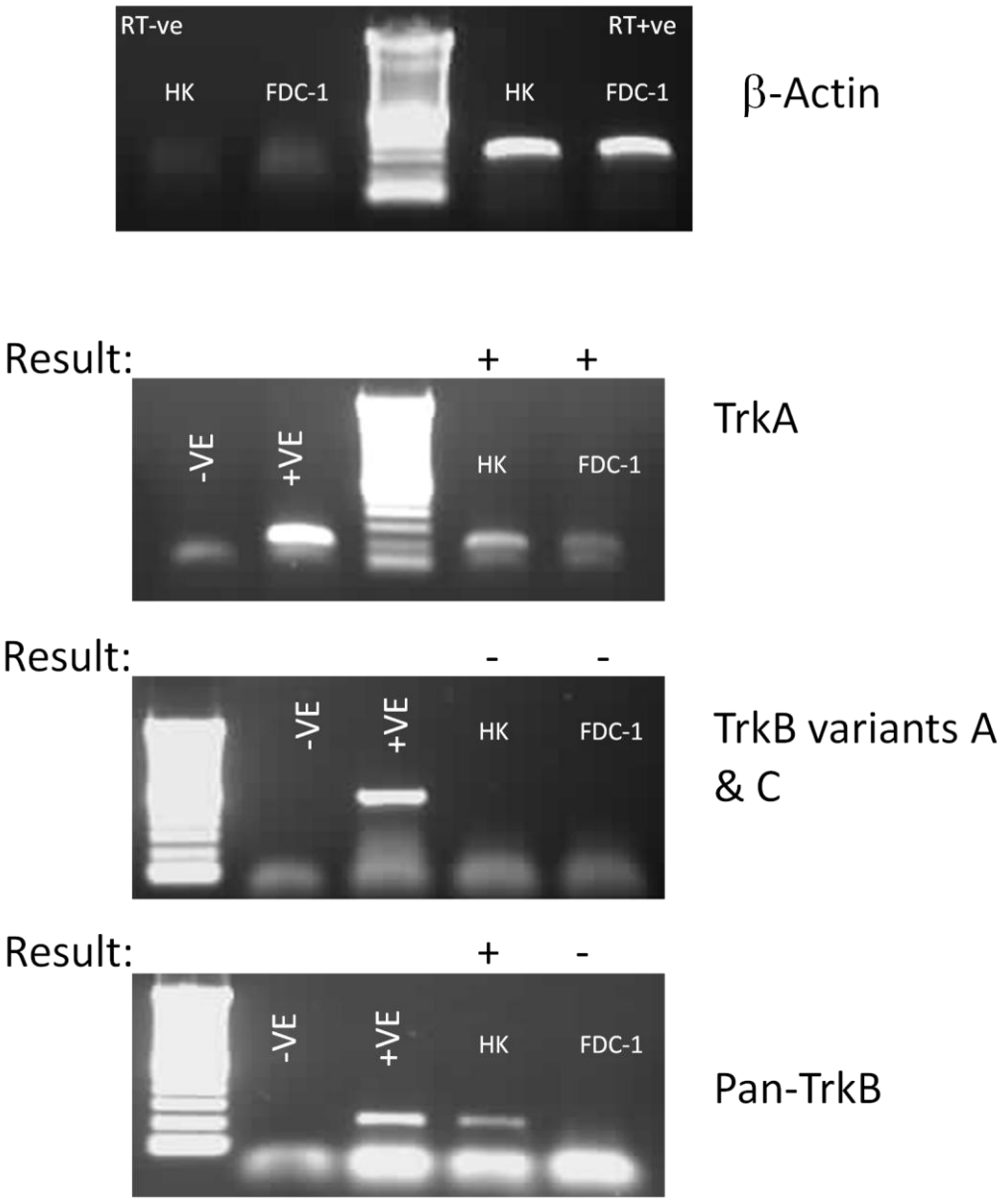

Figure 5.4.1: mRNA transcripts of β-actin, TrkA and TrkB in FDC-like lines HK and FDC-1
RT-PCR primers specific for β-actin were used in an RT-PCR reaction producing a 300bp amplicon. TrkA primers produced a 201bp amplicon and TrkB primers for TrkB Variants A and C prodcued a 574bp amplicon, whereas Pan-TrkB primers produces a 221bp amplicon. RT positive and negative products were separated on a 1.5% agarose gel containing ethidium bromide and visualised under UV light.
Representatives of three independent experiments are shown.

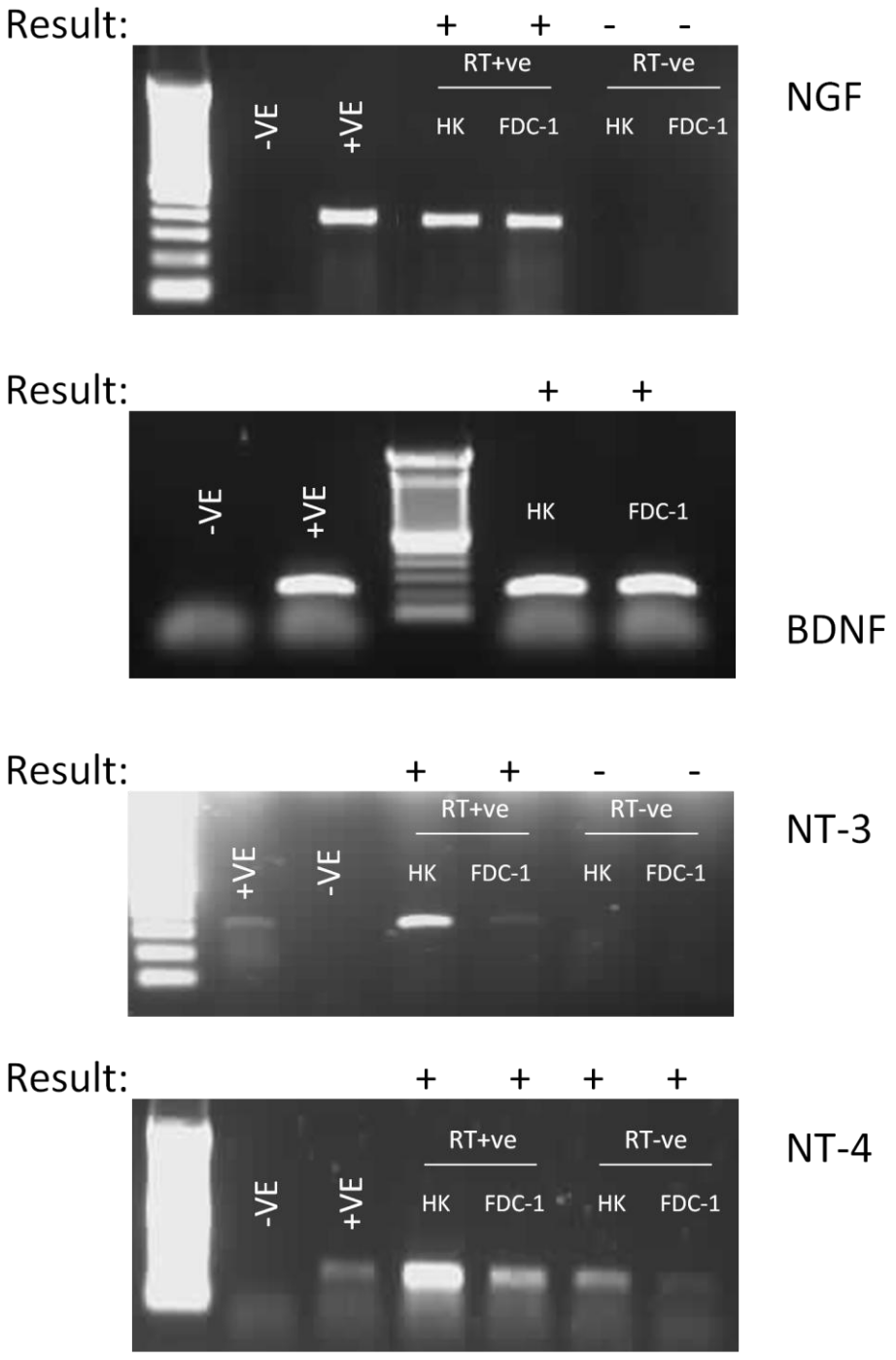

Figure 5.4.2: mRNA transcripts of NGF, BDNF, NT-3 and NT-4 in FDC-like lines HK and FDC-1
RT-PCR primers specific for NGF were used in an RT-PCR reaction producing a 325bp amplicon. BDNF primers produced a 221bp amplicon, NT-3 primers produced a 343bp amplicon and primers for NT-4 produced a 201bp amplicon. RT positive and negative products were separated on a 1.5% agarose gel containing ethidium bromide and visualised under UV light.
Representatives of three independent experiments are shown.

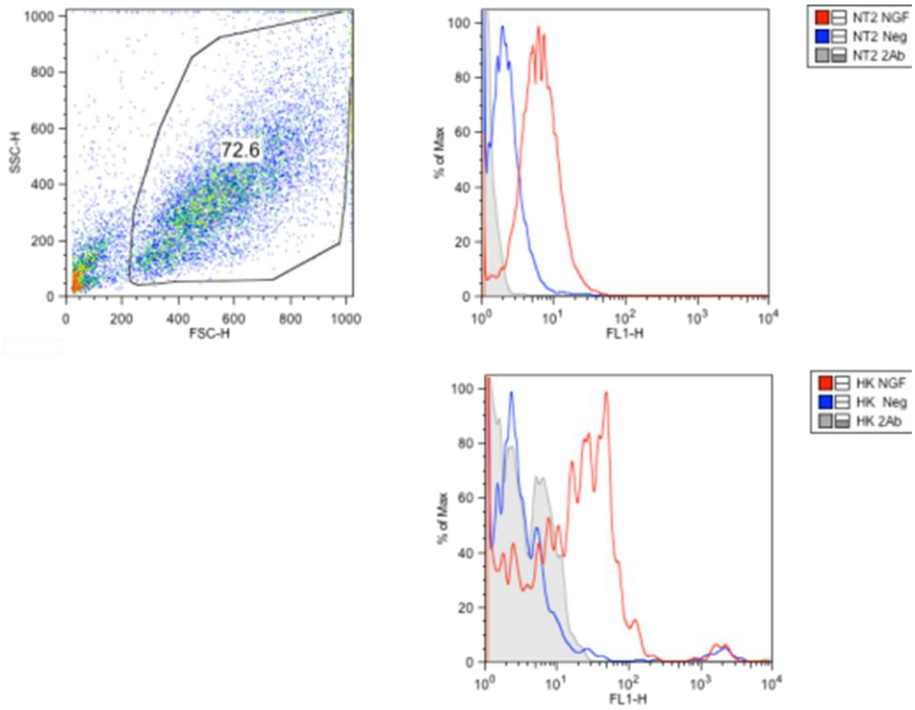

Figure 5.5: The expression of NGF protein in FDC-like cell line, HK by flow cytometry

Permeabilized NT-2 and HK cells stained for flow cytometry analysis using an NGF antibody. The dot plot, shown above, displays the population of cells collected for FITC measurement, gates were drawn from PI low cells taken from culture.

NGF (N3279) was the primary antibody used (NGF) and compared to the isotype control (Neg). A secondary antibody directly conjugated with FITC (2Ab) was used to detect specifically bound NGF antibodies.

A representative of three independent experiments is shown.

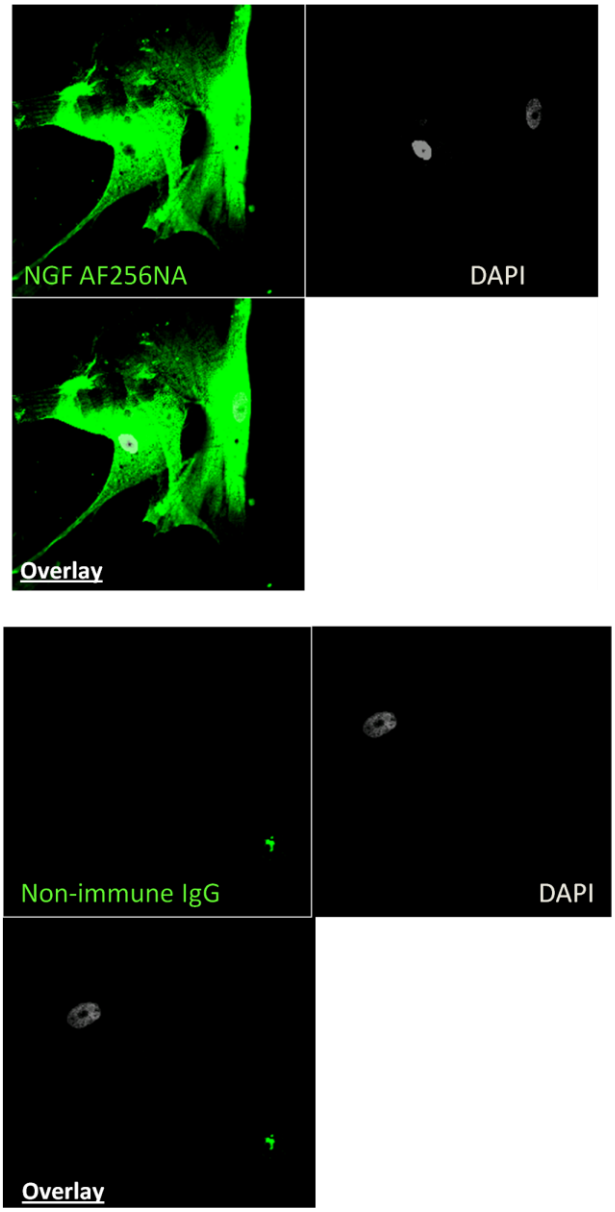

Figure 5.6.1: The expression of NGF protein (AF256NA) in FDC-like lines, HK by confocal microscopy

Confocal images showing permeablised HK cells stained for NGF (AF256NA) primary antibody and DAPI nuclear stain. Specifically bound NGF antibodies were detected by FITC-congugated secondary antibodies then viewed under an LSM laser miscroscope. Immunoglobulin specific isotype controls were also used to compare primary antibody staining. A representative of three independent experiments are shown.

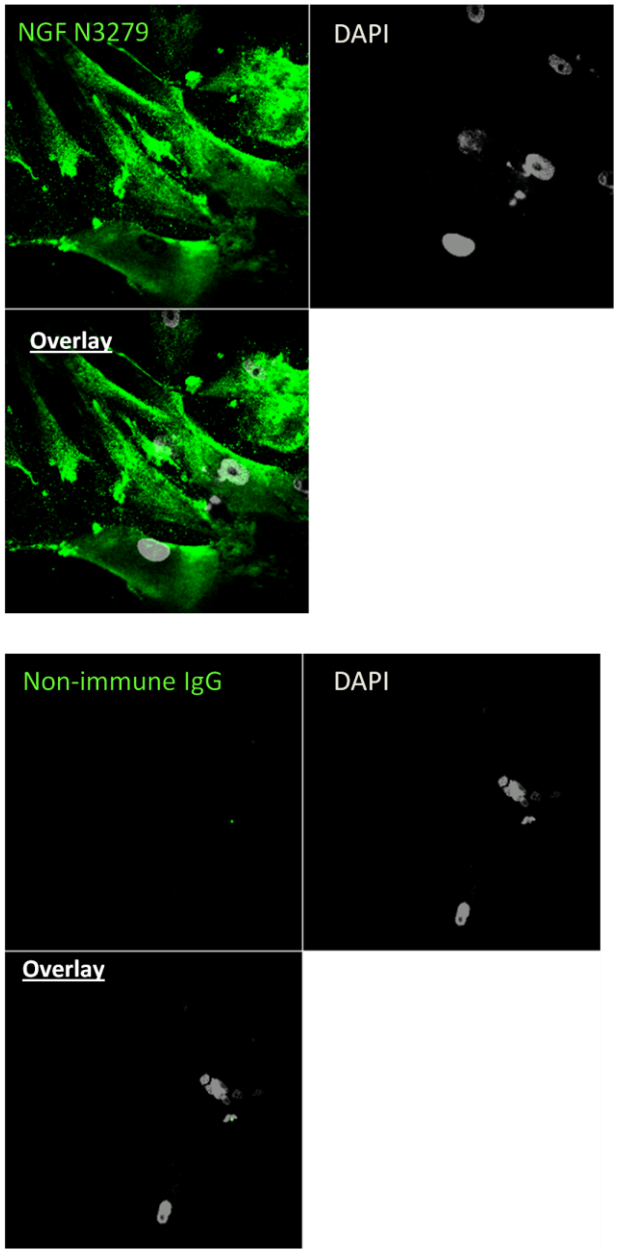

Figure 5.6.2: The expression of NGF protein (N3279) in FDC-like lines, HK by confocal microscopy
Confocal images showing permeablised HK cells stained for NGF (N3279) primary antibody and DAPI nuclear stain. Specifically bound NGF antibodies were detected by FITC-congugated secondary antibodies then viewed under an LSM laser miscroscope. Immunoglobulin specific isotype controls were also used to compare primary antibody staining. A representative of three independent experiments are shown.

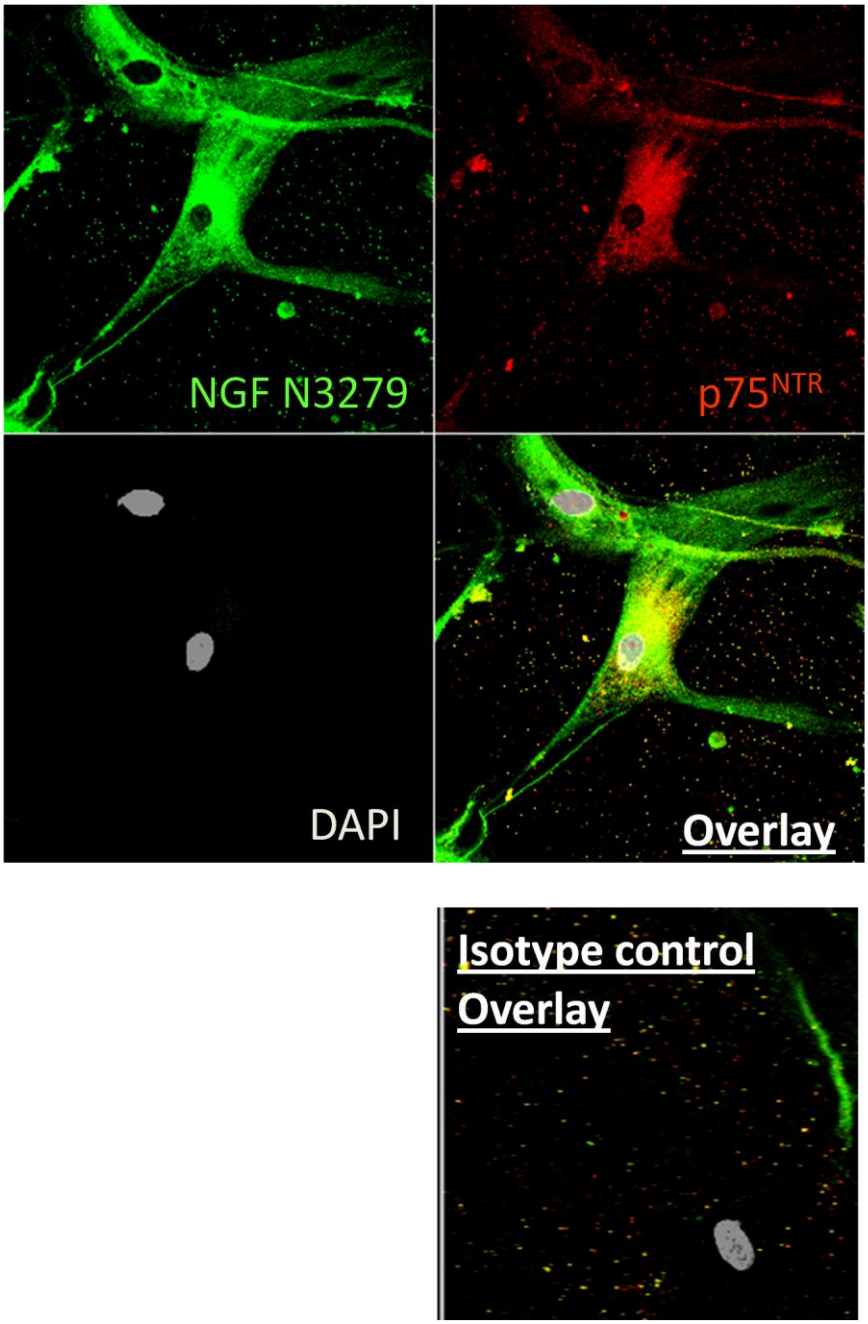

Figure 5.6.3 The expression of p75^{NTR} and NGF protein in FDC-like lines, HK
Confocal images showing permeablised HK cells co-stained for NGF (N3279) and p75^{NTR} primary antibody and DAPI nuclear stain. Specifically bound NGF antibodies were detected by FITC-congugated secondary antibodies then viewed under an LSM laser miscroscope. Immunoglobulin specific isotype controls were also used to compare primary antibody staining.

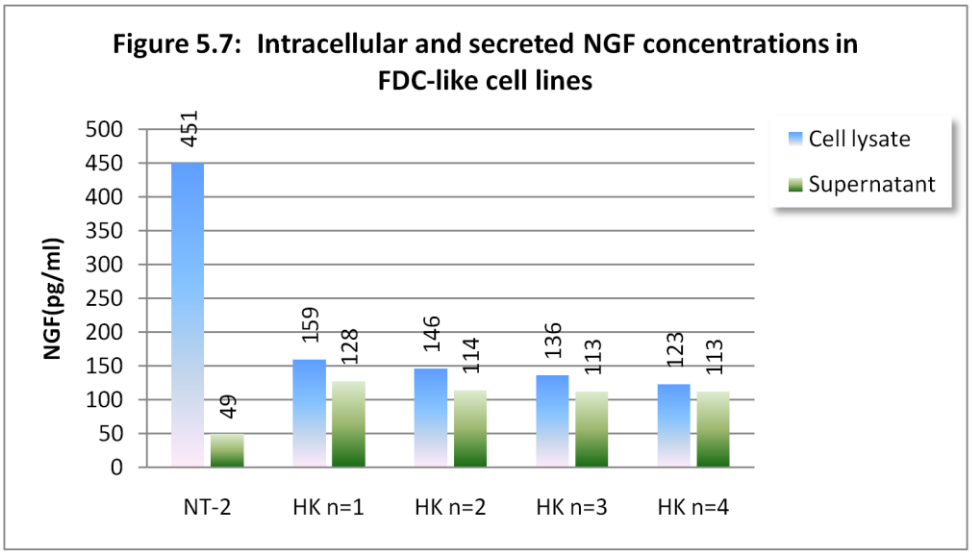

Figure 5.7: Analysis of soluble and intracellular NGF protein levels in FDC-like cell lines
Intracellular and extracellular protein obtained from FDC-like cell lines were added to a NGF antibody pre-coated 96-well plate. Specifically bound antibody was detected by horseradish peroxidise enzyme, colour detection measured on a spectrophotometer at an optical density of 450nM.

Using a linear regression equation (y = 0.0003x + 0.0521) and by subtracting the background standard reading, actual NGF concentrations in the FDC-like lines and the NGF control cell line NT-2 were calculated.
The mean HK cell reading with the standard deviation value is 141±16 for cell lysate samples and 117±7 for cell supernatant.

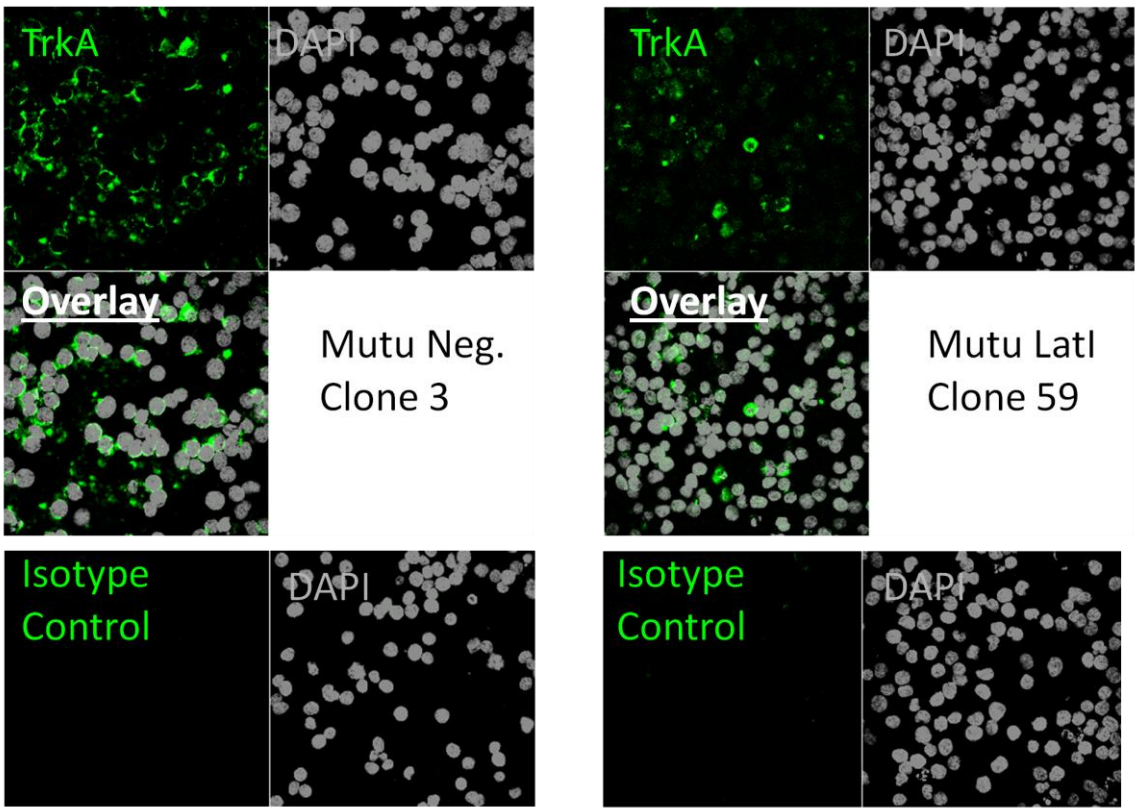

Figure 5.8.1: The expression of TrkA protein in Burkitt's lymphoma B cell lines Mutu negative clone 3 and Mutu latency I clone 59

Confocal images showing permeabilized Burkitt's lymphoma B cells stained for TrkA (C-20) primary antibody and DAPI nuclear stain. Specifically bound TrkA antibodies were detected by FITC-conjugated secondary antibodies then viewed under an LSM laser microscope. Immunoglobulin specific isotype controls were also used to compare primary antibody staining. Representatives of two independent experiments are shown.

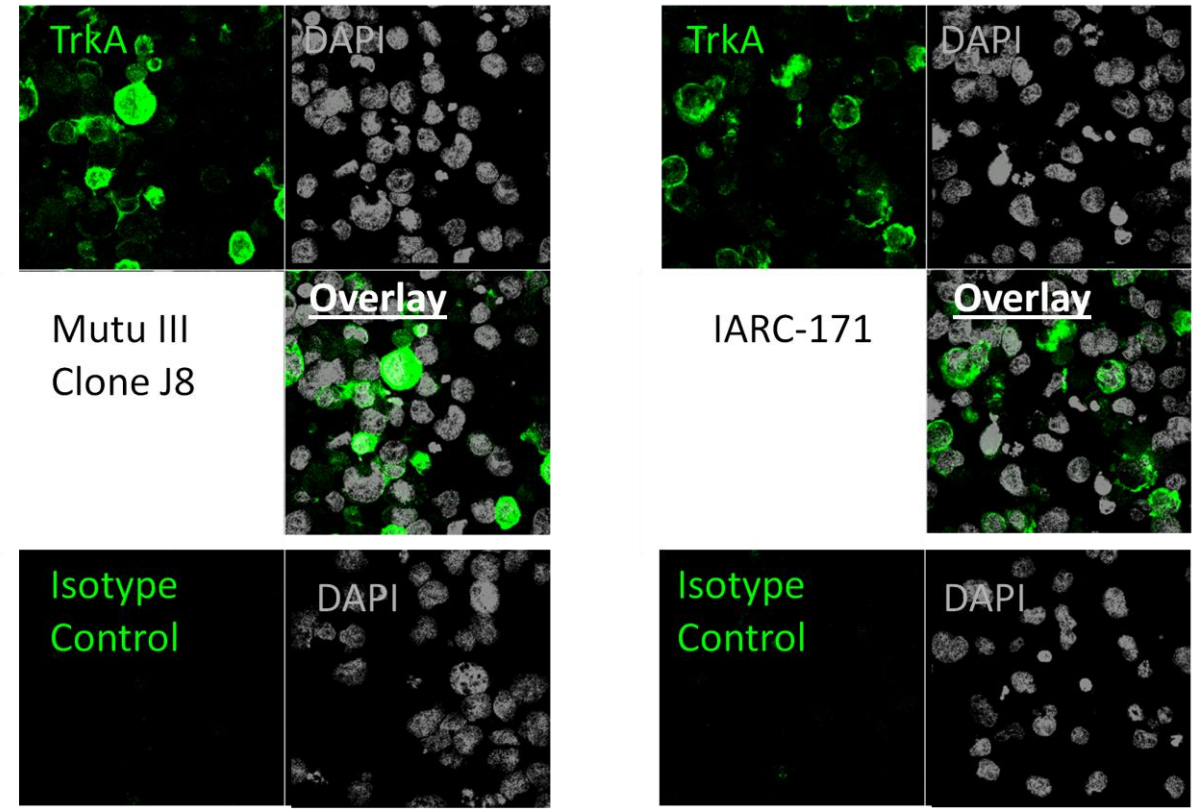

Figure 5.8.2: The expression of TrkA protein in Burkitt's lymphoma B cell lines Mutu latency III and IARC-171

Confocal images showing permeabilized Burkitt's lymphoma B cells stained for TrkA (C-20) primary antibody and DAPI nuclear stain. Specifically bound TrkA antibodies were detected by FITC-conjugated secondary antibodies then viewed under an LSM laser microscope. Immunoglobulin specific isotype controls were also used to compare primary antibody staining. Representatives of two independent experiments are shown.

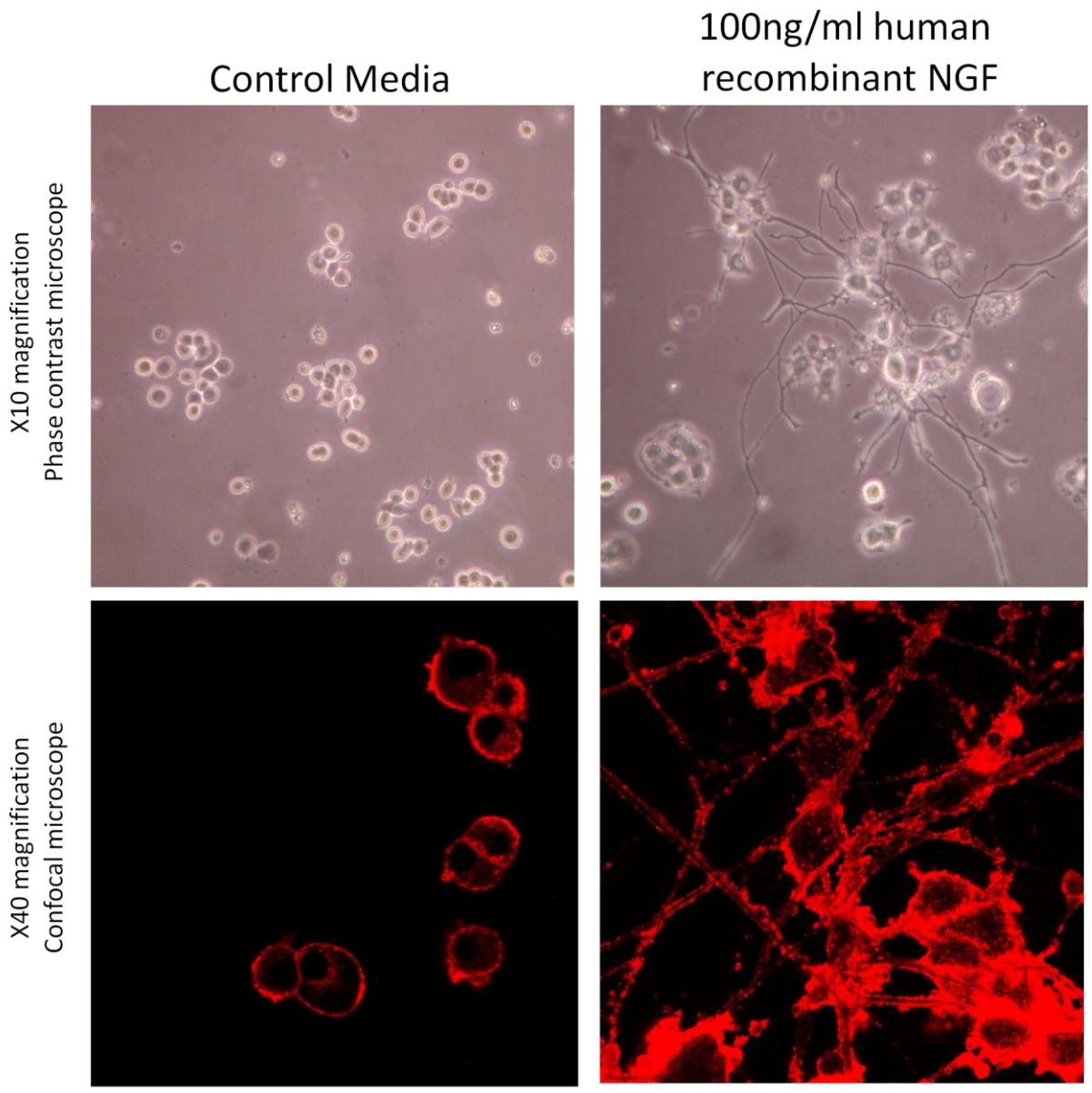

Figure 5.9: Biological assay for human recombinant NGF in PC12 cells
PC12 cells were plated either in control media or media with 100ng/ml human recombinant NGF. Cell morphologies are displayed showing images take by phase contrast microscopy or confocal microscopy. Cells viewed by confocal microscopy were stained with styryl dye (FM 4-64).
Representative images from three independent experiments are shown.

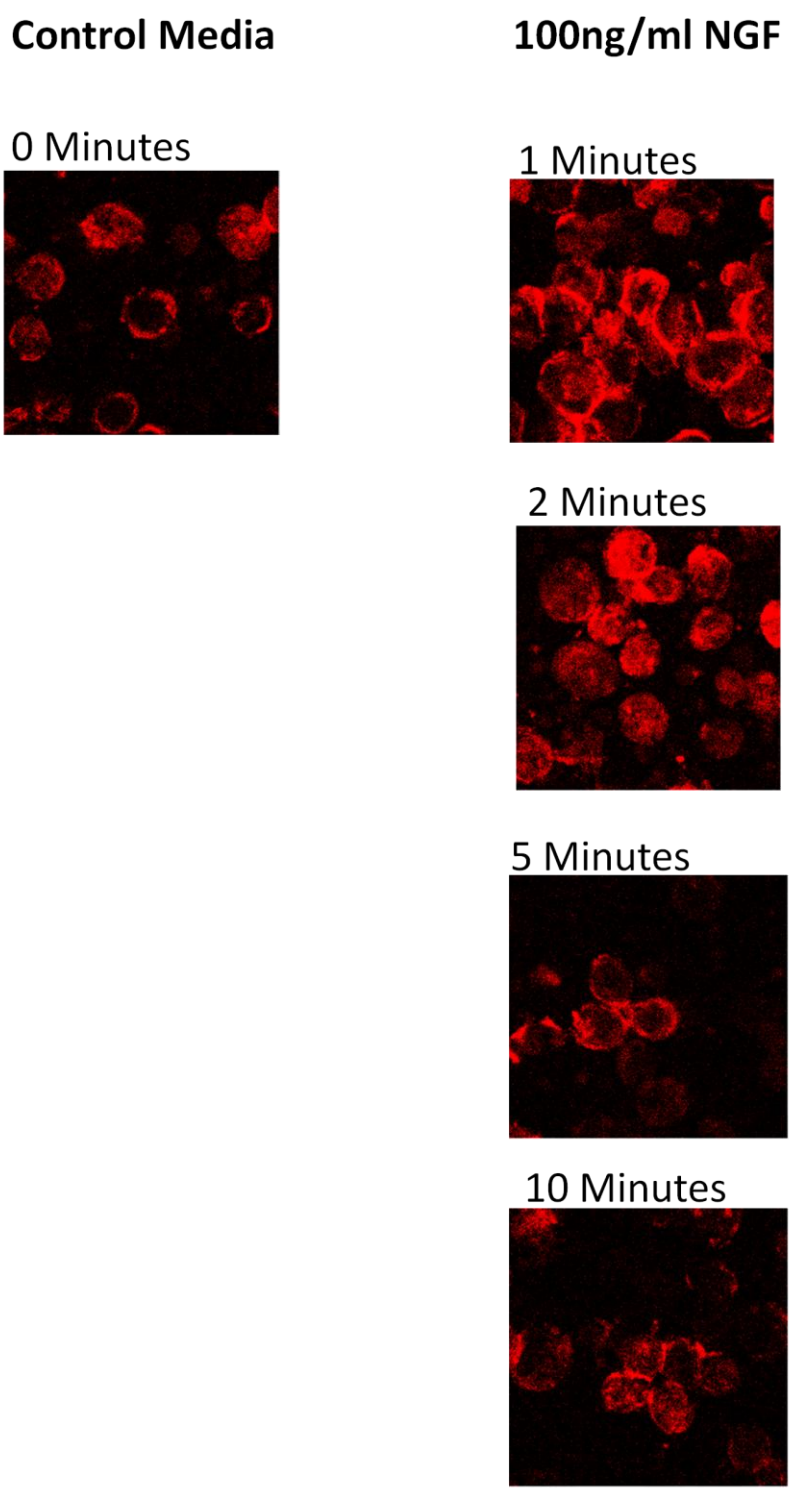

Figure 5.10.1: Mutu negative clone 3 cells stained for F-actin upon NGF treatment

Mutu negative clone 3 cells were treated with NGF at varying time points and stained for F-actin rearrangement using phalloidin dye. Cell images were captured by confocal microscopy.

Representatives from three independent experiments are shown.

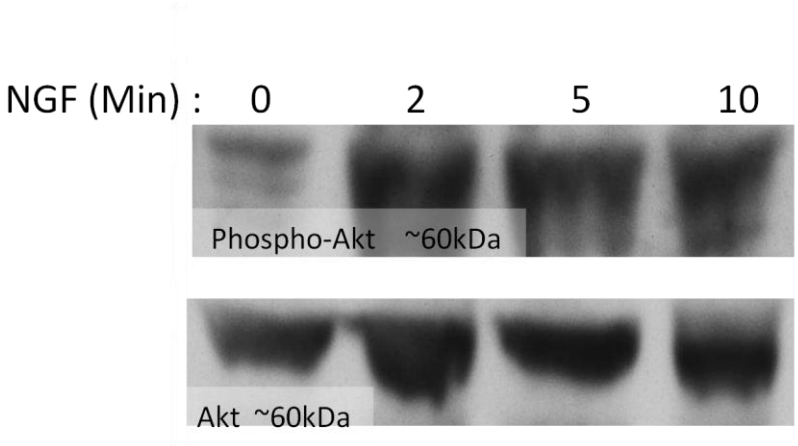

Figure 5.10.2: Mutu negative clone 3 lysates probed for Akt Phosphorylation upon NGF treatment

Western blot showing whole cell extracts (20µg protein) run within 4% to 12% polyacrylamide with SDS gels (Bis-Tris buffer) under reducing conditions. Akt and Phospho-Akt were the primary antibodies used. Specifically bound antibodies were detected by an alkaline phosphatase chemiluminescent method and blots exposed to photographic film.

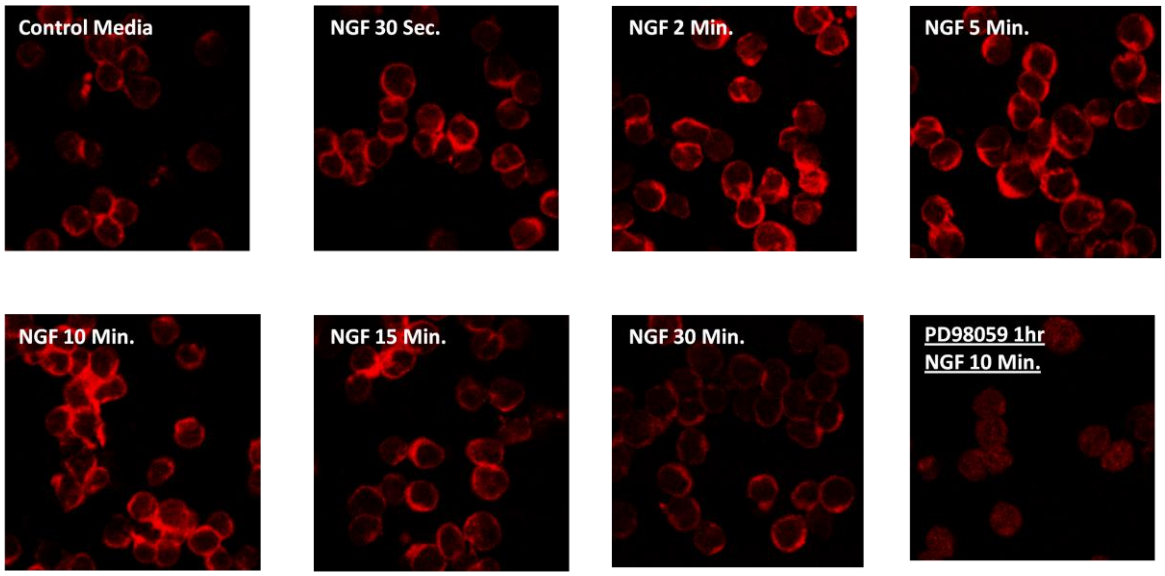

Figure 5.10.3: Mutu negative clone 3 cells stained for Erk Phosphorylation upon NGF treatment

Mutu negative clone 3 cells were treated with 100ng/ml NGF at varying time points. Mutu cells were also pre-treated using the Erk signalling inhibitor, PD98059, then treated with 100ng/ml NGF for 10 minutes. Cells were then fixed and stained for Erk Phosphorylation. Cell images were captured by confocal microscopy.
Representatives from three independent experiments are shown.

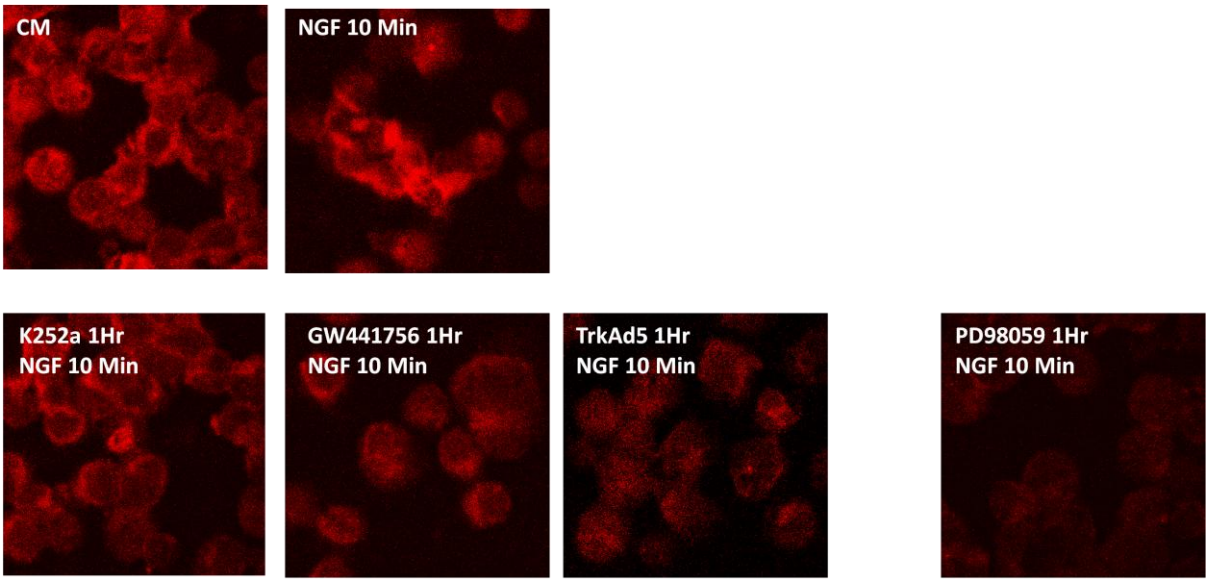

Figure 5.10.4: Mutu negative clone 3 cells stained for Erk Phosphorylation upon NGF treatment and TrkA inhibitors
Mutu negative clone 3 cells were treated with 100ng/ml NGF for 10 minutes. Mutu cells were also pre-treated using the TrkA inhibitors, K252a, GW441756 and TrkA as well as the Erk signalling inhibitor, PD98059. These cells were then treated with NGF for 10 minutes. Cells were then fixed and stained for Erk Phosphorylation. Cell images were captured by confocal microscopy.

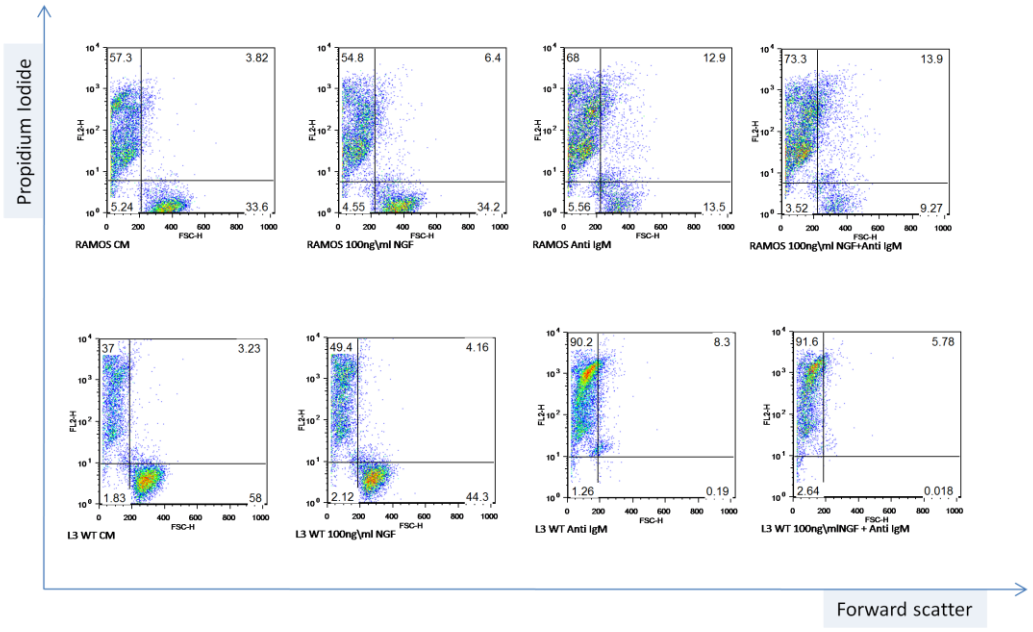

Figure 5.11.1 NGF cell survival assay in Ramos and L3055 cells treated with Anti-IgM
Ramos and L3055 cells were treated with human recombinant NGF (100ng/ml) and/ or anti-IgM (2μg/ml) for 24 hours. Apoptosis was measured by PI uptake on a flow cytometer. Dot plots are displayed showing PI low or viable (bottom right quadrant) and PI high or non-viable (top left quadrant) population percentages.
Representations from three independent experiments are shown.

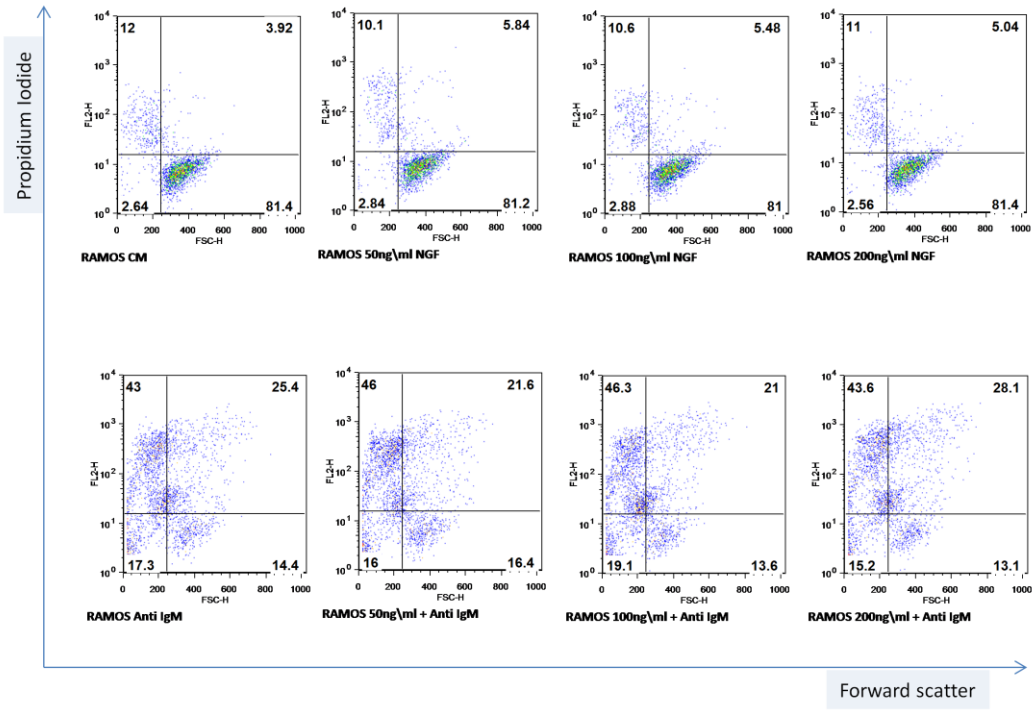

Figure 5.11.2 NGF cell survival assay in Ramos cells treated with Anti-IgM

Ramos cells were treated in varying concentrations of human recombinant NGF and/ or anti-IgM (2μg/ml) for 24 hours. Apoptosis was measured by PI uptake on a flow cytometer. Dot plots are displayed showing PI low (bottom right quadrant) and PI high (top left quadrant) population percentages. Representations from three independent experiments are shown.

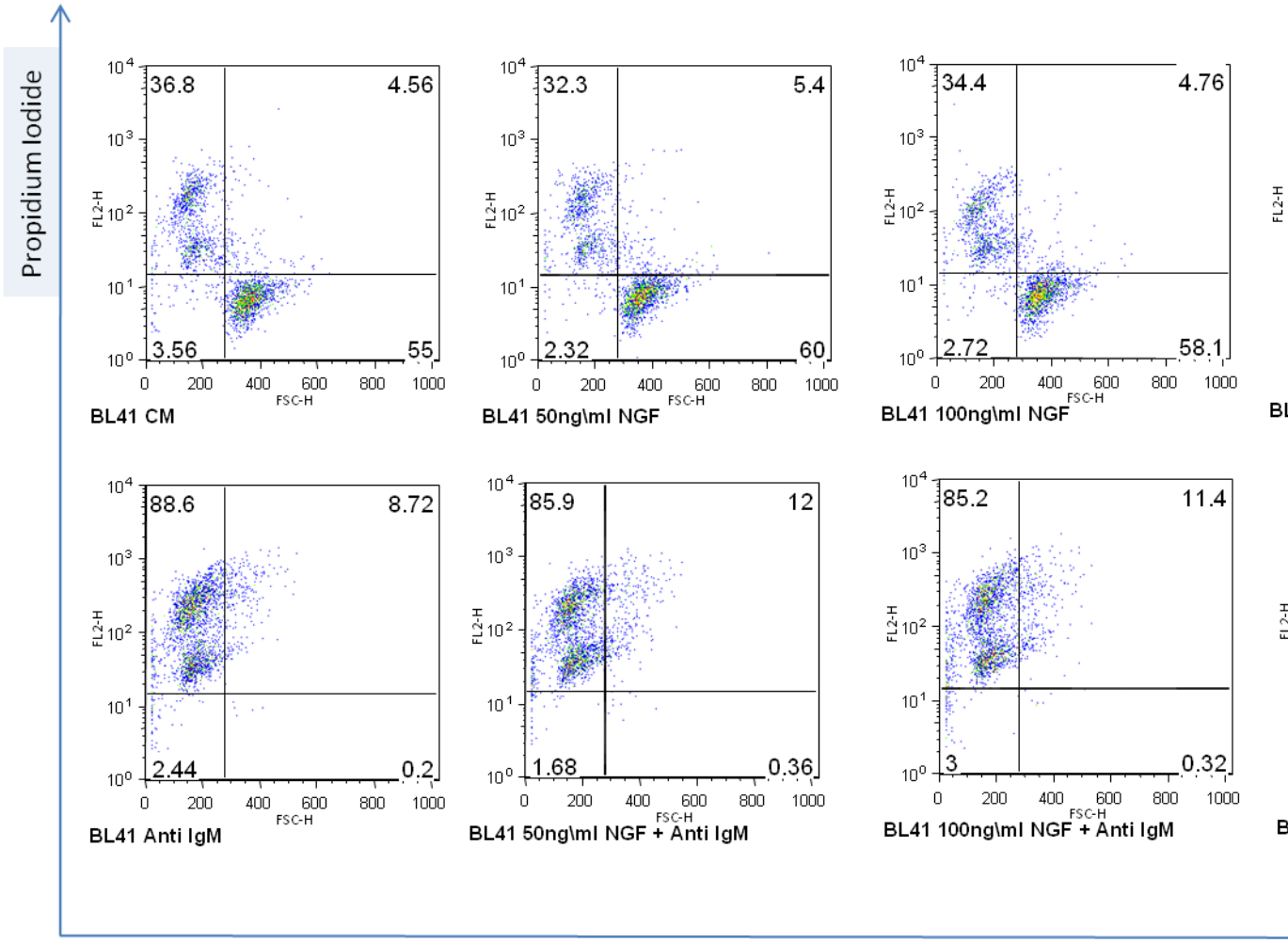

Figure 5.11.3 NGF cell survival assay in BL41 cells treated with Anti-IgM

BL41 cells were treated in varying concentrations of human recombinant NGF and/ or anti-IgM (2μg/ml) for 24 hours uptake on a flow cytometer. Dot plots are displayed showing PI low (bottom right quadrant) and PI high (top left quadran Representations from three independent experiments are shown.

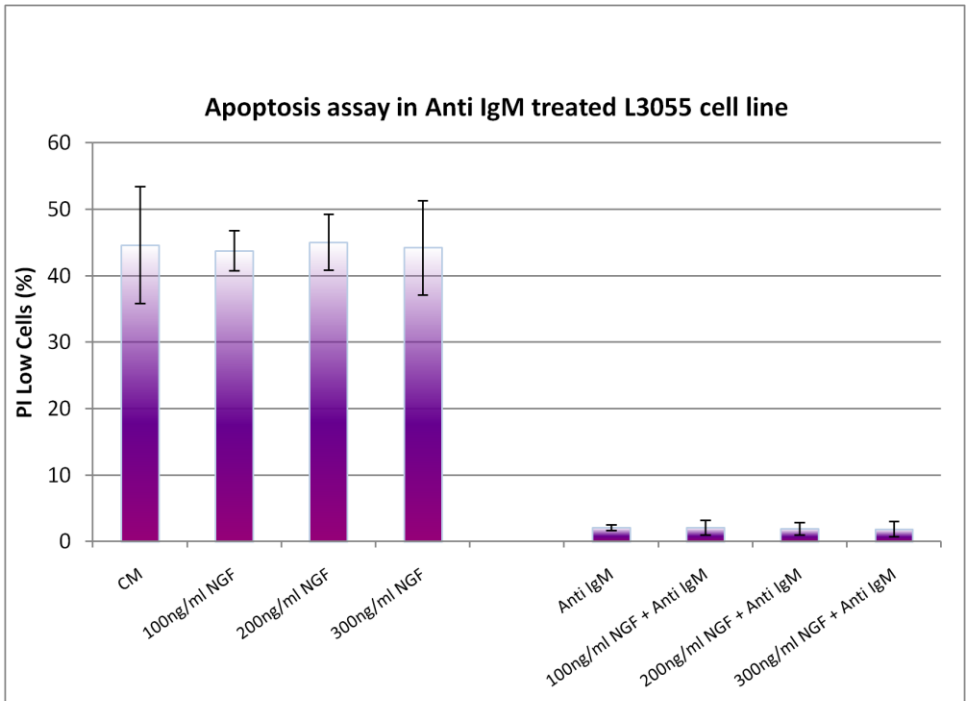

Figure 5.11.4a: NGF cell survival assay in L3055 cells treated with Anti-IgM
L3055 cells were treated with human recombinant NGF (100ng/ml) and/ or anti-IgM (2µg/ml) for 24 hours. Apoptosis was measured by PI uptake on a flow cytometer. Mean PI low cell percentages and SD error bars are displayed, obtained from four independent experiments.

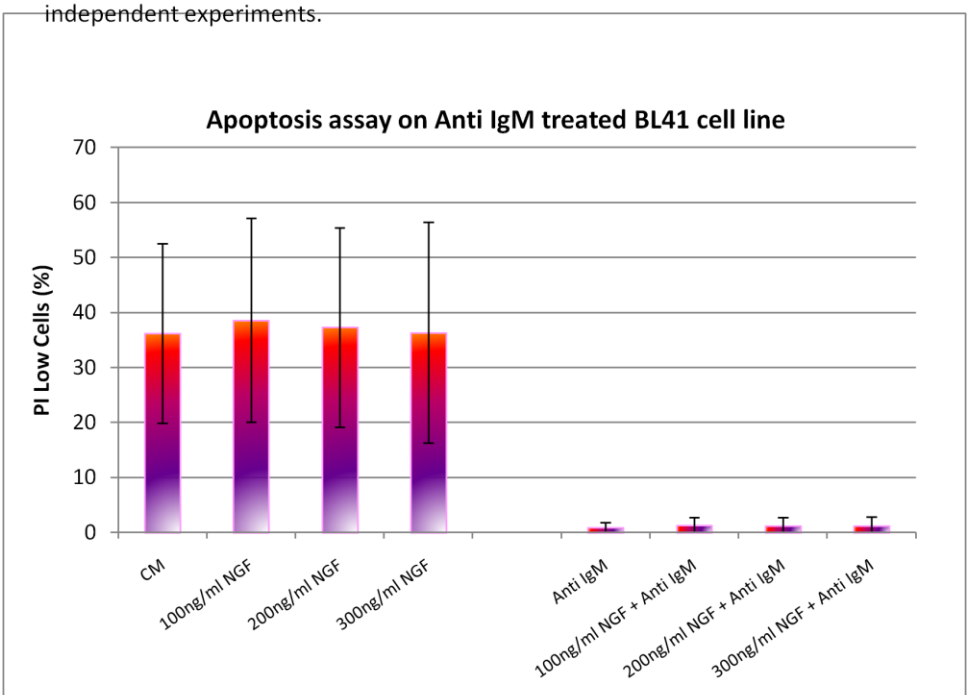

Figure 5.11.4b: NGF cell survival assay in BL41 cells treated with Anti-IgM
BL41 cells were treated with human recombinant NGF (100ng/ml) and/ or anti-IgM (2µg/ml) for 24 hours. Apoptosis was measured by PI uptake on a flow cytometer. Mean PI low cell percentages and SD error bars are displayed, obtained from four independent experiments.

Figure 5.12.1a

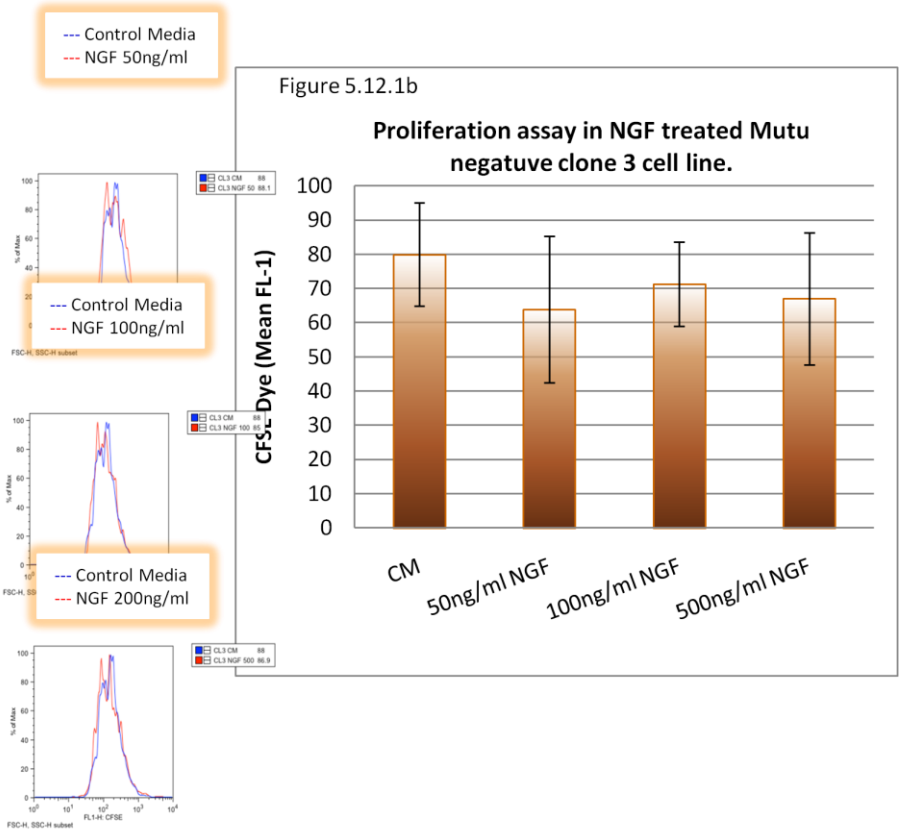

Figure 5.12.1 CFSE cell proliferation assay in Mutu negative clone 3 cells treated with NGF

Mutu negative clone 3 cells (Cl3) were treated in CFSE dye (3μM), then with human recombinant 50ng/ml NGF (NGF 50), 100ng/ml NGF (NGF 100) or 500ng/ml NGF (NGF 500) for 24 hours. Cell proliferation was measured by the loss in CFSE dye.

Histograms displayed in figure 5.12.1a represent one set of data between there independent experiment.

The graph in figure 5.12.1b mean CFSE levels and standard errors bars from three independent experiments.

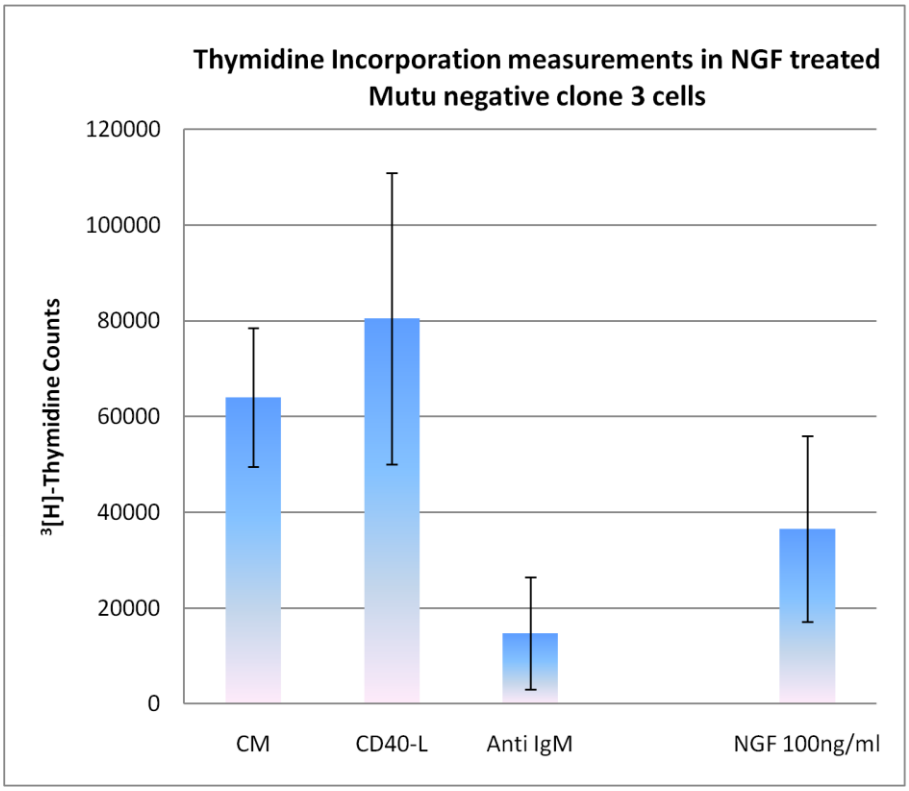

Figure 5.12.2 DNA synthesis assay in Mutu negative clone 3 cells treated with NGF

Mutu negative clone 3 cells were treated with human recombinant 100ng/ml NGF for 20 hours. Cells were then pulsed with 0.5μCi/well, ^{3}[H]-Methyl-Thymidine for 6 hours. Incorporated ^{3}[H]-Thymidine counts from three independent experiments were determined and mean values plotted together with the standard deviation bars.

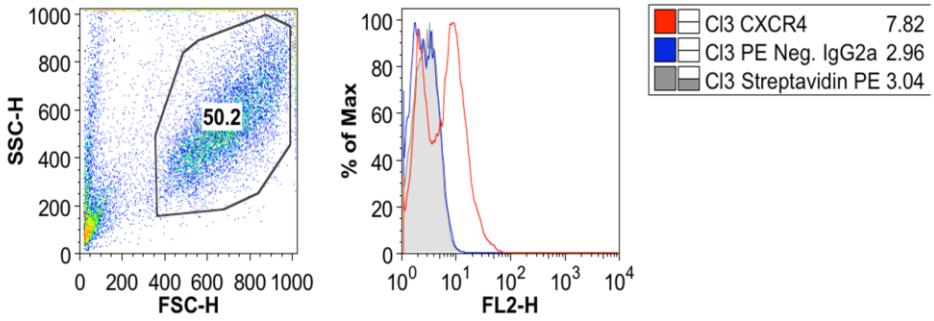

Figure 5.13.1: The expression of CXCR4 in Mutu negative clone 3 cells

Permeabilized Mutu negative clone cells were stained for flow cytometry analysis using a CXCR4 antibody. The dot plot, shown above, displays the population of cells collected for measurement, gates were drawn from PI low cells taken from culture.

The primary antibody used was compared to the isotype control within the histogram displayed. A secondary antibody directly conjugated with PE was used to detect specifically bound primary antibody by streptavidine. Mean PE-Streptavidine, levels are displayed within the histogram.

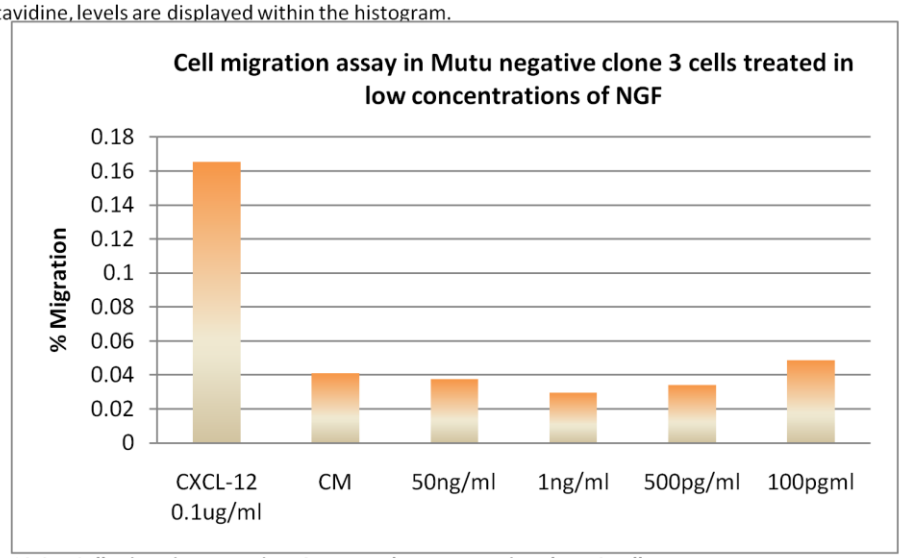

Figure 5.13.2a: Cell migration assay in NGF treated Mutu negative clone 3 cells

Within transwell membrane plates, Mutu negative clone 3 cells within the upper chambers were exposed to varying concentrations of human recombinant NGF (50ng/ml to 100pg/ml) within the bottom chamber for 6 hours. The number of cells within the top and bottom chambers were collected by flow cytomertry, percentage cell migration are displayed within the plotted within the graph.

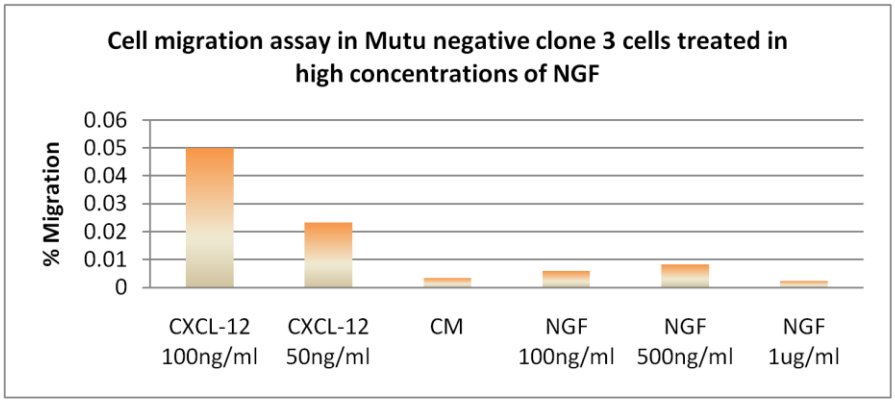

Figure 5.13.2b: Cell migration assay in NGF treated Mutu negative clone 3 cells

Within transwell membrane plates, Mutu negative clone 3 cells within the upper chambers were exposed to varying concentrations of human recombinant NGF (100ng/ml to 100µg/ml) within the bottom chamber for 6 hours. The number of cells within the top and bottom chambers were collected by flow cytomertry , percentage cell migration are displayed within the plotted within the graph (n=3).

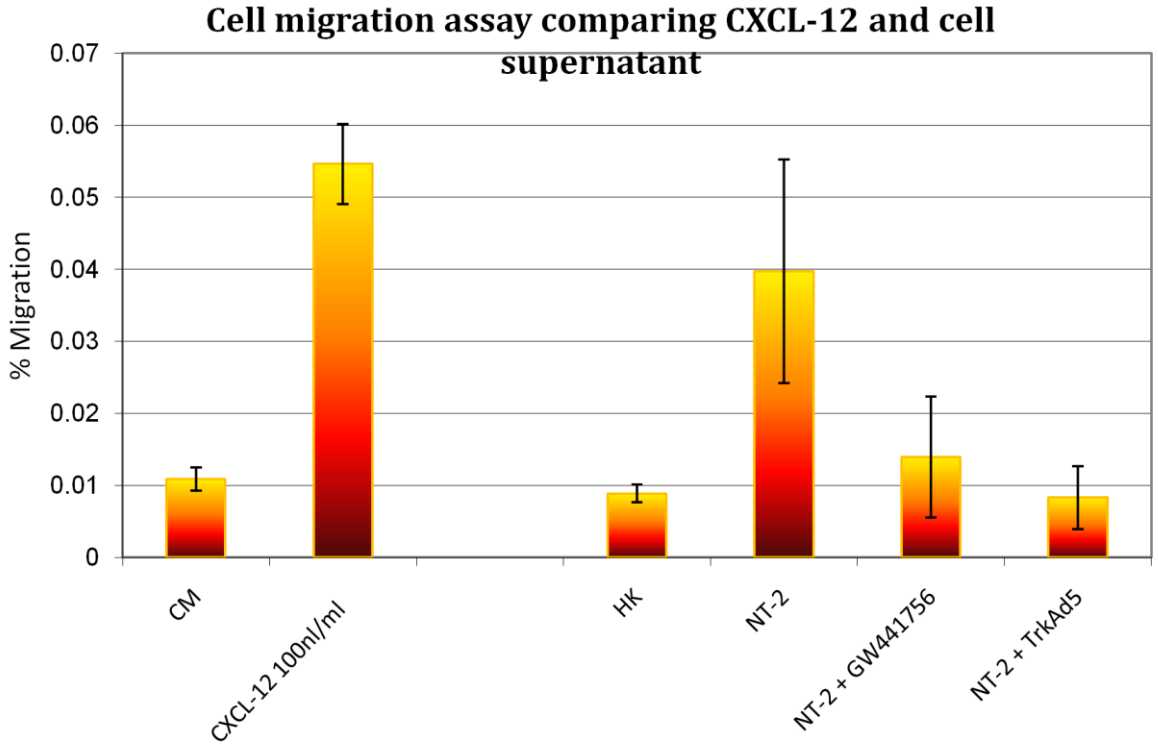

Figure 5.13.3: Cell migration assay in CXCL-12 and cell culture supernatant treated Mutu negative clone 3 cells

Within transwell membrane plates, Mutu negative clone 3 cells within the upper chambers were exposed to varying concentrations of human recombinant NGF (100ng/ml to 100µg/ml) within the bottom chamber for 6 hours. Those cells treated with TrkA inhibitors 4.5µM TrkAd5 or 100nM GW441756, were pre-treated for 1 hour before addition into the transwell plates. The number of cells within the top and bottom chambers were collected by flow cytomertry , percentage cell migration are displayed within the plotted within the graph (n=3).

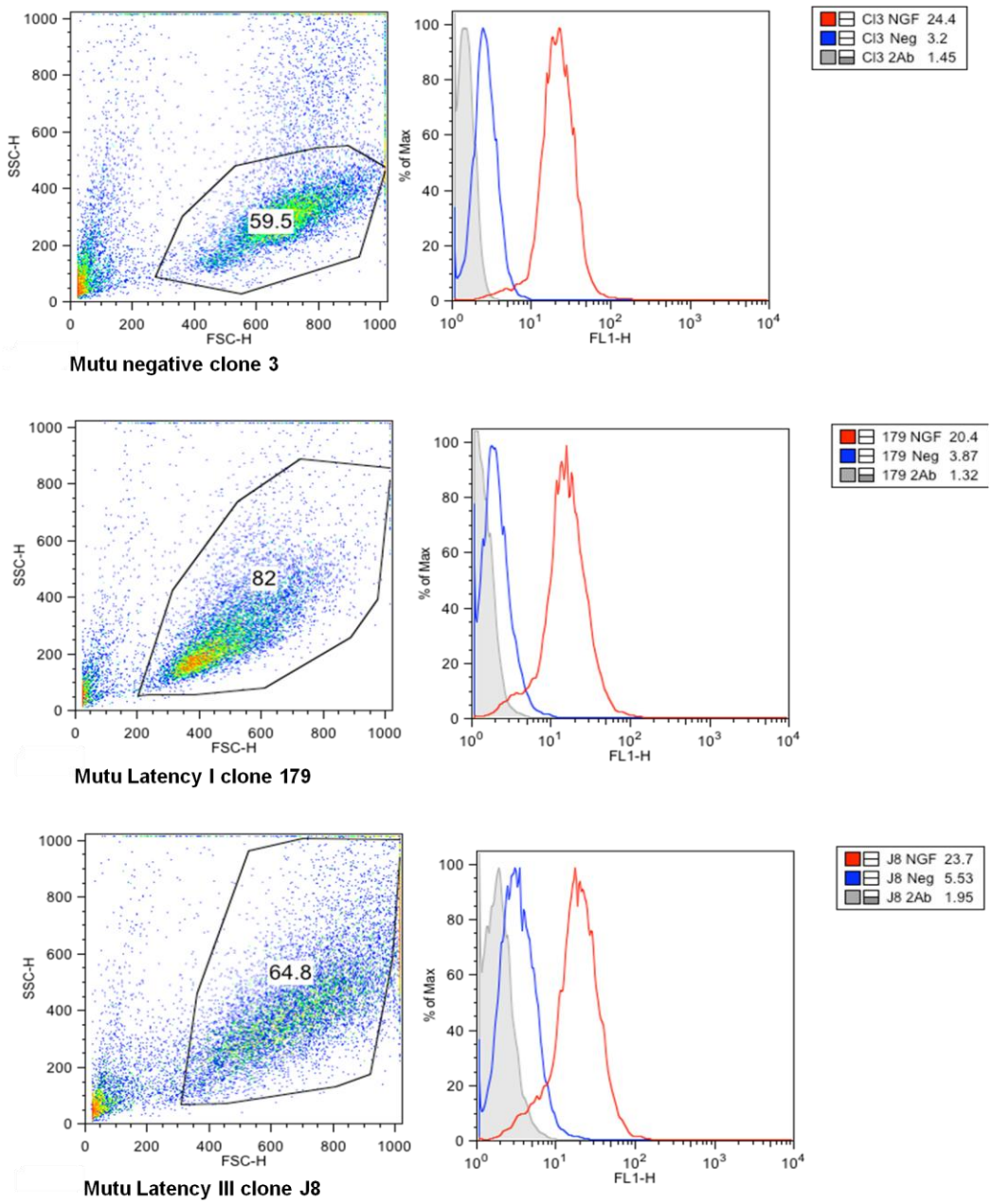

Figure 5.14.1: The expression of NGF in Burkitt's lymphoma B cell lines

Permeabilized Burkitt's lymphoma cell lines stained for flow cytometry analysis using an anti-NGF (N3279) antibody. The dot plot, shown above, displays the population of cells collected for FITC measurement, gates were drawn from PI low cells taken from culture.

The primary antibodies (NGF) used were compared to the isotype control (Neg) within each histogram displayed. A secondary antibody (2Ab) directly conjugated with FITC was used to detect specifically bound primary antibody. Mean FITC levels were displayed from each histogram.

A representative of three independent experiments is shown.

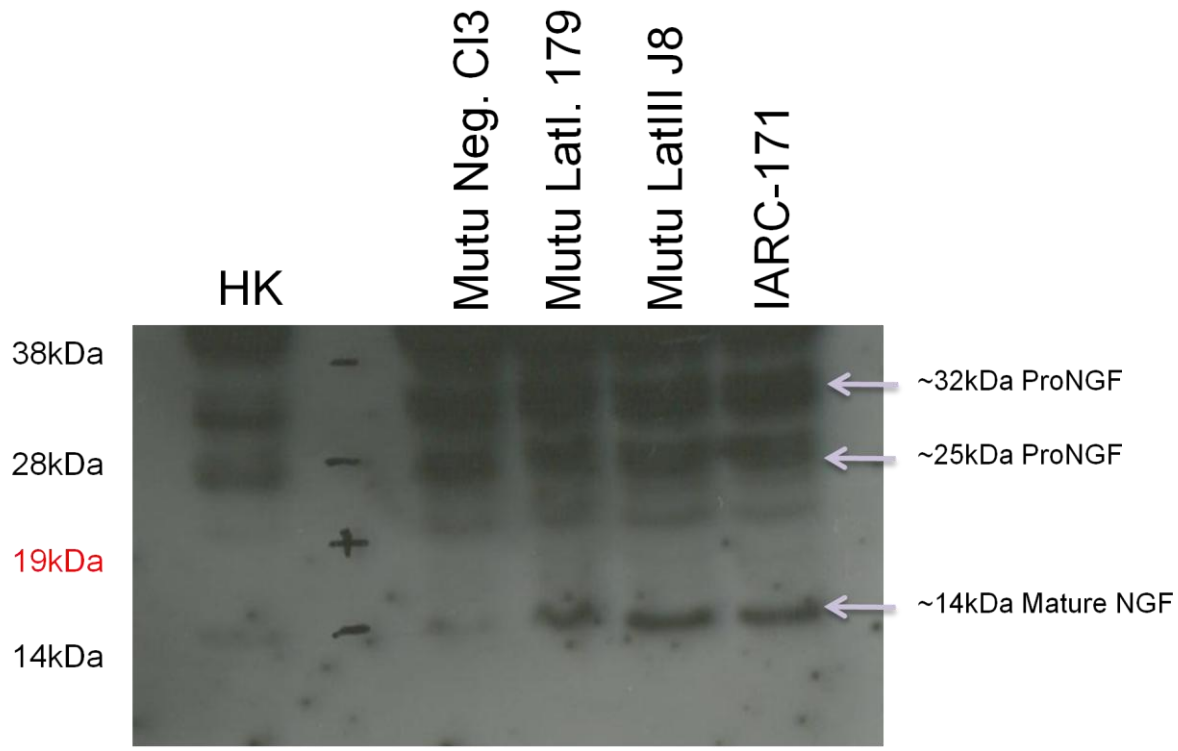

Figure 5.14.2: The expression of NGF protein in Burkitt's lymphoma B cell lines
Western blot results showing whole cell extracts (10µg protein) run within a 4% to 12% acrylamide Bis-Tris NuPAGE gel. Blots were probed for NGF (AF256NA) primary antibody. Specifically bound antibodies were detected by an alkaline phosphatase chemiluminescent method and blots exposed to photographic film ((n=3)).

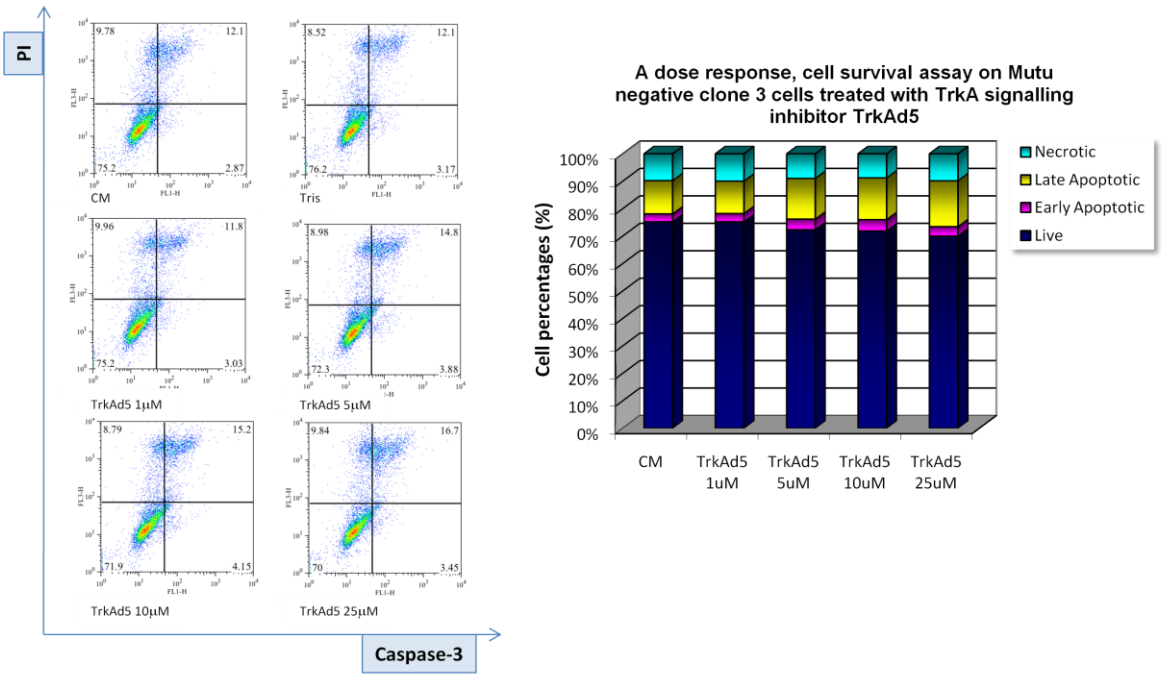

Figure 5.15.1: Cell survival assay on Mutu negative clone 3 cells treated with TrkA signalling inhibitor TrkAd5
Dose response analysis on cells treated with 1µM to 25µM TrkAd5 for 24 hours. PI/PhiPhiLux stained cells were measured by flow cytometry for live cells, early, late apoptotic and necrotic cells.

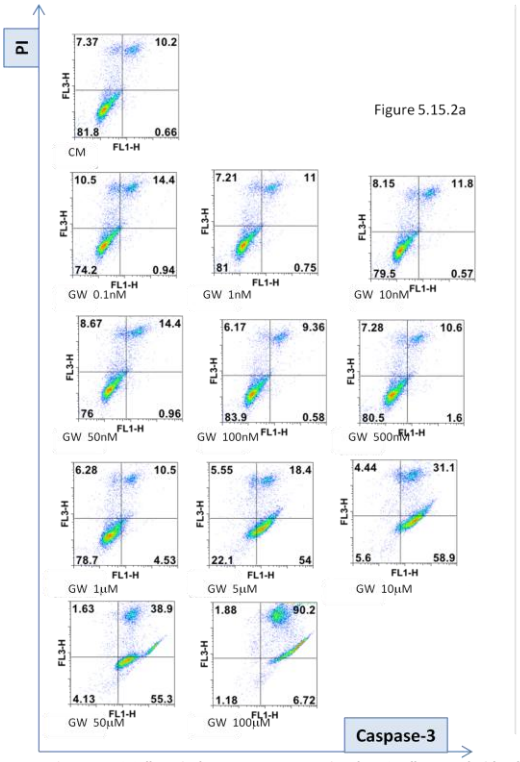

Figure 5.15.2a

Figure 5.15.2b

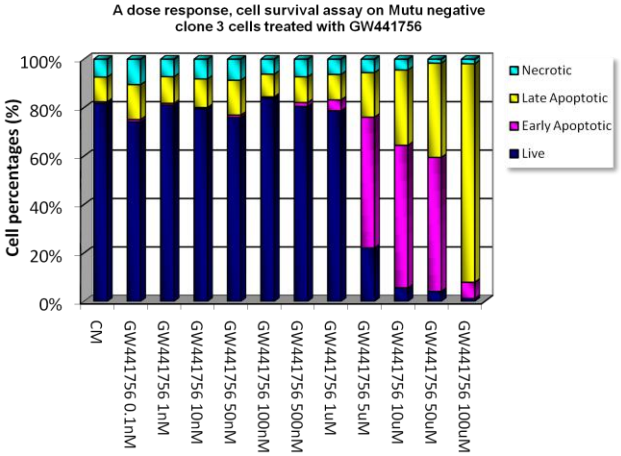

Figure 5.15.2 Cell survival assay on Mutu negative clone 3 cells treated with TrkA signalling inhibitor GW441756
Dose response analysis on cells treated with 0.1nM to 100µM GW441756 for 24 hours. PI/PhiPhiLux stained cells were measured by flow cytometry for live cells, early, late apoptotic and necrotic cells. Dot plots displaying the different stages in cell death are shown in Figure 5.15.a. These percentages are illustrated within a graph shown in figure 5.15.2b

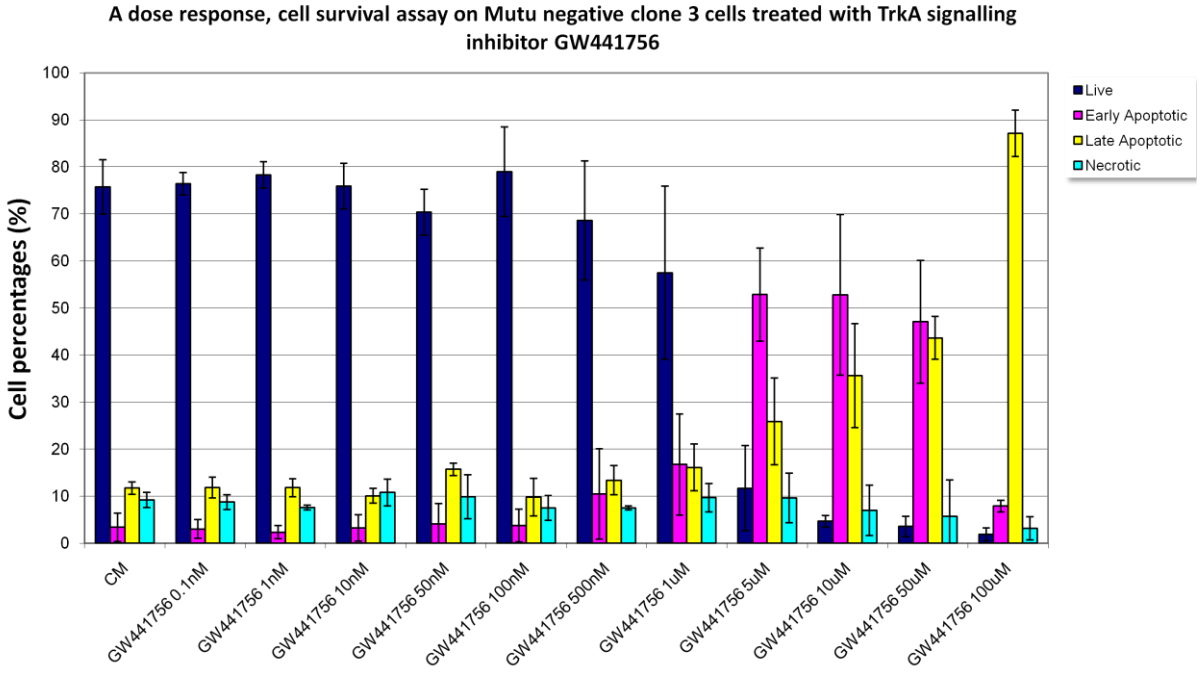

Figure 5.15.3 Cell survival assay on Mutu negative clone 3 cells treated with TrkA signalling inhibitor GW441756 (n=3)
Dose response analysis on cells treated with 0.1nM to 100µM GW441756 for 24 hours. PI/PhiPhiLux stained cells were measured by flow cytometry for live cells, early, late apoptotic and necrotic cells. Mean cell percentages and standard deviation error bars were calculated between three independent experiments.

Figure 5.15.4a

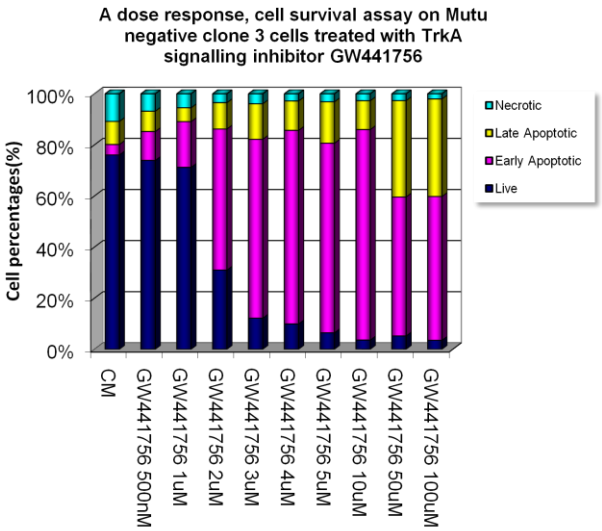

Figure 5.15.4b

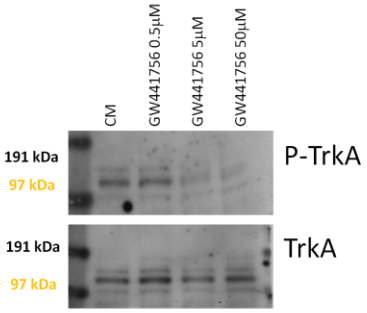

Figure 5.15.4 Cell survival assay and TrkA phosphorylation in Mutu negative clone 3 cells treated with TrkA signalling inhibitor GW441756
Figure 5.15.4a displays a dose response analysis on cells treated with 500nM to 100µM GW441756 for 24 hours. PI/PhiPhiLux stained cells were measured by flow cytometry for live cells, early, late apoptotic and necrotic cells.
Figure 5.15.4b shown western blots for Mutu negative clone 3 cells treated with 0.5mM. 5uM and 50uM HW441756 for 1 hour. Whole cell extracts (20µg protein) run within 4% to 12% polyacrylamide with SDS gels (Bis-Tris buffer) under reducing conditions. Blots were probed for Phospho-TrkA (P-TrkA) primary antibody alone or TrkA antibody . Specifically bound antibodies were detected by an alkaline phosphatase chemiluminescent method and blots exposed to photographic film.

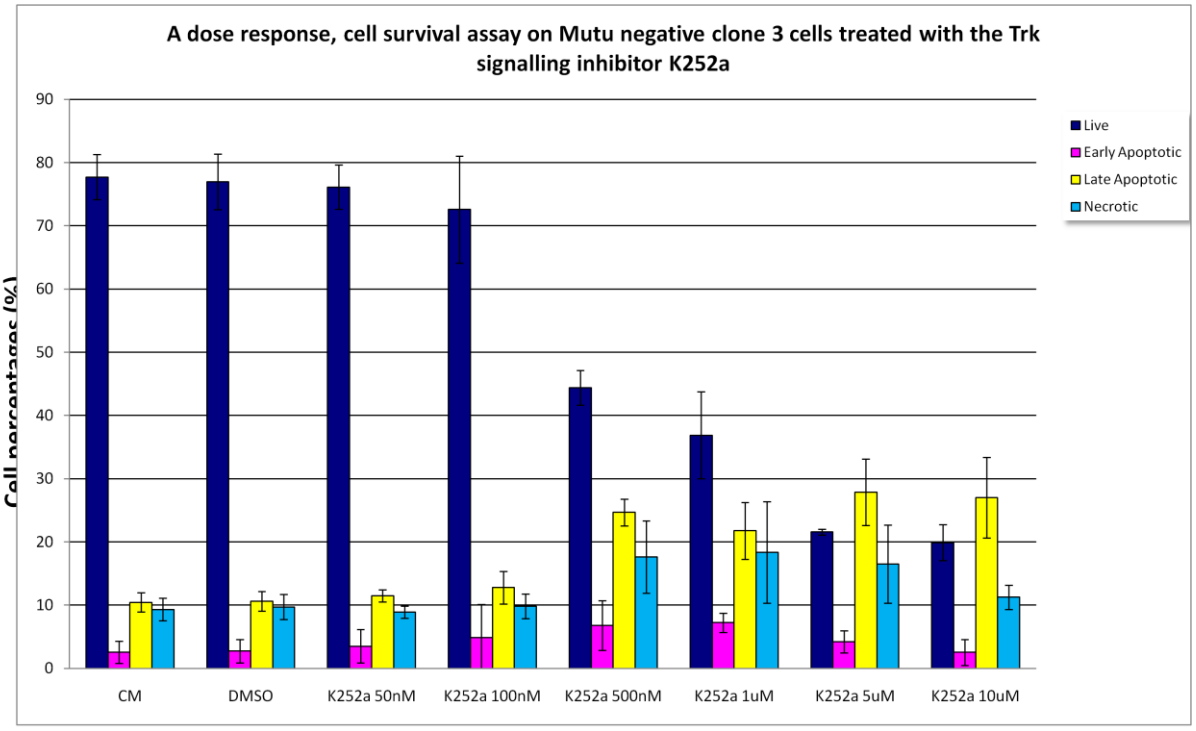

Figure 5.15.5 Cell survival assay on Mutu negative clone 3 cells treated with the Trk signalling inhibitor K252a (n=3)
Dose response analysis on cells treated with 50nM to 10µM K252a for 24 hours. PI/PhiPhiLux stained cells were measured by flow cytometry for live cells, early, late apoptotic and necrotic cells. Mean cell percentages and standard deviation error bars were calculated between three independent experiments.

Figure 5.15.6a

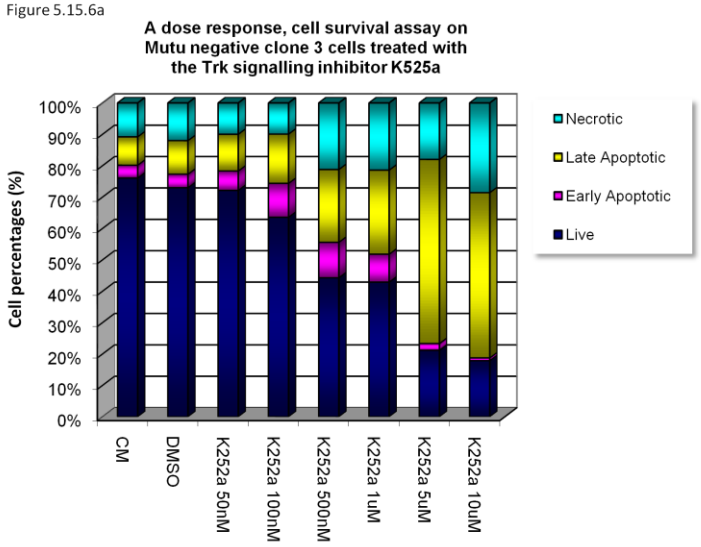

Figure 5.15.6b

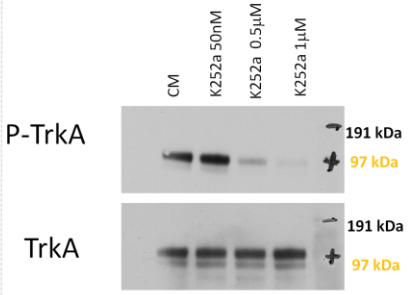

Figure 5.15.6 Cell survival assay on Mutu negative clone 3 cells treated with the Trk signalling inhibitor K252a

Figure 5.15.6a Dose response analysis on cells treated with 50nM to 10µM K252a for 24 hours. PI/PhiPhiLux stained cells were measured by flow cytometry for live cells, early, late apoptotic and necrotic cells. Mean cell percentages and standard deviation error bars were calculated between three independent experiments.

Figure 5.15.6b Western blots for Mutu negative clone 3 cells treated with 5nM, 0.5µM and 1µM K252a for 1 hour. Whole cell extracts (20µg protein) run within 4% to 12% polyacrylamide with SDS gels (Bis-Tris buffer) under reducing conditions. Blots were probed for Phospho-TrkA (P-TrkA) primary antibody alone or TrkA antibody . Specifically bound antibodies were detected by an alkaline phosphatase chemiluminescent method and blots exposed to photographic film.

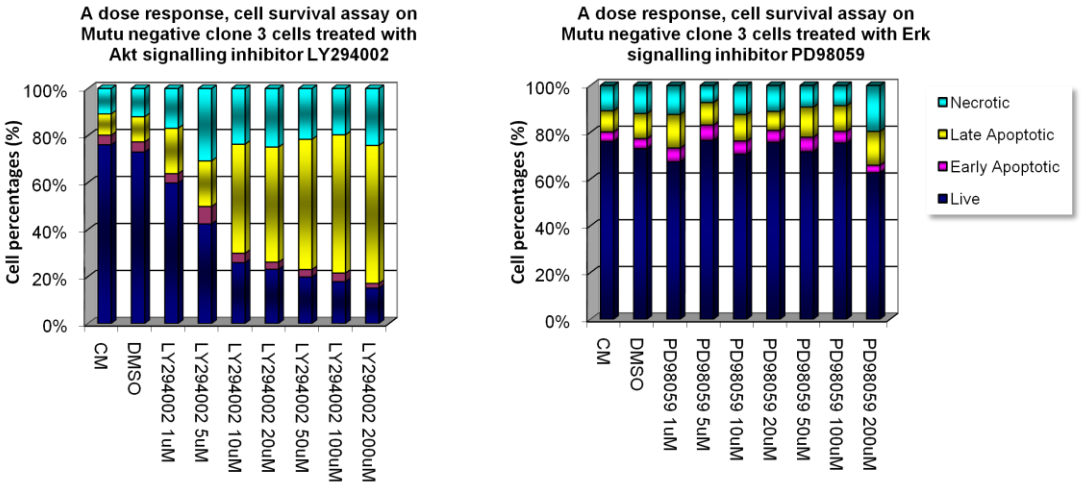

Figure 5.15.7 Cell survival assay on Mutu negative clone 3 cells treated with Akt and Erk signalling inhibitors LY294002 and PD98059

Dose response analysis on cells treated with either LY294002 or PD98059 for 24 hours. PI/PhiPhiLux stained cells were measured by flow cytometry for live cells, early, late apoptotic and necrotic cells.

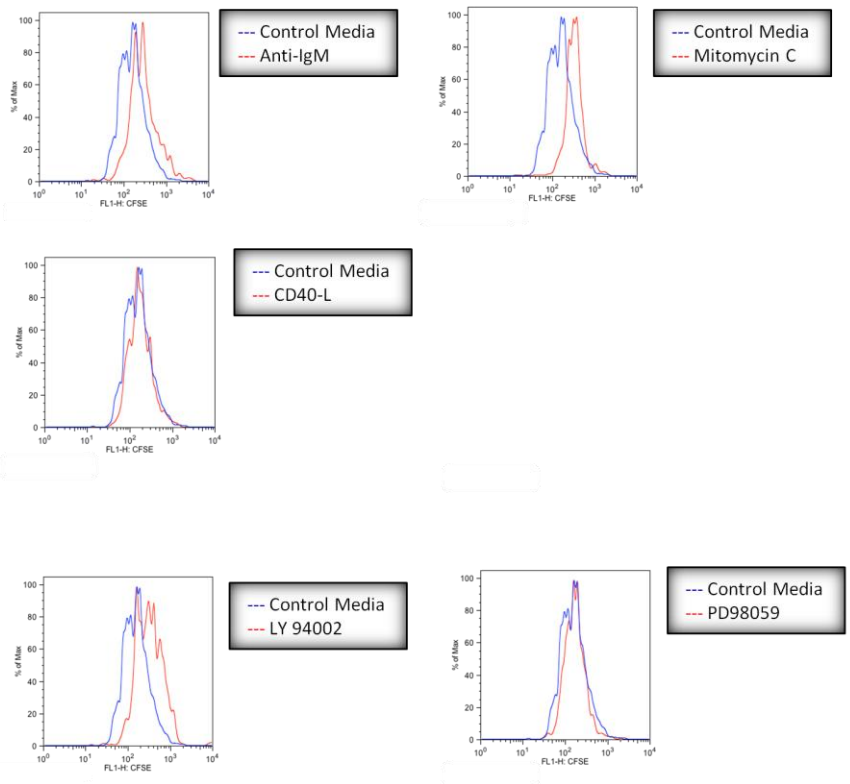

Figure 5.16.1: The effects on cell proliferation in Mutu negative clone 3 cells treated with various TrkA:p75^{NTR} signalling inhibitors

Mutu negative clone 3 cells were treated with CFSE dye then cultured with the inhibitors, Anti IgM, Mitomycin C, CD40-L, Akt inhibitor (LY294002) and Erk inhibitor (PD98059). Cells were treated for 48 hours. CFSE dye levels were measured by flow cytomerty, control treated cells were compared to each inhibitor individually (n=3).

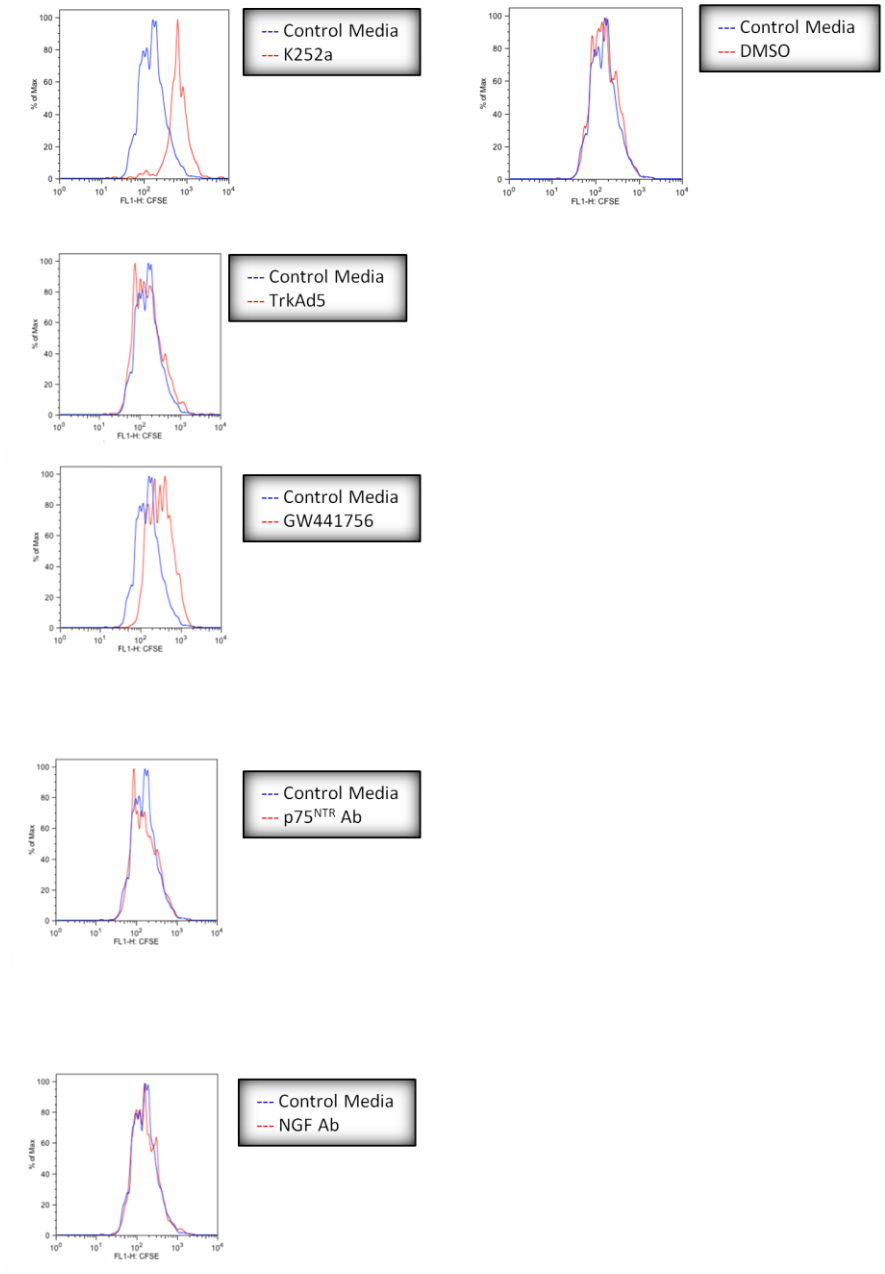

Figure 5.16.2 The effects on cell proliferation in Mutu negative clone 3 cells treated with various TrkA:p75^{NTR} signalling inhibitors

Mutu negative clone 3 cells were treated with CFSE dye then cultured with the inhibitors, TrkAd5, the specific inhibitor for TrkA receptor domain 5 and its vehicle control Tris buffer, GW441756, NGF neutralising antibody, p75^{NTR} neutralising antibody (MLR2). Cells were treated for 48 hours. CFSE dye levels were measured by flow cytomerty, control treated cells were compared to each inhibitor individually (n=3).

Table 5.1: Summary representing the expression of FDC surface markers and RT-PCR mRNA transcript experiments on TNF receptor, BAFF and neurotrophic factors and their receptors within FDC-like cell lines

FDC-like cell lines	FDC1	HK
FDC markers		
BU10	+	+
FD6	-	+
8D6	-	+
CD106	-	+
3C8	+	+
CD19	-	+
TNF receptors		
BAFF	+	+
Neurotrophic Factors		
NGF	+	+
BDNF	+	+
NT-3	+	+
NT-4	Not determinded	
$p75^{NTR}$	-	+
TrkA	+	+
TrkB A&C	-	-
Pan-TrkB	-	+
TrkC	+	+

5.3 Discussion

Based on the initial hypothesis, the main conclusions drawn are that FDCs express NGF protein. Exogenous NGF activates Akt and Erk signalling in EBV negative Burkitt's lymphoma

B cell lines; however NGF alone does not rescue cells from Anti-IgM induced apoptosis, cell proliferation or cell migration. On the other hand it is possible that NGF may act with another chemokine to induce EBV negative, Burkitt's lymphoma B cell migration.

However, NGF protein was detected within all Burkitt's lymphoma lines analysed, therefore, the main conclusions drawn from the second hypothesis are that endogenous NGF signalling in EBV negative Burkitt's lymphoma B cells induces cell proliferation and cell survival, possibly via Akt signalling and not Erk.

FDC interactions with B cells via neurotrophic factors were postulated within this part of the investigation. By immunohistochemisty staining on Human palatine tonsil tissue, it is known that lymphocytes and FDCs express the neurotrophic receptor $p75^{NTR}$ however its functions within FDCs are unknown (Hannestad, Levanti et al. 1995; Maeda, Matsuda et al. 2002). The expression of TrkA and TrkC protein was also observed within lymphocytes and FDCs. TrkA and TrkC expression was noted within paracortical interdigitating cells and endothelial venule cells. As for TrkB expression it was presumed that certain macrophage cell types expressed TrkB.

Within this investigation, HK cells were found to express varying FDC markers, particularly BU10 and 3C8. BU10 is a well documentd FDC marker which provided clear, string staining in FDC-like cells. 3C8 is prostacyclin synthase that inhibits proliferation of T cells. FDCs expressing prostacyclin synthase within a germinal centre may explain why T cells constitute only a minor population compared with B cells within the light zone (Li et al., 2000). Studies by I.Y. Lee et al, used the monoclonal antibody, 3C8 to study HK cells, the advantage of this antibody is that it does not display cross-reactivity with other cells such as those derived from bone-marrow (Lee et al., 2005).

All the FDC markers analysed initiate signalling cascades in vivo for the interaction of FDCs with B cells. These receptors are important for the regulation of B-cell development and prevention of apoptotic. However either low levels or the lack of these markers were observed within the cultured FDC-like lines, with the exception of BU10 and 3C8. As shown by Clark, et al., freshly isolated FDC-like cells extracted from human tonsil were directly compared to long term, in vitro cultured FDC-like cells. Those cultured for long periods of time were observed to have a reduction in FDC, cell surface marker expression levels compared to those freshly isolated (Clark et al., 1992). R. Tsunoda et al. initially found that fresh FDC-like lines which expressed CD21, CD23 and CD35 ceased to express these markers 6 days post isolation (Tsunoda et al., 1990). A reduction in FDC specific markers when FDC1 lines were cultured by E.A. Clark et al, was also observed (Clark et al., 1992). Similar observations were also found in HK lines (Kim et al., 1994). It is therefore worth considering that removing FDCs from their germinal centre microenvironment drastically changes their behaviour and expression patterns. In turn the results obtained from these FDC-like lines are speculations that need to be further investigated using in vivo models. Hence NGF expression is best studies using immunohistochemical staining of human tonsils.

Coincidently, NGF protein expression was detected in Burkitt's lymphoma B cell lines. This was an unexpected result due to the previous RT-PCR experiment results within chapter 3, revealing undetectable NGF mRNA transcripts in all Burkitt's lymphoma B cells. The reason for this is possibly due to low levels of mRNA transcripts expressed by the cell lines that were too low to be detected using RT-PCR methods; hence this method of choice was too insensitive for NGF transcript detection.

Although, NGF expression in B cells, has been shown to be expressed in B cells within the literature. Autocrine NGF signalling was documented by Torcia M., *et al*., where they observe TrkA:$p75^{NTR}$ and NGF autocrine signalling for cell survival in memory B cells (Torcia, Bracci-Laudiero et al. 1996).

Exogenous NGF however does not rescue B cells from Anti-IgM induced apoptosis. Experiments documented by Kronfeld I. *et at*., where Ramos cells were rescued from 10μg/ml Anti-IgM induced apoptosis by 100ng/ml NGF, could not be replicated (Kronfeld, Kazimirsky et al. 2002). In this thesis, lower concentrations of Anti-IgM were used to induce apoptosis in Ramos cells, BL41 and Mutu negative clone 3 cells. Variations in time points (6 hours to 48 hours), NGF concentrations (50μg/ml to 500μg/ml), serum percentages (0% to 20%) and cell densities ($1x10^5$ cells/ml to $1x10^6$ cells /ml) were attempted to replicate the rescue effect from NGF treatment (not all data is shown). Unfortunately all experiments were unsuccessful.

Possible explanations for the discrepancy in results from those published may be due to the cell passage number (Briske-Anderson, Finley et al. 1997; Yu, Cook et al. 1997; Wenger, Senft et al. 2004). The Ramos line used within this investigation may have a higher or lower passage history compared to that used in the study by Kronfeld I. *et at*. It is possible that cell lines at high passage numbers may have alterations in cell morphology, response to stimuli, growth rates, protein expression, transfection and signalling, compared to lower passage cells. As experienced with the use of FDC like lines in this thesis, within 10 passages, cells lose FDC-like surface markers, therefore Ramos cells used by Kronfeld I. *et at*., may have been cells at low passage number, and responsive to NGF stimuli, on the other hand, other EBV negative Burkitt's lines within this results chapter, were also analysed

for a possible rescue effect from Anti-IgM induced cell death by NGF and yet similar results were observed.

Other possible reasons for the lack of an NGF rescue effect in all lines analysed may be due the type of foetal calf serum used within the media. In house experience using the EBV negative Burkitt's lymphoma cells line, L3055, has revealed that cells respond to exogenous treatment depending on the serum they are cultured in. Serum in general, is considered to be an ill-defined component in culture media due to varying unknown peptides and chemicals that may alter signalling pathways in cells (Gstraunthaler 2003). L3055s for example, are more resistant to apoptosis if grown in serum obtained from Cambrex Bioscience Wokingham Ltd. (Berkshire, UK – Cat. Nos. 14-4926) compared to serum from First Link (Birmingham, UK – Cat. Nos. 0205850). According to the publication by Kronfeld I. *et at*., 10% heat inactivated FCS was supplemented within RPMI 1640 tissue culture media. Within this investigation, RPMI 1640 and heat inactivated FCS was also used, however it is unknown whether the same type of FCS was used which may have affect the NGF rescue effect.

Work by Melamed I. *et al*., was also replicated to question the increase in F-actin content, upon NGF stimulation. Equal numbers of Mutu negative clone 3 cells were treated in either 50μg/ml, 100μg/ml, 250μg/ml and 500μg/ml human recombinant NGF for 1 minute, 2 minutes, 3 minutes 4 minutes and 5 minutes. Equal volumes of cell lyates were loaded into a 4 to 12% polyacrylamide with SDS gradient gel (Bis-Tris buffer) under reducing conditions, samples were transferred onto PVDF. Samples were then probed using an actin antibody (data not shown). The experiment was repeated three times and was unsuccessful each time. The levels of actin remained the same in all NGF concentrations and at all time points.

By western blotting methods, NGF does not increase actin levels in Mutu negative clone 3 cells. On the other hand, F-actin levels were increased by confocal analysis of NGF treated Mutu negative cells stained for by phalloidin dye. This lack in detecting an increase in actin protein concentration may also be due to the type of FCS used within the culture media, affecting the cellular response to stimli.

Autocrine NGF and TrkA signalling induced TrkA phosphorylation as seen in control treated Mutu negative cell lysates probed for phospho-TrkA protein observed in western blots (figures 5.15.4b and 5.15.6b). Autocrine signalling also induces basal Erk and Akt phosphorylation, however exogenous NGF increases the level of Erk and Akt phosphorylation in Mutu negative lines (figure 5.10). However Akt inhibition was observed to diminish cell proliferation and cell survival, whereas Erk inhibition had no effect on cell survival or growth (figures 5.15 and 5.16). In mice, is has been shown that TrkA and NGf signalling influences B cell signalling.

Transgenic mice developed to have inactive TrkA in non-neuronal tissues were viable and grossly normal however an accumulation of B1 cells with aging and the deregulation of immunoglobulin production was observed (Coppola, Barrick et al. 2004). TrkA signalling was thought to modulate B cell receptor signalling, hence, NGF may modulate B cell development via TrkA.

Although to a lesser extent compared to mature NGF, ProNGF has also been shown to activate TrkA phosphorylation, Erk and Akt signalling as well as inducing neurite outgrowth in PC12 cells (Boutilier, Ceni et al. 2008). It is probable that mature NGF and proNGF may

signal via TrkA in Mutu negative cells for cell survival and proliferation (figure 5.14.2). This may explain the possible reason why adding neutralising NGF antibody or TrkAd5 to Mutu negative clone 3 cells does not affect their viability or rate of proliferation (figure 5.16.2). Inhibiting extracellular mature NGF may therefore enable ProNGF to bind and signal via TrkA.

To ensure whether ProNGF signalling takes over on Mutu cells treated with extracellular NGF inhibitors, a neutralising antibody for ProNGF could also be added to question the effect on cell survival and proliferation. It would also be important to ensure that TrkA phosphorylation is maintained due to ProNGF signalling in Mutu negative clone 3 cells treated with mature NGF inhibitors.

As previously noted within the last chapter, $p75^{NTR}$ can be cleaved in the middle of the transmembrane domain. Like TrkB, TrkA can form a heterodimer co-receptor complex with $p75^{NTR}$. Studies by Jung K.M. *et al*., show that γ-secretase cleaved $p75^{NTR}$ receptors are unable to co- immunoprecipitate with TrkA receptors, therefore $p75^{NTR}$ cleavage plays a role in controlling TrkA:$p75^{NTR}$ heterodimerization (Jung, Tan et al. 2003).

As reviewed by Bredesena, D. E. and Rabizadeha, S., TrkA and $p75^{NTR}$ co-receptor ratios determine whether the signal is Trk or $p75^{NTR}$ dominant upon neurotrophin binding. At low ratios such as 1 to 10, TrkA to $p75^{NTR}$ dimers, TrkA signalling is thought to be the dominant signalling pathway. Whereas, neuroblastomal cell lines that express 1 to 100, TrkA to $p75^{NTR}$ rations show anti-apoptotic effects mediated by $p75^{NTR}$ signalling, hence higher $p75^{NTR}$ ratios are thought to be the dominant signalling pathway upon neurotrophin binding (Cortazzo, Kassis et al. 1996). This may explain the lack in cell proliferation inhibition in Mutu negative clone 3 cells treated with the neutralising $p75^{NTR}$ antibody (MLR2). Since these cells express

both receptor types, there may be low TrkA:$p75^{NTR}$ ratios enabling TrkA to be the dominant signalling pathway, therefore inhibiting $p75^{NTR}$ signalling would not have had any effect on cell growth.

Overall, EBV infection in B cells may up regulate NGF expression in B cells to signal mainly via TrkA receptors in an autocrine manner involving Akt signalling for cell survival and cell proliferation. However, with the discovery that FDC-like cells express NGF, the next part of the investigation was to question TrkA and NGF signalling between B cells and FDCs within tonsillar germinal centres.

6. Results

Investigating signalling effects of NGF in Germinal centre B cells and questioning possible NGF and TrkA paracrine signalling with Follicular Dendritic Cells

6.1 Introduction

The final part of this thesis is to investigation further, possible NGF and TrkA signalling within the germinal centre environment. From the previous chapter it is known that malignant EBV negative B cells can express and signal via TrkA and NGF in an autocrine manner and that exogenous NGF can induce F-actin re-arrangement, Erk and Akt phosphorylation. This final chapter questions the expression of this neurotrophic factors and its receptor in normal germinal centre B cells as well as considering possible paracrine signalling between germinal centre B cells and FDCs via NGF and TrkA.

6.1.1 B cell development within the germinal centre

As mentioned within the thesis introduction, naive B cells entre the germinal centre for expansion, somatic mutation of surface immunoglobulin, affinity maturation and selection, isotype switching, and differentiation into memory B cells and plasma cells. Cell surface expression patterns are changed depending on the site at which the B cell is within and around the germinal centre. These transcriptional changes observed during B cell transit through the germinal centre are displayed in illustration 6.1. These B cell markers were obtained by purifying naive B cells, centroblasts, centrocytes and memory B cells from human tonsillar mononuclear cells by magnetic cell separation (Pascual, Liu et al. 1994; Agematsu, Hokibara et al. 2000; Klein, Tu et al. 2003).

As discussed within a compilation of reviews, prior to germinal centre entry, B cells are characterised by the expression of cell cycle arrest and anti-apoptotic gene expression. Once within the germinal centre, naive B cells become centroblasts which lack c-Myc expression and proliferation at a fast rate. The cells are pro-apoptotic and have decreased levels of cytokine, chemokine and adhesion receptors. Cell cycle arrest is observed in centrocytes which encounter T cell and FDCs by the upregulation of cytokines, chemokines and adhesion receptors (Berek and Ziegner 1993; Kelsoe 1995; Rajewsky 1996).

As cells leave the germinal centre their phenotype then resembles that of naive B cells. Long-lived, high affinity memory B cells then differentiate into plasma cells upon the encounter of antigen during the secondary immune response) (Stein, Gerdes et al. 1982; Wagner and Neuberger 1996; McHeyzer-Williams and Ahmed 1999)

Add illustration 6.1 here

6.1.2 The extraction of centrocytes from the tonsillar germinal centres

Tonsillar germinal centre B-cell subsets were initially documented by G. Siegel, who separated cells by density gradient then performed quantitative cytological analysis, as well as morphological analysis (Siegel 1978). From cytological analysis, the Kiel classification was applied to depict the B cell subsets from germinal centres. Centrocytes, centroblasts, lymphocytes and plasma cells were described.

The germinal centre cells of interest within this part of the investigation are IgD^{-} $CD38^{+}$ $CD23^{-}$ $CD77^{+}$. These cells are found in the dark zone and known as centrocytes. It is at this stage of B cell differentiation that the initiation of somatic hypermutation occurs within $CD38^{+}$ $CD23^{-}$ $CD77^{+}$ cells (Pascual, Liu et al. 1994).

For these cells to be purified from tonsil tissue, density gradient centrifugation was applied to purity cells at each stage. Initially, tonsils were sheered into FCS negative RPMI media. All cells were spun down in ficoll to separate lymphocytes from other tonsil cells such as red blood cells. Sheep red blood cells pre-treated in 2% AET solution (pH8) were added to the tonsil cells (Kaplan and Clark 1974). This method enables T cells, which express CD2, to bind glycoproteins on sheep red blood cell membranes, forming E-rosettes (Smith and Barker

1973; Bernard, Gay-Bellile et al. 1984). B cells and T cells bound to sheep red blood cells are separated by density gradient centrifugation, enabling T cells to sink to the bottom of the tube. Cells at the interface are obtained, however there is still the possibility that some T cells, macrophages and dentritic cells would remain. To purity germinal centre centroblasts, these cells are incubated in a cocktail of primary mouse monoclonal IgG antibodies.

The four antibodies used include an anti-IgD mouse monoclonal antibody, an anti-CD39, anti CD14 and an anti CD3 antibody. Surface IgD is expressed on naive and peripheral B cells (Mudde, van Dam et al. 1986; Briere, Servet-Delprat et al. 1994). Anti-CD39 monoclonal antibody AC-2 was also included which binds activated B cells, subsets of T cells, macrophages and dendritic cells (Rowe, Hildreth et al. 1982; Kansas, Wood et al. 1991; Maliszewski, Delespesse et al. 1994). CD14 is expressed by macrophages and dendritic cells (Zhou and Tedder 1996) and CD3 is part of the T cell receptor complex on a mature T lymphocytes (van den Elsen, Shepley et al. 1984; Alexander, Goris et al. 1989).

These antibodies bind to IgD, CD39, CD14 and CD3 positive cells of the germinal centre. These cells are depleted by the addition of dynabeads coated with pan mouse IgG antibody which recognises and binds all classes of IgG mouse subclasses and is Fc specific. Cells with surface IgD, CD39, CD14 and CD3 are depleted by magnetic attachment at the side of the universal. The supernatant is collected and presumed to contain germinal centre centroblasts.

These centroblasts were carried forward to question neurotrophic factor expression in germinal centre B cells and possible paracrine neurotrophic communication with FDCs. This

part of the study was with taken to question novel B-cell and FDC interactions within a normal germinal centre microenvironment.

Cell type		Surface marker					
		IgD	CD38	CD23	CD77	CD27	CD19
Naive B cell	NB	+	-	+	-	-	+
Pre-centroblast B cell	PCB	+	+	-	-	-	+
Centroblast	CB	-	+	-	+	-	+
Centrocyte	CC	-	-	-	-	-	+
Memory B cell	MB	+	-	-	-	+	+
Plasma cell	PC	+	+	-	-	+	-
T helper Cell (T^HC)							
Follicular Dendritic Cell (FDC)							
Interdigitating Dendritic Cell (IDC)							
Tingible Body Macrophage (TBM)							

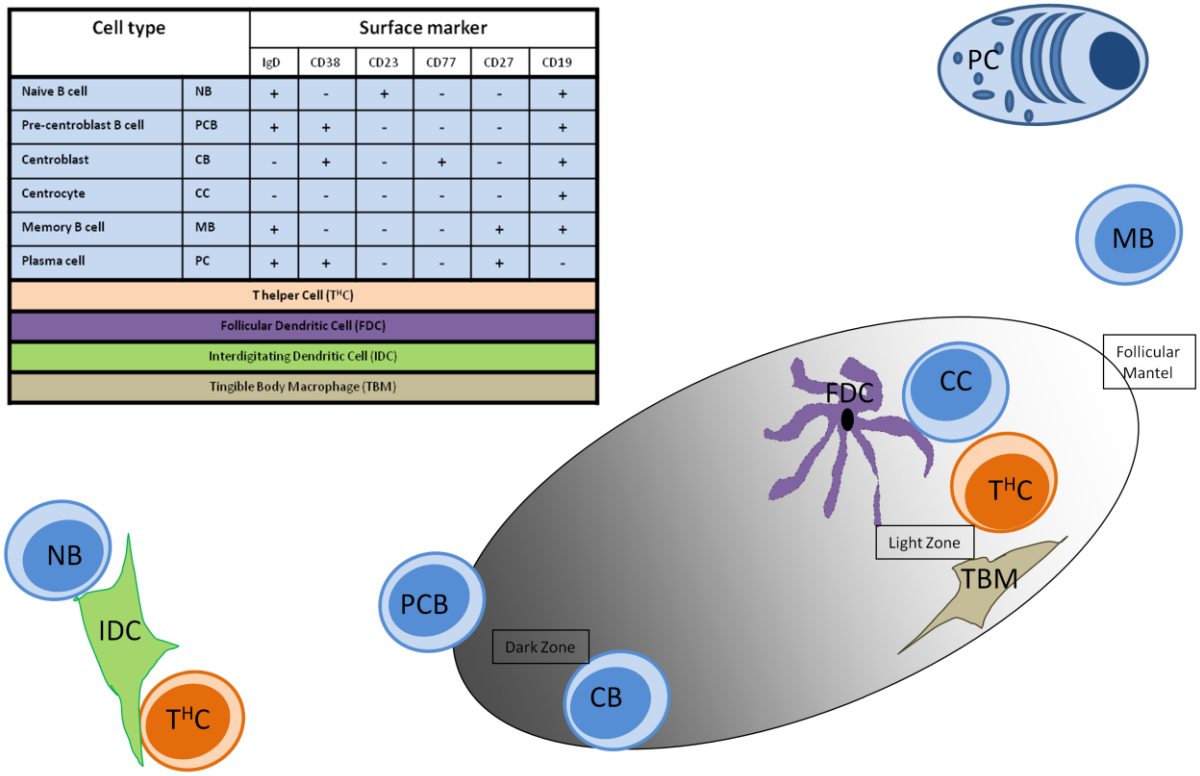

Illustration 6.1 This image depicts B cell maturation through the zones of a germinal centre
The table lists different cells found at the germinal centre microenvironment. A key for each cell line shown is displayed within the table. As naive B cells entre the dark zone they proliferate into centroblasts then migrate to the light zone as centrocytes. Mature B cells then exit the germinal centre as memory B cells which differentiate into plasma cells upon antigen recognition.

6.2 Results

6.2.1 Phenotyping freshly isolated germinal centre B cells

To question possible FDC-B-cell interactions via neurotrophic factors within the germinal centre, germinal centre B cells were initially isolated from human tonsils, then phenotyped for their expression of known germinal centre B cell markers by flow cytometry (figure 6.1).

Cells co-stained for CD38 and IgD were compared to the antibody isotype control as illustrated in figure 6.1a. Whereas, CD3 and CD19 stained cells were compared to the isotype control shown in figure 6.1b. Based on these dotplots, the purified cells isolated from tonsils are mainly $CD19^{+}$, $CD38^{+}$, IgD^{-} and $CD3^{-}$ which coincides with the surface expression patterns observed in centroblasts.

Add fig 6.1 here

6.2.2 Neurotrophic factor and receptor mRNA expression in germinal centre B cells

Once germinal centre B cells were obtained from human tonsils, RNA was extracted and amplified to cDNA for the analysis of neurotrophic factor and receptor mRNA transcripts by RT-PCR analysis (figure 6.2).

In total, eight human tonsils were analysed for the expression of neurotrophic factors and their receptors by RT-PCR. Initially β-actin was used to ensure equal levels of mRNA

transcripts between the tonsil samples (figure 6.2.1). Although comparable β-actin transcripts were detected within all tonsil samples, RT negative cDNA from Tonsil 6 contained residual genomic DNA.

For NGF mRNA transcript analysis, RT negative samples were also included within the PCR reaction since the primers used to recognise NGF transcripts lie within one exon. NGF transcripts within RT positive and negative samples were not detected in any of the germinal centre B cell samples analysed, however all samples, excluding tonsil 3 and tonsil 8, expressed NGF's receptor, TrkA mRNA transcripts (6.2.2).

When tonsil samples 1 and 2 were extracted, their RNA samples were not considered for analysing BDNF and TrkB RT-PCR expression since these tonsil samples were extracted at different stages of the investigation. As for tonsil samples 3 to 8, possible BDNF and TrkB expression was questioned below.

BDNF primers also lie within one exon (6.2.3). By comparing RT positive and negative samples, the expression of BDNF transcripts in RT positive samples and the lack of detectable transcripts in RT negative samples was only observed in tonsil 5, hence positive BDNF mRNA expression was only detected in tonsil sample 5. As for tonsil samples 4, 6,7 and 8, BDNF transcripts were observed in RT negative samples which also may represent genomic DNA. Although the RT positive samples show BDNF transcripts, the true expression of BDNF transcripts within these tonsil samples were not determined. Tonsil sample 3 on the other hand did not display detectable transcripts within the RT positive or negative samples, hence rendered BDNF negative.

As for the BDNF receptor, TrkB, Tonsil samples 4, 5, 6 and 7 show measurable levels of TrkB transcripts specific for all TrkB variants which were not detected within their RT negative equivalents. However mRNA corresponding to TrkB variant A and C were not detected in any tonsil samples. The lack of TrkB mRNA expression from both Pan-TrkB and TrkB variants A and C primers was concluded in Tonsil samples 3 and 8.

RT-PCR transcripts recognising the low affinity receptor $p75^{NTR}$, were also detected in tonsil samples 1, 2, 4, 5, 6, and 7. However tonsils 3 and 8 reveal undetectable levels of $p75^{NTR}$ mRNA expression.

A summary of the RT-PCR results are displayed in table 6.1. It can be concluded that tonsil 3 and tonsil 8 lack the expression of all neurotrophic factors and receptors whereas all other tonsil samples express the receptors TrkA and $p75^{NTR}$. Germinal centre B cell samples 4 to 7 expressed TrkB mRNA corresponding to all TrkB variants however these cells reveal undetectable levels of TrkB variants A and C transcripts. This therefore reveals that germinal centre B cells may express truncated TrkB but not full length TrkB transcripts. As for the neurotrophic factors, the lack of NGF transcripts were observed and only one tonsil sample was concluded to be a true positive for BDNF expression.

Add Fig 6.2 to 6.3 here

Table 6.1

In, all tonsil samples tested, excluding tonsil 3 and 8 expressed mRNA for both NGF receptors $p75^{NTR}$ and TrkA. On the other hand, NGF mRNA was not detected within these germinal centre B cells. To enquire whether these cells expressed TrkA or/ and $p75^{NTR}$ protein, cells were analysed by confocal microscopy and flow cytometry.

6.2.3 The expression of CD19, TrkA and $p75^{NTR}$ protein in germinal centre B cells compared to the Mutu negative clone 3 Burkitt's lymphoma B cell lines

To question the expression of CD19 and TrkA protein in germinal centre B cells, freshly isolated cells from tonsils 4, 5 and 6 were permeabilized and stained for CD19 or TrkA (figure 6.3). Cells were then analysed for the expression by confocal imaging.

Mutu negative clone 3 cells express CD19. The tonsillar B cells also express comparable levels of CD19 protein to Mutu clone 3 cells. As for TrkA expression, Mutu negative cells express stronger staining levels compared to germinal centre B cells. Germinal centre B cells obtained from tonsils 4 and 5 reveal detectable but very weak staining; however cells from tonsil 3 are negative for TrkA protein.

The expression of $p75^{NTR}$ in tonsil samples 4, 5 and 6 were analysed by flow cytometry. Cells were permeabilized then stained using the Anti-$p75^{NTR}$, MLR2 antibody (6.3.3). These germinal centre B cells were compared to Mutu negative clone 3 cells for their expression of $p75^{NTR}$ protein.

Like Mutu negative cells, germinal centre B cells extracted from three separate tonsils expressed $p75^{NTR}$ protein at high levels. In all, germinal centre B cells obtained from tonsils generally expressed the neurotrophin receptors $p75^{NTR}$ and TrkA protein.

Based on previous experience from the last chapter, to analyse NGF mRNA and protein in Burkitt's lymphoma B cell lines, the NGF primers were too sensitive to detect NGF transcripts and yet NGF protein was observed within all Burkitt's lines analysed. With these

results in consideration it was still worth asking weather germinal centre B cells express NGF protein.

6.2.4 NGF protein expression in germinal centre B cells compared to Mutu negative clone 3 Burkitt's lymphoma B cell lines

Initially, NGF expression was considered using confocal imaging methods (figure 6.4.1). Germinal centre B cells and Mutu clone 3 cells were permeabilized and stained for NGF expression using the Anti-NGF (N3279) antibody.

Mutu negative clone 3 cells express NGF protein as previously shown within chapter 5. As shown in figure 6.4.1, some Mutu cells in culture display larger levels of NGF protein staining

compared to the majority of cells which have lower levels and weaker NGF stain. As for the germinal centre B cells obtained from tonsil 4, 5 and 6, very weak to negative levels of NGF staining was observed. The low expression levels are true NGF staining considering the isotype control displayed undetectable staining within the same tonsil samples.

The expression of NGF protein was also scrutinized using flow cytometry analysis (figure 6.4.2). Cells were permeabilized and stained for expression using the Anti-NGF (N3279) antibody.

NT-2 cells, the positive control line for NGF expression, Mutu clone 3 cells and samples from tonsil 4, 5 and 6 were permeabilized then stained. As expected NT-2 show the expression of NGF protein. The expression of NGF in Mutu clone 3 cells is much higher that that observed in germinal centre B cell samples extracted from three separate tonsil samples.

Finally, NGF expression was also investigated by western blotting analysis (figure 6.4.3). Cell lysates were obtained from Mutu clone 3 and germinal centre B cells obtained from tonsils 3, 4, 5, 6, 7 and 8. 20ug of protein was loaded per well within a 4% to 12% polyacrylamide with SDS gradient gel (Bis-Tris buffer) under reducing conditions, samples were transferred onto PVDF. Samples were then probed using an NGF antibody (AF256NA).

Varying levels of NGF expression were detected when comparing germinal centre B cells obtained from six different tonsil preparations. The highest level s of NGF protein detected were within tonsil samples 5 and 7, on the other hand, very low protein levels were observed in tonsil samples 3 and 4. However, the expression of NGF protein in Mutu negative clone 3 cells is very strong compared to all germinal centre B cell samples.

Add fig 6.4 here

In all, Mutu negative clone 3 cell lines express higher levels of TrkA and NGF protein compared to germinal centre B cells obtained from human tonsils. Previously it has been shown that biologically active exogenous NGF added alone does not induce cell survival cell proliferation or cell migration in Mutu negative clone 3 cells and yet induced F-actin re-arrangement and Erk and Akt phosphorylation. Therefore the effects of exogenous NGF were also applied in germinal centre B cells to question NGF signalling functions in normal B cells.

6.2.5 Exogenous CD40-L and NGF treatment on cell proliferation in freshly isolated germinal centre B cells

It is known that freshly isolated centrocytes degenerate rapidly by apoptosis when cultured, however with the addition of CD40-L, cells are rescued from apoptosis (Liu, Joshua et al. 1989; Holder, Wang et al. 1993). To test this, germinal centre B cells obtained from tonsil samples 1, 2, 3, 4 and 5 were either cultured in control media, in varying concentrations of CD40-L or varying exogenous human recombinant NGF protein, then analysed for thymidine incorporation (figure 6.5).

Control treated germinal centre B cells did not synthesis DNA when cultured for 48 hours. As expected, a gradual increase in DNA synthesis was observed in CD40 treated germinal centre cells, although, tonsil 1 and 4 show very high thymidine counts when treated in 1μg/ml CD40-L. NGF treatment on the other hand, had no effect on DNA synthesis within germinal centre B cells from all five tonsil samples. NGF alone therefore, cannot rescue germinal centre centroblasts from apoptosis.

To have a closer look at other possible NGF induced functions in B cells, RNA samples from three tonsils were used within a microarray study to analyse genes that are turned on and off upon the addition of NGF.

6.2.6 The changes in gene expression upon NGF treated germinal centre B cells

Three further germinal centre B cell extractions were performed (tonsil 9, 10 and 11). Once phenotyped, cells were screened for the expression of NGF receptors TrkA and $p75^{NTR}$ mRNA (figure 6.6.1). Cells were then exposed to either control media or media containing 100ng/ml human recombinant NGF, tested for bioactivity prior to the experiment. Cells were treated for 6 hours; RNA was then extracted and used for microarray analysis. The levels of expression were measured using the Robist multichip average method. Readings were analysed using the Linear Models for Microarray Data software package (Limma). To

comparing levels of gene expression changes upon NGF treatment, paired test analysis were competed using significance analysis of microarrays software.

195 genes showed significant changes at p-values less than 0.01 whereas 71 genes showed an average gene expression fold change of 1.5 or more. 25 genes that met both this criteria are displayed in figure 6.6.2.

13 genes were found to be down regulated upon NGF treatment; the known functions of these genes are displayed in table 6.2. 12 genes on the other hand were up regulated and their functions are shown in table 6.3.

As displayed in figure 6.6.1, all there tonsil samples (tonsils 9, 10 and 11) used for micro array analysis expressed NGF receptors, $p75^{NTR}$ and TrkA mRNA. When cultured in 100ng/ml NGF, varying genes were observed to be up regulated and downregulated.

In all, based on tables 6.2 and 6.3, NGF stimulation in GC tonsil B cells could affect RNA processing, induce cytoskeletal re-arrangement, inhibit cell cycle arrest, promote calcium influx, chromosomal organisation re-arrangement and regulate cell proliferation in germinal centre B cells. Although, cell proliferation upon the addition of NGF alone, had no effect in GC tonsil B cells. On the other hand, germinal centre B cells expressed lower levels of NGF

protein compared an EBV negative Mutu line (figure 6.4.1) therefore NGF available within its microenvironment may induce the genes expression alterations observed. To identify possibly sources for this NGF within normal germinal centres NGF staining was completed within human tonsil tissue sections.

6.2.7 Immunohistochemical staining for CD19, $p75^{NTR}$, BU10 and NGF within tonsillar germinal centres

As previously shown in chapter 5, FDC-like cell lines obtained from human tonsils show the expression of NGF mRNA and protein. Within this chapter is has been shown that germinal centre B cells can express TrkA and $p75^{NTR}$ mRNA and protein and yet low levels of NGF. Exogenous NGF has also been shown to induce changes in germinal centre B cell gene expression. It was therefore worth testing the possibilities of TrkA and NGF paracrine between normal germinal centre B cells and cells within the germinal centre.

Freshly excised human tonsil tissue was sliced in 5mm thickness. Cryogenically frozen tissue was sectioned onto glass slides at -20^{o}C. Sections were then acetone fixed then stained. Initially cells were stained for known germinal centre markers BU10, p75^{NTR} and CD19 (figure 6.7).

B cells and FDCs are CD19 and p75^{NTR} positive, therefore cells within the light zone, dark zone and follicular mantel stain were detected by adding the secondary antibodies specific for CD19 and p75^{NTR}. On the other hand, BU10 is an FDC specific antibody which detected staining within the light zone of the germinal centre. The overlay image for all three primary antibodies and the Hoechst nuclear stain is compared with the overlay image taken from the isotope control.

To test the expression of NGF in human germinal centres a serial dilution of the anti-NGF (N3279) antibody was completed and tested in tonsil sections. An optimal concentration was determined which revealed staining within the light zone of the germinal centre (figure 6.8). The concentration of primary antibody used was compared to the same isotype concentration displayed within an overlay image also showing nuclear staining.

To ensure this staining was legitimate FDC staining, cells were co-stained for NGF and BU10 (figure 6.9). Three separate images of stained germinal centres obtained from the same tonsil are displayed within figures 6.9.1, 6.9.2 and 6.9.3. These three figures were compared to their isotype control images; one of which is represented within figure 6.9.4. All three germinal centre images reveal NGF and BU10 co-staining patterns within the light zone of the germinal centre. The different germinal centre zones are illustrated within figure 6.9.5 which is an overlay image obtained from figure 6.9.1.

Cells co-staining for BU10 and NGF were viewed at a higher magnification (figure 6.9.6). The staining pattern observed is that of FDCs (communication with Dr D.L. Hardie, University of Birmingham). Interestingly, some FDCs stain for NGF alone (green), some for BU10 alone (Red) whereas some co-stain for both (yellow) revealing possible heterogeneity of FDC cells within the light zone.

Add fig 6.7 and 6.8 and 6.9 here

Overall, it can be concluded from this data that germinal centre B cells express high levels of the low affinity NGF receptor $p75^{NTR}$ and lower levels of the high affinity receptor, TrkA

protein. Exogenous NGF induces the up regulation and down regulation of genes with varying function in germinal centre B cells and FDCs have been observed to express NGF within a germinal centre environment. NGF and TrkA may therefore signal in a paracrine manner between B cells and FDCs; however the specific functions of this interaction are currently unknown.

For this to be investigated further, questions on more functional outcomes in germinal centre B cells, upon NGF treatment would need to be analysed using varying NGF concentrations of NGF as well as other known germinal centre cytokines. By investigating TrkA and NGF signalling further, within normal germinal microenvironments, more knowledge would be gained on how normal germinal centre B cells interact and the reasons for the upreguation of these neurotrophic factors and receptors in Burkitt's lymphoma B cells.

These important findings could then be applied for better understanding in Burkitt's lymphoma pathogenesis, EBV interaction with B cells, B cell signalling within a germinal centre and provide novel and yet specific, affective therapeutics in the fight against Burkitt's lymphoma.

Figure 6.1a

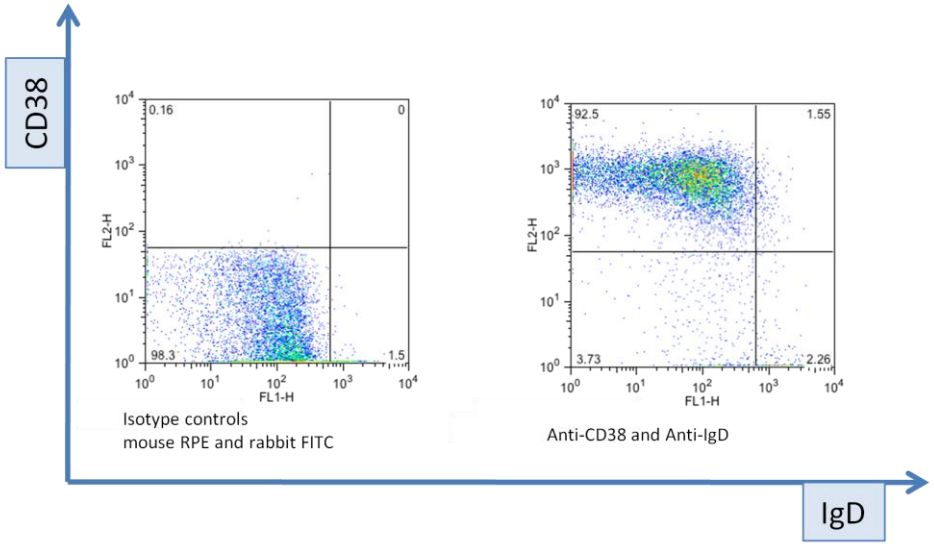

Figure 6.1b

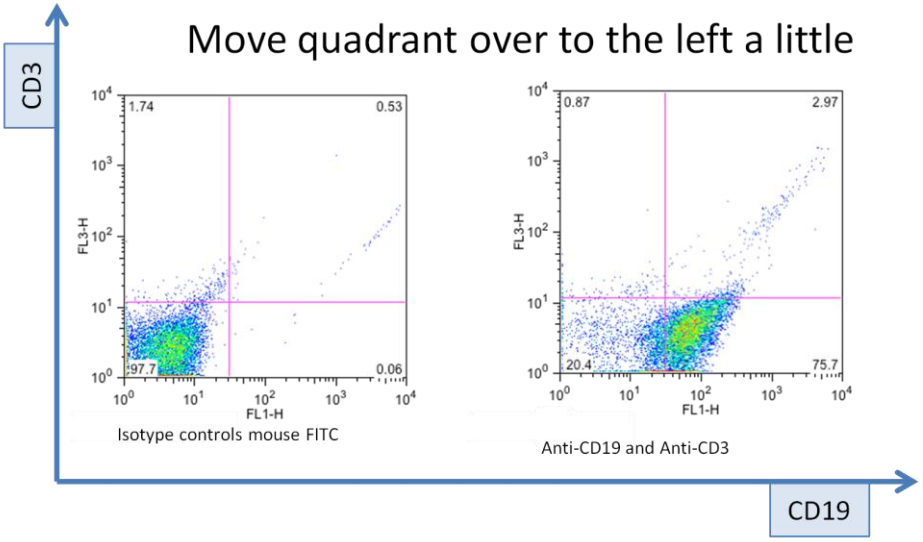

Figure 6.1: Tonsil extracted, germinal centre B-cell phenotype
Freshly isolated germinal centre B cells extracted from human tonsil were extracted then surface stained using Anti-IgD and Anti-CD38 antibodies compared to the isotype controls mouse RPE and rabbit FITC (figure 6.1a). Cells were also stained using Anti-CD19 and Anti-CD3 antibodies compared to their isotype control mouse FITC (figure 6.1b). Cells were then analysed by flow cytometry, dot plots are displayed. Successful germinal centre centroblast B cell extractions were based on high CD38 and CD19 populations and low CD3 and IgD cell phonotypes.

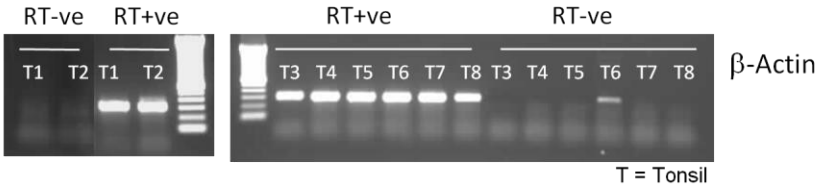

Figure 6.2.1: mRNA transcripts of β-actin in germinal centre tonsil B cells
RT-PCR primers specific for β-actin were used in an RT-PCR reaction producing a 300bp amplicon. RT positive and negative products were separated on a 1.5% agarose gel containing ethidium bromide and visualised under UV light.

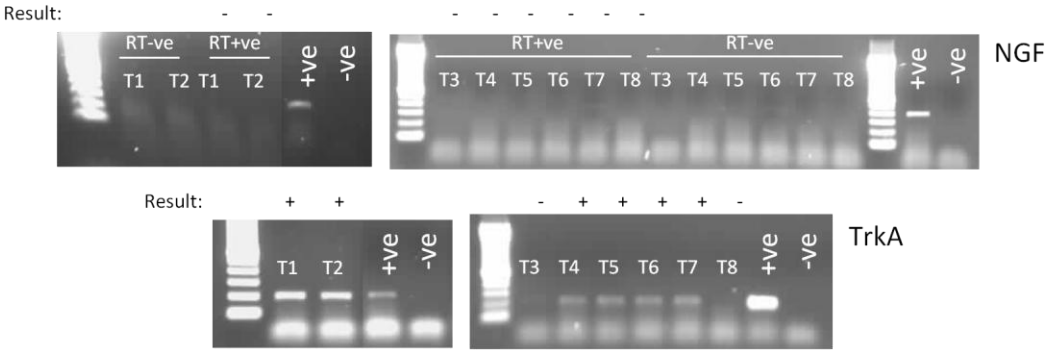

Figure 6.2.2: mRNA transcripts of NGF and its' receptor TrkA in germinal centre tonsil B cells
RT-PCR primers specific for NGF producing a 325bp amplicon, and for TrkA producing a 200bp amplicon were used in RT-PCR reactions. Products were separated on 1.5% agarose gels containing ethidium bromide and visualised under UV light. The interpretation (detected specific product "+" or no specific product "-") of the gels is indicated in the results above each gel image. RNA extracted from NT-2 cells was used as the positive control for NGF whereas RNA from KELLY cells was used for the TrkA RT-PCR control.

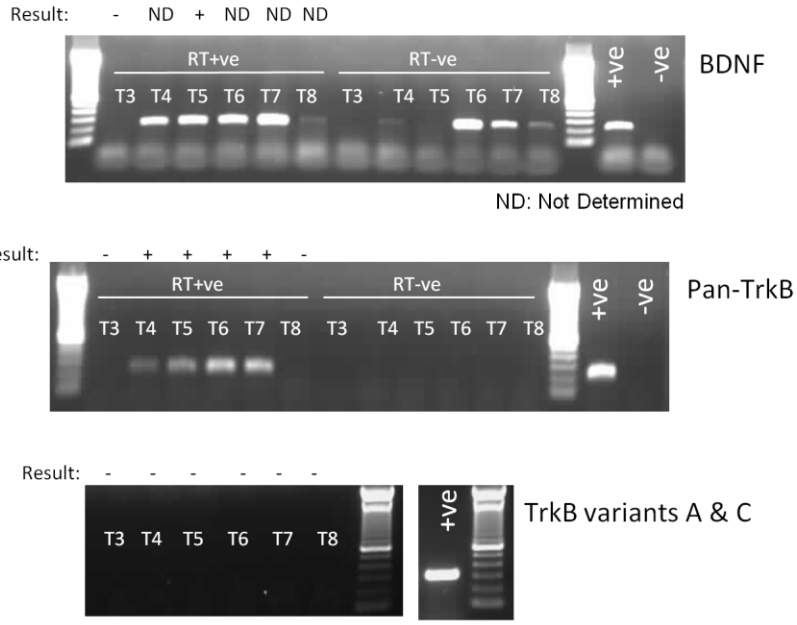

Figure 6.2.3: mRNA transcripts of BDNF and its receptor TrkB in germinal centre tonsil B cells
RT-PCR primers specific for BDNF producing a 221bp amplicon, Pan-TrkB producing a 221bp amplicon and TrkB variants A and C producing a 574bp amplicon were used in an RT-PCR reaction. Products were separated on 1.5% agarose gels containing ethidium bromide and visualised under UV light. The interpretation (detected specific product "+" or no specific product "-") of the gels is indicated in the results above each gel image. The multiple myeloma cell line, KMS-11 was used as a positive control for BDNF expression whereas, cDNA extracted from KMS-11 cell line was used as the control for TrkB mRNA transcripts.

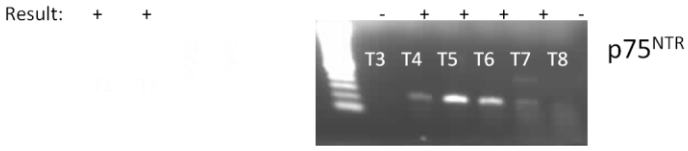

Figure 6.2.4: mRNA transcripts of the low affinity receptor $p75^{NTR}$ in germinal centre tonsil B cells
RT-PCR primers specific for $p75^{NTR}$ producing a 246bp amplicon were used in an RT-PCR reaction. Products were separated on 1.5% agarose gels containing ethidium bromide and visualised under UV light. The interpretation (detected specific product "+" or no specific product "-") of the gels is indicated in the results above each gel image. cDNA extracted from KELLY cells was used as the RT-PCR control.

Table 6.1: Summary representing the expression of RT-PCR mRNA transcript experiments on neurotrophic factors and their receptors within germinal centre tonsil B cells

	Tonsil 1	Tonsil 2	Tonsil 3	Tonsil 4	Tonsil 5	Tonsil 6	Tonsil 7	Tonsil 8
Neurotrophic Factors and Their Receptors								
NGF	-	-	-	-	-	-	-	-
BDNF	Not tested		-	ND	+	Not Determined		
$p75^{NTR}$	+	+	-	+	+	+	+	-
TrkA	+	+	-	+	+	+	+	-
Pan-TrkB	Not tested		-	+	+	+	+	-
TrkB A&C	Not tested		-	-	-	-	-	-

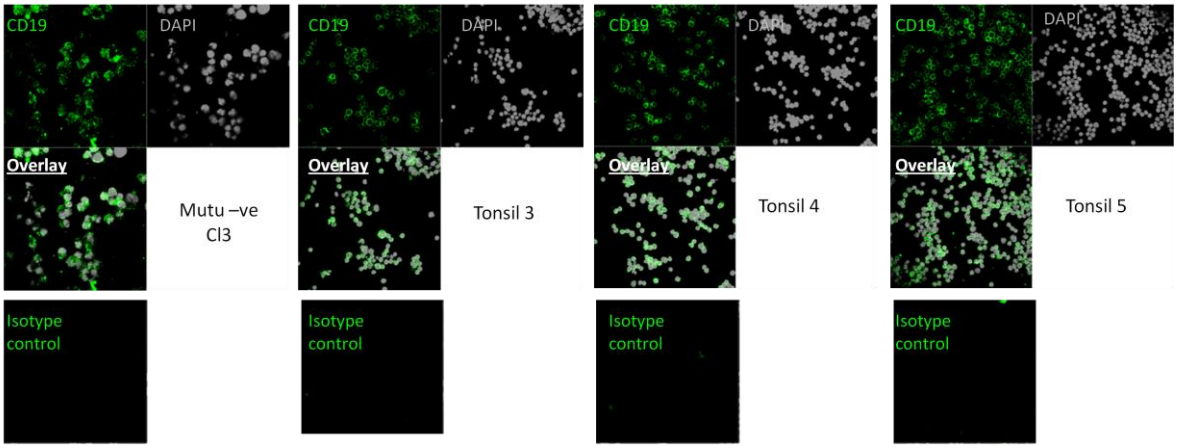

Figure 6.3.1: The expression of CD19 protein in Mutu negative clone 3 cell line and germinal centre tonsil B cells
Confocal images showing permeabilized Mutu negative clone 3 Burkitt's lymphoma B cells and freshly isolated germinal centre B cells from tonsils 3, 4 and 5 stained for CD19 primary antibody and DAPI nuclear stain. Specifically bound CD19 antibodies were detected by FITC-conjugated secondary antibodies then viewed under an LSM laser microscope. Immunoglobulin specific isotype controls were also used to compare primary antibody staining.

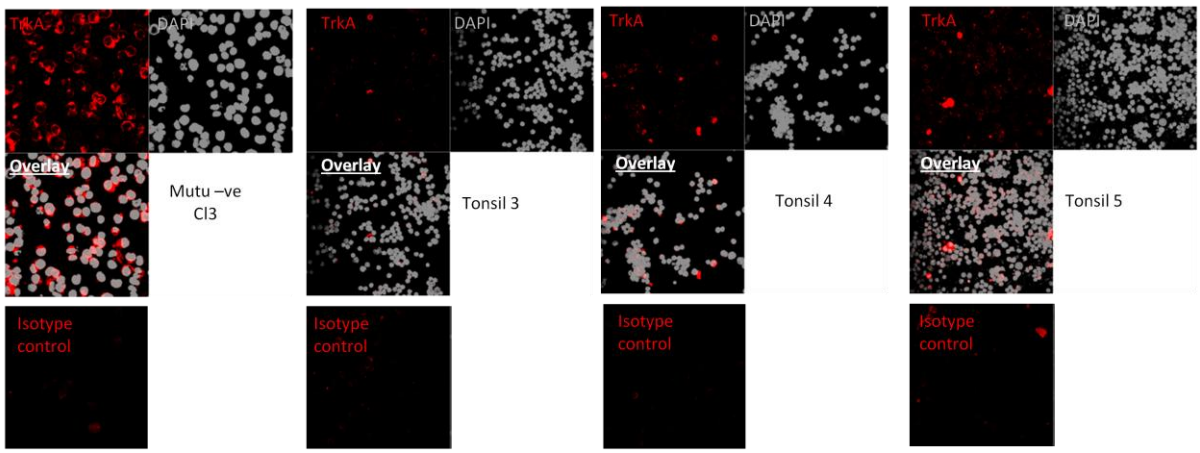

Figure 6.3.2: The expression of TrkA protein in Mutu negative clone 3 cell line and germinal centre tonsil B cells
Confocal images showing permeabilized Mutu negative clone 3 Burkitt's lymphoma B cells and freshly isolated germinal centre B cells from tonsils 3, 4 and 5 stained for TrkA primary antibody and DAPI nuclear stain. Specifically bound TrkA antibodies were detected by FITC-conjugated secondary antibodies then viewed under an LSM laser microscope. Immunoglobulin specific isotype controls were also used to compare primary antibody staining.

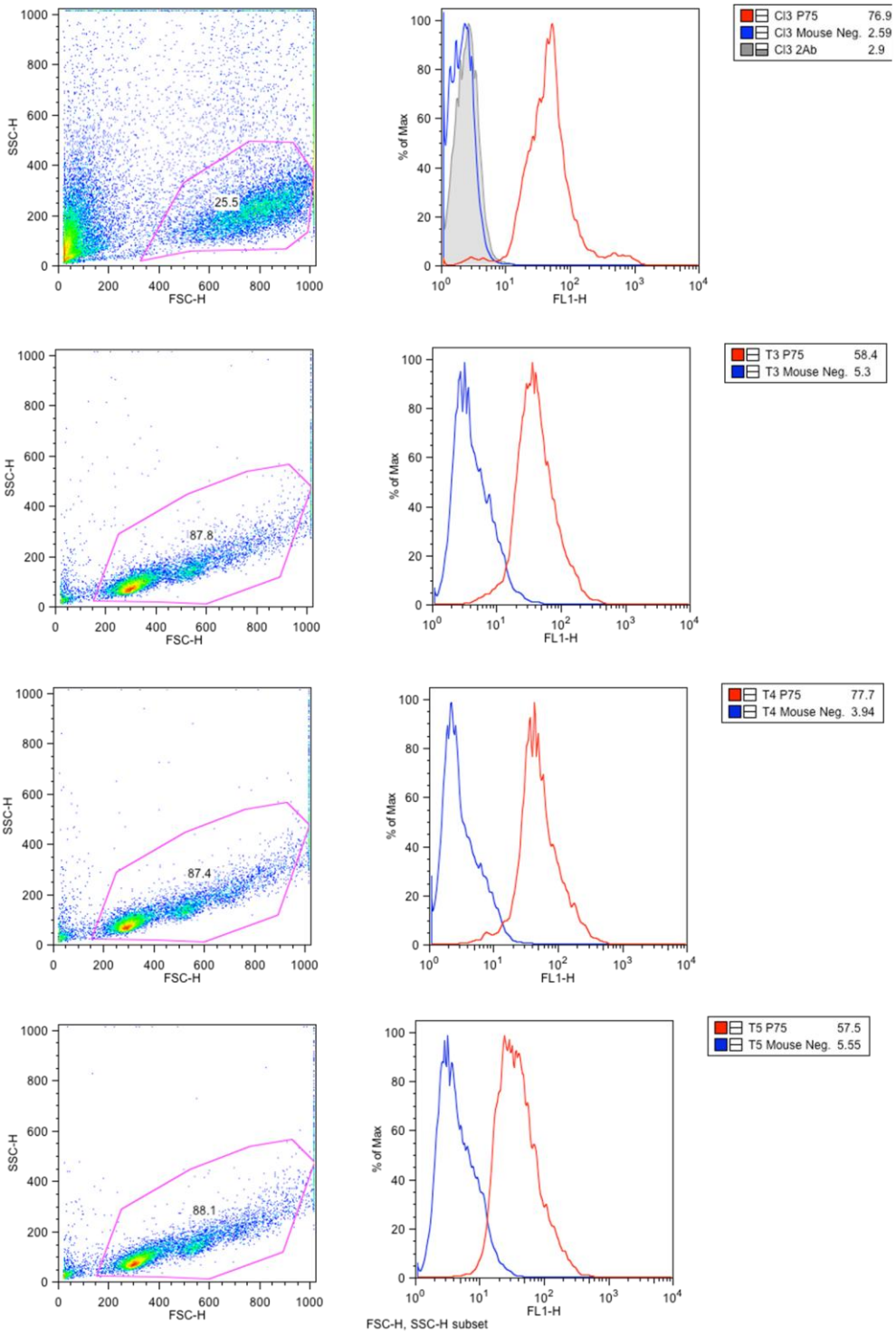

Figure 6.3.3: The expression of NGF in Mutu negative clone 3 cells and tonsillar germinal centre B cells
Permeabilized Mutu negative clone 3 (Cl3) and germinal centre B cells extracted from tonsils 4, 5 and 6 (T4, T5 and T6) were stained for flow cytometry analysis using an anti-NGF (N3279) antibody (P75). The dot plot, shown above, displays the population of cells collected for FITC measurement, gates were drawn from PI low cells taken from culture.
The primary antibodies (NGF) used were compared to the isotype control (Neg) within each histogram displayed. A secondary antibody (2Ab) directly conjugated with FITC was used to detect specifically bound primary antibody. Mean FITC levels were displayed from each histogram.

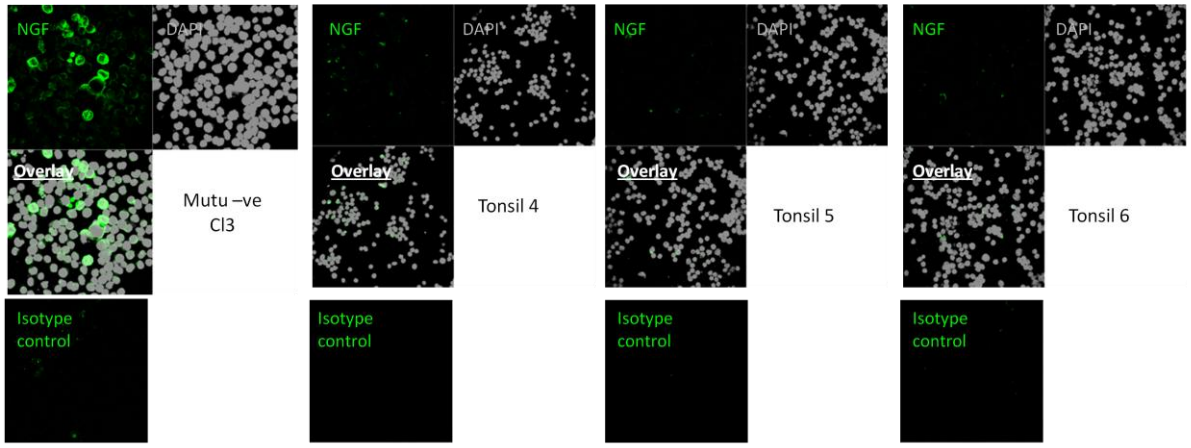

Figure 6.4.1: The expression of NGF protein in Mutu negative clone 3 cell line and germinal centre tonsil B cells by confocal imaging
Confocal images showing permeabilized Mutu negative clone 3 Burkitt's lymphoma B cells and freshly isolated germinal centre B cells from tonsils 4, 5 and 6 stained for NGF primary antibody (N3279) and DAPI nuclear stain. Specifically bound NGF antibodies were detected by FITC-conjugated secondary antibodies then viewed under an LSM laser microscope. Immunoglobulin specific isotype controls were also used to compare primary antibody staining.

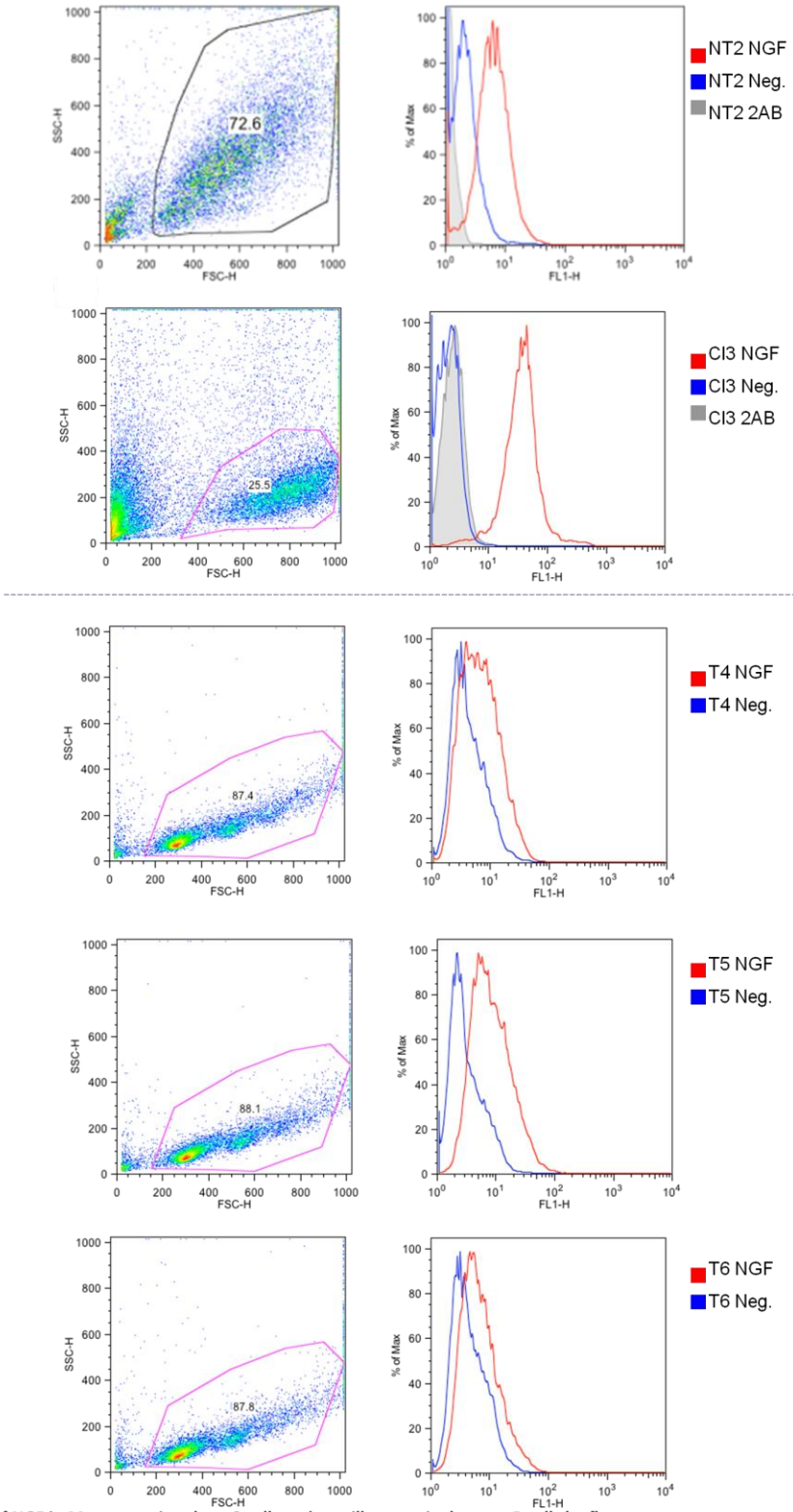

Figure 6.4.2: The expression of NGF in Mutu negative clone 3 cells and tonsillar germinal centre B cells by flow cytometry
Permeabilized Mutu negative clone 3 and germinal centre B cells extracted from tonsils 4, 5 and 6 were stained for flow cytometry analysis using an anti-NGF (N3279) antibody. The dot plot, shown above, displays the population of cells collected for FITC measurement, gates were drawn from PI low cells taken from culture.
The primary antibodies (NGF) used were compared to the isotype control (Neg) within each histogram displayed. A secondary antibody (2Ab) directly conjugated with FITC was used to detect specifically bound primary antibody. Mean FITC levels were displayed from each histogram.

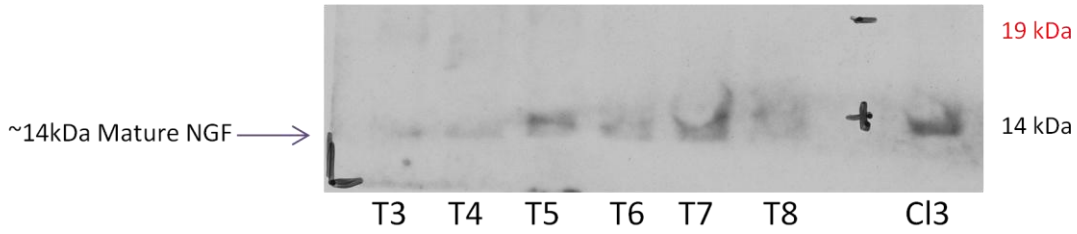

Figure 6.4.2: The expression of NGF protein in Burkitt's lymphoma B cell lines by western blotting

Western blot results showing whole cell extracts (10μg protein) run within a 4% to 12% acrylamide Bis-Tris NuPAGE gel. Blots were probed for NGF (AF256NA) primary antibody. Specifically bound antibodies were detected by an alkaline phosphatase chemiluminescent method and blots exposed to photographic film.

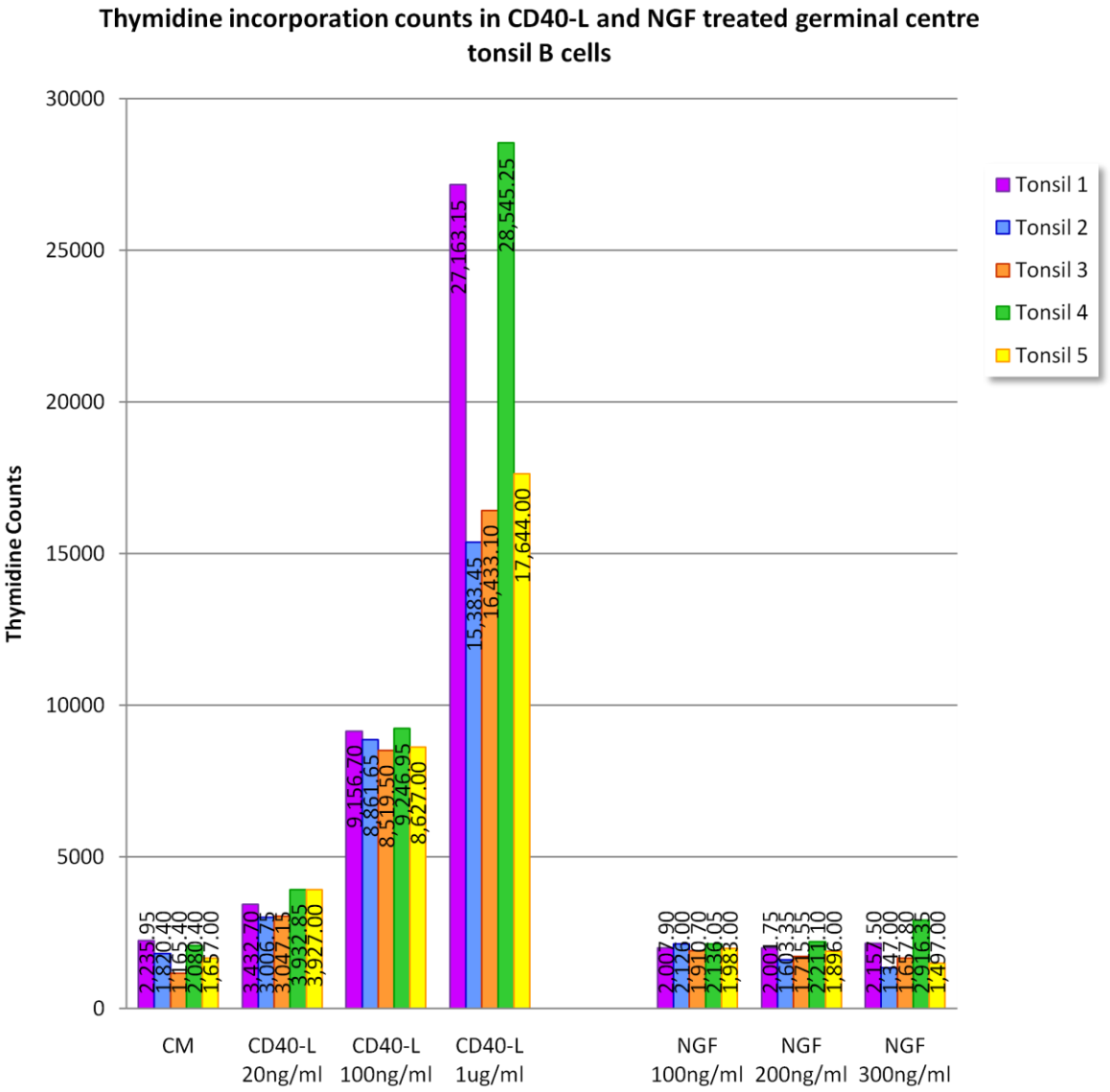

Figure 6.5: Thymidine incorporation counts in germinal centre B cells treated in Cd40-L or exogenous NGF protein

Freshly isolated germinal centre B cells exposed to 20ng/ml, 100ng/ml and 1µg/ml CD40-L and 100ng/ml , 200ng/ml and 300ng/ml human recombinant NGF protein for 36 hours. Cells were then pulsed with 1:100 dilution of thymidine (50µl per well) for 12 hours. Cell were harvested on glass fibre filter pads. Radioactivity counts were determined by liquid scintillation counting over 60 seconds. Mean counts per minute were calculated for quadruplicate wells and plotted within a graph.

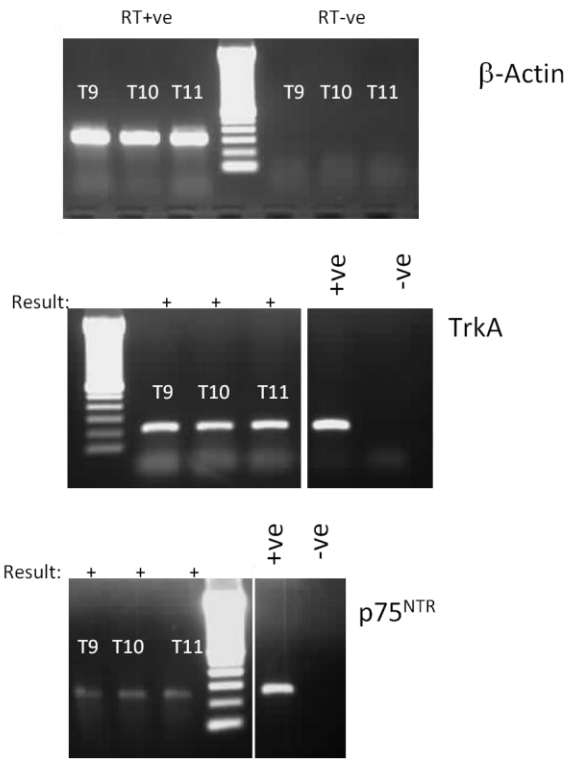

Figure 6.6.1: β-actin, TrkA and p75^{NTR} mRNA transcripts in germinal centre tonsil B cells
RT-PCR primers specific for β-actin (300bp), TrkA (325bp) and p75^{NTR} (246bp) were used within RT-PCR reactions. Products were separated on 1.5% agarose gels containing ethidium bromide and visualised under UV light. The interpretation (detected specific product "+" or no specific product "-") of the gels is indicated in the results above each gel image. cDNA extracted from KELLY cells was used as the RT-PCR control for TrkA and p75^{NTR} expression.

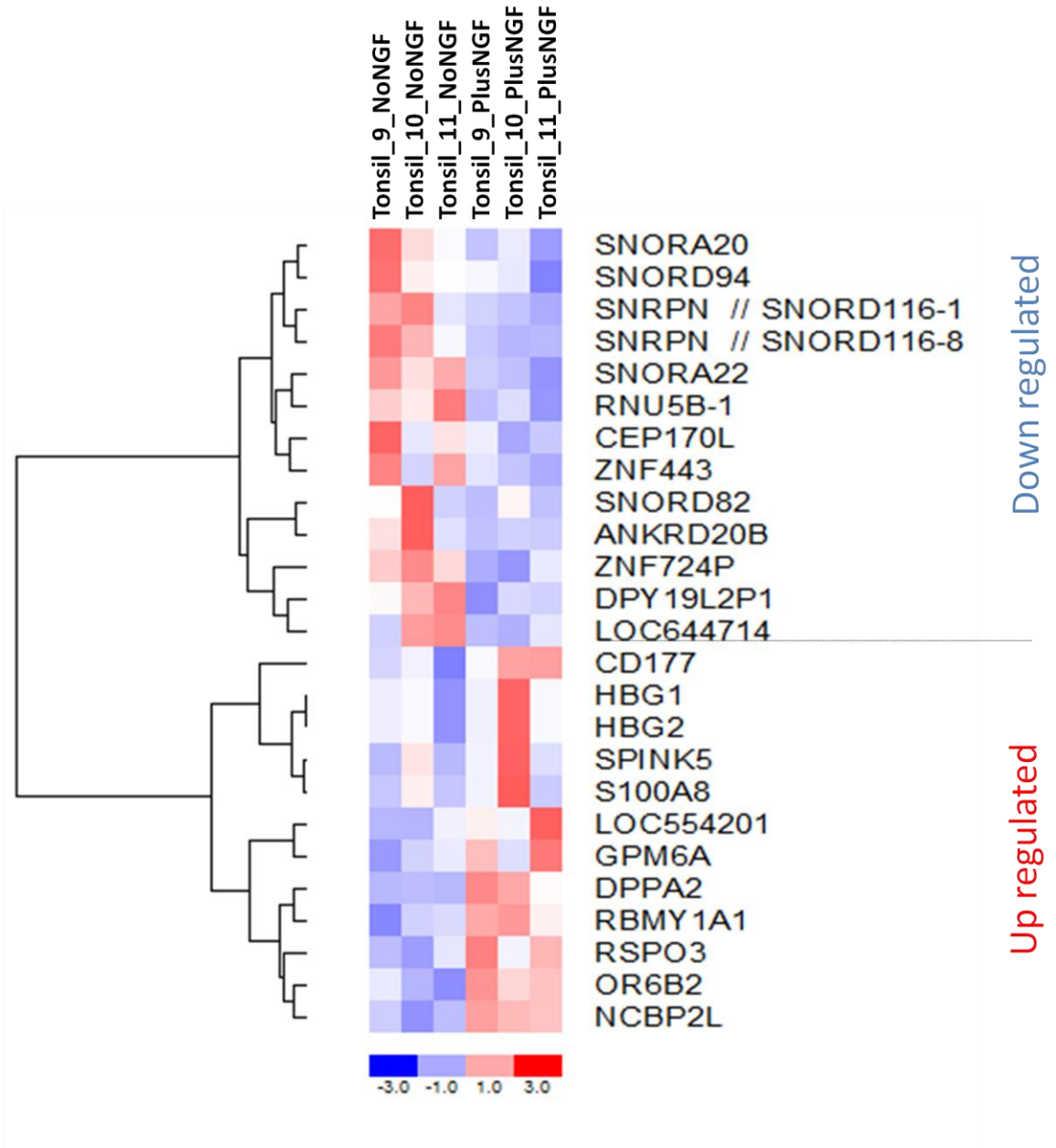

Figure 6.6.2: The changes in gene expression within freshly isolated Germinal centre B cells exposed to NGF

RNA extracted from tonsil samples 9, 10 and 11 were treated either in control media (NoNGF) or in 100ng/ml human recombinant NGF (PlusNGF) and were applied for microarray analysis. 25 genes displaying average gene expression fold changes of 1.5 or more and significant changes at p values less than 0.01 are displayed within a heat map. 13 genes were down regulated, whereas 12 genes were up regulated.

Table 6.2: Down regulated genes in germinal centre tonsil B cells treated with NGF compared to those treated in control media

Gene Symbol	Gene Description	Gene function	Reference
SNORA20	Small nucleolar RNA 20	Both SNORA20 and SNORA22 are members of the H/ACA class of small nuclear RNA which guide the sites for Uridines modification to Pseudouridines.	(Kiss, Jady et al. 2004)
SNORA22	Small nucleolar RNA 22		
SNORD82	Small nucleolar RNA 82	SNORA82, SNORA94, SNRPN // SNORD116-1 and SNRPN // SNORD116-8 contain the conserved sequence motifs known as the C box and the D box. Most of the members of the box C/D family function in directing site-specific 2'-O-methylation of substrate RNAs	(Galardi, Fatica et al. 2002)
SNORD94	Small nucleolar RNA 94		
SNRPN // SNORD116-1	Small nuclear ribonucleoprotein polypeptide N // small nucleolar RNA 116-1		
SNRPN // SNORD116-8	Small nuclear ribonucleoprotein polypeptide N // small nucleolar RNA 116-8		
RNU5B-1	RNA, U5B small nuclear 1	U5 RNA is a non-coding RNA that is a component of both types of known spliceosome. The precise function of this molecule is unknown.	(Hinz, Moore et al. 1996)
CEP170L	Centrosomal protein 170kDa-like	The product of the CEP170 gene is a 170kDa component of the centrosome and a non-membraneous organelle that functions as the major microtubule-organizing center in animal cells. The protein interacts with the intraflagellar transport protein 81 (IFT81) and is phosphorylated by cyclin dependent kinase 1 (CDK1) and polo-like kinase 1 (PLK1), and functions in maintaining microtubule organization, cell morphology and cilium stability.	(Strausberg, Feingold et al. 2002)
ANKRD20B	Ankyrin repeat domain 20B	The ankyrin repeat is a 33-residue motif in proteins consisting of two alpha helices separated by loops. Ankyrin repeats mediate protein-protein interactions and are among the most common structural motifs in known proteins. The repeat has been found in proteins of diverse function such as transcriptional initiators, cell cycle regulators, cytoskeletal, ion transporters and signal transducers.	(Sedgwick and Smerdon 1999)

ZNF443	Zinc finger protein 443	A zinc finger protein is a DNA-binding protein domain consisting of zinc fingers. They occur in nature as the part of transcription factors conferring DNA sequence specificity as the DNA-binding domain.	(Katoh, Oguri et al. 1998)
ZNF724P	Zinc finger protein 724 pseudogene		
DPY19L2P1	Dpy-19-like 2 pseudogene 1 (C. elegans)	DYP19L1 and DYP19L2 genes belong to a transmembrane gene family. The functions for these genes are unknown.	(Carson, Cheung et al. 2006)
LOC644714	Hypothetical protein LOC644714	Function Unknown.	

Table 6.3: Up regulated genes in germinal centre tonsil B cells treated with NGF compared to those treated in control media

Gene Symbol	Gene Description	Gene function	Reference
CD177	CD177 molecule	CD177 is a glycol-phsosphatidylinositol (GPI) linked N-glycosylated cell surface glycoprotein first described in a case of neonatal alloimmune neuropenia. CD177 is also known as neutrophil specific antigen-1. Its function is unknown.	(Lalezari, Murphy et al. 1971)
HBG1	Hemoglobin subunit gamma-1 (gamma A)	Hemoglobin subunit gamma-1 is a protein that in humans is encoded by the HBG1 gene. The gamma globin genes (HBG1 and HBG2) are normally expressed in the fetal liver, spleen and bone marrow. Two gamma chains together with two alpha chains constitute fetal hemoglobin (HbF) which is normally replaced by adult hemoglobin (HbA) at birth. In some beta-thalassemias and related conditions, gamma chain production continues into adulthood. Hemoglobin subunit gamma-2 is a protein that in humans is encoded by the HBG2 gene.	(Higgs, Vickers et al. 1989)
HBG2	Hemoglobin subunit gamma-2 (gamma G)		
SPINK5	Serine peptidase inhibitor, Kazal type 5	Serine protease inhibitor Kazal-type 5 is an enzyme that in humans is encoded by the SPINK5 gene. This gene encodes a multidomain serine protease inhibitor that contains 15 potential inhibitory domains. The inhibitor may play a role in skin and hair morphogenesis and anti-inflammatory and/or antimicrobial protection of mucous epithelia	(Magert, Standker et al. 1999)
S100A8	S100 calcium binding protein A8	The protein encoded by this gene is a member of the S100 family of proteins containing 2 EF-	(Schafer, Wicki et al.

		hand calcium-binding motifs. S100 proteins are localized in the cytoplasm and/or nucleus of a wide range of cells, and involved in the regulation of a number of cellular processes such as cell cycle progression and differentiation	1995)
LOC554201	Hypothetical LOC554201	Function unknown	
GPM6A	Glycoprotein M6A	Neuronal membrane glycoprotein M6-a is a protein that in humans is encoded by the GPM6A gene.	(Renne, Minner et al. 2008)
DPPA2	Developmental pluripotency associated 2	One of the genes recently identified to be expressed specifically in pluripotent cells. Reduced expression of Dppa2 is observed in differentiated mouse ES cells, which also show repressed cell proliferation activity.	
RBMY1A1	RNA binding motif protein, Y-linked, family 1, member A1	RNA-binding motif protein, Y chromosome, family 1 member A1/C protein is encoded	(Chai, Zhou et al. 1998)
RSPO3	R-spondin 3 homolog (Xenopus laevis**)**	This gene encodes a member of the thrombospondin type 1 repeat supergene family. The protein contains a furin-like cysteine-rich region. Furin-like repeat domains have been found in a variety of eukaryotic proteins involved in the mechanism of signal transduction by receptor tyrosine kinases	(Kazanskaya, Glinka et al. 2004)
OR6B2	Olfactory receptor, family 6, subfamily B, member 2	Encodes Olfactory receptor 6B2. Olfactory receptors interact with odorant molecules in the nose, to initiate a neuronal response that triggers the perception of a smell.	(Miwa, Moriizumi et al. 2002)
NCBP2L	Nuclear cap binding protein subunit 2-like	Function unknown	

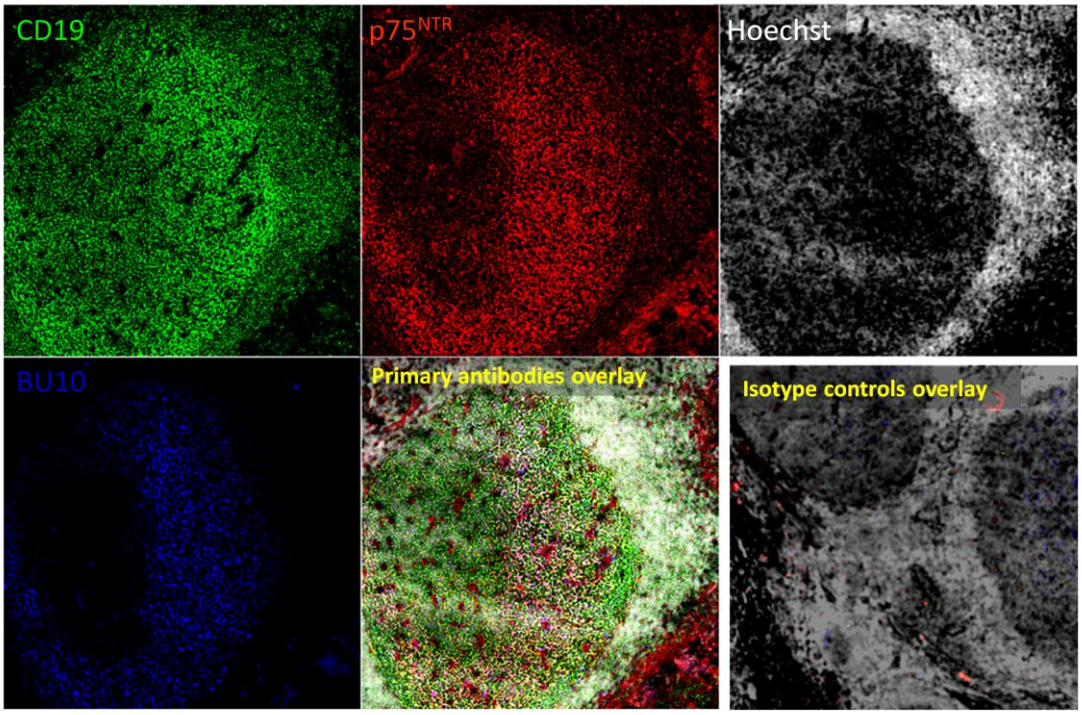

Figure 6.7: Immunohistochemical staining for CD19, p75^{NTR} and BU10 in human tonsil germinal centres
Cryogenically frozen human tonsil tissue sections were stained using the primary antibodies CD19 and p75^{NTR} which detect B cells and FDCs. Sections were also co-stained for and BU10 that detects FDCs. A FITC conjugated secondary antibody (green) was used to detect CD19, a TRITC conjugated secondary (red) was used to detect p75^{NTR}, whereas an Alexa Fluor 633 secondary (blue) was used to detect BU10. Cellular nuclei were detected by Hoechst bis-benzimide dye 33342 (Hoechst). Overlay images for each stain are also shown and compared to the staining observed within isotype control stained cells.

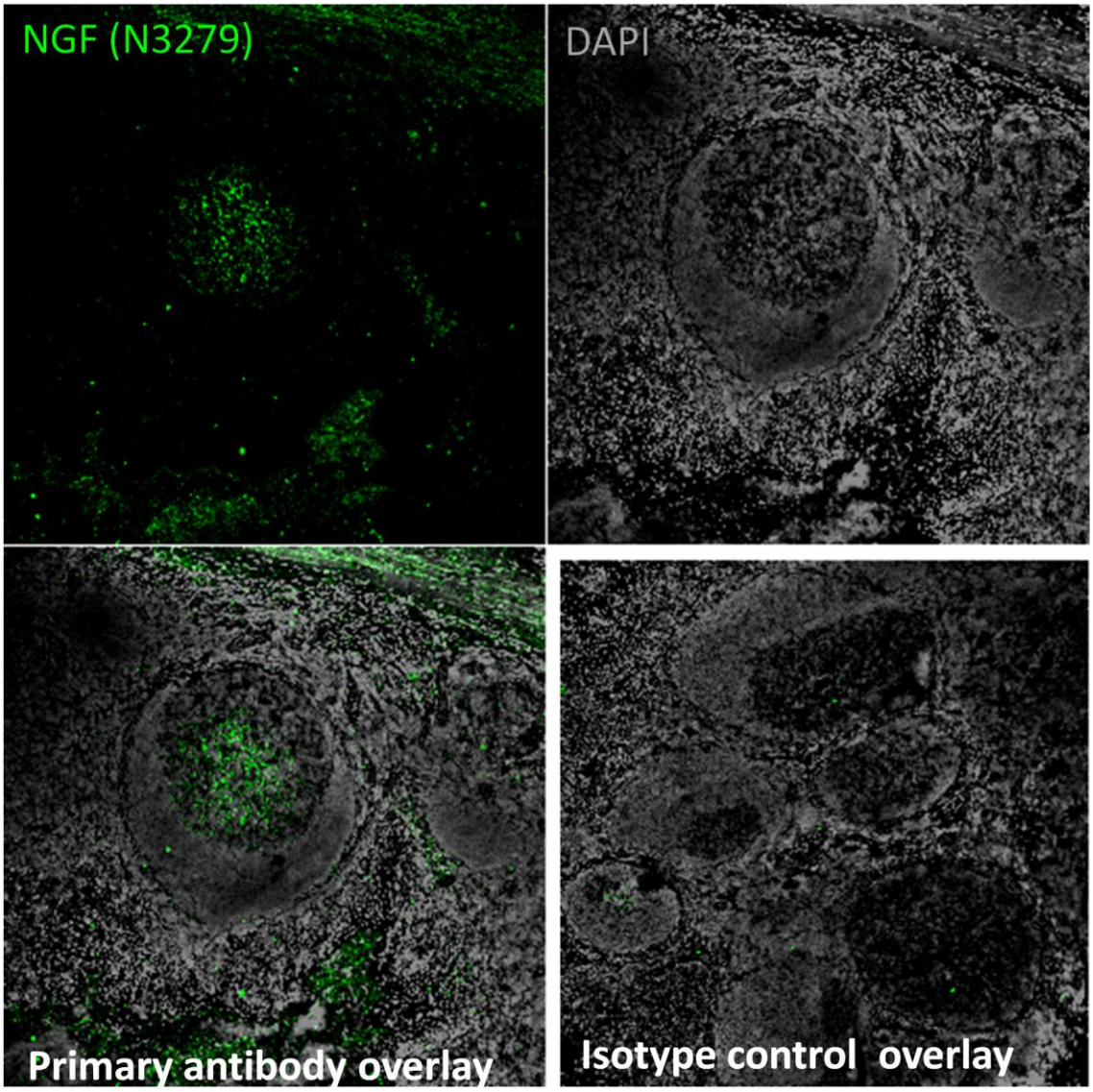

Figure 6.8: Immunohistochemical staining for NGF in human tonsil germinal centres
Cryogenically frozen human tonsil tissue sections were stained using the primary antibody NGF (N3279) detected by the Alexa Fluor 488 secondary antibody. Cellular nuclei were detected by Hoechst bis-benzimide dye 33342 (Hoechst). The overlay image for NGF and Hoechst stain is shown and compared to the overlay image observed in isotype control and Hoechst stained cells. Images are displayed at x10 magnification is displayed.

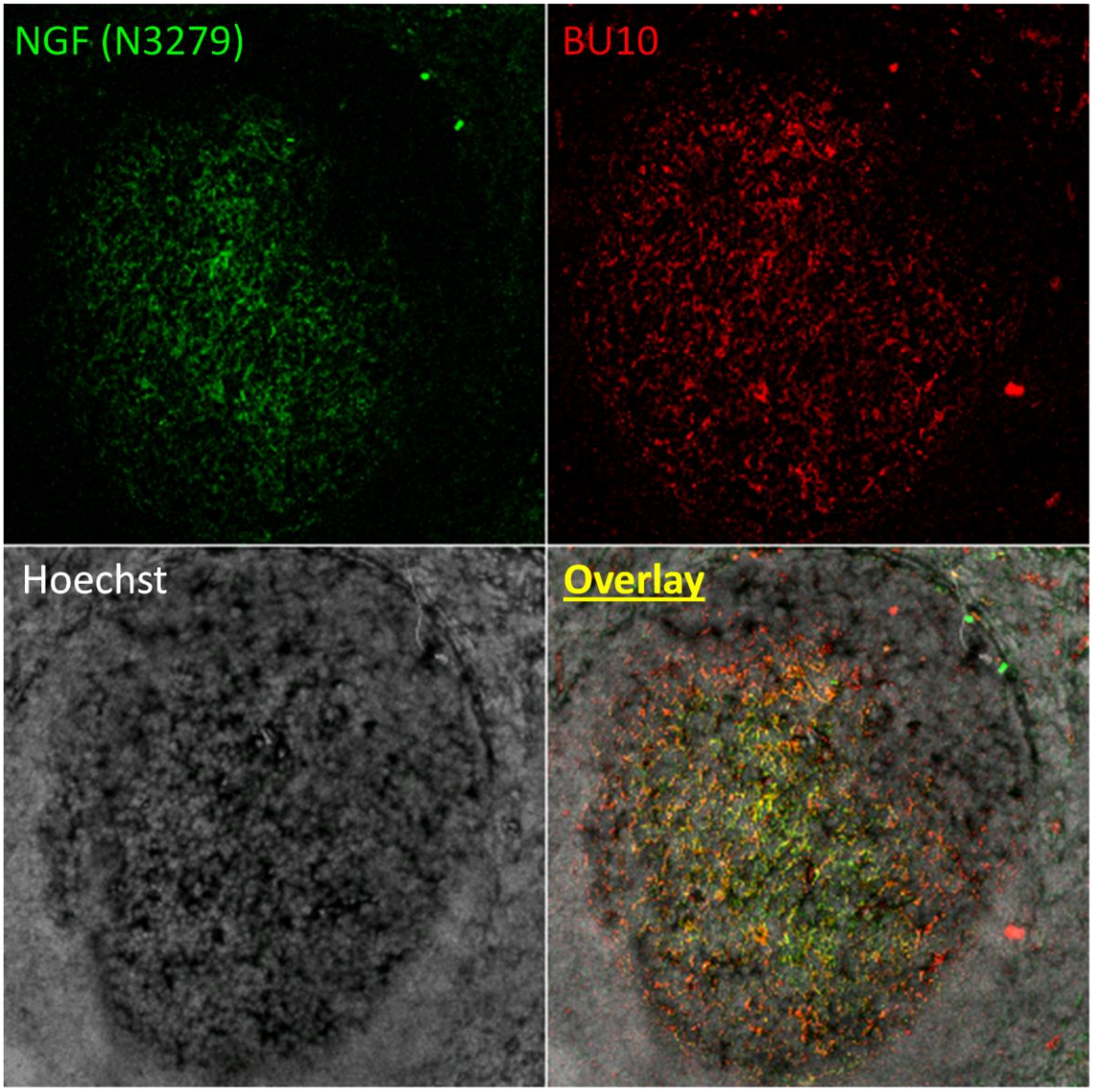

Figure 6.9.1: Immunohistochemical co-staining for NGF and BU10 in human tonsil germinal centres

Cryogenically frozen human tonsil tissue sections were co-stained using the primary antibodies NGF (N3279) and BU10. Cellular nuclei were detected by Hoechst bis-benzimide dye 33342 (Hoechst). To detect NGF primary antibody, Alexa Fluor 488 (green) secondary antibody was used and to detect BU10 primary antibody, Alexa Fluor 633 (red) secondary antibody was added. The overlay image for NGF, BU10 and Hoechst stain is shown. Co-staining overlap between NGF and BU10 is observed in yellow coloured cells. Images are displayed at x10 magnification is displayed.

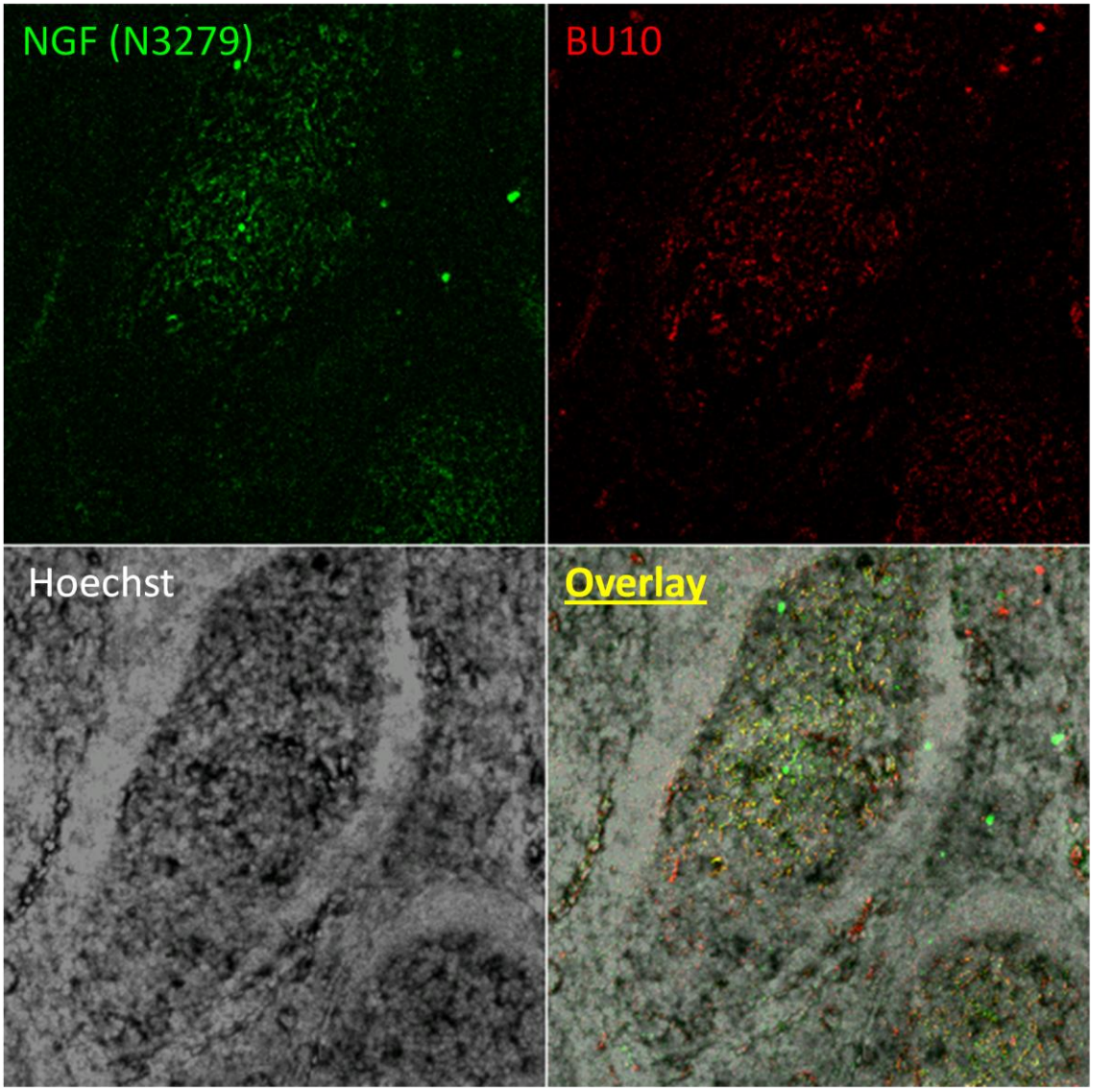

Figure 6.9.2: Immunohistochemical co-staining for NGF and BU10 in human tonsil germinal centres

Cryogenically frozen human tonsil tissue sections were co-stained using the primary antibodies NGF (N3279) and BU10. Cellular nuclei were detected by Hoechst bis-benzimide dye 33342 (Hoechst). To detect NGF primary antibody, Alexa Fluor 488 (green) secondary antibody was used and to detect BU10 primary antibody, Alexa Fluor 633 (red) secondary antibody was added. The overlay image for NGF, BU10 and Hoechst stain is shown. Co-staining overlap between NGF and BU10 is observed in yellow coloured cells. Images are displayed at x10 magnification is displayed.

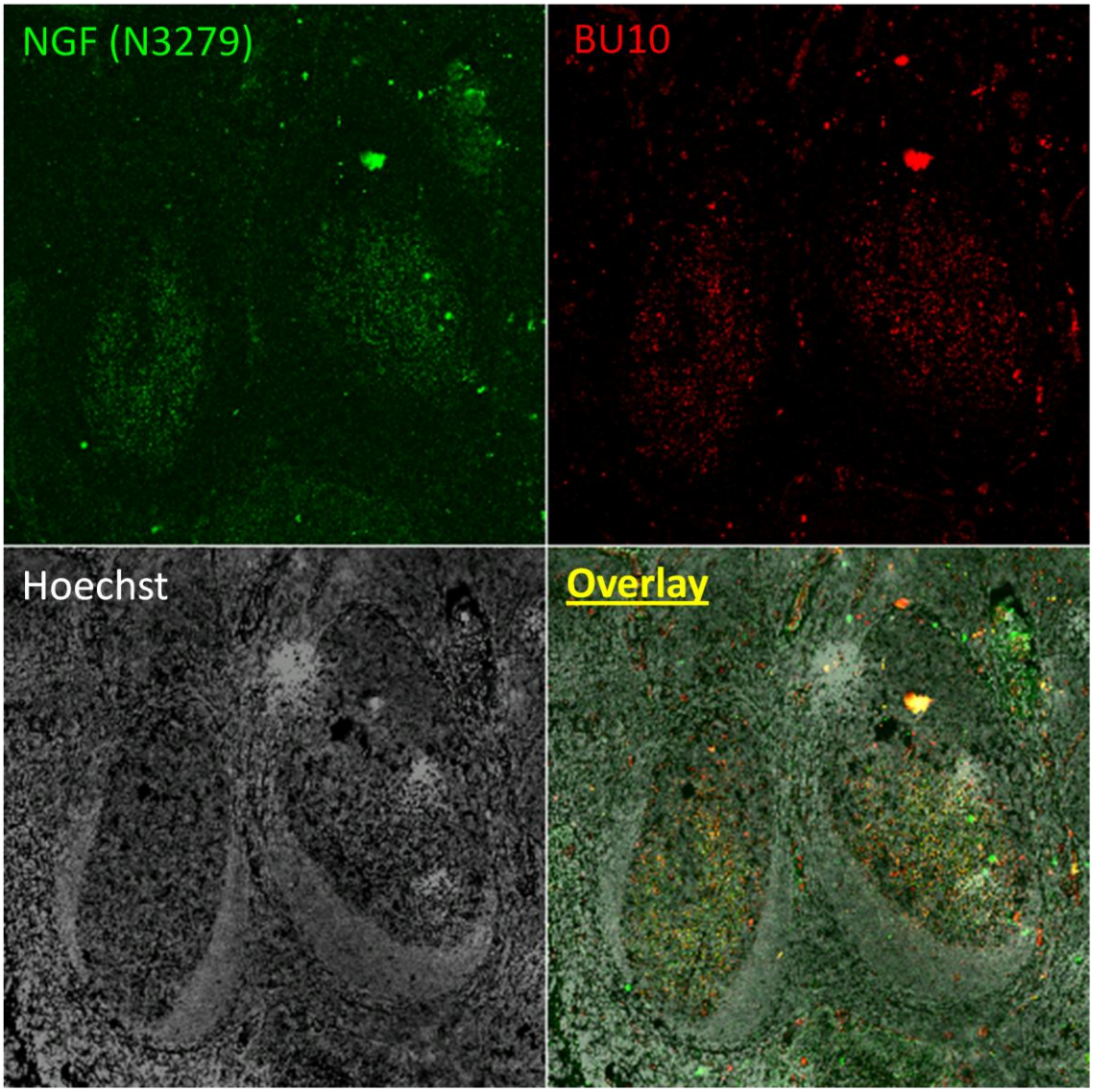

Figure 6.9.3: Immunohistochemical co-staining for NGF and BU10 in human tonsil germinal centres

Cryogenically frozen human tonsil tissue sections were co-stained using the primary antibodies NGF (N3279) and BU10. Cellular nuclei were detected by Hoechst bis-benzimide dye 33342 (Hoechst). To detect NGF primary antibody, Alexa Fluor 488 (green) secondary antibody was used and to detect BU10 primary antibody, Alexa Fluor 633 (red) secondary antibody was added. The overlay image for NGF, BU10 and Hoechst stain is shown. Co-staining overlap between NGF and BU10 is observed in yellow coloured cells. Images are displayed at x10 magnification is displayed.

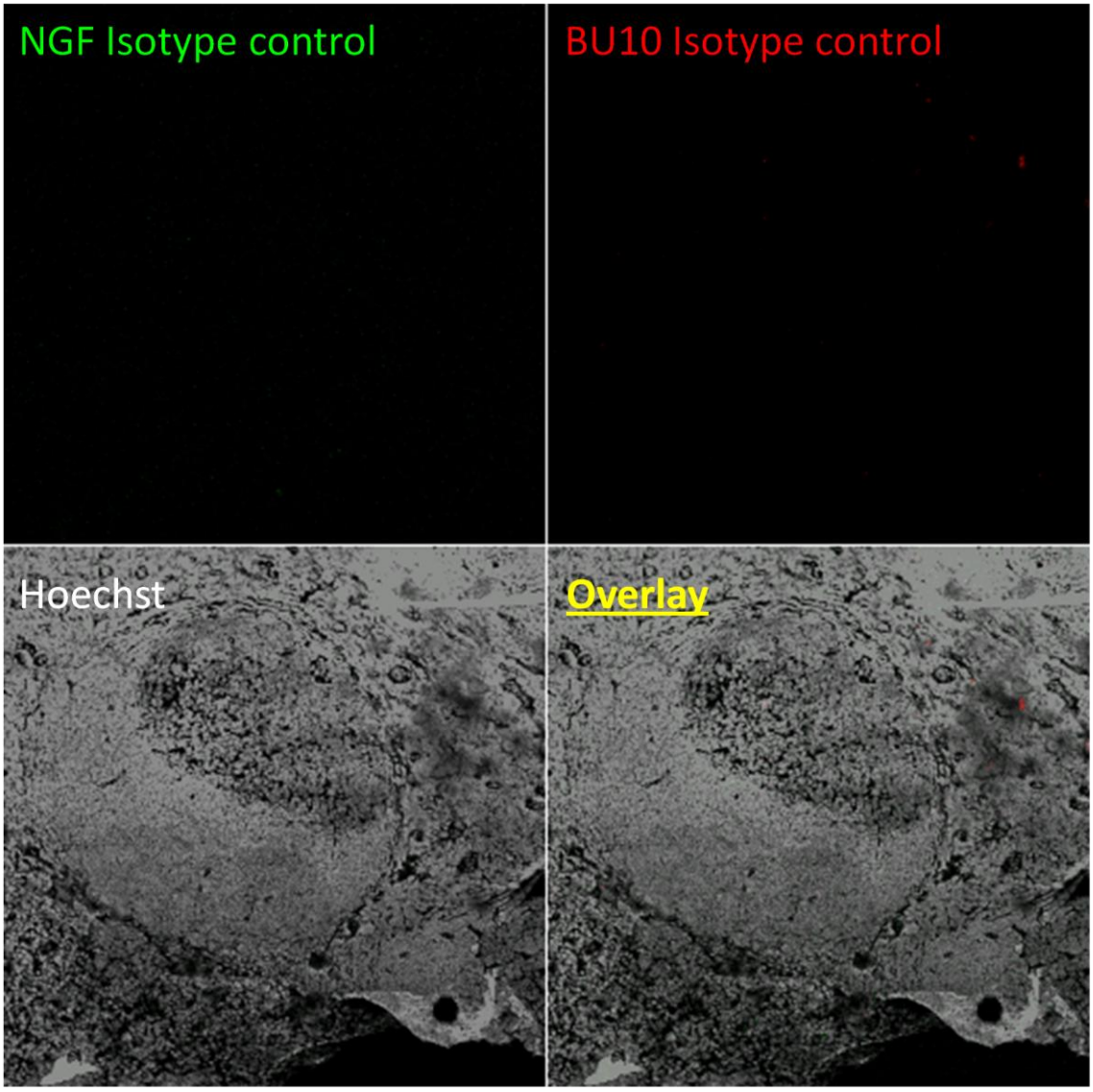

Figure 6.9.4: Immunohistochemical co-staining for NGF and BU10 in human tonsil germinal centres – isotype control

Cryogenically frozen human tonsil tissue sections were co-stained using the isotype controls for the primary antibodies NGF (N3279) and BU10. Cellular nuclei were detected by Hoechst bis-benzimide dye 33342 (Hoechst). Alexa Fluor 488 (green) and Alexa Fluor 633 (red) were the secondary antibodies used to detect primary antibody stainning. Images are displayed at x10 magnification is displayed.

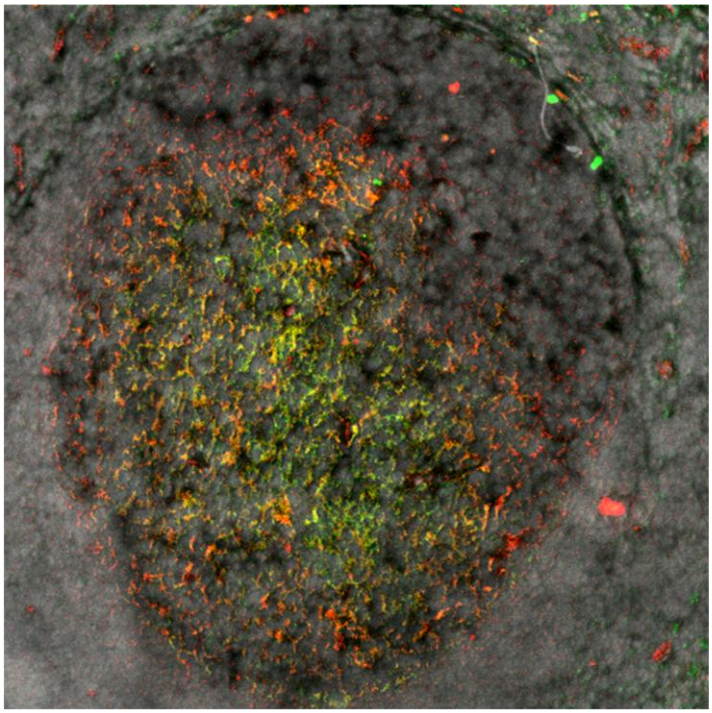

Figure 6.9.5a

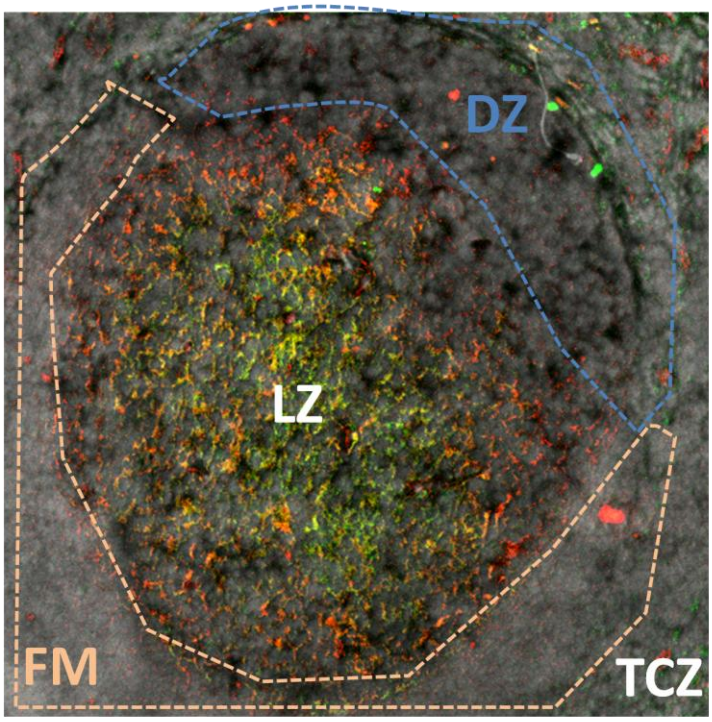

Figure 6.9.5b

Figure 6.9.5: Immunohistochemical co-staining for NGF and BU10 in human tonsil germinal centres – annotated GC zones

An overlay image for NGF, BU10 and Hoechst nuclear stain (figure 6.9.5a). Different zones within the germinal centre are demonstrated (figure 6.9.5b), where FM is the follicular matel, LZ is the light zone, DZ is the dark zone and TCZ is the T cell zone. The Images are displayed at x10 magnification is displayed.

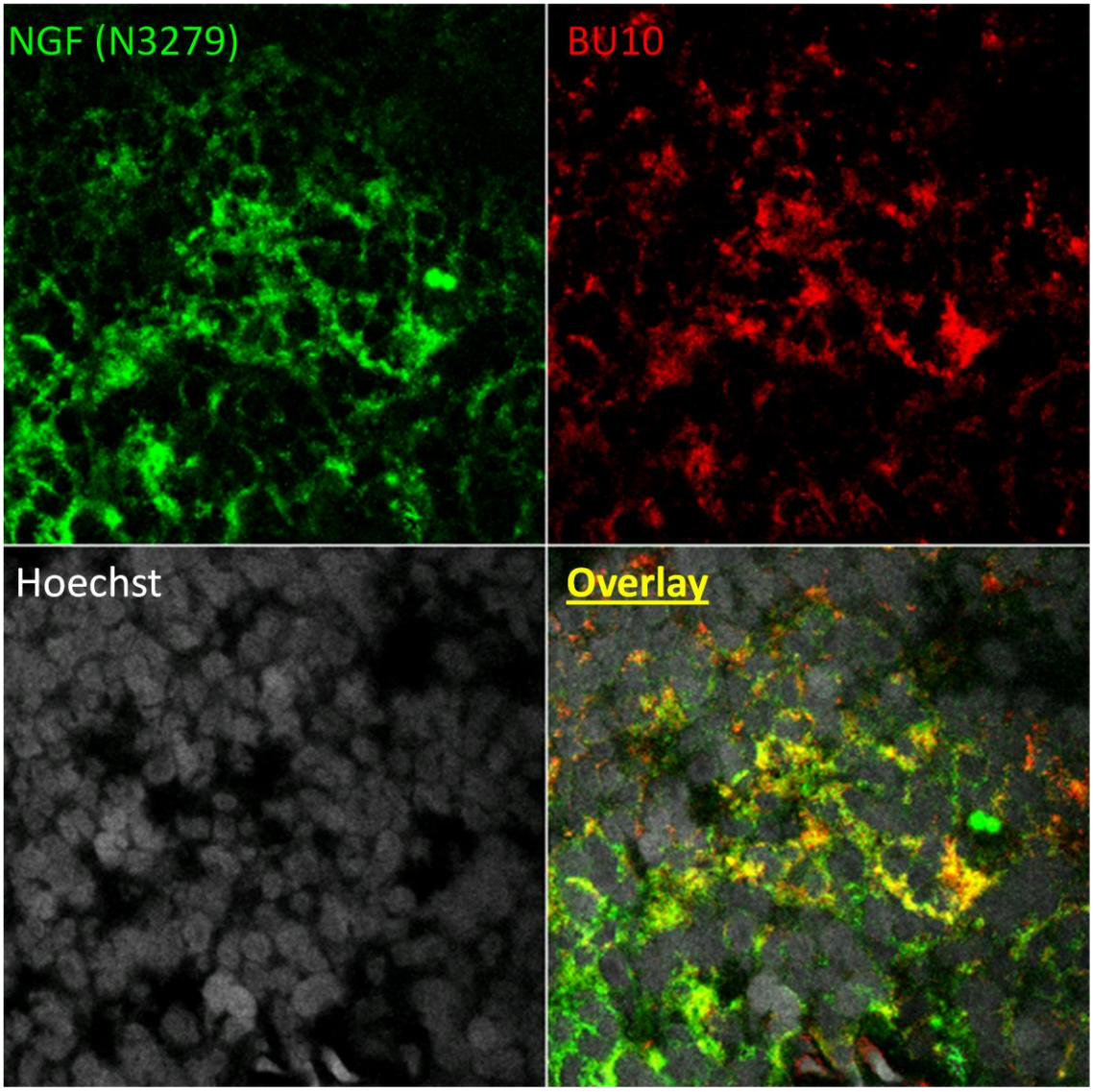

Figure 6.9.6: Immunohistochemical co-staining for NGF and BU10 in human tonsil germinal centres – high magnification

Cryogenically frozen human tonsil tissue sections were co-stained using the primary antibodies NGF (N3279) and BU10. Cellular nuclei were detected by Hoechst bis-benzimide dye 33342 (Hoechst). To detect NGF primary antibody, Alexa Fluor 488 (green) secondary antibody was used and to detect BU10 primary antibody, Alexa Fluor 633 (red) secondary antibody was added. The overlay image for NGF, BU10 and Hoechst stain is shown. Co-staining overlap between NGF and BU10 is observed in yellow coloured cells. Images are displayed at x40 magnification is displayed.

6. Discussion

From the array data, amongst the genes that were down regulated upon NGF treatment in germinal centre B cells, six small nucleolar RNA genes were determined, two of which are also known as small nuclear ribonucleoproteins (snRNPs). snRNPs guide nucleotide modifications within ribosomal RNAs or spliceosomal RNAs and are involved in RNA processing which associate with coiled bodies within neuronal cells (Raska, Ochs et al. 1990; Huttenhofer, Brosius et al. 2002). Coiled bodies are components within nuclear bodies which frequently associate with the nucleous in neuronal cells (Andrade, Tan et al. 1993). Using PC12s as a model for neuronal cell differentiation, snRNPs remained associated with the coiled bodies during NGF induced differentiation in neurones (Janevski, Park et al. 1997). The association between coiled bodies and nucleoli appears to be a feature common to neuronal cells and may represent a nuclear organization associated with neuronal differentiation. The effects on snRNPs in B cells treated with NGF however are unknown.

As for the centrosomal protein, which is a component of the centrosome has been associated with cell shape. By down regulating gene expression of Cep170 by siRNA duplex oligonucleotide, transfected HeLa cells changed from a typical epithelial shape, to a more fibroblastic, elongated appearance whereas, U2OS cells depleted of Cep170 showed an apparent increase in size (Guarguaglini, Duncan et al. 2005). As discussed in chapter 5, NGF induced F-actin rearrangement in EBV negative Burkitt's lymphoma B cells; therefore NGF may alter cytoskeletal arrangements in B cells which may involve the down regulation of Cep170.

Zinc finger protein 443 and the Zinc finger protein 724 pseudogene are also down regulated upon NGF addition in germinal centre B cells. The Schwann factor cell-1 protein (SC-1) belongs to the retinoblastoma interacting zinc finger family of transcription factors, which contains six zinc finger domains and interacts with the cytoplasmic domain on $p75^{NTR}$ (Chittka and Chao 1999).

Nuclear translocation from the cell cytoplasm is observed in cells expressing both SC-1 and $p75^{NTR}$ upon NGF treatment, however the co-expression of TrkA inhibits this translocation (Chittka and

Chao 1999). SC-1 also behaves as a transcriptional repressor upon NGF treatment within cells transfected with both SC-1 and either $p75^{NTR}$ or TrkA.

The expression of $p75^{NTR}$ has previously been linked to cell cycle arrest in sympathoadrenal cells (Verdi, Birren et al. 1994). Since TrkA expression can regulate cellular transformation or promote mitogenesis, restricting nuclear localisation of SC-1 may prevent growth arrest signalling from $p75^{NTR}$ (Chittka, Arevalo et al. 2004).

High $p75^{NTR}$ expression levels in germinal centre B cell treated with NGF may down regulate zinc finger proteins to inhibit the transcriptional repression by SC-1 and may inhibit cell cycle arrest via $p75^{NTR}$. The down regulation of SC-1 may be important in these germinal centre B cells considering low to undetectable levels are TrkA protein are observed.

Human recombinant NGF has also been observed to induce gene up regulation in germinal centre B cells. One of which includes the Hemoglobin subunit gamma-1. NGF is able to induce angiogenesis, increase hemoglobin concentration in a dose-dependent manner and promote wound healing via TrkA and $p75^{NTR}$ (Calza, Giardino et al. 2001; Emanueli, Salis et al. 2002; Graiani, Emanueli et al. 2004; Park, Kwak et al. 2007). However the reason why HBG1 and HBG2 are up regulated in NGF treated germinal centre B cells is unknown.

NGF is also liked to the pathogenesis of various skin conditions such as psoriasis by influencing inflammatory responses within the subcutaneous tissue (Raychaudhuri and Raychaudhuri 2009). Mutating the SPINK6 gene can result in Netherton syndrome, a genetic skin disorder characterised by the appearance of dry, thickened, scaly or flaky skin (Chavanas, Bodemer et al. 2000). However the implications as to why NGF up regulates SPIUNK5 in germinal centre b cells is currently unknown.

The S100 proteins are characterized by the presence of two Calcium binding sites of the EF-hand type and have been implicated in several roles which include interacting with effector proteins within cells, and in turn regulate enzyme activities (Donato 1986; Donato 1999). Examples of these activities include, cytoskeletal arrangement, cell growth, differentiation and Calcium homeostasis (Donato 2001; Donato 2003).

Seven days after the addition of NGF to PC12 cells, neurite projections are observed, however the withdrawal of NGF within the media initiates cellular apoptosis, which is exacerbated upon the treatment of S100 protein (Fulle, Mariggio et al. 1997). These apoptotic effects can be blocked by the readmission of NGF. The S100 genes, S100A1, S100B, and S100A4 have been reported in lymphocytes but their role has not been studied (Singh and Cheng 1996).

As for the S100A8 gene, its expression is up regulated in germinal centre B cells treated with NGF which may regulate certain enzymatic, calcium dependent pathways however these signalling outcomes are unknown.

Originally, glycoprotein M6a was thought to be expressed exclusively by neurons in the central nervous system and the non-neuronal peripheral tissues such as the apical membranes of polarized epithelial cells within the choroid plexus and proximal renal tubules (Yan, Lagenaur et al. 1993; Yan, Narayanan et al. 1996).

Interestingly, PC12 cells transfected with rat M6a cDNA show an increase in calcium influx via protein kinase C upon NGF treatment enabling neuronal differentiation (Mukobata, Hibino et al. 2002). The up regulation of GPM6A gene in NGF treated germinal centre B cells

may increase intracellular calcium for B cell differentiation; however there is currently no literature on these signalling effects.

The DPPA2 gene, on the other hand, encodes for the developmental pluripotency associated-2 protein which has a SAP putative DNA binding motif often found in proteins involved in chromosomal organization and various aspects of RNA biology (Aravind and Koonin 2000). Its gene expression is thought to be restricted in pluripotent cells and the developing germ line, however germinal centre B cells treated with NGF show an up regulation of DPPA2 (Maldonado-Saldivia, van den Bergen et al. 2007).

The R-spondin genes (Rspo1, Rspo2, Rspo3 and Rspo4) encode a novel family of secreted proteins in vertebrates that activate Wnt/β-catenin signalling and interact with LDL receptor-related protein 6 (Kazanskaya, Glinka et al. 2004). It is known that NGF can promote axonal branching and target innervation in developing sympathetic targets by regulating the neuronal expression of Wnt5a. Wnt/β-catenin signalling promotes B cell proliferation via the lymphocyte enhancer factor-1, hence NGF may induce cell proliferation by the up regulation of RSPO3 gene in germinal centre B cells.

Other genes that were observed to be either up regulated or down regulated upon NGF stimulation within germinal centre B cells are either uncharacterised for their function or currently unknown to have any links with B cells and or NGF stimulation. However based on the microarray data analysis NGF stimulation may affect RNA processing, induce cytoskeletal re-arrangement, inhibit cell cycle arrest, promote calcium influx, chromosomal

organisation re-arrangement and regulate cell proliferation in germinal centre B cells. **7.**

Thesis discussion

Based on the results obtained from this thesis it can be concluded that Burkitt's lymphoma B cell lines displaying varying EBV latency phenotypes do express functional neurotrophic factors and their receptors that can signal for either cell survival and or cell proliferation. Hence, inhibiting neurotrophic factors signalling can be considered as a novel axis in suppressing tumour growth in Burkitt's lymphoma.

The EBV latency III phenotype has been observed in lymphoid tissue during infectious mononucleosis primary infection (Anagnostopoulos, Hummel et al. 1995; Joseph, Babcock et al. 2000; Kurth, Hansmann et al. 2003). Hence, since the latency III phenotype is rarely seen *in vivo* due to immune recognition, to discover new therapeutics against Burkitt's lymphoma, focus should be based in targeting B cells displaying a latency I EBV phenotype.

Neurotrophins are classically defined at trophic factors for neuronal cells. With increasing evidence in the expression of functional neurotrophins acting as trophic factors within cells of the immune system, neurotrophic factors can be re-defined as immunotrophic factors. However specific roles of immunotrophins in the development of haematopoietic cells are still a mystery.

Neurotrophins have previously been applied as therapeutics for treatment of varying conditions such as Alzheimer's disease, depression, asthma and Charcot-Marie-Tooth disease.

Both NGF and BDNF levels were shown to be reduced in Alzheimer's disease hippocampus and temporal cortex (Goedert, Fine et al. 1989; Connor, Young et al. 1997). Phase I clinical trial reported by Tuszynski M.H. *et al*, were reported to have successfully stimulated cholinergic function by implanting autologous fibroblasts that secreted NGF within the forebrain (Tuszynski, Thal et al. 2005).

Lower serum BDNF protein levels have been reported in patients with depressive disorders, whereas increased serum BDNF concentrations have been observed after treatment with an antidepressant (Karege, Perret et al. 2002; Shimizu, Hashimoto et al. 2003). Antidepressants such as Mirtazapine, which antagonises the alpha-2 adrenergic receptor was found to increase BDNF mRNA levels in rat hippocampus and cerebral cortex compared to the well known and widely used antidepressant, imipramine (Rogoz, Skuza et al. 2005)

Patients suffering from allergic diseases, in particular asthma, show increased levels of NGF in their serum (Bonini, Lambiase et al. 1996). As shown by Braun *et al.* nasal application of anti-NGF to ovalbumin-sensitized mice reduces IL-4 levels and prevents development of airway hyperreactivity induced by a specific allergen challenge (Braun, Appel et al. 1998).

As for Charcot-Marie-Tooth disease patients, NT-3 therapy can enhance nerve regeneration and in other genetic diseases involving peripheral myelin protein-22 (Pleasure and Chance 2005).

As for currently available Burkitt's lymphoma therapeutics, chemotherapy is still the main type of treatment used. However the cytotoxic drugs applied, which include cyclophosphamide, vincristine and doxorubicin, produce many side effects are not cost effective. Rituximab is an anti-CD20 monoclonal antibody, when combined with cyclophosphamide, doxorubicin, vincristine and prednisolone cytotixic drugs is used as treatment for diffuse large B-cell lymphoma and Burkitt's lymphoma (Golay, Zaffaroni et al. 2000). The down side of these therapeutics are the side effects and the cost of manufacture. Since Burkitt's lymphoma prevalence is the highest in equatorial Africa,

many individuals are unable to pay for and access these prophylaxes. However, with increasing neurotrophic factor research, it is possible that reducing Burkitt's lymphoma tumour growth can be achieved with the use of neurotrophic factors associated prophylaxes.

Despite the achievements gained from this thesis, there is still much work to be completed to gain better understanding of EBV and its relationship with B lymphocytes and how to compact neurotrophic factor exploitation in B cell lymphomas.

8. Bibliography

Agematsu, K., S. Hokibara, et al. (2000). "CD27: a memory B-cell marker." Immunol Today **21**(5): 204-6.

Agerman, K., C. Baudet, et al. (2000). "Attenuation of a caspase-3 dependent cell death in NT4- and p75-deficient embryonic sensory neurons." Mol Cell Neurosci **16**(3): 258-68.

Alderson, R. F., R. Curtis, et al. (2000). "Truncated TrkB mediates the endocytosis and release of BDNF and neurotrophin-4/5 by rat astrocytes and schwann cells in vitro." Brain Res **871**(2): 210-22.

Alexander, D., J. Goris, et al. (1989). "Dephosphorylation of the human T lymphocyte CD3 antigen." Eur J Biochem **181**(1): 55-65.

Allendoerfer, K. L., R. J. Cabelli, et al. (1994). "Regulation of neurotrophin receptors during the maturation of the mammalian visual system." J Neurosci **14**(3 Pt 2): 1795-811.

Anagnostopoulos, I., M. Hummel, et al. (1995). "Morphology, immunophenotype, and distribution of latently and/or productively Epstein-Barr virus-infected cells in acute infectious mononucleosis: implications for the interindividual infection route of Epstein-Barr virus." Blood **85**(3): 744-50.

Andrade, L. E., E. M. Tan, et al. (1993). "Immunocytochemical analysis of the coiled body in the cell cycle and during cell proliferation." Proc Natl Acad Sci U S A **90**(5): 1947-51.

Anton, E. S., G. Weskamp, et al. (1994). "Nerve growth factor and its low-affinity receptor promote Schwann cell migration." Proc Natl Acad Sci U S A **91**(7): 2795-9.

Aravind, L. and E. V. Koonin (2000). "SAP - a putative DNA-binding motif involved in chromosomal organization." Trends Biochem Sci **25**(3): 112-4.

Armanini, M. P., S. B. McMahon, et al. (1995). "Truncated and catalytic isoforms of trkB are co-expressed in neurons of rat and mouse CNS." Eur J Neurosci **7**(6): 1403-9.

Babcock, G. J., L. L. Decker, et al. (1998). "EBV persistence in memory B cells in vivo." Immunity **9**(3): 395-404.

Banfield, M. J., R. L. Naylor, et al. (2001). "Specificity in Trk receptor:neurotrophin interactions: the crystal structure of TrkB-d5 in complex with neurotrophin-4/5." Structure **9**(12): 1191-9.

Barde, Y. A., D. Edgar, et al. (1982). "Purification of a new neurotrophic factor from mammalian brain." Embo J **1**(5): 549-53.

Barde, Y. A., R. M. Lindsay, et al. (1978). "New factor released by cultured glioma cells supporting survival and growth of sensory neurones." Nature **274**(5673): 818.
Barouch, R., E. Appel, et al. (2000). "Differential regulation of neurotrophin expression by mitogens and neurotransmitters in mouse lymphocytes." J Neuroimmunol **103**(2): 112-21.
Barrett, G. L. and P. F. Bartlett (1994). "The p75 nerve growth factor receptor mediates survival or death depending on the stage of sensory neuron development." Proc Natl Acad Sci U S A **91**(14): 6501-5.
Bartkowska, K., A. Paquin, et al. (2007). "Trk signaling regulates neural precursor cell proliferation and differentiation during cortical development." Development **134**(24): 4369-80.
Benedetti, M., A. Levi, et al. (1993). "Differential expression of nerve growth factor receptors leads to altered binding affinity and neurotrophin responsiveness." Proc Natl Acad Sci U S A **90**(16): 7859-63.
Berek, C. and M. Ziegner (1993). "The maturation of the immune response." Immunol Today **14**(8): 400-4.
Berg, M. M., D. W. Sternberg, et al. (1991). "The low-affinity p75 nerve growth factor (NGF) receptor mediates NGF-induced tyrosine phosphorylation." Proc Natl Acad Sci U S A **88**(16): 7106-10.
Berg, M. M., D. W. Sternberg, et al. (1992). "K-252a inhibits nerve growth factor-induced trk proto-oncogene tyrosine phosphorylation and kinase activity." J Biol Chem **267**(1): 13-6.
Bergquist, J., E. Josefsson, et al. (1997). "Measurements of catecholamine-mediated apoptosis of immunocompetent cells by capillary electrophoresis." Electrophoresis **18**(10): 1760-6.
Berkemeier, L. R., J. W. Winslow, et al. (1991). "Neurotrophin-5: a novel neurotrophic factor that activates trk and trkB." Neuron **7**(5): 857-66.
Bernard, A., V. Gay-Bellile, et al. (1984). "A novel human leukocyte differentiation antigen: monoclonal antibody anti-D44 defines a 28 Kd molecule present on immature hematologic cells and a subpopulation of mature T cells." J Immunol **132**(5): 2338-44.
Bibel, M., E. Hoppe, et al. (1999). "Biochemical and functional interactions between the neurotrophin receptors trk and p75NTR." Embo J **18**(3): 616-22.
Biffo, S., N. Offenhauser, et al. (1995). "Selective binding and internalisation by truncated receptors restrict the availability of BDNF during development." Development **121**(8): 2461-70.
Bio-Rad (2006). Bio-Rad Protein Assay. http://www.bio-rad.com/LifeScience/pdf/Bulletin_9004.pdf.
Blalock, J. E. (1984). "The immune system as a sensory organ." J Immunol **132**(3): 1067-70.
Bonini, S., A. Lambiase, et al. (1996). "Circulating nerve growth factor levels are increased in humans with allergic diseases and asthma." Proc Natl Acad Sci U S A **93**(20): 10955-60.
Boutilier, J., C. Ceni, et al. (2008). "Proneurotrophins require endocytosis and intracellular proteolysis to induce TrkA activation." J Biol Chem **283**(19): 12709-16.
Bracci-Laudiero, L., L. Aloe, et al. (2005). "Endogenous NGF regulates CGRP expression in human monocytes, and affects HLA-DR and CD86 expression and IL-10 production." Blood **106**(10): 3507-14.
Bradford, M. M. (1976). "A rapid and sensitive method for the quantitation of microgram quantities of protein utilizing the principle of protein-dye binding." Anal Biochem **72**: 248-54.
Bratke, K., L. Maruschke, et al. (2007). "A role for the neurotrophin receptor TrkB on maturing dendritic cells." J Neuroimmunol **189**(1-2): 88-94.
Braun, A., E. Appel, et al. (1998). "Role of nerve growth factor in a mouse model of allergic airway inflammation and asthma." Eur J Immunol **28**(10): 3240-51.
Briere, F., C. Servet-Delprat, et al. (1994). "Human interleukin 10 induces naive surface immunoglobulin D+ (sIgD+) B cells to secrete IgG1 and IgG3." J Exp Med **179**(2): 757-62.
Briske-Anderson, M. J., J. W. Finley, et al. (1997). "The influence of culture time and passage number on the morphological and physiological development of Caco-2 cells." Proc Soc Exp Biol Med **214**(3): 248-57.
Brodie, C. and E. W. Gelfand (1992). "Functional nerve growth factor receptors on human B lymphocytes. Interaction with IL-2." J Immunol **148**(11): 3492-7.

Bronfman, F. C. and M. Fainzilber (2004). "Multi-tasking by the p75 neurotrophin receptor: sortilin things out?" EMBO Rep **5**(9): 867-71.
Bruni, A., E. Bigon, et al. (1982). "Interaction between nerve growth factor and lysophosphatidylserine on rat peritoneal mast cells." FEBS Lett **138**(2): 190-2.
Burkitt, D. (1958). "A sarcoma involving the jaws in African children." Br J Surg **46**(197): 218-23.
Burkitt, D. (1962). "A lymphoma syndrome in African children." Ann R Coll Surg Engl **30**: 211-9.
Burkitt, D. and G. T. O'Conor (1961). "Malignant lymphoma in African children. I. A clinical syndrome." Cancer **14**: 258-69.
Butcher, E. C., R. V. Rouse, et al. (1982). "Surface phenotype of Peyer's patch germinal center cells: implications for the role of germinal centers in B cell differentiation." J Immunol **129**(6): 2698-707.
Caldwell, R. G., J. B. Wilson, et al. (1998). "Epstein-Barr virus LMP2A drives B cell development and survival in the absence of normal B cell receptor signals." Immunity **9**(3): 405-11.
Calza, L., L. Giardino, et al. (2001). "Nerve growth factor control of neuronal expression of angiogenetic and vasoactive factors." Proc Natl Acad Sci U S A **98**(7): 4160-5.
Carpenter, G. (1987). "Receptors for epidermal growth factor and other polypeptide mitogens." Annu Rev Biochem **56**: 881-914.
Carson, A. R., J. Cheung, et al. (2006). "Duplication and relocation of the functional DPY19L2 gene within low copy repeats." BMC Genomics **7**: 45.
Casaccia-Bonnefil, P., B. D. Carter, et al. (1996). "Death of oligodendrocytes mediated by the interaction of nerve growth factor with its receptor p75." Nature **383**(6602): 716-9.
Casademunt, E., B. D. Carter, et al. (1999). "The zinc finger protein NRIF interacts with the neurotrophin receptor p75(NTR) and participates in programmed cell death." Embo J **18**(21): 6050-61.
Chai, N. N., H. Zhou, et al. (1998). "Structure and organization of the RBMY genes on the human Y chromosome: transposition and amplification of an ancestral autosomal hnRNPG gene." Genomics **49**(2): 283-9.
Chavanas, S., C. Bodemer, et al. (2000). "Mutations in SPINK5, encoding a serine protease inhibitor, cause Netherton syndrome." Nat Genet **25**(2): 141-2.
Chevalier, S., V. Praloran, et al. (1994). "Expression and functionality of the trkA proto-oncogene product/NGF receptor in undifferentiated hematopoietic cells." Blood **83**(6): 1479-85.
Chin, L. S., S. F. Murray, et al. (1999). "K252a induces cell cycle arrest and apoptosis by inhibiting Cdc2 and Cdc25c." Cancer Invest **17**(6): 391-5.
Chittka, A., J. C. Arevalo, et al. (2004). "The p75NTR-interacting protein SC1 inhibits cell cycle progression by transcriptional repression of cyclin E." J Cell Biol **164**(7): 985-96.
Chittka, A. and M. V. Chao (1999). "Identification of a zinc finger protein whose subcellular distribution is regulated by serum and nerve growth factor." Proc Natl Acad Sci U S A **96**(19): 10705-10.
Choe, J., L. Li, et al. (2000). "Distinct role of follicular dendritic cells and T cells in the proliferation, differentiation, and apoptosis of a centroblast cell line, L3055." J Immunol **164**(1): 56-63.
Chun, L. L. and P. H. Patterson (1977). "Role of nerve growth factor in the development of rat sympathetic neurons in vitro. III. Effect on acetylcholine production." J Cell Biol **75**(3): 712-8.
Citron, M., D. Westaway, et al. (1997). "Mutant presenilins of Alzheimer's disease increase production of 42-residue amyloid beta-protein in both transfected cells and transgenic mice." Nat Med **3**(1): 67-72.
Clark, E. A., K. H. Grabstein, et al. (1992). "Cultured human follicular dendritic cells. Growth characteristics and interactions with B lymphocytes." J Immunol **148**(11): 3327-35.
Clarke, P. A., M. Schwemmle, et al. (1991). "Binding of Epstein-Barr virus small RNA EBER-1 to the double-stranded RNA-activated protein kinase DAI." Nucleic Acids Res **19**(2): 243-8.

Clary, D. O. and L. F. Reichardt (1994). "An alternatively spliced form of the nerve growth factor receptor TrkA confers an enhanced response to neurotrophin 3." Proc Natl Acad Sci U S A **91**(23): 11133-7.

Clift, R. A., D. H. Wright, et al. (1963). "Leukemia in Burkitt's Lymphoma." Blood **22**: 243-51.

Cohen, S. and R. Levi-Montalcini (1956). "A Nerve Growth-Stimulating Factor Isolated from Snake Venom." Proc Natl Acad Sci U S A **42**(9): 571-4.

Coico, R. F., B. S. Bhogal, et al. (1983). "Relationship of germinal centers in lymphoid tissue to immunologic memory. VI. Transfer of B cell memory with lymph node cells fractionated according to their receptors for peanut agglutinin." J Immunol **131**(5): 2254-7.

Connor, B., D. Young, et al. (1997). "Brain-derived neurotrophic factor is reduced in Alzheimer's disease." Brain Res Mol Brain Res **49**(1-2): 71-81.

Coppola, V., C. A. Barrick, et al. (2004). "Ablation of TrkA function in the immune system causes B cell abnormalities." Development **131**(20): 5185-95.

Cortazzo, M. H., E. S. Kassis, et al. (1996). "Nerve growth factor (NGF)-mediated protection of neural crest cells from antimitotic agent-induced apoptosis: the role of the low-affinity NGF receptor." J Neurosci **16**(12): 3895-9.

Cuatrecasas, P. (1971). "Insulin--receptor interactions in adipose tissue cells: direct measurement and properties." Proc Natl Acad Sci U S A **68**(6): 1264-8.

D'Onofrio, M., U. de Grazia, et al. (2000). "Expression of neurotrophin receptors in normal and malignant B lymphocytes." Eur Cytokine Netw **11**(2): 283-91.

De Simone, R., E. Ambrosini, et al. (2007). "NGF promotes microglial migration through the activation of its high affinity receptor: modulation by TGF-beta." J Neuroimmunol **190**(1-2): 53-60.

de Vries, A., C. van Rijnsoever, et al. (2001). "The role of sensory nerve endings in nerve growth factor-induced airway hyperresponsiveness to histamine in guinea-pigs." Br J Pharmacol **134**(4): 771-6.

DiStefano, P. S., D. M. Chelsea, et al. (1993). "Involvement of a metalloprotease in low-affinity nerve growth factor receptor truncation: inhibition of truncation in vitro and in vivo." J Neurosci **13**(6): 2405-14.

Dolle, J. P., A. Rezvan, et al. (2005). "Nerve growth factor-induced migration of endothelial cells." J Pharmacol Exp Ther **315**(3): 1220-7.

Donato, R. (1986). "S-100 proteins." Cell Calcium **7**(3): 123-45.

Donato, R. (1999). "Functional roles of S100 proteins, calcium-binding proteins of the EF-hand type." Biochim Biophys Acta **1450**(3): 191-231.

Donato, R. (2001). "S100: a multigenic family of calcium-modulated proteins of the EF-hand type with intracellular and extracellular functional roles." Int J Biochem Cell Biol **33**(7): 637-68.

Donato, R. (2003). "Intracellular and extracellular roles of S100 proteins." Microsc Res Tech **60**(6): 540-51.

Dracopoli, N. C., E. Rose, et al. (1988). "Two thyroid hormone regulated genes, the beta-subunits of nerve growth factor (NGFB) and thyroid stimulating hormone (TSHB), are located less than 310 kb apart in both human and mouse genomes." Genomics **3**(2): 161-7.

Eagle, H., V. I. Oyama, et al. (1956). "The growth response of mammalian cells in tissue culture to L-glutamine and L-glutamic acid." J Biol Chem **218**(2): 607-16.

Eaton, M. J. and S. R. Whittemore (1996). "Autocrine BDNF secretion enhances the survival and serotonergic differentiation of raphe neuronal precursor cells grafted into the adult rat CNS." Exp Neurol **140**(2): 105-14.

Ebina, Y., L. Ellis, et al. (1985). "The human insulin receptor cDNA: the structural basis for hormone-activated transmembrane signalling." Cell **40**(4): 747-58.

Edwards, R. H., M. J. Selby, et al. (1988). "Processing of the native nerve growth factor precursor to form biologically active nerve growth factor." J Biol Chem **263**(14): 6810-5.

Ehrhard, P. B., U. Ganter, et al. (1993). "Expression of functional trk protooncogene in human monocytes." Proc Natl Acad Sci U S A **90**(12): 5423-7.
Eide, F. F., E. R. Vining, et al. (1996). "Naturally occurring truncated trkB receptors have dominant inhibitory effects on brain-derived neurotrophic factor signaling." J Neurosci **16**(10): 3123-9.
Elizabeth R. Leight, B. S. (2000). "EBNA-1: a protein pivotal to latent infection by Epstein-Barr virus." Reviews in Medical Virology **10**(2): 83-100.
Elliott, L. H., S. E. Wilkinson, et al. (1990). "K252a is a potent and selective inhibitor of phosphorylase kinase." Biochem Biophys Res Commun **171**(1): 148-54.
Emanueli, C., M. B. Salis, et al. (2002). "Nerve growth factor promotes angiogenesis and arteriogenesis in ischemic hindlimbs." Circulation **106**(17): 2257-62.
English, J., G. Pearson, et al. (1999). "New insights into the control of MAP kinase pathways." Exp Cell Res **253**(1): 255-70.
Epstein, M. A., B. G. Achong, et al. (1964). "Virus Particles in Cultured Lymphoblasts from Burkitt's Lymphoma." Lancet **1**(7335): 702-3.
Epstein, M. A. and Y. M. Barr (1965). "Characteristics and Mode of Growth of Tissue Culture Strain (Eb1) of Human Lymphoblasts from Burkitt's Lymphoma." J Natl Cancer Inst **34**: 231-40.
Epstein, M. A., G. Henle, et al. (1965). "Morphological and Biological Studies on a Virus in Cultured Lymphoblasts from Burkitt's Lymphoma." J Exp Med **121**: 761-70.
Erikson, J., A. ar-Rushdi, et al. (1983). "Transcriptional activation of the translocated c-myc oncogene in burkitt lymphoma." Proc Natl Acad Sci U S A **80**(3): 820-4.
Ernfors, P., K. F. Lee, et al. (1994). "Lack of neurotrophin-3 leads to deficiencies in the peripheral nervous system and loss of limb proprioceptive afferents." Cell **77**(4): 503-12.
Fan, G., C. Egles, et al. (2000). "Knocking the NT4 gene into the BDNF locus rescues BDNF deficient mice and reveals distinct NT4 and BDNF activities." Nat Neurosci **3**(4): 350-7.
Farinas, I., K. R. Jones, et al. (1994). "Severe sensory and sympathetic deficits in mice lacking neurotrophin-3." Nature **369**(6482): 658-61.
Farrell, P. J., G. J. Allan, et al. (1991). "p53 is frequently mutated in Burkitt's lymphoma cell lines." Embo J **10**(10): 2879-87.
Farrell, P. J., D. T. Rowe, et al. (1989). "Epstein-Barr virus BZLF1 trans-activator specifically binds to a consensus AP-1 site and is related to c-fos." Embo J **8**(1): 127-32.
Fauchais, A. L., F. Lalloue, et al. (2008). "Role of endogenous brain-derived neurotrophic factor and sortilin in B cell survival." J Immunol **181**(5): 3027-38.
Fayard, B., S. Loeffler, et al. (2005). "The secreted brain-derived neurotrophic factor precursor pro-BDNF binds to TrkB and p75NTR but not to TrkA or TrkC." J Neurosci Res **80**(1): 18-28.
Fingeroth, J. D., J. J. Weis, et al. (1984). "Epstein-Barr virus receptor of human B lymphocytes is the C3d receptor CR2." Proc Natl Acad Sci U S A **81**(14): 4510-4.
Flemington, E. and S. H. Speck (1990). "Autoregulation of Epstein-Barr virus putative lytic switch gene BZLF1." J Virol **64**(3): 1227-32.
Flemington, E. and S. H. Speck (1990). "Epstein-Barr virus BZLF1 trans activator induces the promoter of a cellular cognate gene, c-fos." J Virol **64**(9): 4549-52.
Fliedner, T., M. Kesse, et al. (1964). "Cell Proliferation in Germinal Centers of the Rat Spleen." Ann N Y Acad Sci **113**: 578-94.
Foehr, E. D., X. Lin, et al. (2000). "NF-kappa B signaling promotes both cell survival and neurite process formation in nerve growth factor-stimulated PC12 cells." J Neurosci **20**(20): 7556-63.
Franklin, R. A., C. Brodie, et al. (1995). "Nerve growth factor induces activation of MAP-kinase and p90rsk in human B lymphocytes." J Immunol **154**(10): 4965-72.
Frazer, J. K., D. G. Jackson, et al. (2000). "Identification of centerin: a novel human germinal center B cell-restricted serpin." Eur J Immunol **30**(10): 3039-48.
Freedman, A. S., J. M. Munro, et al. (1990). "Adhesion of human B cells to germinal centers in vitro involves VLA-4 and INCAM-110." Science **249**(4972): 1030-3.

Fulle, S., M. A. Mariggio, et al. (1997). "Nerve growth factor inhibits apoptosis induced by S-100 binding in neuronal PC12 cells." Neuroscience **76**(1): 159-66.
Galardi, S., A. Fatica, et al. (2002). "Purified box C/D snoRNPs are able to reproduce site-specific 2'-O-methylation of target RNA in vitro." Mol Cell Biol **22**(19): 6663-8.
Gerdes, J., H. Stein, et al. (1983). "Human dendritic reticulum cells of lymphoid follicles: their antigenic profile and their identification as multinucleated giant cells." Virchows Arch B Cell Pathol Incl Mol Pathol **42**(2): 161-72.
Goedert, M., A. Fine, et al. (1989). "Nerve growth factor receptor mRNA distribution in human brain: normal levels in basal forebrain in Alzheimer's disease." Brain Res Mol Brain Res **5**(1): 1-7.
Golay, J., L. Zaffaroni, et al. (2000). "Biologic response of B lymphoma cells to anti-CD20 monoclonal antibody rituximab in vitro: CD55 and CD59 regulate complement-mediated cell lysis." Blood **95**(12): 3900-8.
Gorzer, I., H. G. M. Niesters, et al. (2006). "Characterization of Epstein-Barr virus Type I variants based on linked polymorphism among EBNA3A, -3B, and -3C genes." Virus Research **118**(1-2): 105-114.
Graiani, G., C. Emanueli, et al. (2004). "Nerve growth factor promotes reparative angiogenesis and inhibits endothelial apoptosis in cutaneous wounds of Type 1 diabetic mice." Diabetologia **47**(6): 1047-54.
Gray, D. (1988). "Recruitment of virgin B cells into an immune response is restricted to activation outside lymphoid follicles." Immunology **65**(1): 73-9.
Gray, D. and T. Leanderson (1990). "Expansion, selection and maintenance of memory B-cell clones." Curr Top Microbiol Immunol **159**: 1-17.
Greene, L. A., E. M. Shooter, et al. (1969). "Subunit interaction and enzymatic activity of mouse 7S nerve growth factor." Biochemistry **8**(9): 3735-41.
Gregory, C. D., T. Tursz, et al. (1987). "Identification of a subset of normal B cells with a Burkitt's lymphoma (BL)-like phenotype." J Immunol **139**(1): 313-8.
Gstraunthaler, G. (2003). "Alternatives to the use of fetal bovine serum: serum-free cell culture." Altex **20**(4): 275-81.
Guarguaglini, G., P. I. Duncan, et al. (2005). "The forkhead-associated domain protein Cep170 interacts with Polo-like kinase 1 and serves as a marker for mature centrioles." Mol Biol Cell **16**(3): 1095-107.
Guiton, M., F. J. Gunn-Moore, et al. (1994). "Identification of in vivo brain-derived neurotrophic factor-stimulated autophosphorylation sites on the TrkB receptor tyrosine kinase by site-directed mutagenesis." J Biol Chem **269**(48): 30370-7.
Haapasalo, A., E. Koponen, et al. (2001). "Truncated trkB.T1 is dominant negative inhibitor of trkB.TK+-mediated cell survival." Biochem Biophys Res Commun **280**(5): 1352-8.
Haapasalo, A., T. Saarelainen, et al. (1999). "Expression of the naturally occurring truncated trkB neurotrophin receptor induces outgrowth of filopodia and processes in neuroblastoma cells." Oncogene **18**(6): 1285-96.
Haapasalo, A., I. Sipola, et al. (2002). "Regulation of TRKB surface expression by brain-derived neurotrophic factor and truncated TRKB isoforms." J Biol Chem **277**(45): 43160-7.
Hallbook, F., C. F. Ibanez, et al. (1991). "Evolutionary studies of the nerve growth factor family reveal a novel member abundantly expressed in Xenopus ovary." Neuron **6**(5): 845-58.
Haniu, M., S. Montestruque, et al. (1997). "Interactions between brain-derived neurotrophic factor and the TRKB receptor. Identification of two ligand binding domains in soluble TRKB by affinity separation and chemical cross-linking." J Biol Chem **272**(40): 25296-303.
Hannestad, J., M. B. Levanti, et al. (1995). "Distribution of neurotrophin receptors in human palatine tonsils: an immunohistochemical study." J Neuroimmunol **58**(2): 131-7.
Hart, B. L. (1988). "Biological basis of the behavior of sick animals." Neurosci Biobehav Rev **12**(2): 123-37.

Hashimoto, S. (1988). "K-252a, a potent protein kinase inhibitor, blocks nerve growth factor-induced neurite outgrowth and changes in the phosphorylation of proteins in PC12h cells." J Cell Biol **107**(4): 1531-9.
Hashimoto, Y., T. Nakayama, et al. (1991). "Potent and preferential inhibition of Ca2+/calmodulin-dependent protein kinase II by K252a and its derivative, KT5926." Biochem Biophys Res Commun **181**(1): 423-9.
Hatchett, C. S., S. Tyler, et al. (2007). "Familial Alzheimer's disease presenilin 1 mutation M146V increases gamma secretase cutting of p75NTR in vitro." Brain Res **1147**: 248-55.
He, L. and M. H. Fox (1996). "Comparison of flow cytometry and western blotting to measure Hsp70." Cytometry **25**(3): 280-6.
He, X. L. and K. C. Garcia (2004). "Structure of nerve growth factor complexed with the shared neurotrophin receptor p75." Science **304**(5672): 870-5.
Hempstead, B. L., D. Martin-Zanca, et al. (1991). "High-affinity NGF binding requires coexpression of the trk proto-oncogene and the low-affinity NGF receptor." Nature **350**(6320): 678-83.
Herrup, K. and E. M. Shooter (1973). "Properties of the beta nerve growth factor receptor of avian dorsal root ganglia." Proc Natl Acad Sci U S A **70**(12): 3884-8.
Higgs, D. R., M. A. Vickers, et al. (1989). "A review of the molecular genetics of the human alpha-globin gene cluster." Blood **73**(5): 1081-104.
Hikawa, S., H. Kobayashi, et al. (2002). "Expression of neurotrophins and their receptors in peripheral lung cells of mice." Histochem Cell Biol **118**(1): 51-8.
Hinz, M., M. J. Moore, et al. (1996). "Domain analysis of human U5 RNA. Cap trimethylation, protein binding, and spliceosome assembly." J Biol Chem **271**(31): 19001-7.
Hofer, M., S. R. Pagliusi, et al. (1990). "Regional distribution of brain-derived neurotrophic factor mRNA in the adult mouse brain." Embo J **9**(8): 2459-64.
Hohn, A., J. Leibrock, et al. (1990). "Identification and characterization of a novel member of the nerve growth factor/brain-derived neurotrophic factor family." Nature **344**(6264): 339-41.
Holden, P. H., V. Asopa, et al. (1997). "Immunoglobulin-like domains define the nerve growth factor binding site of the TrkA receptor." Nat Biotechnol **15**(7): 668-72.
Holder, M. J., H. Wang, et al. (1993). "Suppression of apoptosis in normal and neoplastic human B lymphocytes by CD40 ligand is independent of Bc1-2 induction." Eur J Immunol **23**(9): 2368-71.
Hu, P., L. Sun, et al. (2008). "Crystal structure of Natratoxin, a novel snake secreted phospholipaseA2 neurotoxin from Naja atra venom inhibiting A-type K+ currents." Proteins **72**(2): 673-83.
Huang, E. J. and L. F. Reichardt (2003). "Trk receptors: roles in neuronal signal transduction." Annu Rev Biochem **72**: 609-42.
Huttenhofer, A., J. Brosius, et al. (2002). "RNomics: identification and function of small, non-messenger RNAs." Curr Opin Chem Biol **6**(6): 835-43.
Ibanez, C. F. (1994). "Structure-function relationships in the neurotrophin family." J Neurobiol **25**(11): 1349-61.
Ibanez, C. F. (1998). "Emerging themes in structural biology of neurotrophic factors." Trends Neurosci **21**(10): 438-44.
Ibanez, C. F., P. Ernfors, et al. (1993). "Neurotrophin-4 is a target-derived neurotrophic factor for neurons of the trigeminal ganglion." Development **117**(4): 1345-53.
Ibanez, C. F., L. L. Ilag, et al. (1993). "An extended surface of binding to Trk tyrosine kinase receptors in NGF and BDNF allows the engineering of a multifunctional pan-neurotrophin." Embo J **12**(6): 2281-93.
Inagaki, N., H. Thoenen, et al. (1995). "TrkA tyrosine residues involved in NGF-induced neurite outgrowth of PC12 cells." Eur J Neurosci **7**(6): 1125-33.
Invitrogen (2002). SeeBlue Plus2 Pre-Stained Standard. https://www.invitrogen.com/content/sfs/manuals/seeblueplus2_card.pdf.

Ip, N. Y., C. F. Ibanez, et al. (1992). "Mammalian neurotrophin-4: structure, chromosomal localization, tissue distribution, and receptor specificity." Proc Natl Acad Sci U S A **89**(7): 3060-4.
Janevski, J., P. C. Park, et al. (1997). "Changes in morphology and spatial position of coiled bodies during NGF-induced neuronal differentiation of PC12 cells." J Histochem Cytochem **45**(11): 1523-31.
Joseph, A. M., G. J. Babcock, et al. (2000). "Cells expressing the Epstein-Barr virus growth program are present in and restricted to the naive B-cell subset of healthy tonsils." J Virol **74**(21): 9964-71.
Jung, E. J., C. W. Kim, et al. (2008). "Cytosolic accumulation of gammaH2AX is associated with tropomyosin-related kinase A-induced cell death in U2OS cells." Exp Mol Med **40**(3): 276-85.
Jung, E. J. and D. R. Kim (2008). "Apoptotic cell death in TrkA-overexpressing cells: kinetic regulation of ERK phosphorylation and caspase-7 activation." Mol Cells **26**(1): 12-7.
Jung, K. M., S. Tan, et al. (2003). "Regulated intramembrane proteolysis of the p75 neurotrophin receptor modulates its association with the TrkA receptor." J Biol Chem **278**(43): 42161-9.
Kanning, K. C., M. Hudson, et al. (2003). "Proteolytic processing of the p75 neurotrophin receptor and two homologs generates C-terminal fragments with signaling capability." J Neurosci **23**(13): 5425-36.
Kansas, G. S., G. S. Wood, et al. (1991). "Expression, distribution, and biochemistry of human CD39. Role in activation-associated homotypic adhesion of lymphocytes." J Immunol **146**(7): 2235-44.
Kaplan, D. R. and F. D. Miller (2000). "Neurotrophin signal transduction in the nervous system." Curr Opin Neurobiol **10**(3): 381-91.
Kaplan, M. E. and C. Clark (1974). "An improved rosetting assay for detection of human T lymphocytes." J Immunol Methods **5**(2): 131-5.
Karege, F., G. Perret, et al. (2002). "Decreased serum brain-derived neurotrophic factor levels in major depressed patients." Psychiatry Res **109**(2): 143-8.
Katoh, O., T. Oguri, et al. (1998). "ZK1, a novel Kruppel-type zinc finger gene, is induced following exposure to ionizing radiation and enhances apoptotic cell death on hematopoietic cells." Biochem Biophys Res Commun **249**(3): 595-600.
Kazanskaya, O., A. Glinka, et al. (2004). "R-Spondin2 is a secreted activator of Wnt/beta-catenin signaling and is required for Xenopus myogenesis." Dev Cell **7**(4): 525-34.
Kelsoe, G. (1995). "The germinal center reaction." Immunol Today **16**(7): 324-6.
Kenchappa, R. S., N. Zampieri, et al. (2006). "Ligand-dependent cleavage of the P75 neurotrophin receptor is necessary for NRIF nuclear translocation and apoptosis in sympathetic neurons." Neuron **50**(2): 219-32.
Kerschensteiner, M., E. Gallmeier, et al. (1999). "Activated human T cells, B cells, and monocytes produce brain-derived neurotrophic factor in vitro and in inflammatory brain lesions: a neuroprotective role of inflammation?" J Exp Med **189**(5): 865-70.
Khursigara, G., J. R. Orlinick, et al. (1999). "Association of the p75 neurotrophin receptor with TRAF6." J Biol Chem **274**(5): 2597-600.
Kim, H. S., X. Zhang, et al. (1994). "Activation and proliferation of follicular dendritic cell-like cells by activated T lymphocytes." J Immunol **153**(7): 2951-61.
Kimata, H., A. Yoshida, et al. (1991). "Nerve growth factor specifically induces human IgG4 production." Eur J Immunol **21**(1): 137-41.
Kiss, A. M., B. E. Jady, et al. (2004). "Human box H/ACA pseudouridylation guide RNA machinery." Mol Cell Biol **24**(13): 5797-807.
Kitagawa, N., M. Goto, et al. (2000). "Epstein-Barr virus-encoded poly(A)(-) RNA supports Burkitt's lymphoma growth through interleukin-10 induction." Embo J **19**(24): 6742-50.
Klaus, G. G., J. H. Humphrey, et al. (1980). "The follicular dendritic cell: its role in antigen presentation in the generation of immunological memory." Immunol Rev **53**: 3-28.

Klein, G., B. Giovanella, et al. (1975). "An EBV-genome-negative cell line established from an American Burkitt lymphoma; receptor characteristics. EBV infectibility and permanent conversion into EBV-positive sublines by in vitro infection." Intervirology **5**(6): 319-34.
Klein, R., D. Conway, et al. (1990). "The trkB tyrosine protein kinase gene codes for a second neurogenic receptor that lacks the catalytic kinase domain." Cell **61**(4): 647-56.
Klein, R., L. F. Parada, et al. (1989). "trkB, a novel tyrosine protein kinase receptor expressed during mouse neural development." Embo J **8**(12): 3701-9.
Klein, U., Y. Tu, et al. (2003). "Transcriptional analysis of the B cell germinal center reaction." Proc Natl Acad Sci U S A **100**(5): 2639-44.
Kobayashi, H. and A. P. Mizisin (2001). "Nerve growth factor and neurotrophin-3 promote chemotaxis of mouse macrophages in vitro." Neurosci Lett **305**(3): 157-60.
Kreil, G. (1981). "Transfer of proteins across membranes." Annu Rev Biochem **50**: 317-48.
Kronfeld, I., G. Kazimirsky, et al. (2002). "NGF rescues human B lymphocytes from anti-IgM induced apoptosis by activation of PKCzeta." Eur J Immunol **32**(1): 136-43.
Kruse, N., S. Cetin, et al. (2007). "Differential expression of BDNF mRNA splice variants in mouse brain and immune cells." J Neuroimmunol **182**(1-2): 13-21.
Kunkl, A. and G. G. Klaus (1981). "The generation of memory cells. IV. Immunization with antigen-antibody complexes accelerates the development of B-memory cells, the formation of germinal centres and the maturation of antibody affinity in the secondary response." Immunology **43**(2): 371-8.
Kurth, J., M. L. Hansmann, et al. (2003). "Epstein-Barr virus-infected B cells expanding in germinal centers of infectious mononucleosis patients do not participate in the germinal center reaction." Proc Natl Acad Sci U S A **100**(8): 4730-5.
Kuwako, K., H. Taniura, et al. (2004). "Necdin-related MAGE proteins differentially interact with the E2F1 transcription factor and the p75 neurotrophin receptor." J Biol Chem **279**(3): 1703-12.
Laemmli, U. K. (1970). "Cleavage of structural proteins during the assembly of the head of bacteriophage T4." Nature **227**(5259): 680-5.
Lagadec, C., S. Meignan, et al. (2009). "TrkA overexpression enhances growth and metastasis of breast cancer cells." Oncogene **28**(18): 1960-70.
Lalezari, P., G. B. Murphy, et al. (1971). "NB1, a new neutrophil-specific antigen involved in the pathogenesis of neonatal neutropenia." J Clin Invest **50**(5): 1108-15.
Lamballe, F., R. Klein, et al. (1991). "trkC, a new member of the trk family of tyrosine protein kinases, is a receptor for neurotrophin-3." Cell **66**(5): 967-79.
Lambiase, A., L. Bracci-Laudiero, et al. (1997). "Human CD4+ T cell clones produce and release nerve growth factor and express high-affinity nerve growth factor receptors." J Allergy Clin Immunol **100**(3): 408-14.
Laurenzi, M. A., T. Beccari, et al. (1998). "Expression of mRNA encoding neurotrophins and neurotrophin receptors in human granulocytes and bone marrow cells--enhanced neurotrophin-4 expression induced by LTB4." J Leukoc Biol **64**(2): 228-34.
Lawyer, F. C., S. Stoffel, et al. (1989). "Isolation, characterization, and expression in Escherichia coli of the DNA polymerase gene from Thermus aquaticus." J Biol Chem **264**(11): 6427-37.
Lee, R., P. Kermani, et al. (2001). "Regulation of cell survival by secreted proneurotrophins." Science **294**(5548): 1945-8.
Levi-Montalcini, R. and P. U. Angeletti (1968). "Nerve growth factor." Physiol Rev **48**(3): 534-69.
Li, L., S. O. Yoon, et al. (2004). "Novel follicular dendritic cell molecule, 8D6, collaborates with CD44 in supporting lymphomagenesis by a Burkitt lymphoma cell line, L3055." Blood **104**(3): 815-21.
Li, L., X. Zhang, et al. (2000). "Identification of a human follicular dendritic cell molecule that stimulates germinal center B cell growth." J Exp Med **191**(6): 1077-84.
Lindhout, E., M. L. Mevissen, et al. (1993). "Direct evidence that human follicular dendritic cells (FDC) rescue germinal centre B cells from death by apoptosis." Clin Exp Immunol **91**(2): 330-6.

Linggi, M. S., T. L. Burke, et al. (2005). "Neurotrophin receptor interacting factor (NRIF) is an essential mediator of apoptotic signaling by the p75 neurotrophin receptor." J Biol Chem **280**(14): 13801-8.
Liot, G., C. Gabriel, et al. (2004). "Neurotrophin-3-induced PI-3 kinase/Akt signaling rescues cortical neurons from apoptosis." Exp Neurol **187**(1): 38-46.
Liu, Q. R., L. Lu, et al. (2006). "Rodent BDNF genes, novel promoters, novel splice variants, and regulation by cocaine." Brain Res **1067**(1): 1-12.
Liu, Y. J., D. E. Joshua, et al. (1989). "Mechanism of antigen-driven selection in germinal centres." Nature **342**(6252): 929-31.
Longo, F. M., M. Manthorpe, et al. (1997). "Synthetic NGF peptide derivatives prevent neuronal death via a p75 receptor-dependent mechanism." J Neurosci Res **48**(1): 1-17.
Lu, V. B., J. E. Biggs, et al. (2009). "Brain-derived neurotrophic factor drives the changes in excitatory synaptic transmission in the rat superficial dorsal horn that follow sciatic nerve injury." J Physiol **587**(Pt 5): 1013-32.
Lyons, A. B. and C. R. Parish (1994). "Determination of lymphocyte division by flow cytometry." J Immunol Methods **171**(1): 131-7.
MacLennan, I. C. and D. Gray (1986). "Antigen-driven selection of virgin and memory B cells." Immunol Rev **91**: 61-85.
Maeda, K., M. Matsuda, et al. (2002). "Immunohistochemical recognition of human follicular dendritic cells (FDCs) in routinely processed paraffin sections." J Histochem Cytochem **50**(11): 1475-86.
Magert, H. J., L. Standker, et al. (1999). "LEKTI, a novel 15-domain type of human serine proteinase inhibitor." J Biol Chem **274**(31): 21499-502.
Maisonpierre, P. C., L. Belluscio, et al. (1990). "Neurotrophin-3: a neurotrophic factor related to NGF and BDNF." Science **247**(4949 Pt 1): 1446-51.
Maldonado-Saldivia, J., J. van den Bergen, et al. (2007). "Dppa2 and Dppa4 are closely linked SAP motif genes restricted to pluripotent cells and the germ line." Stem Cells **25**(1): 19-28.
Maliszewski, C. R., G. J. Delespesse, et al. (1994). "The CD39 lymphoid cell activation antigen. Molecular cloning and structural characterization." J Immunol **153**(8): 3574-83.
Mangeney, M., C. A. Lingwood, et al. (1993). "Apoptosis induced in Burkitt's lymphoma cells via Gb3/CD77, a glycolipid antigen." Cancer Res **53**(21): 5314-9.
Mangeney, M., Y. Richard, et al. (1991). "CD77: an antigen of germinal center B cells entering apoptosis." Eur J Immunol **21**(5): 1131-40.
Manolov, G. and Y. Manolova (1972). "Marker band in one chromosome 14 from Burkitt lymphomas." Nature **237**(5349): 33-4.
Martens, L. K., K. M. Kirschner, et al. (2007). "Hypoxia-inducible factor-1 (HIF-1) is a transcriptional activator of the TrkB neurotrophin receptor gene." J Biol Chem **282**(19): 14379-88.
Martin-Zanca, D., S. H. Hughes, et al. (1986). "A human oncogene formed by the fusion of truncated tropomyosin and protein tyrosine kinase sequences." Nature **319**(6056): 743-8.
Martin-Zanca, D., R. Oskam, et al. (1989). "Molecular and biochemical characterization of the human trk proto-oncogene." Mol Cell Biol **9**(1): 24-33.
McCarty, J. H. and S. C. Feinstein (1998). "Activation loop tyrosines contribute varying roles to TrkB autophosphorylation and signal transduction." Oncogene **16**(13): 1691-700.
McCarty, J. H. and S. C. Feinstein (1999). "The TrkB receptor tyrosine kinase regulates cellular proliferation via signal transduction pathways involving SHC, PLCgamma, and CBL." J Recept Signal Transduct Res **19**(6): 953-74.
McGinnis, K. M., K. K. Wang, et al. (2001). "Calcium/calmodulin-dependent protein kinase inhibition potentiates thapsigargin-mediated cell death in SH-SY5Y human neuroblastoma cells." Neurosci Lett **301**(2): 99-102.
McHeyzer-Williams, M. G. and R. Ahmed (1999). "B cell memory and the long-lived plasma cell." Curr Opin Immunol **11**(2): 172-9.

McKenna, F., P. J. McLaughlin, et al. (2002). "Dopamine receptor expression on human T- and B-lymphocytes, monocytes, neutrophils, eosinophils and NK cells: a flow cytometric study." J Neuroimmunol **132**(1-2): 34-40.
Melamed, I., C. A. Kelleher, et al. (1996). "Nerve growth factor signal transduction in human B lymphocytes is mediated by gp140trk." Eur J Immunol **26**(9): 1985-92.
Melamed, I., H. Patel, et al. (1999). "Activation of Vav and Ras through the nerve growth factor and B cell receptors by different kinases." Cell Immunol **191**(2): 83-9.
Melamed, I., C. E. Turner, et al. (1995). "Nerve growth factor triggers microfilament assembly and paxillin phosphorylation in human B lymphocytes." J Exp Med **181**(3): 1071-9.
Meurs, E., K. Chong, et al. (1990). "Molecular cloning and characterization of the human double-stranded RNA-activated protein kinase induced by interferon." Cell **62**(2): 379-90.
Middlemas, D. S., R. A. Lindberg, et al. (1991). "trkB, a neural receptor protein-tyrosine kinase: evidence for a full-length and two truncated receptors." Mol Cell Biol **11**(1): 143-53.
Middlemas, D. S., J. Meisenhelder, et al. (1994). "Identification of TrkB autophosphorylation sites and evidence that phospholipase C-gamma 1 is a substrate of the TrkB receptor." J Biol Chem **269**(7): 5458-66.
Miller, C. L., J. H. Lee, et al. (1994). "An Integral Membrane Protein (LMP2) Blocks Reactivation of Epstein-Barr Virus from Latency Following Surface Immunoglobulin Crosslinking." PNAS **91**(2): 772-776.
Mitra, G., D. Martin-Zanca, et al. (1987). "Identification and biochemical characterization of p70TRK, product of the human TRK oncogene." Proc Natl Acad Sci U S A **84**(19): 6707-11.
Miwa, T., T. Moriizumi, et al. (2002). "Role of nerve growth factor in the olfactory system." Microsc Res Tech **58**(3): 197-203.
Moore, G. E., R. E. Gerner, et al. (1967). "Culture of normal human leukocytes." Jama **199**(8): 519-24.
Morgan, R. T., L. K. Woods, et al. (1980). "Human cell line (COLO 357) of metastatic pancreatic adenocarcinoma." Int J Cancer **25**(5): 591-8.
Mowla, S. J., S. Pareek, et al. (1999). "Differential sorting of nerve growth factor and brain-derived neurotrophic factor in hippocampal neurons." J Neurosci **19**(6): 2069-80.
Mudde, G. C., D. van Dam, et al. (1986). "Human peripheral blood B cell subpopulations: surface IgD+ cells respond to pokeweed mitogen with plasma cell differentiation." Clin Exp Immunol **64**(1): 150-7.
Mukobata, S., T. Hibino, et al. (2002). "M6a acts as a nerve growth factor-gated Ca(2+) channel in neuronal differentiation." Biochem Biophys Res Commun **297**(4): 722-8.
Narisawa-Saito, M., Y. Iwakura, et al. (2002). "Brain-derived neurotrophic factor regulates surface expression of alpha-amino-3-hydroxy-5-methyl-4-isoxazoleproprionic acid receptors by enhancing the N-ethylmaleimide-sensitive factor/GluR2 interaction in developing neocortical neurons." J Biol Chem **277**(43): 40901-10.
Naylor, R. L., A. G. Robertson, et al. (2002). "A discrete domain of the human TrkB receptor defines the binding sites for BDNF and NT-4." Biochem Biophys Res Commun **291**(3): 501-7.
Newsholme, P., R. Curi, et al. (1999). "Glutamine metabolism by lymphocytes, macrophages, and neutrophils: its importance in health and disease." J Nutr Biochem **10**(6): 316-24.
Nimnual, A. S., B. A. Yatsula, et al. (1998). "Coupling of Ras and Rac guanosine triphosphatases through the Ras exchanger Sos." Science **279**(5350): 560-3.
Ninkina, N., J. Adu, et al. (1996). "Expression and function of TrkB variants in developing sensory neurons." Embo J **15**(23): 6385-93.
Ninkina, N., M. Grashchuck, et al. (1997). "TrkB variants with deletions in the leucine-rich motifs of the extracellular domain." J Biol Chem **272**(20): 13019-25.
Nykjaer, A., R. Lee, et al. (2004). "Sortilin is essential for proNGF-induced neuronal cell death." Nature **427**(6977): 843-8.
O'Conor, G. T. and J. N. Davies (1960). "Malignant tumors in African children. With special reference to malignant lymphoma." J Pediatr **56**: 526-35.

Ohmichi, M., S. J. Decker, et al. (1991). "Phospholipase C-gamma 1 directly associates with the p70 trk oncogene product through its src homology domains." J Biol Chem **266**(23): 14858-61.
Ojika, K. and S. H. Appel (1984). "Neurotrophic effects of hippocampal extracts on medial septal nucleus in vitro." Proc Natl Acad Sci U S A **81**(8): 2567-71.
Old, L. J., E. A. Boyse, et al. (1966). "Precipitating Antibody in Human Serum to an Antigen Present in Cultured Burkitt's Lymphoma Cells." Proc Natl Acad Sci U S A **56**(6): 1699-1704.
Otten, U., J. B. Baumann, et al. (1984). "Nerve growth factor induces plasma extravasation in rat skin." Eur J Pharmacol **106**(1): 199-201.
Otten, U., P. Ehrhard, et al. (1989). "Nerve growth factor induces growth and differentiation of human B lymphocytes." Proc Natl Acad Sci U S A **86**(24): 10059-63.
Pan, J., Q. G. Zhang, et al. (2005). "The neuroprotective effects of K252a through inhibiting MLK3/MKK7/JNK3 signaling pathway on ischemic brain injury in rat hippocampal CA1 region." Neuroscience **131**(1): 147-59.
Park, M. J., H. J. Kwak, et al. (2007). "Nerve growth factor induces endothelial cell invasion and cord formation by promoting matrix metalloproteinase-2 expression through the phosphatidylinositol 3-kinase/Akt signaling pathway and AP-2 transcription factor." J Biol Chem **282**(42): 30485-96.
Pascual, V., Y. J. Liu, et al. (1994). "Analysis of somatic mutation in five B cell subsets of human tonsil." J Exp Med **180**(1): 329-39.
Paterson, M. A., A. J. Horvath, et al. (2007). "Molecular characterization of centerin, a germinal centre cell serpin." Biochem J **405**(3): 489-94.
Pearse, R. N., S. L. Swendeman, et al. (2005). "A neurotrophin axis in myeloma: TrkB and BDNF promote tumor-cell survival." Blood **105**(11): 4429-36.
Pleasure, D. E. and P. F. Chance (2005). "Neurotrophin-3 therapy for Charcot-Marie-Tooth disease type 1A." Neurology **65**(5): 662-3.
Pruunsild, P., A. Kazantseva, et al. (2007). "Dissecting the human BDNF locus: bidirectional transcription, complex splicing, and multiple promoters." Genomics **90**(3): 397-406.
Radeke, M. J., T. P. Misko, et al. (1987). "Gene transfer and molecular cloning of the rat nerve growth factor receptor." Nature **325**(6105): 593-7.
Rajewsky, K. (1996). "Clonal selection and learning in the antibody system." Nature **381**(6585): 751-8.
Raska, I., R. L. Ochs, et al. (1990). "Association between the nucleolus and the coiled body." J Struct Biol **104**(1-3): 120-7.
Raychaudhuri, S. K. and S. P. Raychaudhuri (2009). "NGF and its receptor system: a new dimension in the pathogenesis of psoriasis and psoriatic arthritis." Ann N Y Acad Sci **1173**: 470-7.
Reichardt, L. F. (2006). "Neurotrophin-regulated signalling pathways." Philos Trans R Soc Lond B Biol Sci **361**(1473): 1545-64.
Renne, C., S. Minner, et al. (2008). "Autocrine NGFbeta/TRKA signalling is an important survival factor for Hodgkin lymphoma derived cell lines." Leuk Res **32**(1): 163-7.
Renovanz, H. D. (1960). "[Results of newer pulmonary function tests in children.]." Tuberkulosearzt **14**: 621-30.
Ricci, A., S. Greco, et al. (2001). "Neurotrophins and neurotrophin receptors in human lung cancer." Am J Respir Cell Mol Biol **25**(4): 439-46.
Riccio, A., S. Ahn, et al. (1999). "Mediation by a CREB family transcription factor of NGF-dependent survival of sympathetic neurons." Science **286**(5448): 2358-61.
Rickinson, A. B., L. S. Young, et al. (1987). "Influence of the Epstein-Barr virus nuclear antigen EBNA 2 on the growth phenotype of virus-transformed B cells." J Virol **61**(5): 1310-7.
Robertson, A. G., M. J. Banfield, et al. (2001). "Identification and structure of the nerve growth factor binding site on TrkA." Biochem Biophys Res Commun **282**(1): 131-41.
Rogers, M. L., I. Atmosukarto, et al. (2006). "Functional monoclonal antibodies to p75 neurotrophin receptor raised in knockout mice." J Neurosci Methods **158**(1): 109-20.

Rogoz, Z., G. Skuza, et al. (2005). "Repeated treatment with mirtazepine induces brain-derived neurotrophic factor gene expression in rats." J Physiol Pharmacol **56**(4): 661-71.
Roland, K., J. Stefan, et al. (1994). "Characterisation of Neurotrophin Dimers and Monomers." European Journal of Biochemistry **225**(3): 995-1003.
Rouse, R. V., J. A. Ledbetter, et al. (1982). "Mouse lymph node germinal centers contain a selected subset of T cells--the helper phenotype." J Immunol **128**(5): 2243-6.
Rowe, M., J. E. Hildreth, et al. (1982). "Monoclonal antibodies to Epstein-Barr virus-induced, transformation-associated cell surface antigens: binding patterns and effect upon virus-specific T-cell cytotoxicity." Int J Cancer **29**(4): 373-81.
Rubio, N. (1997). "Mouse astrocytes store and deliver brain-derived neurotrophic factor using the non-catalytic gp95trkB receptor." Eur J Neurosci **9**(9): 1847-53.
Ruegg, U. T. and G. M. Burgess (1989). "Staurosporine, K-252 and UCN-01: potent but nonspecific inhibitors of protein kinases." Trends Pharmacol Sci **10**(6): 218-20.
Sakamoto, Y., Y. Kitajima, et al. (2001). "Expression of Trk tyrosine kinase receptor is a biologic marker for cell proliferation and perineural invasion of human pancreatic ductal adenocarcinoma." Oncol Rep **8**(3): 477-84.
Salehi, A. H., P. P. Roux, et al. (2000). "NRAGE, a novel MAGE protein, interacts with the p75 neurotrophin receptor and facilitates nerve growth factor-dependent apoptosis." Neuron **27**(2): 279-88.
Samah, B., F. Porcheray, et al. (2008). "Neurotrophins modulate monocyte chemotaxis without affecting macrophage function." Clin Exp Immunol **151**(3): 476-86.
Sawada, J., A. Itakura, et al. (2000). "Nerve growth factor functions as a chemoattractant for mast cells through both mitogen-activated protein kinase and phosphatidylinositol 3-kinase signaling pathways." Blood **95**(6): 2052-8.
Schafer, B. W., R. Wicki, et al. (1995). "Isolation of a YAC clone covering a cluster of nine S100 genes on human chromosome 1q21: rationale for a new nomenclature of the S100 calcium-binding protein family." Genomics **25**(3): 638-43.
Schenone, A., J. S. Gill, et al. (1996). "Expression of high- and low-affinity neurotrophin receptors on human transformed B lymphocytes." J Neuroimmunol **64**(2): 141-9.
Schneider, R. and M. Schweiger (1991). "A novel modular mosaic of cell adhesion motifs in the extracellular domains of the neurogenic trk and trkB tyrosine kinase receptors." Oncogene **6**(10): 1807-11.
Schriever, F., A. S. Freedman, et al. (1989). "Isolated human follicular dendritic cells display a unique antigenic phenotype." J Exp Med **169**(6): 2043-58.
Schuhmann, B., A. Dietrich, et al. (2005). "A role for brain-derived neurotrophic factor in B cell development." J Neuroimmunol **163**(1-2): 15-23.
Scott D. Z. Eggers and Anthony J. Windebank, M. (1996). "Epstein-Barr Virus Transformation Induces Expression of trk b mRNA in Human B Lymphocytes." Contemporary Neurology(1): 1.
Sedgwick, S. G. and S. J. Smerdon (1999). "The ankyrin repeat: a diversity of interactions on a common structural framework." Trends Biochem Sci **24**(8): 311-6.
Seidah, N. G., S. Benjannet, et al. (1996). "Cellular processing of the nerve growth factor precursor by the mammalian pro-protein convertases." Biochem J **314 (Pt 3)**: 951-60.
Selby, M. J., R. Edwards, et al. (1987). "Mouse nerve growth factor gene: structure and expression." Mol Cell Biol **7**(9): 3057-64.
Shelton, D. L., J. Sutherland, et al. (1995). "Human trks: molecular cloning, tissue distribution, and expression of extracellular domain immunoadhesins." J Neurosci **15**(1 Pt 2): 477-91.
Shimizu, E., K. Hashimoto, et al. (2003). "Alterations of serum levels of brain-derived neurotrophic factor (BDNF) in depressed patients with or without antidepressants." Biol Psychiatry **54**(1): 70-5.
Shonukan, O., I. Bagayogo, et al. (2003). "Neurotrophin-induced melanoma cell migration is mediated through the actin-bundling protein fascin." Oncogene **22**(23): 3616-23.

Siegel, G. (1978). "Cell fractionation and cytological analysis of human lymphatic cells from tonsil and blood." Arch Otorhinolaryngol **221**(1): 15-21.
Singh, V. K. and J. F. Cheng (1996). "Immunoreactive S100 proteins of blood immunocytes and brain cells." J Neuroimmunol **64**(2): 135-9.
Skaper, S. D. (2008). "The biology of neurotrophins, signalling pathways, and functional peptide mimetics of neurotrophins and their receptors." CNS Neurol Disord Drug Targets **7**(1): 46-62.
Smith, A. P., S. Varon, et al. (1968). "Multiple forms of the nerve growth factor protein and its subunits." Biochemistry **7**(9): 3259-68.
Smith, J. L. and C. R. Barker (1973). "T and B cell separation by sheep-red-cell rosetting." Lancet **1**(7802): 558-9.
Smith, R. J., J. M. Justen, et al. (1988). "Effects of a protein kinase C inhibitor, K-252a, on human polymorphonuclear neutrophil responsiveness." Biochem Biophys Res Commun **152**(3): 1497-503.
Snider, W. D. (1994). "Functions of the neurotrophins during nervous system development: what the knockouts are teaching us." Cell **77**(5): 627-38.
Soppet, D., E. Escandon, et al. (1991). "The neurotrophic factors brain-derived neurotrophic factor and neurotrophin-3 are ligands for the trkB tyrosine kinase receptor." Cell **65**(5): 895-903.
Stein, H., J. Gerdes, et al. (1982). "The normal and malignant germinal centre." Clin Haematol **11**(3): 531-59.
Stephan, H., J. L. Zakrzewski, et al. (2008). "Neurotrophin receptor expression in human primary retinoblastomas and retinoblastoma cell lines." Pediatr Blood Cancer **50**(2): 218-22.
Stephens, R. M., D. M. Loeb, et al. (1994). "Trk receptors use redundant signal transduction pathways involving SHC and PLC-gamma 1 to mediate NGF responses." Neuron **12**(3): 691-705.
Stewart, S., C. W. Dawson, et al. (2004). "Epstein-Barr virus-encoded LMP2A regulates viral and cellular gene expression by modulation of the NF-{kappa}B transcription factor pathway." PNAS **101**(44): 15730-15735.
Stoilov, P., E. Castren, et al. (2002). "Analysis of the human TrkB gene genomic organization reveals novel TrkB isoforms, unusual gene length, and splicing mechanism." Biochem Biophys Res Commun **290**(3): 1054-65.
Strausberg, R. L., E. A. Feingold, et al. (2002). "Generation and initial analysis of more than 15,000 full-length human and mouse cDNA sequences." Proc Natl Acad Sci U S A **99**(26): 16899-903.
Szekely, L., G. Selivanova, et al. (1993). "EBNA-5, an Epstein-Barr Virus-Encoded Nuclear Antigen, Binds to the Retinoblastoma and p53 Proteins." PNAS **90**(12): 5455-5459.
Tam, S. Y., M. Tsai, et al. (1997). "Expression of functional TrkA receptor tyrosine kinase in the HMC-1 human mast cell line and in human mast cells." Blood **90**(5): 1807-20.
Taub, R., I. Kirsch, et al. (1982). "Translocation of the c-myc gene into the immunoglobulin heavy chain locus in human Burkitt lymphoma and murine plasmacytoma cells." Proc Natl Acad Sci U S A **79**(24): 7837-41.
Teng, H. K., K. K. Teng, et al. (2005). "ProBDNF induces neuronal apoptosis via activation of a receptor complex of p75NTR and sortilin." J Neurosci **25**(22): 5455-63.
Tepper, C. G. and M. F. Seldin (1999). "Modulation of caspase-8 and FLICE-inhibitory protein expression as a potential mechanism of Epstein-Barr virus tumorigenesis in Burkitt's lymphoma." Blood **94**(5): 1727-37.
Tervonen, T. A., F. Ajamian, et al. (2006). "Overexpression of a truncated TrkB isoform increases the proliferation of neural progenitors." Eur J Neurosci **24**(5): 1277-85.
Tessarollo, L., P. Tsoulfas, et al. (1993). "trkC, a receptor for neurotrophin-3, is widely expressed in the developing nervous system and in non-neuronal tissues." Development **118**(2): 463-75.
Thoenen, H., C. Bandtlow, et al. (1987). "The physiological function of nerve growth factor in the central nervous system: comparison with the periphery." Rev Physiol Biochem Pharmacol **109**: 145-78.

Thress, K., T. Macintyre, et al. (2009). "Identification and preclinical characterization of AZ-23, a novel, selective, and orally bioavailable inhibitor of the Trk kinase pathway." Mol Cancer Ther **8**(7): 1818-27.
Tomkinson, B., E. Robertson, et al. (1993). "Epstein-Barr virus nuclear proteins EBNA-3A and EBNA-3C are essential for B-lymphocyte growth transformation." J Virol **67**(4): 2014-25.
Torcia, M., L. Bracci-Laudiero, et al. (1996). "Nerve growth factor is an autocrine survival factor for memory B lymphocytes." Cell **85**(3): 345-56.
Towbin, H., T. Staehelin, et al. (1979). "Electrophoretic transfer of proteins from polyacrylamide gels to nitrocellulose sheets: procedure and some applications." Proc Natl Acad Sci U S A **76**(9): 4350-4.
Turner, B. J., S. S. Murray, et al. (2004). "Effect of p75 neurotrophin receptor antagonist on disease progression in transgenic amyotrophic lateral sclerosis mice." J Neurosci Res **78**(2): 193-9.
Tuszynski, M. H., L. Thal, et al. (2005). "A phase 1 clinical trial of nerve growth factor gene therapy for Alzheimer disease." Nat Med **11**(5): 551-5.
Ultsch, M. H., C. Wiesmann, et al. (1999). "Crystal structures of the neurotrophin-binding domain of TrkA, TrkB and TrkC." J Mol Biol **290**(1): 149-59.
van den Elsen, P., B. A. Shepley, et al. (1984). "Isolation of cDNA clones encoding the 20K T3 glycoprotein of human T-cell receptor complex." Nature **312**(5993): 413-8.
Varon, S., J. Nomura, et al. (1967). "Subunit structure of a high-molecular-weight form of the nerve growth factor from mouse submaxillary gland." Proc Natl Acad Sci U S A **57**(6): 1782-9.
Verdi, J. M., S. J. Birren, et al. (1994). "p75LNGFR regulates Trk signal transduction and NGF-induced neuronal differentiation in MAH cells." Neuron **12**(4): 733-45.
Waage, A., N. Liabakk, et al. (1992). "p55 and p75 tumor necrosis factor receptors in patients with chronic lymphocytic leukemia." Blood **80**(10): 2577-83.
Wagner, S. D. and M. S. Neuberger (1996). "Somatic hypermutation of immunoglobulin genes." Annu Rev Immunol **14**: 441-57.
Walker, U. A. and E. A. Schon (1998). "Neurotrophin-4 is up-regulated in ragged-red fibers associated with pathogenic mitochondrial DNA mutations." Ann Neurol **43**(4): 536-40.
Watson, J. J., M. S. Fahey, et al. (2006). "TrkAd5: A novel therapeutic agent for treatment of inflammatory pain and asthma." J Pharmacol Exp Ther **316**(3): 1122-9.
Wenger, S. L., J. R. Senft, et al. (2004). "Comparison of established cell lines at different passages by karyotype and comparative genomic hybridization." Biosci Rep **24**(6): 631-9.
Windisch, J. M., B. Auer, et al. (1995). "Specific neurotrophin binding to leucine-rich motif peptides of TrkA and TrkB." FEBS Lett **374**(1): 125-9.
Wood, E. R., L. Kuyper, et al. (2004). "Discovery and in vitro evaluation of potent TrkA kinase inhibitors: oxindole and aza-oxindoles." Bioorg Med Chem Lett **14**(4): 953-7.
Wooten, M. W., M. L. Seibenhener, et al. (1999). "Overexpression of atypical PKC in PC12 cells enhances NGF-responsiveness and survival through an NF-kappaB dependent pathway." Cell Death Differ **6**(8): 753-64.
Xie, C. W., D. Sayah, et al. (2000). "Deficient long-term memory and long-lasting long-term potentiation in mice with a targeted deletion of neurotrophin-4 gene." Proc Natl Acad Sci U S A **97**(14): 8116-21.
Xing, J., J. M. Kornhauser, et al. (1998). "Nerve growth factor activates extracellular signal-regulated kinase and p38 mitogen-activated protein kinase pathways to stimulate CREB serine 133 phosphorylation." Mol Cell Biol **18**(4): 1946-55.
Yacoubian, T. A. and D. C. Lo (2000). "Truncated and full-length TrkB receptors regulate distinct modes of dendritic growth." Nat Neurosci **3**(4): 342-9.
Yamada, K., K. Iwahashi, et al. (1987). "K252a, a new inhibitor of protein kinase C, concomitantly inhibits 40K protein phosphorylation and serotonin secretion in a phorbol ester-stimulated platelets." Biochem Biophys Res Commun **144**(1): 35-40.

Yan, H. and M. V. Chao (1991). "Disruption of cysteine-rich repeats of the p75 nerve growth factor receptor leads to loss of ligand binding." J Biol Chem **266**(18): 12099-104.
Yan, Y., C. Lagenaur, et al. (1993). "Molecular cloning of M6: identification of a PLP/DM20 gene family." Neuron **11**(3): 423-31.
Yan, Y., V. Narayanan, et al. (1996). "Expression of members of the proteolipid protein gene family in the developing murine central nervous system." J Comp Neurol **370**(4): 465-78.
Yarden, Y., J. A. Escobedo, et al. (1986). "Structure of the receptor for platelet-derived growth factor helps define a family of closely related growth factor receptors." Nature **323**(6085): 226-32.
Yeiser, E. C., N. J. Rutkoski, et al. (2004). "Neurotrophin signaling through the p75 receptor is deficient in traf6-/- mice." J Neurosci **24**(46): 10521-9.
Young, L. S. and A. B. Rickinson (2004). "EPSTEIN-BARR VIRUS: 40 YEARS ON." Nature Reviews Cancer **4**(10): 757-768.
Yu, H., T. J. Cook, et al. (1997). "Evidence for diminished functional expression of intestinal transporters in Caco-2 cell monolayers at high passages." Pharm Res **14**(6): 757-62.
Zacny, V. L., J. Wilson, et al. (1998). "The Epstein-Barr virus immediate-early gene product, BRLF1, interacts with the retinoblastoma protein during the viral lytic cycle." J Virol **72**(10): 8043-51.
Zampieri, N., C. F. Xu, et al. (2005). "Cleavage of p75 neurotrophin receptor by alpha-secretase and gamma-secretase requires specific receptor domains." J Biol Chem **280**(15): 14563-71.
Zech, L., U. Haglund, et al. (1976). "Characteristic chromosomal abnormalities in biopsies and lymphoid-cell lines from patients with Burkitt and non-Burkitt lymphomas." Int J Cancer **17**(1): 47-56.
Zhang, Q., D. Gutsch, et al. (1994). "Functional and physical interaction between p53 and BZLF1: implications for Epstein-Barr virus latency." Mol Cell Biol **14**(3): 1929-38.
Zhao, B. and C. E. Sample (2000). "Epstein-Barr virus nuclear antigen 3C activates the latent membrane protein 1 promoter in the presence of Epstein-Barr virus nuclear antigen 2 through sequences encompassing an Spi-1/Spi-B binding site." Journal of Virology **74**(11): 5151-5160.
Zhou, L. J. and T. F. Tedder (1996). "CD14+ blood monocytes can differentiate into functionally mature CD83+ dendritic cells." Proc Natl Acad Sci U S A **93**(6): 2588-92.
Zola, H., L. Flego, et al. (1993). "Expression of membrane receptor for tumour necrosis factor on human blood lymphocytes." Immunol Cell Biol **71 (Pt 4)**: 281-8.